

**FUCOIDAN IN BONE TISSUE  
REGENERATION:  
FROM CELL TYPE SPECIFIC BIOACTIVITIES TO  
THE DEVELOPMENT OF A HYDROGEL-BASED  
DELIVERY SYSTEM**

DISSERTATION

zur Erlangung des Doktorgrades  
der Mathematisch-Naturwissenschaftlichen Fakultät  
der Christian-Albrechts-Universität zu Kiel

vorgelegt von

Julia Maria Ohmes

Kiel, 2022



Erste Gutachterin: Prof. Dr. Sabine Fuchs  
Zweite Gutachterin: Prof. Dr. Susanne Alban

Tag der mündlichen Prüfung: 21.10.2022



---

## Eigenständigkeitserklärung

Hiermit erkläre ich, dass

1. es sich bei der eingereichten Arbeit zum Thema "Fucoidan in Bone Tissue Regeneration: From Cell Type Specific Bioactivities to the Development of a Hydrogel-based Delivery System" um meine eigenständig erbrachte Leistung handelt.
2. ich keine anderen, als die angegebenen Hilfsmittel verwendet habe.
3. die Arbeit gemäß den Regeln zur guten wissenschaftlichen Praxis der Deutschen Forschungsgemeinschaft angefertigt wurde.
4. ich nicht mit demselben Thema zeitgleich an einer anderen Fakultät im In- oder Ausland die Zulassung zur Promotion beantragt habe oder beantragen werde.
5. ich noch an keiner anderen Hochschule oder an keiner anderen Fakultät dieser Hochschule ein Promotionsvorhaben endgültig nicht bestanden habe.
6. mir noch kein akademischer Grad entzogen wurde.

Kiel, 2022

---

Julia Ohmes



---

## Summary

Fucoidans are sulfated polysaccharides found in the cell wall of brown algae. Due to their ample effects on angiogenesis, osteogenesis and inflammation, these polysaccharides are promising bioactive compounds for the application in regenerative medicine. However, the chemical structure of fucoidan which determines the bioactivities is dependent on many parameters such as algae species, location, season and extraction technique and can therefore vary tremendously between extracts. Due to the heterogeneity of fucoidan and the largely unknown relation between chemical structure and function, it remains challenging to use fucoidan in a medical context.

The presented dissertation investigates the biological activity of different fucoidan extracts on molecular processes relevant for bone tissue regeneration. Mono- and co-cultures of human outgrowth endothelial cells (OEC) isolated from peripheral blood and human mesenchymal stem cells isolated from cancellous bone and differentiated towards an osteoblast lineage (MSC) were used as cell model systems to mimic the bone tissue environment. To come one step closer to the utilization of fucoidan as a therapeutic agent, a hydrogel-based delivery system with incorporated fucoidan was developed.

**Part I** of the dissertation studies the bioactivity of enzymatically-extracted fucoidans on angiogenesis, osteogenesis and inflammation, all processes which are relevant for bone regeneration. The chemical characterization revealed that all extracts were high molecular weight (HMW) fucoidans (> 400 kDa) which mainly differed in their sulfate and fucose content. It was found that treatment of cells with the HMW fucoidans inhibited osteogenesis and angiogenesis indicated by reduced expression and secretion of angiogenic and osteogenic markers, such as vascular endothelial growth factor (VEGF), angiopoietin 1 (ANG-1) and stromal derived factor 1 (SDF-1). Additionally, an impaired formation of prevascular structures was observed. The anti-angiogenic and anti-osteogenic effect was strongest for extracts with a high fucose and sulfate content, indicating that the chemical composition of fucoidans is closely related to their bioactivity. Likely, the chemical properties define fucoidan's affinity to specific molecular mediators, thereby causing the observed effects.

**Part II** of the dissertation examines the potential of defined enzymatic hydrolysis after extraction as a tool to produce fucoidan extracts with tailored bioactivities. Therefore, HMW fucoidan F3 which was studied in Part I was cleaved by fucoidanase Fhf1 obtaining a 10-209 kDa medium (MMW) and a 2 kDa low molecular weight (LMW) extract. The anti-angiogenic effect of the HMW fucoidan which was described in Part I of the dissertation was no longer observed for MMW and LMW fucoidan extracts. Treatment with MMW and LMW fucoidans did not affect the expression and protein levels of relevant molecular mediators, nor impaired the formation of angiogenic structures. In contrast to high doses of MMW, LMW did not provoke an inflammatory response. These results demonstrate that enzymatic hydrolysis clearly changes the bioactivities of the obtained extracts and therefore represents a promising tool to select and tailor fucoidans for individual medical purposes.

**Part III** of the dissertation analyzes the effect of chemically extracted and H<sub>2</sub>O<sub>2</sub>-

---

degraded fucoidans on angiogenic processes. It was found that chemically extracted and degraded fucoidans exhibited a comparable bioactivity on angiogenic processes as observed for enzymatically-extracted fucoidans with similar molecular weights.

Finally, **Part IV** of the dissertation describes the development of a hydrogel-based delivery system for fucoidan. The composite hydrogel consisted of chitosan, collagen type I and  $\beta$ -glycerophosphate. The sol was injectable at room temperature, but gelled within 1 min at 37°C. The incorporation of fucoidan had only minor impacts on the physicochemical parameters of the hydrogel. Further, the biomaterial was compatible with MSC and OEC, indicating its potential for the use in regenerative medicine.

Taken together, the presented dissertation contributes to the elucidation of structure-function relationships of fucoidan in the context of bone regeneration. Based on the findings, different mechanisms of action of fucoidan are pointed out. By comparing the bioactivity of fucoidan from different extraction methods, by evaluating post extraction processing techniques and by developing a fucoidan delivery system, this dissertation provides valuable information which help to make the utilization of fucoidan in the medical context possible.

---

## Zusammenfassung

Fucoidane sind sulfatierte Polysaccharide, welche in der Zellwand von Braunalgen lokalisiert sind. Aufgrund ihrer vielseitigen Effekte im Bereich der Angiogenese, Osteogenese und bei Entzündungsprozessen sind diese Polysaccharide vielversprechende bioaktive Moleküle für die Anwendung in der regenerativen Medizin. Allerdings ist die chemische Struktur von Fucoidan, welche die Bioaktivität bestimmt, abhängig von verschiedenen Faktoren wie Algenspezies, Ursprung, Jahreszeit und Extraktionsmethode und kann deshalb von Extrakt zu Extrakt sehr unterschiedlich sein. Diese Heterogenität der Fucoidane erschwert die Anwendung im medizinischen Kontext.

Die vorliegende Dissertation untersucht die biologische Aktivität verschiedener Fucoidanextrakte auf molekulare Prozesse, welche relevant für die Knochenregeneration sind. Als zelluläre Modelle für das Knochengewebe wurden Mono- und Kokulturen aus humanen Endothelzellen (OEC) und humanen mesenchymalen Stammzellen, welche in Richtung Osteoblasten differenziert wurden, verwendet. Die OEC wurden aus dem peripheren Blut isoliert, während die MSC aus dem Spongiosaknochen gewonnen wurden. Um der Anwendung von Fucoidanen in der Medizin einen Schritt näher zu kommen, wurde ein hydrogelbasiertes Trägersystem für Fucoidan entwickelt.

**Teil I** der Dissertation untersucht die Wirkung von enzymatisch-extrahierten Fucoidanen auf die Angiogenese, Osteogenese und Entzündungsprozesse. Alle der genannten Prozesse spielen eine wichtige Rolle während der Knochenregeneration. Die chemische Charakterisierung erbrachte, dass es sich bei allen Extrakten um hochmolekulare (HMW) Fucoidane (> 400 kDa) handelte, welche sich hauptsächlich durch ihren Fucose- und Sulfatgehalt unterschieden. Durch die verringerte Expression und Sekretion verschiedener angiogener und osteogener Mediatoren wie vascular endothelial growth factor (VEGF), angiopoietin 1 (ANG-1) und stromal derived factor 1 (SDF-1) konnte gezeigt werden, dass die Behandlung der Zellen mit den Fucoidanextrakten eine anti-angiogene und anti-osteogene Wirkung hatte. Zusätzlich wurde eine reduzierte Bildung prävasculärer Strukturen beobachtet. Der hemmende Effekt war am stärksten bei Extrakten mit einem hohen Fucose- und Sulfatgehalt. Dies zeigt, dass die chemische Struktur der Fucoidane eng mit der biologischen Wirkung zusammenhängt. Es scheint wahrscheinlich, dass die chemische Struktur die Affinität von Fucoidan zu verschiedenen physiologischen Molekülen bestimmt und somit verantwortlich für die beobachteten Effekte ist.

**Teil II** der Dissertation untersucht, ob definierte enzymatische Hydrolyse nach der Extraktion ein geeignetes Werkzeug darstellt, um die Bioaktivität von Fucoidanen für spezifische medizinische Anwendungen maßzuschneidern. Hierfür wurde das HMW Fucoidan F3, welches im ersten Teil beschrieben wurde, spezifisch mit der Fucoidanase Fhfl verdaut. Aus dem Verdau ergaben sich ein 10-209 kDa mittel molekularer (MMW) und ein 2 kDa niedermolekularer (LMW) Extrakt. Der anti-angiogene Effekt der HMW Fucoidane, welcher in Teil I beschrieben wurde, konnte bei dem MMW und LMW Extrakt nicht mehr gezeigt werden. Eine Behandlung mit MMW und LMW beeinflusste weder die Expression und Sekretion relevanter Mediatoren, noch beeinträchtigte sie die Bildung prävasculärer Strukturen. Im Gegensatz zu einer hohen MMW Konzentration, löste

---

LMW keine Entzündungsreaktion aus. Diese Ergebnisse machen deutlich, dass enzymatische Hydrolyse die Bioaktivität der gewonnenen Extrakte verändert und somit ein vielversprechendes Werkzeug darstellt, um Fucoidane und ihre Bioaktivität entsprechend dem medizinischen Zweck anzupassen.

**Teil III** der Dissertation analysiert den Effekt von chemisch extrahierten und H<sub>2</sub>O<sub>2</sub>-degradierten Fucoidanen auf angiogene Prozesse. Es wurde gezeigt, dass chemisch extrahierte und degradierte Fucoidane vergleichbare Effekte auf angiogene Prozesse ausübten wie die enzymatisch extrahierten Fucoidane mit einem ähnlichem Molekulargewicht.

**Teil IV** der Dissertation beschreibt schließlich die Entwicklung eines hydrogelbasierten Trägersystems für Fucoidan. Das aus Chitosan, Kollagen Typ I und  $\beta$ -Glycerophosphat zusammengesetzte Hydrogel war bei Raumtemperatur injizierbar, gelierte jedoch in weniger als 1 min bei 37°C. Die Integration von Fucoidan in das Hydrogel hatte keinen erheblichen Einfluss auf die physikochemischen Parameter. Zusätzlich zeigte die Kompatibilität des Biomaterials mit OEC und MSC sein Potential für die Anwendung in der regenerativen Medizin.

Zusammengefasst leistet die vorgelegte Dissertation einen Beitrag zur Aufklärung der Struktur-Funktion Beziehungen von Fucoidan im Kontext der Knochenregeneration. Basierend auf den Ergebnissen wird auf verschiedene Wirkungsmechanismen von Fucoidan hingedeutet. Durch den Vergleich verschiedener Extraktionsmethoden, die Beurteilung von enzymatischer Prozessierung nach der Extraktion und durch die Entwicklung eines Fucoidan Trägermaterials, stellt diese Dissertation wertvolle Ergebnisse zur Verfügung, die dabei helfen können die Anwendung von Fucoidanen in der Medizin zu realisieren.

---

## Publications

### First author publications

OHMES, Julia; XIAO, Yuejun; WANG, Fanlu; MIKKELSEN, Maria D.; NGUYEN, Thuan T.; SCHMIDT, Harald; SEEKAMP, Andreas; MEYER, Anne S.; FUCHS, Sabine: Effect of Enzymatically Extracted Fucoidans on Angiogenesis and Osteogenesis in Primary Cell Culture Systems Mimicking Bone Tissue Environment. In: *Mar Drugs* 18 (2020)

OHMES, Julia; MIKKELSEN, Maria D.; NGUYEN, Thuan T.; TRAN, Vy H. N.; MEIER, Sebastian; NIELSEN, Mads S.; DING, Ming; SEEKAMP, Andreas; MEYER, Anne S.; FUCHS, Sabine: Depolymerization of Fucoidan with Endo-Fucoidanase Changes Bioactivity in Processes Relevant for Bone Regeneration. In: *Carbohydrate Polymers* 286 (2022)

OHMES, Julia; SAURE, Lena M.; SCHÜTT, Fabian; TRENKEL, Marie; SEEKAMP, Andreas; SCHERLIEß, Regina; ADELUNG, Rainer; FUCHS, Sabine: Injectable Thermosensitive Chitosan-Collagen Hydrogel as a Delivery System for Marine Polysaccharide Fucoidan. In: *Mar Drugs* 20 (2022)

### Co-author publications

WANG, Fanlu; XIAO, Yuejun; NEUPANE, Sandesh; PTAK, Signe H.; RÖMER, Ramona; XIONG, Junyu; OHMES, Julia; SEEKAMP, Andreas; FRETTE, Xavier; ALBAN, Susanne; FUCHS, Sabine: Influence of Fucoidan Extracts from Different Fucus Species on Adult Stem Cells and Molecular Mediators in In Vitro Models for Bone Formation and Vascularization. In: *Mar Drugs* 19 (2021)

NIELSEN, Mads S.; MIKKELSEN, Maria D.; PTAK, Signe H.; KILDALL, Eva H.; OHMES, Julia; NGUYEN, Thuan T.; TRAN, Vy H. N.; FRETTE, Xavier; FUCHS, Sabine; MEYER, Anne S.; SCHRÖDER, Henrik D.; DING, Ming: Efficacy of marine bioactive compound fucoidan for bone regeneration and implant fixation in sheep. *J Biomed Mater Res.* 110 (2022)

KIRSTEN, Nora; OHMES, Julia, MIKKELSEN, Maria D.; NGUYEN, Thuan T.; WANG, Fanlu; SEEKAMP, Andreas; MEYER, Anne S.; FUCHS, Sabine: Impact of purified Fucoidan Fractions on Endothelial Functionality, Activation and Inflammatory Response during Bacterial Infections. (in preparation)

### Conference contributions

2<sup>nd</sup> International Workshop on Advanced Materials for Healthcare Applications in Funchal, Madeira, Portugal 2019 (poster contribution)

---

FucoSan - from Science to Innovation Day in Kiel, Germany 2019 (poster contribution)

The ABC Conference: Algae Bioactive Compounds - From Research to Innovation, virtual conference 2020 (oral contribution)

6<sup>th</sup> Euro BioMat - European Symposium on Biomaterials and Related Areas, virtual symposium 2021 (poster contribution)

Advancing the interface: biomaterials & regenerative cells, virtual symposium 2021 (oral contribution)

### **Awards**

1st place poster award winner at the 6<sup>th</sup> Euro BioMat - European Symposium on Biomaterials and Related Areas, virtual symposium 2021

---

## Danksagung

Mein Dank gilt Prof. Dr. Sabine Fuchs und Prof. Dr. Andreas Seekamp, welche die Forschung für die vorliegende Doktorarbeit finanziell und durch tatkräftige Betreuung unterstützt und begleitet haben. Sabine war stets am aktuellen Stand meiner Arbeit interessiert und immer bereit sich mit mir zu treffen und die Fortschritte zu diskutieren - auch wenn es spontan sein musste. Deine Erfahrungen und Vorschlägen haben mir geholfen mich auf die richtigen Dinge zu fokussieren und immer nach dem roten Faden zu suchen. Ich bin sehr dankbar für den Freiraum, den du mir gegeben hast und für das Vertrauen, welches du mir entgegen gebracht hast, insbesondere beim Hydrogelprojekt. Mein Dank gilt auch Prof. Dr. Susanne Alban vom Pharmazeutischen Institut. Als Teil des FucoSan Projekts haben ihre Einschätzungen und ihre Expertise im Bereich der Fucoidane meine Arbeit stets bereichert.

A huge thanks goes to Fanlu, Anne-Rose and Junyu who introduced me to the lab and made the acclimatization so easy for me. Fanlu, thanks for always trying to answer my questions, finding protocols and chemicals for me.

Neben Anne-Rose hatte ich das Glück mit den Technikern Angelika und Lennard zusammenarbeiten zu dürfen. Ihre Hilfe und Labororganisation haben meine Arbeit enorm unterstützt.

Danke auch an die Masterandin Julie für die vielen Gespräche, geteiltes Teewasser und natürlich all die Weisheit!

Mein Dank gilt allen Medizin- und Zahnmedizinierenden, die ich in den letzten Jahren kennenlernen und im Labor begleiten durfte - und das waren einige. Eure Anwesenheit hat mir stets Freude bereitet. Ihr habt mich, besonders in einsamen Laborzeiten, aufgebaut, die Räume belebt und mich immer nach meinem Befinden gefragt. Danke an: Caro, Alex, Steffi, Felix, Leah, Julia, Veit und Malte. Ganz besonders danken möchte ich Nora. Durch die Nähe deines Projekts zu meinem haben wir unzählige fachliche Gespräche geführt und generell haben wir immer viel zusammen erlebt (Mittagspausen, Eselpatenschaften, Persönlichkeitstests...).

Thanks to the medical exchange student Yuejun and to Ngoc, our short-term HiWi, for the direct support of my experiments.

A big thanks goes to the whole FucoSan project team. Our regular meetings in Kiel and Denmark were always inspiring to me. I not only gained so much scientific knowledge, but had direct insight on how such a big project is managed and organized. A special thanks goes to the young researchers Kaya, Sandesh, Rafael, Signe, Jana, Daniel and Philipp with whom I always had a good and fun time!

Ich danke Sandesh aus der AG Alban für die Bereitstellung von Fucoidanextrakten und all die Erklärungen in Hinblick auf die chemische Charakterisierung.

A massive thanks goes to Maria who together with her students Thuan and Vy produced the enzymatically-extracted fucoidans. Maria was always extremely helpful and whenever I had questions about something she was immediately available to explain, answer and to discuss. I also thank Prof. Dr. Anne Meyer for her time to discuss results and publications.

---

I thank Anca Remes from AG Müller for her endless helpfulness and expertise with every confocal microscopy issue.

Ein großes Dankeschön geht an Lena Marie Saure aus der AG Adeling, die sich die Zeit genommen hat tolle Bilder von meinen Proben am SEM zu machen.

Mein Dank gilt auch Prof. Dr. Stanislav Gorb, der mir sein SEM zur Verfügung gestellt hat. Danke an Dr. Alexander Kovalev, der mir die Funktionen des SEM ganz genau erklärt hat und immer zur Stelle war, falls ich eine Frage hatte.

Danke an Marie Trenkel aus der AG Scherließ, die sich die Zeit genommen hat mich bei den rheologischen Messungen zu unterstützen.

Vielen Dank an Prof. Dr. Andreas Tholey für die beratenden Treffen ganz am Anfang des Hydrogelprojekts und die Bereitstellung von Abzügen, pH-Metern und der Gefriertrocknung. Ein besonderer Dank geht auch an Jan, der mir so oft die Gefriertrocknung ein- und ausgeschaltet hat und während der Trocknung immer ein Auge auf meine Proben hatte.

Danke an Dr. Sebastian Meier für seine NMR Expertise und die Hilfe bei der Aufklärung von chemischen Fucoidanstrukturen.

Danke auch an Dr. Harald Schmidt für die Hilfe bei der Quantifizierung von angiogenen Strukturen.

Danke an die AG Sebens für die Bereitstellung einiger Geräte, sowie für die vielen gemeinsamen Mittagsessen und Frühsporthinweise im botanischen Garten oder an der Förde. Ein großer Dank geht an meine Mindener Gang, die Heidelbuddies und neu gewonnene Kieler Freunde: Eure Unterstützung war mir immer sicher. Die Naturwissenschaftler unter euch konnten meine Erfolge und Sorgen bestens nachvollziehen und entsprechend mit mir feiern oder mir Hinweise geben und Mut zusprechen. Aber auch die Nicht-Biologen unter euch waren immer interessiert am Inhalt und Stand meiner Arbeit und haben sich mit mir gefreut oder mich in schwierigen Phasen mental unterstützt.

Mein Dank gilt insbesondere auch meinen Eltern und Geschwistern, die immer mitgefiebert haben. Ihr wusstet immer vom aktuellen Stand, mit welchen Schwierigkeiten ich zu kämpfen hatte und welche Erfolge ich verbuchen konnte. Danke, dass ihr immer für mich da seid. Ein Dank geht auch an Horst, der irgendwie auch mitverantwortlich dafür war, dass ich mich zur Promotion entschieden habe.

Finalmente, quiero agradecer a mi novio y mejor amigo. Viste mis lagrimas de alegría, pero también de desesperación y frustración. Siempre me animaste y me apoyaste en todo.





# Contents

---

Eigenständigkeitserklärung . . . . .	i
Abstract . . . . .	iii
Zusammenfassung . . . . .	v
Publications . . . . .	vii
Danksagung . . . . .	ix
<b>1 Introduction</b>	<b>1</b>
1.1 Bone Regeneration . . . . .	2
1.1.1 Inflammation . . . . .	3
1.1.2 Angiogenesis . . . . .	5
1.1.3 Osteogenesis . . . . .	7
1.2 Cell Model Systems . . . . .	9
1.2.1 Mesenchymal stem cells . . . . .	9
1.2.2 Outgrowth endothelial cells . . . . .	9
1.2.3 Co-culture of MSC and OEC . . . . .	10
1.3 Fucoidan . . . . .	10
1.3.1 Chemical structure . . . . .	11
1.3.2 Extraction techniques . . . . .	11
1.3.3 Bioactivities . . . . .	13
1.3.4 Challenges for medical applications . . . . .	14
1.4 Biomaterials for Bone Regeneration . . . . .	14
1.4.1 Hydrogels . . . . .	15
1.4.2 Thermosensitive chitosan-collagen hydrogel . . . . .	16
1.5 Aims of the Presented Thesis . . . . .	16
<b>2 Material &amp; Methods</b>	<b>19</b>
2.1 Ethical Approval . . . . .	20
2.2 Fucoidan Extraction . . . . .	20
2.2.1 Algal material . . . . .	20
2.2.2 Enzyme-assisted fucoidan extraction . . . . .	20
2.2.3 Fucoidan hydrolysis by fucoidanase Fhf1 . . . . .	20
2.2.4 Chemical fucoidan extraction . . . . .	21
2.2.5 Fucoidan fractionation by H <sub>2</sub> O <sub>2</sub> . . . . .	21
2.2.6 Endotoxin quantification in fucoidan extracts . . . . .	22

2.3	Chemical Characterization of Fucoidan Extracts . . . . .	22
2.3.1	Monosaccharide content . . . . .	22
2.3.2	Sulfate content . . . . .	23
2.3.3	Polyphenol and protein content . . . . .	23
2.3.4	Molecular weight . . . . .	23
2.3.5	$^1\text{H}$ - $^{13}\text{C}$ NMR . . . . .	23
2.4	Human Cell Models & Fucoidan Treatment . . . . .	24
2.4.1	OEC isolation and culture conditions . . . . .	24
2.4.2	MSC isolation and culture conditions . . . . .	25
2.4.3	MSC-OEC co-culture conditions . . . . .	25
2.4.4	Fucoidan treatment . . . . .	25
2.5	Biological Assays . . . . .	27
2.5.1	MTS and LDH assay . . . . .	27
2.5.2	DNA quantification . . . . .	27
2.5.3	Quantitative real-time PCR . . . . .	27
2.5.4	ELISA . . . . .	28
2.5.5	ALP activity . . . . .	29
2.5.6	Alizarin red staining . . . . .	29
2.5.7	Immunocytochemistry . . . . .	30
2.6	Image Analysis . . . . .	32
2.6.1	Quantification of angiogenic tube-like structures . . . . .	32
2.6.2	Quantification of the integrity of the endothelial cell layer . . . . .	33
2.6.3	Quantification of fucoidan staining . . . . .	33
2.7	Chitosan-Collagen Hydrogel as a Delivery System for Fucoidan . . . . .	33
2.7.1	Hydrogel preparation . . . . .	33
2.7.2	Gelation time by the tube-inverting method . . . . .	34
2.7.3	pH . . . . .	34
2.7.4	Turbidity . . . . .	34
2.7.5	Absorption kinetics . . . . .	34
2.7.6	Equilibrium swelling ratio . . . . .	34
2.7.7	Rheological measurements . . . . .	35
2.7.8	Scanning electron microscopy . . . . .	35
2.7.9	Fucoidan detection with SYBR Gold . . . . .	37
2.7.10	Cell cultivation in and on the hydrogel . . . . .	38
2.7.11	Life/Dead staining of 2D- and 3D-cultured MSC and OEC . . . . .	39
2.7.12	DNA quantification of 3D-cultured MSC . . . . .	39
2.7.13	VEGF protein level in supernatant of 3D-cultured MSC . . . . .	39
2.8	Statistics . . . . .	39
2.9	Materials . . . . .	40

---

<b>3</b>	<b>Results I: Bioactivity of Enzymatically-Extracted Fucoidans</b>	<b>43</b>
3.1	Chemical Characterization of Enzymatically-Extracted Fucoidans . . . . .	44
3.2	Tolerance of OEC and MSC Towards Enzymatically-Extracted Fucoidans	45
3.3	Angiogenesis, Osteogenesis and Inflammation in Mono-cultures . . . . .	47
3.3.1	Angiogenic signaling molecules VEGF, ANG-1 and SDF-1 in MSC	47
3.3.2	Early and late osteogenic markers in MSC . . . . .	47
3.3.3	Influence of fucoidan concentration on angiogenic and osteogenic mediators . . . . .	47
3.3.4	Affinity of fucoidan to VEGF & impact on VEGFR2 phosphorylation	50
3.3.5	Inflammatory and angiogenic signaling molecules in OEC . . . . .	51
3.4	Angiogenesis in MSC-OEC Co-cultures . . . . .	53
3.4.1	Development of angiogenic structures . . . . .	53
3.4.2	Angiogenic signaling molecules in MSC-OEC co-cultures . . . . .	53
<b>4</b>	<b>Results II: Bioactivity of Enzymatically-Degraded Fucoidans</b>	<b>57</b>
4.1	Chemical Characterization of MMW and LMW . . . . .	58
4.1.1	Monosaccharide composition, molecular weight, sulfate, polyphenolic and protein content . . . . .	58
4.1.2	Chemical structures of MMW and LMW . . . . .	58
4.2	Tolerance of OEC Towards MMW and LMW . . . . .	60
4.3	Angiogenesis and Inflammation in Mono-cultures . . . . .	61
4.3.1	Angiogenic signaling molecules VEGF, ANG-1 and SDF-1 in MSC	61
4.3.2	VEGFR2 phosphorylation in OEC . . . . .	62
4.3.3	Inflammatory and angiogenic signaling molecules in OEC . . . . .	63
4.4	Angiogenesis and Inflammation in MSC-OEC Co-cultures . . . . .	65
4.4.1	Integrity of the endothelial cell barrier . . . . .	65
4.4.2	Development of angiogenic structures . . . . .	66
4.4.3	Angiogenic signaling molecules in MSC-OEC co-cultures . . . . .	68
4.5	Interaction of Fucoidan Extracts with MSC and OEC . . . . .	68
<b>5</b>	<b>Results III: Bioactivity of Chemically Extracted Fucoidans</b>	<b>73</b>
5.1	Chemical Characterization of Chemically Extracted and Degraded Fucoidans . . . . .	74
5.2	Angiogenesis in MSC-OEC Co-cultures . . . . .	74
5.2.1	Development of angiogenic structures . . . . .	75
5.2.2	Angiogenic signaling molecules in MSC-OEC co-cultures . . . . .	75
5.3	Interaction of Chemically Extracted Fucoidans with MSC and OEC . . . . .	79
<b>6</b>	<b>Results IV: Development of a Fucoidan Delivery System</b>	<b>83</b>
6.1	Protocol Development for Thermosensitive Hydrogels . . . . .	84
6.1.1	Glycerophosphate and incorporation of fucoidan . . . . .	84
6.1.2	$\beta$ -GP concentration . . . . .	84
6.1.3	Collagen type I integration . . . . .	87
6.2	Physicochemical Properties . . . . .	88

6.2.1	Gelation time, temperature, pH, swelling and turbidity . . . . .	88
6.2.2	Internal microstructure visualized by SEM . . . . .	92
6.2.3	Fucoidan detection and release . . . . .	93
6.3	Biological Performance . . . . .	95
6.3.1	MSC . . . . .	95
6.3.2	OEC . . . . .	98
<b>7</b>	<b>Discussion</b>	<b>99</b>
7.1	Bioactivity of Enzymatically-Extracted Fucoidans on Angiogenesis and Osteogenesis . . . . .	100
7.2	Effect of Enzymatic Hydrolysis on the Bioactivity of the Resulting Fucoidans	103
7.3	Preliminary Effect of Chemically Extracted and Degraded Fucoidans . . .	107
7.4	Injectable Chitosan-Collagen Hydrogel as a Delivery System for Fucoidan	109
7.5	Conclusions & Future Perspectives . . . . .	112
	<b>Bibliography</b>	<b>132</b>
	<b>Acronyms</b>	<b>133</b>
	<b>List of Figures</b>	<b>137</b>
	<b>List of Tables</b>	<b>139</b>
<b>A</b>	<b>Appendix</b>	<b>141</b>
A.1	OEC and MSC Donor Information . . . . .	142
A.2	NMR Spectroscopy . . . . .	143
A.3	Certificate of Analysis Chitosan 95/100 . . . . .	144





# 1

## Introduction

---

*The first chapter gives an introduction into bone regeneration on a molecular level and how angiogenesis, inflammation and osteogenesis are involved in the repair mechanisms. Fucoidans, polysaccharides from brown algae, are introduced and their relevance in the medical context is described. Further, the use of biomaterials, especially hydrogels, in regenerative medicine is pointed out.*

### Contents

---

<b>1.1</b>	<b>Bone Regeneration</b>	<b>2</b>
<b>1.2</b>	<b>Cell Model Systems</b>	<b>9</b>
<b>1.3</b>	<b>Fucoidan</b>	<b>10</b>
<b>1.4</b>	<b>Biomaterials for Bone Regeneration</b>	<b>14</b>
<b>1.5</b>	<b>Aims of the Presented Thesis</b>	<b>16</b>

---

## 1.1 Bone Regeneration

Bones have multiple important functions in the human body. They provide structural stability, allow movement by providing levers for muscles, protect inner organs, are reservoirs for growth factors and represent the site where hematopoiesis takes place [32, 19]. Depending on their shape, bones can be categorized into long (e.g. clavicles and femurs), short (e.g. carpal and tarsal bones), flat (e.g. the skull and ribs), and irregular bones (e.g. vertebrae and hyoid bone) [20]. Long bones as depicted in Figure 1.1 are separated into the diaphysis representing the long hollow shaft in the middle, the cone-shaped metaphyses and the round epiphyses at both ends. While metaphyses and epiphyses are composed of spongy soft trabecular bone, the diaphysis mainly consists of dense cortical bone [32]. Trabecular and cortical bone consist of the same matrix components, but significantly differ in porosity, three-dimensional structure and metabolic activity. Cortical bone makes up 80 % of the adult skeleton. It has only a porosity of 5-10 %, thereby providing resistance and mechanical strength. 20 % of the adult skeleton are composed of trabecular bone which is characterized by a porosity of 50-90 % [47, 32, 20]. To cope with external and internal stimuli, bone tissue is constantly remodeled, at which the metabolic activity in the trabecular bone is higher than in the cortical bone. During the remodeling processes old bone is resorbed by osteoclasts and new bone is formed by osteoblasts [67, 19].

Healing of bone tissue after a fracture can be categorized into three partly overlapping steps: inflammation, repair and remodeling. The inflammatory phase occurs directly after bone fracture and is crucial for the activation of regenerative processes and the healing success [119]. A complex network of blood vessels runs through the bone tissue. Upon bone fracture, blood vessels get ruptured. For successful bone regeneration, it is indispensable to restore these vessels in order to ensure the supply of the tissue with nutrients, minerals and oxygen. Only if inflammatory and angiogenic processes are activated, bone formation (osteogenesis) can proceed [65, 119]. Osteogenesis is regulated by two molecular mechanisms called intramembranous and endochondral ossification. During the intramembranous ossification hard callus is formed directly, while during the endochondral ossification soft callus is formed first which is then replaced by hard callus afterwards [57]. Both processes occur during embryonic development, but also proceed in a very similar way during fracture healing. During a long bone fracture, endochondral ossification occurs at the central callus, while intramembranous ossification takes place at the periosteum [95]. In the final step, the bone tissue is remodeled until complete regeneration is accomplished.

In contrast to other tissues, bone has great self-healing capacities. However, critical-sized fractures, diseases such as diabetes and arthritis, or anti-inflammatory and anti-coagulant drugs bare the risk to impede complete bone regeneration [71]. In these cases, bone tissue engineering together with the application of bioactive compounds can help to support healing processes [9]. Fucoidans are bioactive sulfated polysaccharides which naturally occur in brown algae and other marine invertebrates. Many studies have shown that fucoidan exhibits effects on a multitude of physiological processes in-

cluding angiogenesis, osteogenesis and inflammation all of which are important during bone regeneration [136, 91, 122]. However, some challenges need to be tackled in order to benefit from fucoidan's bioactivities in the medical context. Structure-function relationships, standardized extraction procedures and the development of a formulation for fucoidan are only some focal points.

As stated above the repair of bone tissue and its maintenance in a healthy state is matter of different molecular processes which need to occur in perfect balance and involve multiple cell types communicating and interacting with each other [163, 119]. The following sections will highlight the contribution of inflammation, angiogenesis and osteogenesis to bone regeneration in more detail.

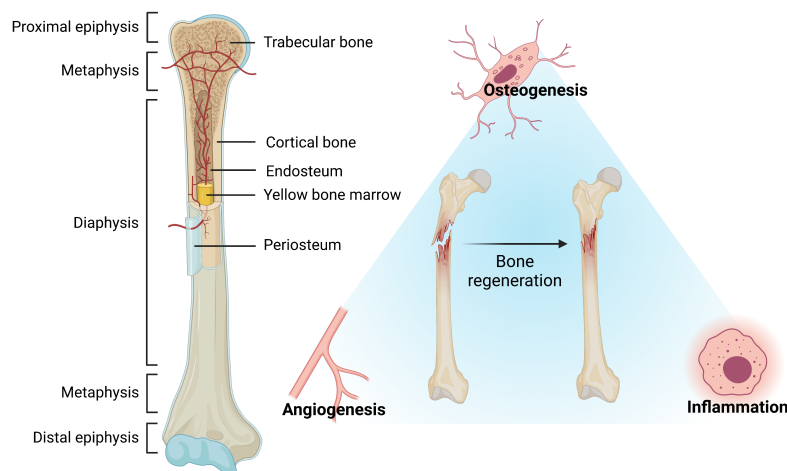


**Figure 1.1:** Long bone anatomy and regeneration. Bone healing is a complex process which relies on a well orchestrated interplay of inflammatory responses, angiogenic processes and bone tissue formation.

### 1.1.1 Inflammation

Immediately after bone fracture, an acute inflammation occurs. An inflammatory response is necessary to initiate bone repair and therefore represents the first important process contributing to bone regeneration and health next to angiogenesis and osteogenesis [119]. Underlying molecular processes are depicted in Figure 1.2.

Inflammation is defined as the response to a harmful stimulus and the initiation of tissue regeneration. In the absence of a noxious stimulus, endothelial cells (EC) rest. The expression of leukocyte-interactive proteins (P-selectin and other chemokines) and adhesion molecules (E-selectin, intercellular adhesion molecule-1 (ICAM-1), vascular cell adhesion molecule-1 (VCAM-1)) is suppressed. Similar to the quiescent angiogenic state, EC are characterized by tight cell-cell contacts via adherens junctions [141]. The inflammatory response, respectively the activation of EC, can be triggered by damage-associated

molecular patterns (DAMPs) such as apoptotic cells or pathogen-associated molecular patterns (PAMPs) such as endotoxins [195]. Phase I activation of EC occurs directly after the stimulus and lasts approximately 10-20 min. If a ligand binds to a G-protein coupled receptor (GPCR) on the EC surface, cytosolic calcium levels increase via the activation of phospholipase C (PLC) [15]. This leads to the release of nitric oxide (NO) and prostaglandin I<sub>2</sub> (PGI<sub>2</sub>). NO together with PGI<sub>2</sub> acts as a vasodilator [171]. The increased blood flow results in the well-known inflammatory properties heat and redness. GPCR also activates downstream signaling Rho which leads to the phosphorylation of myosin light chain (MLC). Phosphorylated MLC in turn contracts actin filaments resulting in the dissociation of tight and adherens junctions [165]. Plasma protein-rich fluid leaks into the tissue through the loose endothelial cell layer causing a swelling of the injured site. Additionally, active MLC initiates the exocytosis of P-selectin from Weibel-Palade bodies to the EC surface [15]. P-selectin serves as an anchor point for neutrophils, which are the first immune cells arriving to an injured tissue. They clear the tissue from harmful substances and release chemokines to support the migration of monocytes. Monocytes recruit other immune cells and differentiate into macrophages promoting tissue repair [119].

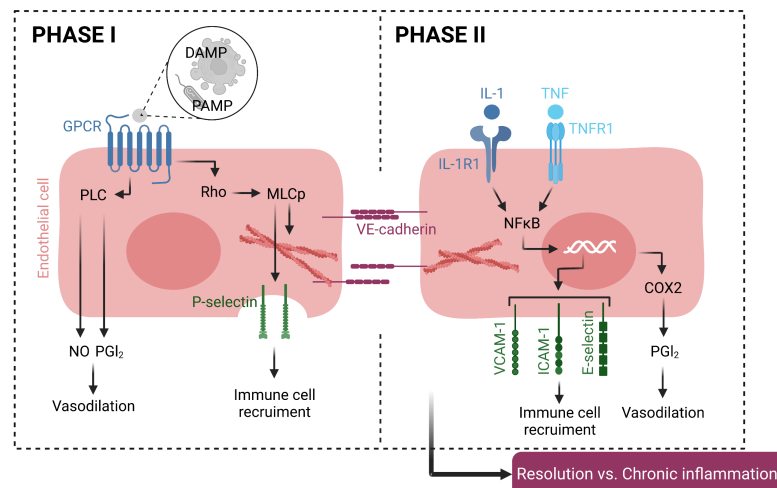


**Figure 1.2:** Phase I and phase II inflammation in endothelial cells. The acute immune response after bone fracture can be separated into the very first reaction occurring 10-20 min after the stimulus (phase I) and into the more sustained phase II response. If the inflammation is not resolved, a chronic inflammatory state develops.

GPCR signaling only lasts for 10-20 min [56]. In order to get a more sustained inflammatory response, EC activation type II takes place. Activated leukocytes, for example M1 macrophages, release inflammatory cytokines such as interleukin-1 (IL-1) and tumor-necrosis factor (TNF) which bind to the respective receptors on the EC surface. The subsequent formation of intracellular protein complexes triggers the activation of tran-

scription factor nuclear factor  $\kappa$ B (NF $\kappa$ B). Pro-inflammatory proteins such as E-selectin, ICAM-1 and VCAM-1 are expressed and positioned on the EC surface. NF $\kappa$ B also regulates the production of cyclooxygenase 2 (COX2) which initiates the release of PGI<sub>2</sub>. Comparable to type I activation, type II activation leads to an increased blood flow, a loose endothelial layer and leukocyte recruitment [141]. It becomes evident that the effect on EC is similar after a pro-angiogenic (as described in the next section) and a pro-inflammatory stimulus. Even though the mechanisms and the purpose are different, both processes are interwoven.

While EC type I activation resolves automatically due to GPCR desensibilization, the duration of type II activation is dependent on the presence of pro-inflammatory cytokines and can therefore persist for a long period of time. If the inflammatory stimulus cannot be resolved, the inflammatory response shifts to a chronic form. Causes for a chronic inflammation can be microbial infections, surgical intervention or injury. During a chronic infection, TNF- $\alpha$  and NF $\kappa$ B signaling are constantly upregulated resulting in the continuous presence of monocytes, macrophages and lymphocytes in the affected tissue. Macrophages differentiate rather into the pro-inflammatory M1 type than into the tissue repair M2 type. The upregulation of the mentioned pathways also results in the differentiation and activation of osteoclasts [86, 114]. Taken together, the perfect balance of inflammatory homeostasis is crucial for a successful bone repair. An initial stage of acute inflammation is necessary to trigger the repair process. If inflammation however cannot be resolved and evolves into a chronic state, bone repair is impaired and can result in a non-union.

### 1.1.2 Angiogenesis

Angiogenesis describes the formation of new blood vessels from already existing ones. Blood vessels deliver nutrients, minerals and oxygen to the tissue, but they also serve as niches and guiding structures for bone and blood progenitor cells [64]. Therefore, functioning angiogenesis is indispensable for successful bone regeneration. The molecular processes guiding angiogenesis are depicted in Figure 1.3.

During a bone defect, blood vessels rupture which results in the formation of a hematoma. The acidic and hypoxic hematoma environment activates hypoxia inducible factor (HIF). This transcription factor is the main regulator of cell responses during hypoxia. The binding of HIF to a specific hypoxia responsive element in the promoter region triggers the expression of genes involved in anaerobic metabolism and angiogenesis [155].

The most important angiogenic mediator which is produced upon HIF signaling is vascular endothelial growth factor A. Next to VEGF A, the VEGF family consists of four other members: VEGF B, C, D and placenta growth factor, all of which play a crucial role during angiogenesis in different tissues [72]. However, VEGF A, in the following referred to as VEGF, is the best-described member and the most relevant one for the presented dissertation. VEGF is mostly secreted by cells which contribute to skeleton development and repair such as smooth muscle cells, osteoblasts and chondrocytes. But it can also be produced by macrophages for example. The release of VEGF stimulates EC in a paracrine manner to initiate angiogenesis via VEGF receptor 2 (VEGFR2) [166].

VEGF is also able to bind to VEGF receptor 1. However, the exact function of this receptor is still unknown [49].

Angiogenesis is initiated by a step called sprouting. The basement membrane extracellular matrix (ECM) which surrounds stable resting blood vessels is degraded by matrix metalloproteinases (MMP) which are secreted during pro-angiogenic stimuli. The degradation of the matrix results in the release of additional angiogenic mediators and clears space for the new vessels [148]. VEGF isoforms have different affinities to heparan sulfate proteoglycans. The ratio between freely diffusible and proteoglycan-bound VEGF forms a gradient resulting in the formation of a tip cell which is activated and responds to angiogenic cues. [62]

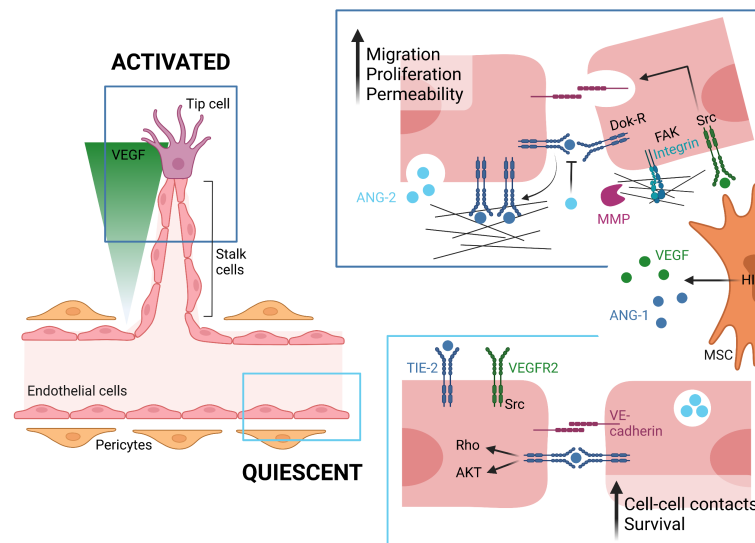


**Figure 1.3:** Molecular processes during angiogenesis. Quiescent cells are characterized by strong cell-cell contacts and a high survival. Via paracrine pro-angiogenic signaling, endothelial cells initiate the formation of new blood vessels. Activated cells are motile, highly proliferative and the cell layer is permeable.

Next to VEGF-VEGFR2 signaling, the angiopoietin (ANG)-TIE2 system is responsible for the transition of EC from a quiescent into an activated state. The quiescent state of EC is characterized by tight cell-cell contacts, low migration and low permeability [10]. ANG-1, mainly secreted by mesenchymal stem cells (MSC) or pericytes binds to the TIE2 receptor which is located at inter-EC junctions forming complexes with other ANG-1-TIE2 complexes from adjacent EC [150, 55]. Together with VE-cadherin-mediated adherens junctions stable cell-cell contacts are formed. Resting EC are also characterized by a high survival triggered by the PI3K (phosphoinositide 3-kinase)/AKT pathway [135].

On an external signal (high VEGF levels for example), the transition from a quiescent

into an activated state is performed. ANG-2 is released from EC where it is stored in Weibel-Palade bodies until secretion [50]. ANG-2 binds to the ANG-1-TIE2 complexes and functions as an antagonist for ANG-1 [118]. This results in the translocation of TIE2 receptors to the cell site facing the ECM [150, 55]. In conjunction with integrins, Dok-R and FAK (focal adhesion kinase) pathways are activated which promote migration of EC [120].

Translocation of TIE2 towards the ECM, together with the internalization of VE-cadherin (via src and Rho signaling) results in loose cell-cell contacts and an increased permeability of the endothelial cell layer [59].

Leading tip cells develop filopodia to sense the environment and start to migrate into the tissue stroma. The so-called stalk cells follow the tip cells and start to build the new blood vessel. Stalk cells have the ability to proliferate fast and to stabilize prevascular structures. The encounter of two tip cells results in the fusion of the newly established blood vessels and a lumen is formed [79]. To attract EC and endothelial progenitor cells (EPC) for the expansion of blood vessels, MSC secrete the chemokine stromal-derived factor 1 (SDF-1). SDF-1 binds to the CXCR4 receptor which is mainly expressed on the surface of EC and EPC [184].

It becomes evident that angiogenesis is a complex molecular process which involves many more signaling molecules than the ones explained in this section. However, the function of the most important ones which are also matter of this thesis were stated and put into context.

### 1.1.3 Osteogenesis

Osteogenesis is the general term to describe the formation of bone tissue. As mentioned earlier, regeneration of a bone defect can be categorized into the inflammatory, repair and remodeling phase [119]. The repair phase is characterized by the formation of callus which can proceed through two different mechanisms depending on the bone anatomy. The intramembranous ossification occurs mainly at the periosteum, while the endochondral ossification occurs at the endosteum and in the bone marrow (for long bone anatomy see Figure 1.1) [90]. Intramembranous and endochondral ossification including the involved cell types are illustrated in Figure 1.4.

During the intramembranous ossification, hard callus is formed directly. MSC differentiate into preosteoblasts which then differentiate into osteoblasts. The differentiation from MSC to osteoblasts is triggered by the activation of the transcription factor Runx2 [149]. The osteoblast maturation occurs in three steps of which each is characterized by different molecular markers [164]. First, osteoblasts produce the so-called osteoid which mainly contains collagen type I, but also other proteins such as fibronectin and osteopontin. Upon maturation, osteoblasts start to secrete alkaline phosphatase (ALP). Via dephosphorylation, ALP provides phosphate moieties which are necessary building elements for the osteoid mineralization. In the last maturation step, osteoblasts calcify the new bone matrix. Therefore, they secrete osteocalcin which helps to deposit hydroxyapatite, a combination of calcium and phosphate molecules. Inside the mineralized osteoid, an ossification center is formed which allows osteoblasts to finally differentiate

into osteocytes.

In contrast to the intramembranous ossification, during the endochondral ossification, soft callus is formed first, followed by the development of hard callus. MSC differentiate into chondrocytes which is controlled by the transcription factor Sox9 [2]. Chondrocytes secrete a cartilage matrix that mainly consists of collagen type I and proteoglycans. Following hypertrophic differentiation, chondrocytes differentiate first into preosteoblasts and finally into osteoblasts [149].

In the remodeling phase, the final shape and mechanics of the bone are achieved by establishing a balance between bone deposition by osteoblasts and bone resorption by osteoclasts [119].

Next to the master transcription factors Runx2 or Sox9, there are also paracrine mechanisms that are involved in MSC differentiation. Bone morphogenic proteins (BMP) for example are a group of cytokines which can activate Runx2 expression via SMAD signaling and therefore influence osteoblast differentiation [143]. The release of osteogenic factors like BMP-2 and BMP-4 from EC is controlled by VEGF, amongst others. Even though, VEGF is known as a regulator for angiogenesis, some non-endothelial cells such as preosteoblasts or pericytes are able to express VEGF receptors. Hence, next to its paracrine regulation of EC, it can also act on osteoblast differentiation directly via auto- and intracrine mechanisms [163]. It becomes clear that osteogenesis is directly interwoven with angiogenic activities and that repair of bone tissue relies on adequate vascularization and the cross-talk between EC and bone cells.

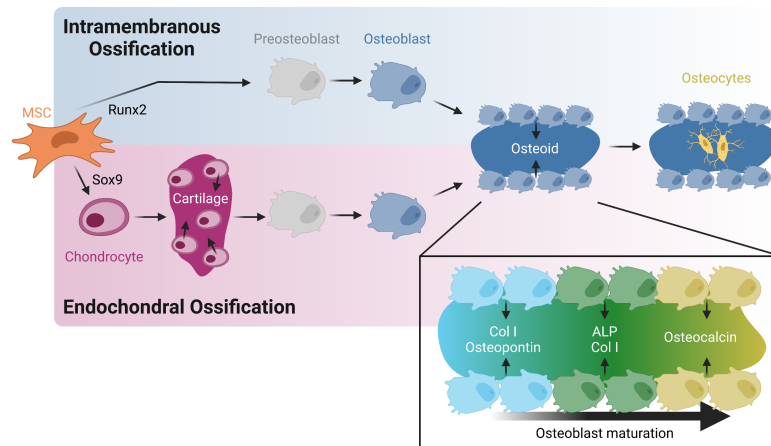


**Figure 1.4:** Bone regeneration via intramembranous and endochondral ossification. During intramembranous ossification, hard callus is formed directly by osteoblasts. During endochondral ossification, soft callus is formed first by chondrocytes, followed by the formation of hard callus.

## 1.2 Cell Model Systems

To mimic molecular processes occurring during regeneration and maintenance of bone health in the tissue, osteoblast-like MSC and outgrowth endothelial cells (OEC) were used as model systems for the current thesis. The next section describes both cell types and their properties in further detail.

### 1.2.1 Mesenchymal stem cells

MSC are multipotent cells which means they can differentiate into various more specified lineages including fat, muscle, cartilage and bone tissue [149].

Currently, MSC cannot be distinguished from other cell types by the definition of specific surface markers. However, certain criteria exist which should be fulfilled by cells to define them as MSC in vitro: a) MSC should remain adherent to plastic under standard culture conditions; b) MSC should express CD105, CD73 and CD90 and should not express hematopoietic markers CD45, CD34, CD14 or CD11b, CD79a or CD19 and HLA-DR (Other molecules which are usually expressed by MSC are CD13, CD29, CD44 and CD10); c) MSC should be able to differentiate into osteoblasts, adipocytes and chondrocytes in vitro [44, 12, 85]. The most popular source for MSC is the bone marrow, however other sources like adipose tissue [46], placenta [54] or peripheral blood [173] can also be considered for MSC isolation. It must be pointed out that an isolated MSC population is very heterogeneous containing cells with different lineage commitments, varying expression patterns of proteins and cytokines, as well as unequal differentiation potencies [117].

The differentiation of MSC in vitro towards the osteoblastic lineage is accomplished by treatment with a cocktail of dexamethasone, ascorbic acid and  $\beta$ -glycerophosphate ( $\beta$ -GP) [104]. Dexamethasone induces Runx2 expression (master transcription factor for osteoblast differentiation as described in section 1.1.3) by FHL2/ $\beta$ -catenin-mediated transcriptional activation [69]. It further enhances Runx2 activity by upregulation of TAZ and MKP1 [73, 140]. Ascorbic acid facilitates the secretion of collagen type I into the ECM. Xiao and colleagues suggest that differentiation is promoted when cells are in contact with collagen-containing ECM. Integrin binding to the secreted ECM activates mitogen-activated protein kinase (MAPK) signaling which triggers the activation of Runx2 [189].  $\beta$ -GP represents a source for the formation of hydroxyapatite. Additionally, inorganic phosphate enters the cell and acts as a signaling molecule to regulate the expression of osteogenic genes such as osteopontin and BMP-2 [48, 168].

The multipotency and paracrine signaling (as described in further detail in the prior sections) of MSC turns them into ideal candidates for regenerative medicine and respective research purposes.

### 1.2.2 Outgrowth endothelial cells

EC build up the blood vessels and are important regulators of inflammatory responses. The discovery of endothelial progenitor cells (EPC) led to the realization that blood

vessels could not only be formed as branch-offs from already existing vessels, but that de novo blood vessel formation was possible [169]. EPC are a heterogeneous cell population with a roundish spindle-shaped morphology. They secrete pro-angiogenic molecules and therefore support vascularization through paracrine mechanisms. So-called outgrowth endothelial cells are late EPC which differ in shape and function. Even though no clear definition of EPC and OEC exists in terms of morphology, function and surface markers, both cell types can be distinguished by these before-mentioned parameters. In contrast to EPC, OEC possess a cobblestone-like morphology, have a high proliferative potential and the ability to develop tube-like angiogenic structures in vitro [51]. EPC express CD31, CD45, CD34, CD14 and CD133, while OEC lack the expression of CD45, CD14 and CD133. In contrast to EPC, OEC express CD164 [169, 60, 144, 172, 39]. In terms of surface marker expression and key functions, OEC highly resemble EC. Both, EPC and OEC can be isolated by gradient centrifugation from peripheral blood [96]. While EPC make up the majority of the mononuclear cells, the density of OEC is very small. After isolation, OEC appear after two to three weeks as adherent cobblestone-shaped colonies. The strong resemblance of OEC with EC and their ability to form angiogenic tube-like structures in vitro makes them ideal model systems to investigate angiogenic processes.

### 1.2.3 Co-culture of MSC and OEC

As described before, mechanisms in bone tissue are a result of orchestrated molecular processes involving different types of cells. The co-culture system of MSC and OEC allows to mimic the physiological environment of bone tissue in a different way than cultures of only one cell type. In the co-culture, MSC and OEC are able to interact with each other, giving the possibility to study paracrine mechanisms involved in the differentiation of bone cells or the establishment of blood vessels [97]. As stated before, MSC secrete pro-angiogenic mediators of which VEGF and angiopoietins are the most important ones in the context of the presented dissertation. These influence OEC and result in the development of tube-like prevascular structures. On the other hand, OEC secrete osteogenic mediators such as BMP-2 which have an effect on the differentiation of MSC. Even though the co-culture system resembles the physiological situation more than mono-cultures, it is still important to perform biological experiments also with only one cell type. The reduction in complexity with only one cell type allows to understand the molecular processes better which cause observed phenotypes in the co-culture system.

## 1.3 Fucoidan

More than 250 genera of brown algae are known today, encompassing 1,500-2,000 different species [159]. Brown algae represent the largest biomass producers in the coastal regions. The cell wall of algae of the order of Fucales is mainly composed of two different polysaccharide-based networks. Fucose-containing sulfated polysaccharides, including fucoidan, are bound to  $\beta$ -glucans which are embedded into an alginate matrix. Cross-

linking polyphenols and proteins are also part of the cell wall next to different ions such as calcium [40]. On a biological level, fucoidan is involved in osmotic adjustments of the alga as a response to different levels of salinity. Since the first discovery of fucoidan by Kylin in 1913, fucoidan isolation, characterization and biological activities have been extensively studied [100]. The following sections provide further details in regard to fucoidan structure, extraction methods and bioactivities. Finally, it is pointed out why the use of fucoidan in the medical context remains challenging.

### 1.3.1 Chemical structure

Fucoidans are generally described as sulfated polysaccharides with a backbone of  $\alpha$ -L-fucopyranose residues. However, there is no specific chemical formula which defines the fucoidan molecule. Fucoidans rather represent a heterogeneous mixture of polysaccharides which sometimes share common features such as the molecule backbone or the presence of substituted sulfates. Next to sulfate groups, the backbone can also be substituted with other chemical residues such as acetate or glycosyl side branches. Even though fucose usually makes up the biggest part of the fucoidan molecule, it can also contain smaller portions of other monosaccharides such as glucose, galactose, xylose or mannose. These monosaccharides can be part of the fucoidan molecule as covalently bound substitutes or represent a contamination due to co-extraction from the algal material. Especially alginate (mannuronic and guluronic acids) co-extractions are a common source of contamination [4].

The current thesis deals exclusively with fucoidans from two algae species from the order of Fucales: *Fucus evanescens* (FE) and *Fucus vesiculosus* (FV). The backbone of fucoidans from *F. evanescens* consists of alternating  $\alpha(1\rightarrow3)$ - and  $\alpha(1\rightarrow4)$ -linked L-fucopyranose residues. Sulfates are bound at C2 or C4 [14, 13]. Fucoidans from *F. vesiculosus* are characterized by repeating  $\alpha(1\rightarrow3)$ -linked L-fucopyranose units which are sulfated at C2. These  $\alpha(1\rightarrow3)$ -L-fucopyranose units can be linked to  $\alpha(1\rightarrow4)$ -L-fucopyranose which are disulfated at C2 and C3 [28]. Photos of the brown algae and their backbone structures are shown in Figure 1.5.

Next to the backbone structure, sulfate content and monosaccharide composition, the molecular weight is an important factor to characterize fucoidans. The size of the molecules can range from low molecular weight (LMW), over middle molecular weight (MMW) to high molecular weight (HMW). Up to date, no generally accepted definition exists which categorizes fucoidans into LMW, MMW and HMW molecules. Here, fucoidans  $< 10$  kDa,  $10$ - $100$  kDa and  $> 100$  kDa are defined as LMW, MMW and HMW, respectively.

### 1.3.2 Extraction techniques

As we know today, the way how fucoidans are isolated from the algal material has a great impact on the chemical properties of the obtained extract. Fucoidan extraction can be grouped into conventional techniques which mostly use acids or hot water and into advanced techniques such as microwave or enzyme-assisted extraction [42].

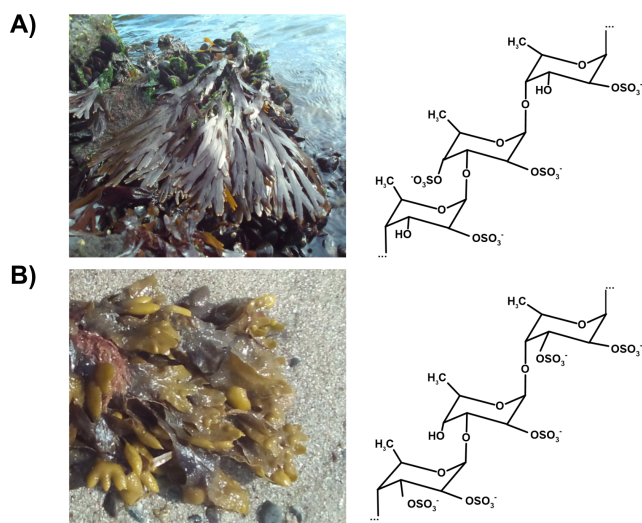


**Figure 1.5:** Photos and backbone structures of brown algae A) *Fucus evanescens* and B) *Fucus vesiculosus*. Photos were taken and kindly provided by Rafael Meichßner.

The majority of the conventional methods involve extractions in acid (for example HCl) at high temperatures. The yield can be increased if the acid hydrolysis treatment is repeated for several times [17]. The incubation of algal material in hot water (80-90°C) is also often used to extract fucoidan [5]. Pretreatments with ethanol or chloroform have shown to remove lipids from the sample [185]. An additional treatment with calcium helps to remove co-extracted alginate. Ethanol precipitation is used to remove ethanol-soluble contaminants such as salts. With the realization that harsh extraction conditions alter the chemical composition of fucoidan and often reduce the yield, more advanced techniques are developed [68].

Enzyme-assisted extractions have shown to proceed faster, consume less energy, need less solvents and obtain increased yields. This technique takes advantage of specific enzymes which degrade cell wall components of the algal material in order to release the fucoidan molecules [127]. These enzymatic cocktails can include for example alginate lyases (catalyze the degradation of alginate), cellulases (cleave glycosidic linkages in cellulose) or alcalases (protease which hydrolyzes peptide bonds) [130, 3].

Purification processes after fucoidan extraction can additionally help to remove co-extracted compounds. Chromatographies such as ion-exchange chromatography separate the complex fucoidan extract into more defined fractions facilitating the biological characterization and elucidation of structure-function relationships [42, 129].

The awareness that the chemical properties of fucoidan are determinant for its bioactivity have raised the need to create fucoidans with defined chemical characteristics. In past studies, oversulfated fucoidans were created or fucoidans lacking acetyl groups [74, 105]. Other post-extraction steps can be applied to create fucoidans with different molecular weights. The incubation of fucoidan in H<sub>2</sub>O<sub>2</sub> hydrolyzes fucoidan into smaller frag-

ments [101]. While hydrolysis using chemicals occurs mostly randomly, fucoidan-specific enzymes, so-called fucoidanases, offer the advantage of a defined cleavage. Different fucoidanases have been discovered in marine organisms, but only few of them are functionally characterized [99]. The fucoidanase Fhf1 was recently discovered in the marine bacterium *Formosa haliotis*. It was characterized in detail and found to cleave fucoidans at  $\alpha$ -(1,4) glycosidic linkages into fractions with a smaller molecular weight. [179].

It becomes evident that structure-function relationships of fucoidan can only be elucidated if chemical properties are known and at best can be reproduced in different extraction cycles. Reproducibility of extracts depends on the isolation technique, purification steps and on post-processing measures.

### 1.3.3 Bioactivities

Fucoidan exhibits a wide range of biological activities. Effects were proven on many physiological processes including angiogenesis, osteogenesis, inflammation, coagulation and cancer [136, 134, 91, 105]. In the following, only a few studies are mentioned which prove fucoidan's impact on molecular processes relevant for bone regeneration. Multiple studies have pointed out fucoidan's effect on angiogenesis, including pro- and anti-angiogenic activities. Commercially available crude fucoidan from *F. vesiculosus* impaired the formation of angiogenic tube-like structures in MSC-OEC and MG63-OEC co-cultures which was related to reduced protein levels of VEGF and SDF-1 [180]. The comparison of HMW fucoidans from three different algae species (*F. serratus*, *F. evanescens* and *F. vesiculosus*) showed that all extracts lowered levels of angiogenic mediators such as VEGF and angiopoietins in MSC and OEC cell cultures [181]. A fucoidan extract from *Sargassum fusifore* inhibited tube formation and migration of human microvascular endothelial cells in a dose-dependent manner [34]. On the other hand, fucoidan from *Laminaria japonica* in combination with fibroblast growth factor 2 had a supporting effect on tube formation and migration in human umbilical vein endothelial cells (HUVEC) [92]. Another study reported that 15-20 kDa fucoidans enhanced HUVEC migration and did not inhibit tube formation [123].

In regard to osteogenesis, fucoidan from *Laminaria japonica* was shown to induce osteoblast differentiation in human alveolar bone marrow-derived MSC via BMP-2-SMAD signaling [91]. Another study showed that osteogenesis-related genes such as ALP, osteopontin and collagen type I were increased in human adipose-derived stem cells after fucoidan treatment [137]. On the other hand, fucoidan from *Fucus evanescens* decreased the expression of ALP and the deposition of calcium in osteoblast-like MSC [133].

An increasing number of studies report anti-inflammatory properties of fucoidan extracts. Fucoidan from *Sargassum swartzii* decreased the NO production in lipopolysaccharide (LPS)-stimulated RAW 264.7 macrophages by suppression of TLR (toll-like receptor) and  $\text{NF}\kappa\text{B}$  signaling [80]. A similar study demonstrates that fucoidan from *Saccharina japonica* decreased the production of NO and cytokines such as  $\text{TNF-}\alpha$  and IL-6 in LPS-stimulated RAW 264.7 and zebrafish. The effect was also associated with a downregulation of the MAPK/ $\text{NF}\kappa\text{B}$  pathway [131]. Accordingly, in a study from our group it is shown that the expression and protein production of pro-inflammatory

cytokines such as IL-6 and adhesion molecules such as ICAM-1 were downregulated in LPS-stimulated OEC (manuscript in preparation).

By only mentioning this limited number of studies, it becomes evident that fucoidan exhibits many different effects on physiological molecular processes. However, the heterogeneity of fucoidans (different species and extraction techniques) and varying experimental set-ups used in these studies make results difficult to compare and to draw final conclusions. Even though some chemical key features such as sulfate content and molecular weight seem to play a major role in defining fucoidan's bioactivities, the exact structure-function relationship and mechanisms of action underlying the observed effects remain unclear.

### 1.3.4 Challenges for medical applications

Brown algae biomass for fucoidan isolation is abundantly available. Extraction techniques are widely investigated and under constant development. Numerous studies prove beneficial effects of fucoidan on the human body. Nevertheless, so far fucoidan is not used as a bioactive compound in the medical context.

Today it is understood that fucoidan's bioactivity relies on its chemical properties. These properties however are influenced by many different parameters such as algae species, season of harvest and extraction technique. Last, but not least, observed bioactivities depend strongly on the investigated model system and how fucoidan is applied. Due to its heterogeneity, the structure-function relationship of fucoidan is not fully elucidated and many underlying mechanisms of action remain unsolved.

To apply fucoidan in a medical context, it is indispensable (as for any other drug) to know how fucoidan treatment will affect the patient. Therefore, extraction techniques are needed which guarantee the isolation of reproducible fucoidan molecules with equal chemical properties from batch to batch. Post-extraction processing for example can help to reach this goal and create fucoidans with defined chemical characteristics.

Fucoidans are natural compounds which always bare a higher risk of insufficient purity or endotoxin contamination. The biological safety of fucoidans must be guaranteed in a standardized procedure to avoid cytotoxicity and other unwanted side effects.

To apply fucoidan in the context of bone regeneration and maintenance of bone health, the bioactivity of fucoidans must meet specific requirements. To support bone healing, fucoidan should promote angiogenesis and osteogenesis. On the other hand, the application of fucoidan should not cause a sustained inflammatory response in the affected tissue to avoid the development of a chronic inflammation. Finally, it is noteworthy that the formulation or delivery of fucoidan into the bone tissue is crucial to achieve desired therapeutic effects.

## 1.4 Biomaterials for Bone Regeneration

Usually bone tissue will regenerate completely after a fracture. However, 5-10 % of bone fractures fail to heal. These so called non-unions result in long-term disability and pain

in the patient. Severe or complex fractures bare the risk to develop into a non-union. But also diseases such as diabetes and arthritis or taking of certain drugs [71] can impede the healing process. The regenerative medicine is constantly developing and trying to find life-saving and live-improving solutions to help these patients. Conventional approaches include the implantation of xeno-, allo-, and autografts which all come with certain disadvantages. The implantation of xenografts and allografts always bares the risk of disease transmission or causing an immunological reaction in the patient. Autografts require an additional surgical intervention in the patient and the bone material is limited [11]. Tissue engineering represents an advanced approach to overcome these disadvantages. Here, stem cells are isolated from the patient and expanded in vitro. Cells are seeded onto a scaffold or encapsulated into a suitable biomaterial before they are transplanted back into the injured tissue. Additional encapsulation of bioactive compounds into the material can support bone regeneration processes, such as angiogenesis and osteoblast differentiation [9].

The investigation and development of suitable biomaterials for bone regeneration is constantly progressing. Bioceramics consisting of calcium phosphate, bioactive glass or metallic materials such as titanium are already widely used as bone substitutes. While bioceramics mimic the inorganic phase of bone tissue and thereby stimulate regenerative processes, metallic implants provide high mechanical support [63, 7]. However, these traditional biomaterials often possess low biological activity. New approaches try to develop materials with enhanced biological integrity and activity. For these purposes, synthetic polymers such as polylactic acid or polycaprolactone are investigated, as well as natural polymers such chitosan, collagen, gelatin, hyaluronic acid, alginate and fibroin [170]. An ideal biomaterial for bone regeneration should mimic the surrounding tissue to promote regenerative processes. Further, it should be mechanically stable, but also biocompatible and degradable. Hydrogels meet many of these requirements and are promising materials for regenerative medicine. In the following, hydrogels are introduced as an option to deliver bioactive compounds and stem cells into bone tissue to support healing processes.

### 1.4.1 Hydrogels

Hydrogels are three dimensional networks built of hydrophilic polymers. They have the ability to store high amounts of water which turns them into a soft, viscoelastic material. The structure of hydrogels resembles the ECM and allows exchange and diffusion of molecules, as well as adhesion and migration of cells. In regard to bone tissue engineering, they can serve as delivery systems for stem cells and/or bioactive compounds [21, 161]. Especially injectable hydrogels became a popular topic of research in the last years, because they offer certain advantages over conventional hydrogels. [111]. These hydrogels are liquid during application and only gelate upon a specific stimulus such as radiation, pH or temperature changes [108, 146, 76]. Hence, their application is minimally invasive because no surgical intervention is needed. Additionally, their shape can adjust exactly to the shape of the defect. The following subsection introduces a particular injectable hydrogel system which is relevant for the presented dissertation.

### 1.4.2 Thermosensitive chitosan-collagen hydrogel

Naturally occurring building elements for hydrogels often offer advantages over synthetic components. They are characterized by an increased biocompatibility, degradation and structural resemblance with physiological structures such as bone tissue [23].

Chitosan is a linear co-polymer of randomly arranged  $\beta$ -(1-4)-linked glucosamine and N-acetyl-D-glucosamine units from the exoskeleton of crustaceans. It is usually obtained by deacetylation of chitin, the second most abundant polysaccharide in nature after cellulose [145]. Due to its resemblance with glycosaminoglycans, the main component of bone ECM, it has become a promising candidate for biomaterials [111]. Its cationic charge allows interactions with anionic molecules, such as growth factors and receptors [157]. Further, it is biodegradable, biocompatible and shows antibacterial properties [121]. Together with anionic  $\beta$ -GP, chitosan forms an ionically-crosslinked hydrogel [27].  $\beta$ -GP can be found in the human body and is often used as an osteogenic supplement for the differentiation of MSC towards the osteoblast lineage (see section 1.2.1). Addition of  $\beta$ -GP to a chitosan solution results in the formation of a thermosensitive sol which is liquid and injectable at low temperatures, but forms a hydrogel upon temperature increase.

Chitosan alone is not a thermosensitive molecule. The mixture of GP into a chitosan solution modulates electrostatic and hydrophobic interactions, as well as hydrogen bonds. GP reduces electrostatic repulsion and favors the formation of hydrogen bonds between chitosan chains. Anionic phosphate groups of GP form electrostatic interactions with the cationic amino groups of the chitosan. At low temperatures, chitosan aggregation is prevented by its interaction with water molecules. However, on temperature increase, water molecules are removed by the glycerol moieties supporting chitosan aggregation via hydrophobic interactions and therefore hydrogel formation. At low temperature, chitosan is characterized by a coiled structure due to the presence of intramolecular hydrogen bonds. Temperature increase reduces the amount of hydrogen bonds, allowing chitosan to unfold and to promote gelation [29, 106].

Collagen type I is the main structural component of the ECM and plays a major role in defining the properties of the bone and its fracture susceptibility [178]. The addition of collagen type I to the chitosan- $\beta$ -GP system increases the biocompatibility, cell adhesion and gelation properties [41, 183, 151].

Multiple studies have already pointed out the potential of thermosensitive chitosan-collagen hydrogels for the use in regenerative medicine. The current thesis investigates its potential as a delivery system for fucoidan in the context of bone regeneration.

## 1.5 Aims of the Presented Thesis

This thesis compares the bioactivity of different fucoidan extracts in regard to bone regeneration in mono- and co-culture systems of human MSC and OEC. Cell distinct effects are studied using fucoidans with varying chemical properties. Subsequently, fucoidan extracts are selected for further investigation. To accumulate fucoidans inside the tissue of interest, a hydrogel-based delivery system for the potential use in regenerative

medicine is presented. To accomplish these tasks, the thesis is separated into four parts which deal with:

- I Investigating the effect of enzymatically-extracted fucoidans on angiogenesis, osteogenesis and inflammation and relating the chemical properties of the extracts with the observed bioactivities.
- II Evaluating the potential of defined enzymatic hydrolysis to tailor the bioactivity of fucoidans. Therefore, comparing the bioactivities of enzymatically degraded fucoidans of lower molecular weight with the effects of the native high molecular weight extract on angiogenic and inflammatory processes.
- III Studying the effect of chemically extracted and H<sub>2</sub>O<sub>2</sub>-degraded fucoidans on angiogenesis.
- IV Developing a hydrogel system to deliver fucoidan for the potential use in regenerative medicine. Characterizing the physicochemical properties and the biocompatibility of the hydrogel.

The comparison of different fucoidan extracts shall contribute to the further elucidation of structure-function relationships and reveal possible mechanisms of action. By comparing fucoidans extracted with different methods, by evaluating potential post extraction processing techniques and by developing a fucoidan delivery system, this thesis shall provide information which help to make the utilization of fucoidan in the medical context possible.



# 2

## Material & Methods

---

*The second chapter introduces all materials and methods used for the current thesis. It gives information about fucoïdan extraction, the human cell model systems and performed biological assays. It further explains the development of a chitosan-collagen hydrogel functioning as a delivery system for fucoïdan.*

### Contents

---

2.1	Ethical Approval . . . . .	20
2.2	Fucoïdan Extraction . . . . .	20
2.3	Chemical Characterization of Fucoïdan Extracts . . . . .	22
2.4	Human Cell Models & Fucoïdan Treatment . . . . .	24
2.5	Biological Assays . . . . .	27
2.6	Image Analysis . . . . .	32
2.7	Chitosan-Collagen Hydrogel as a Delivery System for Fucoïdan . . . . .	33
2.8	Statistics . . . . .	39
2.9	Materials . . . . .	40

---

## 2.1 Ethical Approval

The use of human material was approved by the local ethics committee of the University Medical Center Schleswig-Holstein. Isolation of primary cells from human tissue was performed with the consent of the donors.

## 2.2 Fucoidan Extraction

This section gives information about the origin of the algal material and introduces different fucoidan extraction techniques, as well as fucoidan fractionation using a fucoidanase and H<sub>2</sub>O<sub>2</sub>. The enzyme-assisted extraction and fucoidanase hydrolysis were performed by Thuan Thi Nguyen, Vy Ha Nguyen Tran and Dr. Maria Dalgaard Mikkelsen (Group of Prof. Dr. Anne S. Meyer, Department of Biotechnology and Biomedicine, Danish Technical University). The chemical extraction and H<sub>2</sub>O<sub>2</sub> fractionation were performed by Sandesh Neupane (Group of Prof. Dr. Susanne Alban, Department of Pharmaceutical Biology, Kiel University)

### 2.2.1 Algal material

Over two years old *Fucus distichus* subsp. *evanescens* was collected in March 2017 from 1 m water depth at the Kiel canal, Germany. The upper 2/3 part was harvested and kindly provided by Coastal Research & Management GmbH.

### 2.2.2 Enzyme-assisted fucoidan extraction

The enzyme-assisted extraction is explained in detail in [130]. In the following, only the main steps will be specified. Before extraction, algal material was washed, lyophilized and grounded into powder. To break down the cell wall components and release fucoidan, dried seaweed was treated with Cellic<sup>®</sup>Ctec2 cellulase and alginate lyase from *Sphingomonas* sp. High molecular weight alginate was removed by precipitating with CaCl<sub>2</sub>. Crude fucoidan (FE\_crude) was precipitated using ethanol and subsequently lyophilized. To obtain purified extracts, aqueous FE\_crude was fractionated into FE\_F1, FE\_F2 and FE\_F3 using ion-exchange chromatography (IEX). Finally, the fractions were filtered (10 kDa membrane) and lyophilized.

### 2.2.3 Fucoidan hydrolysis by fucoidanase Fhf1

After identifying fucoidan FE\_F3 as the purest and most bioactive fraction in angiogenesis- and osteogenesis-related studies [133], FE\_F3 was chosen for enzymatic hydrolysis. The expression and purification of recombinant endo- $\alpha$ -(1,4)-fucoidanase Fhf1 from *Formosa haliotis* (Fhf1 $\Delta$ 470) in *E. coli*, as well as optimal fucoidan hydrolysis conditions and Fhf1 cleaving mechanism are explained in more detail in [179]. The hydrolysis reaction conditions used for FE\_F3 cleavage will be described briefly in the following. 800 mg FE\_F3 were incubated for 24 h with 100 mg/l Fhf1 and 2 mM CaCl<sub>2</sub> in 10 mM Tris-HCl

(pH = 8) at 37°C. After stopping the reaction by heating at 80°C for 10 min, the reaction products were centrifuged at 20°C and 19000 rpm for 45 min. The medium molecular weight products were separated from the low molecular weight reaction products by precipitation with 75 % ethanol and subsequent centrifugation at 4°C and 19000 rpm for 15 min. LMW was concentrated under vacuum and lyophilized.

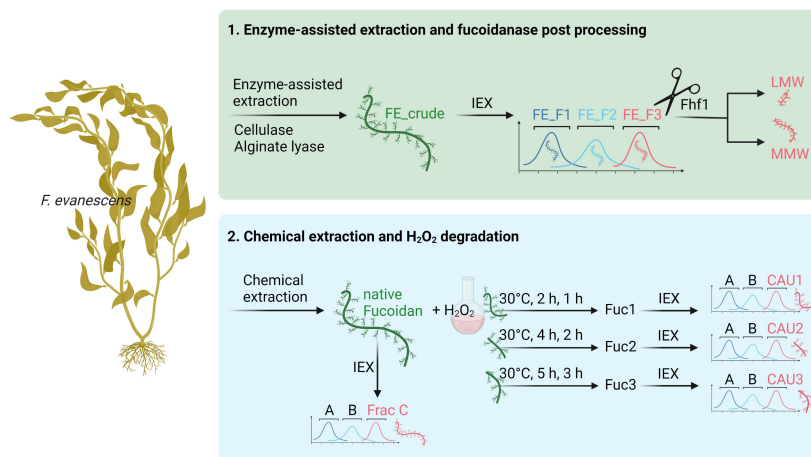


**Figure 2.1:** Extraction and processing of fucoidan extracts. For the presented thesis, fucoidans were gained by two extraction methods: 1. Enzyme-assisted extraction coupled with defined enzymatic degradation by fucoidanase Fhf1. 2. Chemical extraction and subsequent random degradation by  $\text{H}_2\text{O}_2$ .

#### 2.2.4 Chemical fucoidan extraction

The chemical extraction of fucoidan from *Fucus evanescens* is described in detail in previous publications [45, 147]. In brief, the algal materials was defatted with 99 % ethanol for 6 h with a Soxhlet extraction, followed by the removal of alginate and proteins using 2 % calcium chloride for 2 h at 85°C. Fucoidan was precipitated using 60 % ice-cold ethanol, dialyzed and lyophilized to obtain the native extract (NatF). The native fucoidan was further purified using IEX. Biological experiments were conducted with the third eluted fraction (FracC). The extraction process is schematically illustrated in Figure 2.1.

#### 2.2.5 Fucoidan fractionation by $\text{H}_2\text{O}_2$

Fucoidan was fractionated using 3 %  $\text{H}_2\text{O}_2$  [102]. The native extract was incubated in  $\text{H}_2\text{O}_2$  at 30°C for different periods of time to obtain fucoidans with varying molecular weights (2 and 1 h for Fuc1, 4 and 2 h for Fuc2, 5 and 3 h for Fuc3). Each degraded extract was purified using IEX. Biological experiments were conducted with the third eluted fractions CAU1, CAU2 and CAU3.

### 2.2.6 Endotoxin quantification in fucoidan extracts

To exclude bacterial impurities in the fucoidan extracts originating from the extraction procedure, fractionation or enzymatic hydrolysis, the endotoxin content was quantified using the Endolisa kit according to the manufacturer's instruction. The endotoxin levels were negligibly low for all tested fucoidan extracts. The results are listed in Table 2.1.

**Table 2.1:** Endotoxin levels of fucoidan extracts used in the current thesis. (nd=not detectable)

	FE_crude	FE_F1	FE_F2	FE_F3	MMW	LMW
Endotoxins [EU/ml]	0.138	0.058	0.003	0.004	0.016	0.538
	CAU1	CAU2	CAU3			
Endotoxins [EU/ml]	nd	nd	nd			

## 2.3 Chemical Characterization of Fucoidan Extracts

The following section provides information regarding the chemical characterization of the extracted fucoidans including molecular weight, structural information, degree of sulfation, monosaccharide, protein and polyphenolic content. Chemical characterization of FE\_crude, FE\_F1, FE\_F2, FE\_F3, MMW and LMW was performed by Thuan Thi Nguyen, Vy Ha Nguyen Tran and Dr. Maria Dalgaard Mikkelsen (Group of Prof. Dr. Anne S. Meyer, Department of Biotechnology and Biomedicine, Danish Technical University).  $^1\text{H}$ - $^{13}\text{C}$  NMR of MMW and LMW was performed by Dr. Sebastian Meier (Department of Chemistry, Danish Technical University). The chemical characterization of CAU1, CAU2, CAU3, FracC and NatF was performed by Sandesh Neupane (Group of Prof. Dr. Susanne Alban, Department of Pharmaceutical Biology, Kiel University).

### 2.3.1 Monosaccharide content

Fucoidans were hydrolyzed with a two-step acid hydrolysis applying 72 %  $\text{H}_2\text{SO}_4$  at 30°C for 1 h and 4 %  $\text{H}_2\text{SO}_4$  at 120°C for 40 min. Monosaccharide content of hydrolysates was determined by high performance anion-exchange chromatography with pulsed amperometric detection (HPEAC-PAD) using deionized water, 200 mM NaOH and 200 mM NaOH together with 1 M NaOAc as eluents. Further details are given in [130].

The fucose content of CAU1, CAU2, CAU3, FracC and NatF was determined by gas-liquid chromatography as specified in [147].

### 2.3.2 Sulfate content

Fucoidans were hydrolyzed in 2 M TFA at 100°C for 6 h. After evaporating and removing residual TFA, the sulfate content was determined using the BaCl<sub>2</sub> gelatin method [43]. Briefly, 10  $\mu$ l of hydrolysate was mixed with 160  $\mu$ l TCA and 100  $\mu$ l 0.5 % BaCl<sub>2</sub>-gelatine reagent. After 30 min at room temperature, the absorption of released BaSO<sub>4</sub> was measured at 360 nm. Potassium sulfate was used as a standard. Further details are given in [130].

The sulfate content of CAU1, CAU2, CAU3, FracC and NatF was determined by elemental analysis as specified in [16].

### 2.3.3 Polyphenol and protein content

The total phenolic content of the fucoidan extracts was determined using an adapted Folin-Ciocalteu method. Briefly, aqueous fucoidan sample was mixed with 0.025 N Folin-Ciocalteu reagent and incubated for 5 min. After adding 2 M Na<sub>2</sub>CO<sub>3</sub> and incubating for 2 h, the absorption was measured at 600 nm. Gallic acid was used as a reference. The total phenolic content is expressed in gallic acid equivalents (GAE) in mg per g dried substance.

The protein content of the fucoidan extracts was quantified using the Bradford method. Bovine serum albumin (BSA) was used as a standard.

### 2.3.4 Molecular weight

The molecular weight of the fucoidan extracts was quantified by high performance size exclusion chromatography (SEC). Therefore, 3 mg/ml sample dissolved in 100 mM sodium acetate, pH=6, were injected into a Shodex SB-806 HQ GPC column coupled with a Shodex SB-G guard column. Elution flow rate was 0.5 ml/min at 40°C. Pullulan was used as a standard. Further details are given in [130].

The molecular weight of CAU1, CAU2, CAU3, FracC and NatF were determined by size exclusion chromatography coupled with MALS-VIS (multi-angle light scattering-viscosity) detection (Neupane et al., manuscript in preparation).

### 2.3.5 <sup>1</sup>H-<sup>13</sup>C NMR

NMR spectroscopy was employed to gain insights into the chemical structure of the fucoidan extracts MMW and LMW. LMW (7.5 mg) and MMW (9.3 mg) were dissolved under agitation in 500  $\mu$ l <sup>2</sup>H<sub>2</sub>O and NMR spectra were acquired at 50°C on an 800 MHz Bruker Avance III instrument equipped with an 18.7 T Oxford magnet and a TCI cryoprobe (5 mm). A suite of 2D NMR experiments was acquired with standard Bruker pulse sequences. Spectra including 1D <sup>1</sup>H NMR spectra (of 16384 complex data points sampling the FID for 1.7 seconds), 2D <sup>1</sup>H-<sup>1</sup>H TOCSY (2048 x 256 complex data points sampling the FID for 128 ms and 16 ms in the direct and indirect dimension, respectively), <sup>1</sup>H-<sup>1</sup>H COSY (2048 x 256 complex data points sampling the FID for 128 ms and 16 ms in the direct and indirect dimension, respectively), <sup>1</sup>H-<sup>13</sup>C HMBC (2048 x 128

complex data points sampling the FID for 256 ms and 6.3 ms, in the direct and indirect dimension, respectively) and  $^1\text{H}$ - $^{13}\text{C}$  HSQC (2048 x 512 complex data points sampling the FID for 160 ms and 21.2 ms in the direct and indirect dimension, respectively) were acquired. All NMR spectra were processed with ample zero filling in all dimensions and baseline correction using Bruker Topspin 3.5 pl7 software. The spectra were analyzed using the same software.

## 2.4 Human Cell Models & Fucoidan Treatment

The following section gives information about the isolation and cultivation of human MSC and OEC. It further provides details regarding the experimental procedure of fucoidan treatment.

### 2.4.1 OEC isolation and culture conditions

Human endothelial progenitor cells were isolated from buffy coats by gradient centrifugation using Biocoll. Afterwards, cells were resuspended in Endothelial Basal Medium (EBM-2) including 5 % fetal bovine serum (FBS) and 1 % Penicillin/Streptomycin (PS) and all endothelial growth medium 2 (EGM-2) associated supplements. Isolated cells were seeded in collagen type I-coated 24-well plates at a density of  $5 \times 10^6$  cells/cm<sup>2</sup>. After one week, cells were detached and sub-cultured in new collagen type I-coated 24-well plates at a density of  $5 \times 10^5$  cells/cm<sup>2</sup>. Colonies of cobblestone-shaped OEC adhered within two to three weeks (see Figure 2.2). Further information regarding OEC isolation from peripheral blood can be found in [52].

Obtained OEC were cultivated in fibronectin-coated plates or flasks in EGM-2 (EBM-2, EGM-2 associated supplements, 7 % FBS and 1 % PS). Cells were sub-cultured every two to three days after reaching confluency and the medium was exchanged every second or third day. OEC in passages 4 to 11 were used for biological assays. If not stated otherwise, OEC were seeded at a density of 40,000 cells/cm<sup>2</sup> in adequate fibronectin-coated plates or flasks for biological assays. For further OEC donor information see supplementary Table A.1.

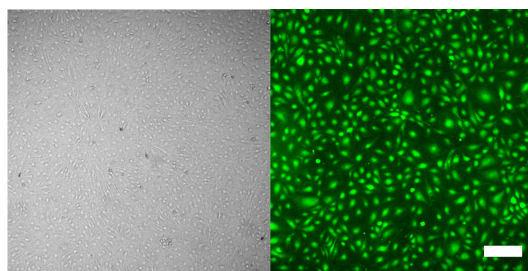


**Figure 2.2:** Human outgrowth endothelial cells (OEC) isolated from peripheral blood. Scale bar = 200  $\mu\text{m}$ .

### 2.4.2 MSC isolation and culture conditions

Human mesenchymal stem cells derived from cancellous bone were isolated from femoral heads as described in the previous publication [97]. Briefly, bone segments were washed in phosphate-buffered saline (PBS) and cells were collected by centrifugation. Obtained MSC were resuspended in Dulbecco's Modified Eagle's Medium (DMEM)/Ham's F-12 including 20 % FBS and 1 % PS and seeded into collagen type I-coated flasks at a density of  $2 \times 10^6$  cells/cm<sup>2</sup>. After reaching confluency, MSC were sub-cultured and seeded into collagen type I-coated flasks in DMEM/Ham's F-12 including 10 % FBS and 1 % PS. To differentiate MSC towards an osteoblast-like lineage, cells from passage number 2 were cultured in collagen- or fibronectin-coated flasks using osteogenic differentiation medium (ODM: DMEM/Ham's F-12 supplemented with 10 % FBS, 1 % PS, 50  $\mu$ M L-ascorbic acid 2-phosphate, 10 mM  $\beta$ -GP and 0.1  $\mu$ M dexamethasone). The medium was exchanged every second or third day. MSC in passage 4 or 5 were used for biological assays. Osteoblast-like MSC are shown in Figure 2.3. If not stated otherwise, MSC were seeded at a density of 40,000 cells/cm<sup>2</sup> in adequate collagen- or fibronectin-coated plates or flasks for biological assays. For further MSC donor information see supplementary Table A.1.

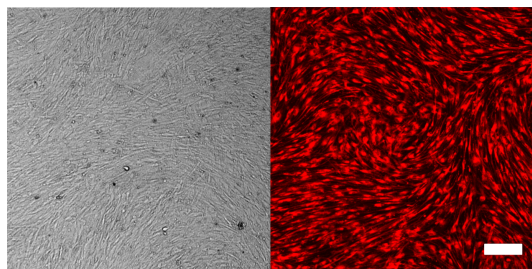


**Figure 2.3:** Human osteoblast-like mesenchymal stem cells (MSC) isolated from cancellous bone. Scale bar = 200  $\mu$ m.

### 2.4.3 MSC-OEC co-culture conditions

For MSC-OEC co-cultures, MSC were seeded in fibronectin-coated plates at a density of 40,000 cells/cm<sup>2</sup> in ODM on the first day. After 24 h, OEC were seeded at the same density in EGM-2 on top of the MSC.

### 2.4.4 Fucoidan treatment

Lyophilized fucoidan extracts were dissolved in distilled water to create 5 mg/ml stock solutions. For cell treatment, the fucoidan stock solution was diluted to the desired concentration in respective cell culture medium and filtered through a membrane with a pore size of 0.2  $\mu$ m. 24 h after cell seeding, the culture medium was removed and replaced by fresh medium containing the desired fucoidan concentration. The medium including fucoidan was refreshed on the third treatment day if the experiment would last for seven

days. Control cells were cultured equally in regular growth medium without fucoidan. The timeline of biological experiments with fucoidan treatment is schematically depicted in Figure 2.4. Table 2.2 lists all fucoidan extracts used for the current thesis. Fucoidans from Danish Technical University were extracted by Dr. Maria Dalgaard Mikkelsen, Thuan Ti Nguyen and Vy Ha Nguyen Tran. Fucoidans from Christian-Albrechts University were extracted by Sandesh Neupane. Commercially available crude and pure fucoidan from Sigma-Aldrich were used as reference substances.

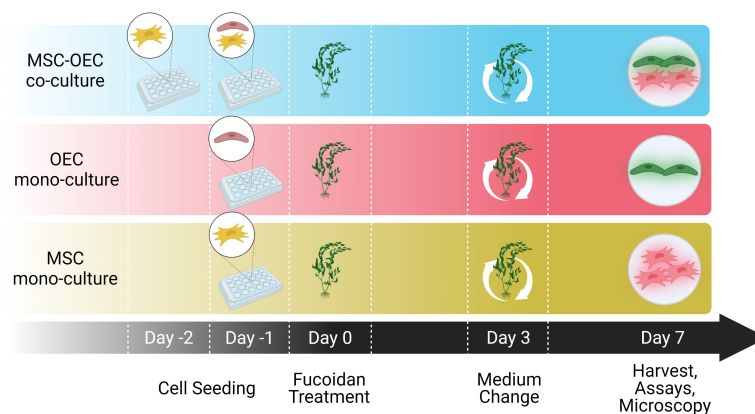


**Figure 2.4:** Workflow for biological experiments using MSC and OEC mono- and co-cultures as model systems. After cell seeding, cultures were treated with fucoidan on day zero. For seven day experiments, medium including fucoidan treatment was refreshed on day three.

**Table 2.2:** Fucoidan extracts from *Fucus evanescens* (FE) and *Fucus vesiculosus* (FV) used in the presented thesis.

Extract	Species	Source
FE_crude	FE	Danish Technical University
FE_F1	FE	Danish Technical University
FE_F2	FE	Danish Technical University
FE_F2	FE	Danish Technical University
MMW	FE	Danish Technical University
LMW	FE	Danish Technical University
CAU1	FE	Christian-Albrechts-University Kiel
CAU2	FE	Christian-Albrechts-University Kiel
CAU3	FE	Christian-Albrechts-University Kiel
NatF	FE	Christian-Albrechts-University Kiel
FracC	FE	Christian-Albrechts-University Kiel
FV_crude	FV	F5631, Sigma-Aldrich
FV_pure	FV	F8190, Sigma-Aldrich

## 2.5 Biological Assays

The following section provides information about the performed biological assays and analyses after fucoidan treatment. Assays for cell viability, DNA quantification, osteogenic potential, gene expression, intra-, and extracellular protein levels, as well as immunocytochemistry stainings were applied to reveal the effect of fucoidan on MSC and OEC mono- and co-culture systems.

### 2.5.1 MTS and LDH assay

MSC or OEC mono-cultures were seeded in 96-well plates and treated with fucoidan as described in section 2.4.4. Lactate dehydrogenase (LDH) release and metabolic activity of the cells were determined after one, three and seven days of treatment using Pierce LDH Cytotoxicity Assay Kit and CellTiter 96 Aqueous One Solution Cell Proliferation Assay, respectively. Both assays were performed according to the manufacturer's protocols.

### 2.5.2 DNA quantification

MSC were treated with fucoidan for seven days as described in section 2.4.4. After seven days, cells were washed with PBS and collected by scraping. The DNA was released from MSC by repeated freeze-thaw cycles and sonication. The DNA was quantified using the Quant-iT<sup>TM</sup> PicoGreen<sup>TM</sup> dsDNA Assay Kit. 100  $\mu$ l TE-buffer, followed by 72  $\mu$ l PicoGreen reagent per well were added into a 96-well plate. 28  $\mu$ l sample or standard were added into the wells and incubated for 10 min at 200 rpm. The fluorescence was measured at 485 nm and 535 nm excitation and emission wavelength, respectively.

### 2.5.3 Quantitative real-time PCR

MSC and OEC mono- and co-cultures were treated with fucoidan for seven days as described in section 2.4.4. For lysis, cells were incubated with 100  $\mu$ l RNA Lysis Buffer T per well for 10 min at 37°C. The cell lysate was collected and RNA was isolated using the peqGOLD Total RNA kit according to the manufacturer's protocol. DNase I treatment for DNA digestion was included into the isolation procedure. 1  $\mu$ g RNA was transcribed into cDNA using the High-Capacity RNA-to-cDNA<sup>TM</sup> Kit following the manufacturer's instructions. The cDNA was diluted in the ratio 1:5 in nuclease-free water before it was used for qPCR.

For qPCR, 3.2  $\mu$ l cDNA was mixed with 10  $\mu$ l SYBR<sup>TM</sup> Select Master Mix, 2  $\mu$ l QuantiTect Primer Assays and 4.8  $\mu$ l nuclease-free water. RPL13A was used as the housekeeping gene. qPCR was ran with a two-step program (50°C 2 min, 95°C 2 min, 40 cycles 95°C 15 s and 60°C 60 s). The relative gene expression was calculated using the  $\Delta\Delta_{ct}$  method. All primers used for the current thesis are listed in Table 2.3.

**Table 2.3:** QuantiTect Primer Assays (Qiagen) for qPCR used in the current thesis.

Gene	QuantiTect Primer Assay	Catalog Number
Alkaline phosphatase (ALP)	Hs_ALPL_1_SG	QT00012957
Angiopoietin 1 (ANG-1)	Hs_ANGPT1_1_SG	QT00046865
Angiopoietin 2 (ANG-2)	Hs_ANGPT2_1_SG	QT00100947
Intercellular Adhesion Molecule 1 (ICAM-1)	Hs_ICAM1_1_SG	QT00074900
Interleukin 6 (IL-6)	Hs_IL6_1_SG	QT00083720
Matrix Metalloproteinase 14 (MMP14)	Hs_MMP14_1_SG	QT00001533
Nuclear Factor NF-kappa-B p105 subunit (NF $\kappa$ B)	Hs_NFKB1_1_SG	QT00063791
Stromal-derived Factor 1 (SDF-1/CXCL12)	Hs_CXCL12_1_SG	QT00087591
Vascular Cell Adhesion Molecule 1 (VCAM-1)	Hs_VCAM1_1_SG	QT00018347
Vascular Endothelial Cadherin (VE-cad)	Hs_CDH5_1_SG	QT00013244
Vascular Endothelial Growth Factor A (VEGF)	Hs_VEGFA_2_SG	QT01036861
Zona Occludens 1 (ZO-1)	HS_TJP1_1_SG	QT00077308
60S Ribosomal Protein L13a (RPL13A)	Hs_RPL13A_1_SG	QT00089915

#### 2.5.4 ELISA

##### Extracellular proteins

MSC and OEC mono- and co-cultures were treated with fucoidan as described in section 2.4.4. For the quantification of secreted proteins, the culture medium was harvested on day four and/or seven after fucoidan treatment. Protein levels were quantified using DuoSet<sup>®</sup> ELISA Development Systems according to the manufacturer's protocol. A list of all used ELISA DuoSets<sup>®</sup> for secreted proteins can be found in Table 2.4.

##### Transmembrane proteins

For the quantification of transmembrane VEGFR2 and phosphorylated VEGFR2 (VEGFR2p),  $10^6$  OEC per well ( $104,000$  cells/cm<sup>2</sup>) were seeded in 6-well plates and cultivated for 24 h in regular EGM-2 medium. On the next day, OEC were starved for 24 h in EBM-2 containing 0.2 % FBS and 1 % PS. After 24 h, the medium was replaced by fresh starving medium containing  $100 \mu\text{g/ml}$  fucoidan and  $100 \text{ ng/ml}$  VEGF-165 to stimulate the VEGFR2 phosphorylation. Control cells 1 were stimulated with  $100 \text{ ng/ml}$  VEGF-165

in the absence of fucoidan. Control cells 2 were cultured in starving medium without fucoidan and VEGF-165. OEC were stimulated for 15 min at 37°C. Subsequently, the 6-well plates were placed immediately on ice and cells were washed with ice-cold PBS. 600  $\mu$ l freshly prepared lysis buffer #9 (containing leupeptin and aprotinin, for preparation see manufacturer's protocol) was added per well and cells were incubated for 15 min on ice. Afterwards, the cell lysates were collected and stored at -80°C until use. The DuoSet<sup>®</sup> ELISA for quantifying VEGFR2 and VEGFR2p were performed according to the manufacturer's protocol.

A list of all used ELISA DuoSets<sup>®</sup> for transmembrane proteins can be found in Table 2.4.

**Table 2.4:** DuoSet<sup>®</sup> ELISA Development Systems (R&D) used in the current thesis.

Secreted protein	Catalog number
Angiopoietin 1 (ANG-1)	DY923
Angiopoietin 2 (ANG-2)	DY623
Intercellular Adhesion Molecule 1 (ICAM-1)	DY720
Interleukin 6 (IL-6)	DY206
Stromal-derived Factor 1 (SDF-1/CXCL12)	DY350
Vascular endothelial growth factor (VEGF)	DY293B
Transmembrane protein	
Human Total VEGF R2/KDR (VEGFR2)	DYC1780-2
Human Phospho-VEGF R2/KDR (VEGFR2p)	DYC1766-2

### ELISA competitive binding assay

To investigate the binding affinity of fucoidan to VEGF, 300 pg/ml VEGF was mixed with 0, 1, 5 and 10  $\mu$ g/ml fucoidan. The VEGF DuoSet<sup>®</sup> ELISA Development System (for further information see table 2.4) was used to quantify the VEGF concentration which was still available after mixing with different fucoidan concentrations.

#### 2.5.5 ALP activity

MSC were treated with fucoidan as described in section 2.4.4 for seven days. After seven days, the culture medium was harvested and ALP activity was measured using the Alkaline Phosphatase Assay Kit according to the manufacturer's protocol.

#### 2.5.6 Alizarin red staining

MSC were treated with fucoidan as described in section 2.4.4 for 14 days. After two weeks, cells were fixed with 4% paraformaldehyde (PFA) followed by the addition of

1 ml 40 mM Alizarin Red S Stain Solution per well. After 30 min incubation, cells were washed with distilled water until rinsed water became clear. To extract the bound dye, 600  $\mu$ l 10 % cetylpyridinium chloride (CPC) was added into each well and incubated overnight. On the next day, 150  $\mu$ l CPC with the extracted dye were transferred to a new 96-well plate and the absorbance was measured at 560 nm. Alizarin Red dilutions in CPC were used as a standard.

### 2.5.7 Immunocytochemistry

MSC and OEC mono- or co-cultures were seeded on Thermanox coverslips in 24-well plates or in 8-well  $\mu$ -slides and treated with fucoidan as described in section 2.4.4. For immunostaining, cells were fixed with 4 % PFA for 15 min and subsequently washed with PBS three times for 5 min. After fixation, cells were permeabilized with 0.5 % Triton<sup>TM</sup> X-100 for 15 min, followed by blocking of unspecific binding sites using 1 % BSA for 30 min.

#### VE-cadherin staining

MSC-OEC co-cultures were treated with fucoidan for seven days and subsequently prepared for VE-cadherin immunostaining as described in the prior paragraph 2.5.7. After blocking with BSA, the samples were incubated with 4  $\mu$ g/ml in 1 % BSA Human VE-cadherin primary antibody (AF938, R&D) for 1 h at room temperature. Subsequently, samples were washed three times for 5 min with PBS and 2  $\mu$ g/ml secondary antibody (AlexaFluor488/anti-goat (A11055, invitrogen)) in 1 % BSA was applied for 1 h. Nuclei were stained for 15 min with 2  $\mu$ g/ml Hoechst 33258. After washing three times for 5 min, the samples were mounted using Fluoromount<sup>TM</sup> and imaged with the Evos FL Auto 2 fluorescence microscope.

#### Fucoidan staining

To investigate whether the studied fucoidan extracts interacted with the MSC or OEC, a protocol for fucoidan staining was established using the BAM antibodies (developed by SeaProbes, Roscoff, France). MSC and OEC were treated with 100  $\mu$ g/ml fucoidan for three days. After three days, cells were repeatedly washed with PBS to remove remaining fucoidan solution and prepared for immunostaining as described in the prior paragraph 2.5.7. BAM-1 or BAM-4 primary antibody was applied in a 1:10 dilution in 1 % BSA and samples were incubated overnight at 4°C. Following the manufacturer's specification, BAM-1 binds to an unsulfated epitope and BAM-4 to a sulfated epitope [174]. 2  $\mu$ g/ml secondary antibody (AlexaFluor647/anti-rat (A21247, invitrogen)) was applied for 1 h at room temperature after 3 times 5 min washing with PBS. Nuclei and actin were stained for 15 min with 2  $\mu$ g/ml Hoechst 33258 and 5  $\mu$ g/ml Phalloidin-TRITC, respectively. OEC were additionally stained for VE-cadherin using the antibodies and concentrations as described in the prior paragraph 2.5.7. After washing three times for

5 min, the samples were mounted using Fluoromount<sup>TM</sup> and imaged with the Zeiss confocal laser scanning microscope LSM 800.

Preliminary staining experiments with BAM-1 and BAM-4 revealed that BAM-1 had a strong unspecific binding to MSC, making a differentiation between unspecific and fucoidan staining difficult. For this reason, following fucoidan staining experiments were performed using the BAM-4 antibody. Exemplary stainings of MSC control and fucoidan-treated cells are shown in Figure 2.5.

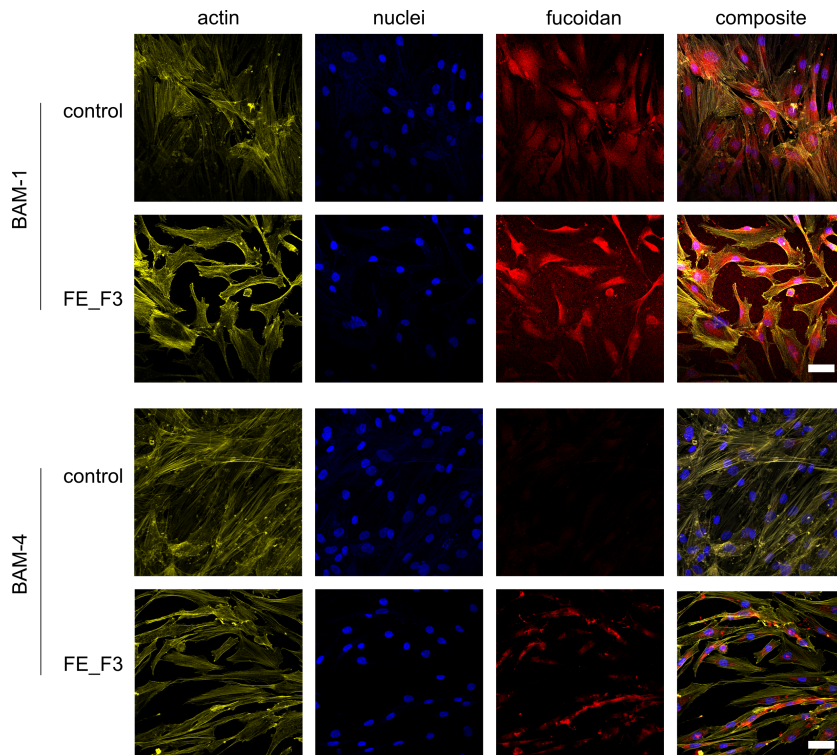


**Figure 2.5:** Fucoidan staining with primary antibodies BAM-1 and BAM-4. MSC were treated with fucoidan FE\_F3 for three days, control cells were cultured in medium without fucoidan. Cells were stained for fucoidan (red), actin (yellow) and nuclei (blue). Scale bar=50  $\mu$ m.

### Dot blot for BAM-4

To confirm that the BAM-4 antibody is able to bind to the studied fucoidan extracts, a simple dot blot was performed. 2  $\mu$ l aqueous fucoidan solution (0.1 and 5 mg/ml) were dotted on 0.45  $\mu$ m nitrocellulose membranes. After air-drying the membranes for 15 min, they were blocked in 5 % low fat milk powder (LFMP) under constant shaking for 1 h. 1 ml of BAM-4 antibody (1:10 dilution in 5 % LFMP) was carefully applied to the membrane surface and incubated for 2 h. Afterwards, the membranes were washed three times for 10 min with PBS under constant shaking and then incubated with secondary anti-

body anti-rat IgG-ALP (A6066, Sigma Aldrich, 1:10,000 dilution in 5 % LFMP) for 2 h under constant shaking. After washing the membranes three times with PBS for 10 min under constant shaking, they were developed by carefully applying 1 ml BCIP/NBT liquid substrate per membrane stripe. After dot development, the membranes were air-dried and scanned. The resulting dot blots are shown in Figure 2.6. As expected, dots with the higher fucoidan concentration of 5 mg/ml developed much darker than dots that contained only 0.1 mg/ml fucoidan. The dot containing LMW only developed for the higher fucoidan concentration, indicating that BAM-4 affinity to LMW is weaker compared to the other fucoidans or LMW was not able to bind appropriately to the membrane. Nevertheless, the dot blot proved that BAM-4 antibody was able to bind to the studied fucoidans.

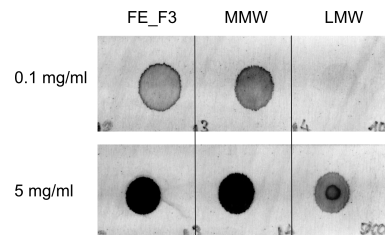


**Figure 2.6:** Dot blot for proving the affinity of primary antibody BAM-4 to the studied fucoidan extracts. 0.1 and 5 mg/ml FE\_F3, MMW and LMW were dotted on a nitrocellulose membrane, incubated with BAM-4 primary antibody, anti-rat IgG-ALP secondary antibody and developed using BCIP/NBT.

## 2.6 Image Analysis

In the following section, computational approaches are described which were used to quantify stained structures from microscopy images.

### 2.6.1 Quantification of angiogenic tube-like structures

Co-cultures of MSC and OEC were seeded and cultured for seven days as described in section 2.4.3. After one week, cells were fixed and stained for VE-cadherin as described in section 2.5.7. For quantifying the number, area and length of the formed angiogenic structures, three stitched pictures consisting of nine frames were taken for each sample. A shading correction was performed for the stitched images using the BASiC plug-in in FIJI [138, 152]. Area and length of the angiogenic skeleton were quantified semi-automatically using the software ImageJ Version 1.42 [153] as described in a previous publication [53].

### 2.6.2 Quantification of the integrity of the endothelial cell layer

Co-cultures of MSC and OEC were seeded and cultured for seven days as described in section 2.4.3. After one week, cells were fixed and stained for VE-cadherin as described in section 2.5.7. Three stitched microscopy pictures consisting of nine frames were taken for each sample and corrected as stated in the prior section 2.6.1. The integrity of the endothelial cell layer was expressed by quantifying the area which was not covered by OEC using FIJI [152]. Therefore, fluorescent images were converted into binary images and black areas (areas without OEC) were measured.

### 2.6.3 Quantification of fucoidan staining

MSC and OEC mono- and co-cultures were seeded, treated with fucoidan, cultured for three days and stained for fucoidan as described in section 2.5.7. Red fluorescence intensity (fucoidan) in reference to the cell number was measured for three frames of each sample. For determining the number of cells in each frame, the channel with nucleus staining was converted into a binary image, followed by a particle analysis. The red fluorescence intensity was divided by the number of nuclei in order to obtain the fucoidan amount in relation to the number of cells. The analysis was conducted using FIJI [152].

## 2.7 Chitosan-Collagen Hydrogel as a Delivery System for Fucoidan

This section describes the protocol for the preparation of a thermosensitive chitosan-collagen hydrogel serving as a delivery system for fucoidan. It further describes how physicochemical properties like gelation time, temperature, pH, turbidity and swelling were determined. Rheological measurements were performed with the help of Marie Trenkel (Group of Prof. Dr. Regina Scherließ, Department of Pharmaceutics and Biopharmaceutics, Kiel University). To reveal the morphology of the hydrogels, scanning electron microscopy (SEM) was applied with the help of Lena Marie Saure (Group of Prof. Dr. Rainer Adelung, Institute for Materials Science, Kiel University) and Dr. Alexander Kovalev (Group of Prof. Dr. Stanislav N. Gorb, Zoological Institute, Kiel University). Finally, this section provides information about MSC or OEC cultivation on and inside the hydrogel.

### 2.7.1 Hydrogel preparation

The entire hydrogel preparation was performed on ice and under constant stirring. A cool solution of 2 % Chitosan in 0.1 M acetic acid was pipetted into a glass vial. Second, the desired volume of cooled rat tail collagen type 1 was slowly pipetted into the chitosan solution to reach a final concentration of 1.5 mg/ml. Cooled aqueous  $\beta$ -GP (stock: 50 %) and fucoidan solution (commercially available FV\_pure, stock: 5 mg/ml) were premixed and immediately added dropwise into the chitosan-collagen mix to reach final

concentrations of 7% and 10, 100 or 500  $\mu\text{g}/\text{ml}$ , respectively. The hydrogel mix was incubated on ice under constant stirring for 15 min and afterwards stored on ice until further use. The hydrogel sols were always used within three hours after preparation. If not stated otherwise, this protocol was used to produce the hydrogels. For preliminary experiments, the effect of different concentrations and procedures was studied. In these cases, experimental variations will be mentioned in the corresponding result sections.

### 2.7.2 Gelation time by the tube-inverting method

To roughly determine the gelation time of the hydrogels, the tube-inverting method was applied. Therefore, the glass vial with the liquid sol was placed into a 37°C water bath. The flow of the sol was checked every minute by inverting the vial. The sol was declared as gelled if flow could no longer be observed.

### 2.7.3 pH

The pH of the sols was measured before and after gelation using a SevenEasy pH meter S20 with an InLab Micro Pro-ISM pH electrode.

### 2.7.4 Turbidity

To determine the turbidity, 200  $\mu\text{l}$  sol per well was pipetted into a 96-well plate on ice. The absorption of the sols was measured at 600 nm with an infinite M200 Pro plate reader.

### 2.7.5 Absorption kinetics

When sols gelate into hydrogels, their color turns from transparent to opaque. To monitor and compare the gelation processes of different hydrogels, the absorptions of sols and later gels, were measured over time. Therefore, 200  $\mu\text{l}$  sol per well was pipetted into a 96-well plate on ice. The plate reader was heated to 37°C and the absorption was measured at 600 nm every minute for one hour.

### 2.7.6 Equilibrium swelling ratio

To quantify the swelling capacities of the different hydrogels, the equilibrium swelling ratio (ESR) was determined. Therefore, 500  $\mu\text{l}$  sol was pipetted into a tube and gelled at 37°C for 30 min. Subsequently, the hydrogels inside the tubes were quick-frozen using liquid nitrogen and lyophilized. Dried hydrogels were weighted ( $w_d$ ) and rehydrated in PBS for three days at 37°C. After three days, the swollen hydrogels were weighted again ( $w_s$ ). The ESR was calculated using the following formula:

$$ESR = \frac{w_s - w_d}{w_d}$$

### 2.7.7 Rheological measurements

The rheological studies were performed with the Bohlin CVO 120 HRNF plate-to-plate rheometer (plate diameter: 40 mm). 1 ml of sample covered with a solvent trap to prevent evaporation was used for each measurement. Storage ( $G'$ ) and loss moduli ( $G''$ ) were determined to characterize the viscoelastic properties of the hydrogels with and without fucoidan. At the beginning, an amplitude sweep test was carried out at  $37^\circ\text{C}$  and at a constant frequency of 1 Hz to determine the viscoelastic region of the hydrogels. As shown in Figure 2.7, a strain of 5% resulted to be adequate for both hydrogels. All oscillatory measurements were therefore performed with a strain of 5%. Time sweep tests at a constant frequency of 1 Hz were performed to determine the time until sol-gel transition and the duration of the gelation process at  $37^\circ\text{C}$ . Temperature sweep tests were performed to determine the exact gelation temperature.  $G'$  and  $G''$  were quantified for a temperature gradient from 10- $60^\circ\text{C}$  ( $2^\circ\text{C}/\text{min}$ ) at a constant frequency of 1 Hz.

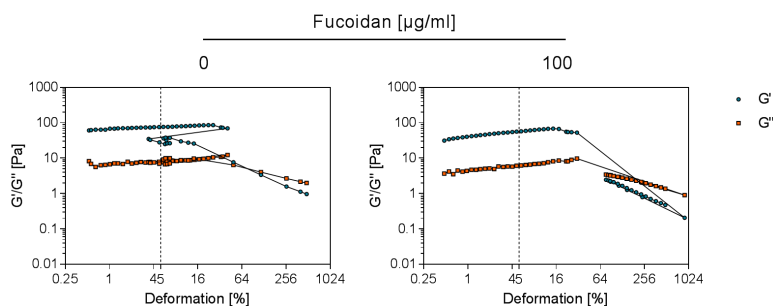


**Figure 2.7:** Amplitude sweep test to determine the linear viscoelastic region of the hydrogels without and with  $100\ \mu\text{g}/\text{ml}$  fucoidan. The measurements were performed at  $37^\circ\text{C}$  and at a constant frequency of 1 Hz. A strain of 5% (marked with a dashed line) resulted to be in the linear region for both hydrogels.

### 2.7.8 Scanning electron microscopy

To reveal the microstructure of the hydrogels, SEM was applied. The samples were dried with two different approaches, lyophilization and critical point drying (CPD), which are described in the following.

#### Lyophilization

Sols with and without fucoidan were prepared, pipetted into a tube ( $500\ \mu\text{l}$ ) and gelled at  $37^\circ\text{C}$ . Subsequently, gels were quick-frozen in liquid nitrogen and lyophilized.

To image the cross-section of the dried gels, the samples were carefully cut in half with a scalpel, mounted on a holder using conductive carbon tape or glue and sputtered with gold for 90 s. The samples were imaged with a Zeiss Supra 55VP and a Hitachi S-4800.

### Critical point drying

Sols with and without fucoidan were prepared; 200  $\mu\text{l}$  were pipetted into a 8-well  $\mu\text{-Slide}$  and gelated at 37°C. To facilitate the removal of the soft hydrogel without destroying it, the 8-well  $\mu\text{-Slide}$  was specially prepared as illustrated in Figure 2.8. Thermanox coverslips were cut into the size of a  $\mu\text{-Slide}$  well, followed by attaching thin transparent tape to the bottom side of the Thermanox coverslip. The modified coverslip was placed into the well. The tape stripes allowed to easily lift the hydrogel out of the  $\mu\text{-Slide}$  well using tweezers.

After gelation, the hydrogels were incubated in PBS for 24 h at 37°C. On the next day, the hydrogels were fixed with 3 % glutaraldehyde in 4 % PFA for 30 min at room temperature and subsequently washed three times with PBS for 5 min. Then, the aqueous solution was exchanged gradually to ethanol beginning with a 50 % ethanol dilution. The hydrogels were incubated with 200  $\mu\text{l}$  50 % ethanol for 15 min at room temperature. This step was repeated with 60, 70, 80, 90, 95 and 100 % ethanol solutions. The hydrogels were stored in 100 % ethanol until critical point drying.

Before drying, the hydrogels were carefully lifted out of the wells and cut in half with a scalpel to be able to image the cross-sections. The hydrogels were always kept in 100 % ethanol.

The soft dried hydrogels were carefully mounted on a holder using conductive carbon tape or glue and sputtered with gold for 90 s. The samples were imaged with a Zeiss Supra 55VP and a Hitachi S-4800.

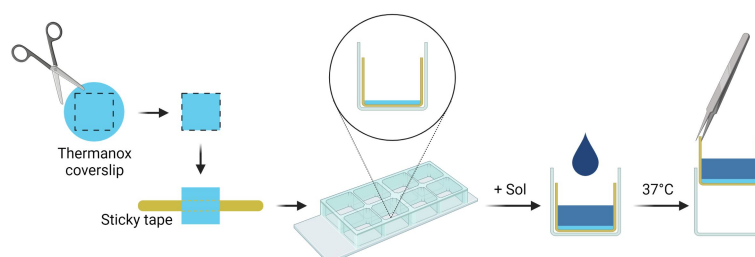


**Figure 2.8:** Preparations for critical point drying. Thermanox coverslips were cut into the size of a  $\mu\text{-Slide}$  well. Sticky tape was fixed on the bottom of the Thermanox to facilitate removal of the hydrogel after gelation.

### SEM of MSC cultured on hydrogels

Hydrogels were prepared and placed on modified Thermanox coverslips inside 8-well  $\mu\text{-Slides}$  as described in the prior section and illustrated in Figure 2.8. MSC were cultured on top of the hydrogels for seven days as specified in the later section 2.7.10. After seven days, MSC were fixed and the hydrogels were dried using critical point drying (for

further details see the prior section). The dried samples were mounted on SEM holders using conductive tape or glue and imaged with the Zeiss Supra 55VP.

### 2.7.9 Fucoidan detection with SYBR Gold

#### Quantification of fucoidan in solution

The quantification of fucoidan in solution was established using the SYBR Gold nucleic acid gel stain following the protocol of Yamazaki et al. [190]. Pure fucoidan from *Fucus vesiculosus* (Sigma-Aldrich) was used to establish the protocol. 150  $\mu\text{l}$  per well aqueous fucoidan solution was pipetted into a black 96-well plate, followed by adding 50  $\mu\text{l}$  per well of the diluted SYBR Gold solution (1:625 in 80 mM Tris-HCl, pH 7.5).

The excitation and emission optima were determined by emission and excitation scans as shown in Figure 2.9 A). The excitation scan was performed at an emission wavelength of 600 nm. The optimum excitation wavelength was determined to be 470 nm. The emission scan was performed at an excitation wavelength of 470 nm. The optimum emission wavelength was determined to be 600 nm. A standard curve of different fucoidan dilutions was prepared and a linear relation between concentration and fluorescence could be detected for concentrations ranging from 0 to 3.2  $\mu\text{g}/\text{ml}$  as shown in Figure 2.9 B).

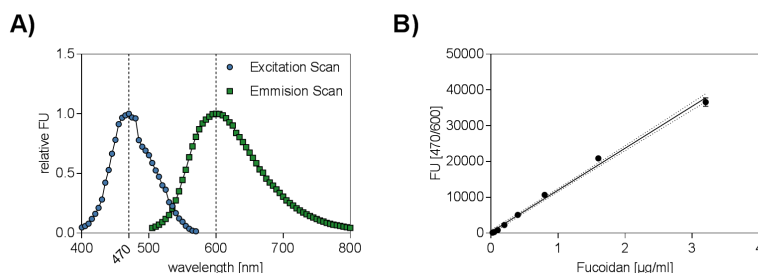


**Figure 2.9:** SYBR Gold nucleic acid gel stain for quantifying fucoidan in solution according to the protocol of Yamazaki et al. [190] A) Excitation scan at emission wavelength 600 nm, emission scan at excitation wavelength 470 nm. The wavelength optima were determined as 470 nm and 600 nm for excitation and emission, respectively. B) Linear relation between fluorescence and fucoidan concentrations ranging from 0 to 3.2  $\mu\text{g}/\text{ml}$ .

#### Fucoidan detection inside the hydrogel using fluorescence microscopy

The protocol described in the prior section 2.7.9 was adapted to detect fucoidan inside the hydrogel using fluorescence microscopy. Therefore, sols containing fucoidan concentrations ranging from 0 to 500  $\mu\text{g}/\text{ml}$  were pipetted into a  $\mu$ -Slide Angiogenesis (10  $\mu\text{l}$  sol per well) and gelled at 37°C. After gelation, 50  $\mu\text{l}$  SYBR Gold dilution was added to each well as described in the prior section and samples were incubated for one hour at

room temperature. Subsequently, the staining solution was removed and hydrogels were washed with PBS. The hydrogels were imaged using the Evos FL Auto 2 fluorescence microscope.

Three frames per sample were taken for fluorescence quantification. A region of interest (ROI) covering approximately 1/4 of the frame was defined and inserted into each frame. The fluorescence intensity was measured for each ROI.

### **Fucoidan detection inside the hydrogel using a plate reader**

The protocol described in the prior section 2.7.9 was adapted to detect fucoidan inside the hydrogel using a plate reader. Therefore, sols containing fucoidan concentrations ranging from 0 to 500  $\mu\text{g}/\text{ml}$  were pipetted into a black 96-well plate (100  $\mu\text{l}$  sol per well) and gelled at 37°C. After gelation, 50  $\mu\text{l}$  SYBR Gold dilution was added to each well as described in the prior section and samples were incubated for one hour at room temperature. Subsequently, the staining solution was removed and hydrogels were washed with PBS. The fluorescence was measured at 470 nm and 600 nm excitation and emission wavelength, respectively.

### **Fucoidan release from the hydrogel**

To measure the fucoidan release from the hydrogel over time, the fucoidan was detected with the plate reader on three different time points using the established method. Therefore, 100  $\mu\text{l}$  sol with and without fucoidan was added into a black 96-well plate and gelled at 37°C. After gelation, the hydrogels were incubated in PBS at 37°C. On day zero, two and six, the PBS was removed and the fluorescence was measured as described in the prior section.

### **2.7.10 Cell cultivation in and on the hydrogel**

For cell culture experiments, the hydrogel was prepared as described in section 2.7.1 and afterwards filtered through a membrane with a pore size of 0.2  $\mu\text{m}$ . Sols were always stored on ice.

#### **2D cell culture**

The sterile-filtered sols were pipetted into a suitable dish and gelled at 37°C for 30 min. Subsequently, OEC or MSC were seeded in a density of 80,000 cells/ $\text{cm}^2$  on top of the hydrogels. If not stated otherwise, the medium was gently exchanged every day or every second day. Therefore, only part of the old medium was removed and replaced by fresh medium.

#### **3D cell culture**

For encapsulating cells into the hydrogel, the MSC or OEC suspension was centrifuged and the pellet was resuspended in the cold sterile-filtered sol (1000 cells/ $\mu\text{l}$ ). Sols mixed

---

with the cells were pipetted into a suitable dish and incubated at 37°C for 30 min until the sol gelled. After 30 min, cell culture medium was added on top of the hydrogels. If not stated otherwise, the medium was gently exchanged every day or every second day. Therefore, only part of the old medium was removed and replaced by fresh medium.

### 2.7.11 Life/Dead staining of 2D- and 3D-cultured MSC and OEC

Vital and dead cells were stained on day two and six with calcein-AM and propidium iodide, respectively. Therefore, MSC or OEC were cultured in or on the hydrogels in Angiogenesis  $\mu$ -Slides as described in the previous section 2.7.10 (10  $\mu$ l sol, 50  $\mu$ l medium per well). The medium on the hydrogels was removed and replaced by fresh medium containing calcein-AM and propidium iodide in dilutions of 1:500. The staining solution was incubated on the hydrogels at 37°C for 30 min. Subsequently, the staining solution was removed and replaced by fresh medium. The cells were imaged with the Evos FL Auto 2 fluorescence microscope immediately after staining.

### 2.7.12 DNA quantification of 3D-cultured MSC

The DNA of MSC encapsulated in the hydrogels was quantified on day one and six. Therefore, MSC were cultured inside the hydrogels in 24-well plates as described in the previous section 2.7.10 (400  $\mu$ l sol, 600  $\mu$ l medium per well). On day two and six, the medium was removed and replaced by 500  $\mu$ l PBE (PBS supplemented with 10 mM EDTA) buffer containing 1 mg/ml proteinaseK. The hydrogels with cells were destroyed using the pipette tip and resuspended by pipetting up and down. For the quantification, hydrogels from two wells were pooled. The hydrogel-proteinaseK suspension was incubated for 24 h at 55°C. After 24 h, the samples were stored at -80°C until use. Before DNA quantification, samples were centrifuged for 10 min at 2000 rpm and the supernatant was transferred into a clean tube. The DNA quantification was performed using the Quant-iT<sup>TM</sup> PicoGreen<sup>TM</sup> dsDNA Assay Kit as described in section 2.5.2.

### 2.7.13 VEGF protein level in supernatant of 3D-cultured MSC

MSC were cultured inside the hydrogels in 24-well plates as described in section 2.7.10 (400  $\mu$ l sol, 600  $\mu$ l medium per well). The medium was harvested on day one, three and six and stored at -80°C until further use. To quantify VEGF protein levels in the supernatant, ELISA DuoSet<sup>®</sup> was used according to the manufacturer's protocol. For the catalog number see Table 2.4.

## 2.8 Statistics

The presented plots show the mean value and standard deviation of three independent experiments, if not stated otherwise. Experiments containing MSC or OEC were always performed with cells from three different donors. To control the technical error, biological assays like qPCR, ELISA or DNA quantification were always performed with at least

two replicates. The statistical significance, mostly indicated by asterisks, was calculated with Welch's t-test or ANOVA with post-hoc Dunnett test using GraphPad Prism 7, as specifically indicated in the figure captions. Values were declared as significantly different when  $p < 0.05$  (\* $p < 0.05$ , \*\* $p < 0.01$ , \*\*\* $p < 0.001$ , \*\*\*\* $p < 0.0001$ ).

## 2.9 Materials

The following table lists all the materials and important machines used for the presented thesis. Tables for used QuantiTect Primer Assays and DuoSet<sup>®</sup> ELISA Development Systems are shown separately in the corresponding qPCR (section 2.5.3) and ELISA (section 2.5.4) sections.

**Table 2.5:** List of materials used for the presented thesis.

Material	Company
Leupeptin hemisulfate salt	Sigma-Aldrich, Steinheim, Germany
Aprotinin from bovine lung	Sigma-Aldrich
Calcein-AM	Sigma-Aldrich
Propidium Iodide solution	Sigma-Aldrich
Glutaraldehyde	Sigma-Aldrich
Fetal bovine serum	Sigma-Aldrich
L-ascorbic acid 2-phosphate	Sigma-Aldrich
Dexamethasone	Sigma-Aldrich
$\beta$ -glycerophosphate	Sigma-Aldrich
Triton <sup>TM</sup> X-100	Sigma-Aldrich
Hoechst 33258	Sigma-Aldrich
Fluoromount <sup>TM</sup>	Sigma-Aldrich
Phalloidin-TRITC	Sigma-Aldrich
anti-rat IgG-ALP	Sigma-Aldrich
BCIP/NBT liquid substrate	Sigma-Aldrich
Fucoidan $\geq 95\%$ <sup>1</sup>	Sigma-Aldrich
Fucoidan crude <sup>1</sup>	Sigma-Aldrich
Endothelial Basal Medium-2	Promocell, Heidelberg, Germany
Endothelial growth medium-2 supplements	Promocell
Biocoll	Biochrom, Berlin, Germany
Dulbecco's Modified Eagle's Medium/Ham's F-12	Biochrom
Penicillin/Streptomycin	gibco, Grand Island NY, USA
Phosphate buffered saline	gibco

---

<sup>1</sup>for further information see Table 2.2

**Table 2.5:** List of all materials used for the presented thesis (continued).

Material	Company
Rat tail collagen type-I	Corning, Bedford, MA, USA
Fibronectin	Millipore, Temecula, CA, USA
Bovine serum albumin	Millipore
Alizarin Red S Stain Solution	Millipore
Proteinase K	Carl Roth GmbH, Karlsruhe, Germany
Cetylpyridinium chloride	Carl Roth GmbH
Acetic acid 100 %	Carl Roth GmbH
Tris Ultra Qualität $\geq 99.9$ %	Carl Roth GmbH
VEGF-165	biomol, Hamburg, Germany
Low fat milk powder	Bio-Rad, Hercules, CA, USA
Cellic <sup>®</sup> CTec2 cellulase	Novozymes, Bagsværd, Denmark
EDTA disodium	Serva, Heidelberg, Germany
Endolisa kit	Hyglos GmbH, Bernfried am Starnberger See, Germany
Pierce LDH Cytotoxicity Assay Kit	Thermo Scientific, Rockford, IL, USA
CellTiter 96 AQueous Solution Cell Proliferation Assay	Promega, Madison, WI, USA
Alkaline Phosphatase Assay Kit	abcam, Cambridge, UK
peqGOLD Total RNA kit	VWR, Leuven, Belgium
DNase I	VWR
High-Capacity RNA-to-cDNA <sup>TM</sup> Kit	Applied Biosystems, Vilnius, Lithuania
SYBR <sup>TM</sup> Select Master Mix	Applied Biosystems
SYBR Gold nucleic acid gel stain	invitrogen, Eugene, OR, USA
Quant-iT <sup>TM</sup> PicoGreen <sup>TM</sup> dsDNA Assay Kit	invitrogen
AlexaFluor647/anti-rat (A21247)	invitrogen
AlexaFluor488/anti-goat (A11055)	invitrogen
BAM-1	SeaProbes, Roscoff, France
BAM-4	SeaProbes
DuoSet <sup>®</sup> ELISA Development Systems <sup>2</sup>	R&D Systems, Minneapolis, USA
VE-cadherin antibody (AF938)	R&D
QuantiTect Primer Assays <sup>3</sup>	Qiagen, Hilden, Germany
Angiogenesis $\mu$ -slides	Ibidi, Gräfelfing, Germany

<sup>2</sup>for further information see Table 2.4<sup>3</sup>for further information see Table 2.3

**Table 2.5:** List of all materials used for the presented thesis (continued).

Material	Company
8-well $\mu$ -slides	Ibidi
Thermanox coverslips	Nunc, Rochester, NY, USA
Paraformaldehyde	Morphisto, Frankfurt am Main, Germany
Chitosan 95/100 <sup>4</sup>	Heppe Medical Chitosan GmbH, Halle, Germany
Ethanol, absolute for analysis	Merck, Darmstadt, Germany
InLab Micro Pro-ISM pH electrode	Mettler-Toledo GmbH, Gießen, Germany
Rotor-GeneQ	Qiagen
infinite M200 Pro plate reader	Tecan, Männedorf, Switzerland
CVO 120 HRNF plate-to-plate rheometer	Bohlin Instruments, Pforzheim, Germany
Evos FL Auto 2 fluorescence microscope	Thermo Fisher Scientific, Massachusetts, USA
Confocal laser scanning microscope LSM 800	Zeiss, Jena, Germany
Supra 55VP	Zeiss
S-4800	Hitachi, Tokio, Japan

---

<sup>4</sup>for the Certificate of Analysis see Appendix A.3

# 3

## Results I

---

*This chapter investigates the biological effect of four enzymatically-extracted fucoidans (FE\_crude, FE\_F1, FE\_F2, FE\_F3) in cell culture models relevant for bone regeneration. Fucoidan extracts were chemically characterized and structural properties were associated with bioactivities. The most important findings are summarized in the following publication:*

**Effect of Enzymatically Extracted Fucoidans on Angiogenesis and Osteogenesis in Primary Cell Culture Systems Mimicking Bone Tissue Environment.**

Julia Ohmes, Yuejun Xiao, Fanlu Wang, Maria Dalgaard Mikkelsen, Thuan Thi Nguyen, Harald Schmidt, Andreas Seekamp, Anne S. Meyer and Sabine Fuchs (2020). *Mar. Drugs* 18, 481

### Contents

---

<b>3.1</b>	<b>Chemical Characterization of Enzymatically-Extracted Fucoidans . . . . .</b>	<b>44</b>
<b>3.2</b>	<b>Tolerance of OEC and MSC Towards Enzymatically-Extracted Fucoidans . . . . .</b>	<b>45</b>
<b>3.3</b>	<b>Angiogenesis, Osteogenesis and Inflammation in Mono-cultures</b>	<b>47</b>
<b>3.4</b>	<b>Angiogenesis in MSC-OEC Co-cultures . . . . .</b>	<b>53</b>

---

### 3.1 Chemical Characterization of Enzymatically-Extracted Fucoidans

Fucoidan extracts were isolated from *F. evanescens* using an enzyme-assisted extraction technique. The crude extract (FE\_crude) was released by digesting cell wall components with cellulases and alginate lyases. Afterwards, it was purified by IEX to obtain the three fucoidan fractions FE\_F1 (eluted first), FE\_F2 (eluted second) and FE\_F3 (eluted third). The extraction process is schematically illustrated in Figure 2.1.

**Table 3.1:** Chemical characterization of enzymatically-extracted fucoidans FE\_crude, FE\_F1, FE\_F2 and FE\_F3 including monosaccharide composition, sulfate content, molecular weight, total phenolic and total protein content. For further details see publication [130].

		FE_crude	FE_F1	FE_F2	FE_F3
Neutral sugars [%mol]	Fucose	24.8±2.9	34±3.1	74.7±0.8	87.8±1.4
	Rhamnose	0.2±0.1	0.3±0.1	0.8±0.1	0.5±0.1
	Galactose	0.9±0.1	4.6±0.4	15.4±0.4	9.0±0.9
	Glucose	0.7±0.1	7.7±0.7	1.4±0.1	0.3±0.1
	Xylose	0.8±0.1	5.3±0.5	2.8±0.1	1.5±0.3
	Mannose	0.4±0.0	3.2±0.5	2.3±0.1	0.3±0.1
Uronic acid [%mol]	GluA	1.0±0.2	3.8±0.3	0.3±0.0	0.5±0.1
	ManA	58.4±2.6	32.2±0.6	0.2±0.0	0.0±0.0
	GuluA	12.6±1.8	9.1±0.5	2.2±0.2	0.0±0.0
Sulfate content	SO <sub>4</sub> <sup>2-</sup> [%]	21.7±0.5	20.4±3.4	34.8±2.0	38.7±1.0
	SO <sub>4</sub> <sup>2-</sup> :Fuc <sup>1</sup>	1.4	0.8	1.0	1.0
Molecular weight	Range [kDa]	12-800 <sup>2</sup>	12-800 <sup>2</sup>	12-800	110-800
	Peak [kDa]	~400	~40, ~400	~40, ~600	~600
Total phenolic content [GAE/g]		5.19±0.07	2.93±0.11	3.02±0.02	0.76±0.04
Total protein content [%]		≤0.15	≤0.15	≤0.15	≤0.15

<sup>1</sup> weight ratio

<sup>2</sup> contains an additional alginate oligosaccharide peak at 2-3 kDa

Fucose was the most represented neutral sugar in the fucoidan extracts. The crude extract contained 25 % fucose and a high portion of alginate, in total 59 % (mainly manuronic acid). IEX purification reduced the alginate and increased the fucose content. FE\_F1, FE\_F2 and FE\_F3 contained 34 %, 75 % and 88 % fucose, respectively. The alginate content was reduced from 36 % in FE\_F1 to 0.5 % in FE\_F3. All other quantified

sugars represented 15 % or less (FE\_F2 had the highest galactose content with 15 %, the highest glucose content was quantified for FE\_F1 with 8 %) of the total monosaccharide content. IEX purification also reduced the polyphenolic content from 5 GAE/g in the crude extract to 0.8 GAE/g in FE\_F3. The third eluted fucoidan fraction FE\_F3 can be defined as very pure, taking high fucose and low alginate and polyphenolic contents as measures for purity. The total sulfate content ranged between 22 and 39 % and was highest for FE\_F3. All extracts are defined as high molecular weight fucoidans with peaks around 400 and 600 kDa. The protein content was  $\leq 0.15$  % for all extracts and therefore negligibly low. Further information regarding the process of enzyme-assisted extraction and chemical characterizations can be found in [130].

## 3.2 Tolerance of OEC and MSC Towards Enzymatically-Extracted Fucoidans

To study whether fucoidan treatment affected the metabolic activity and the membrane integrity of MSC and OEC, MTS and LDH assays were applied. MSC and OEC monocultures were treated with FE\_crude, FE\_F1, FE\_F2 and FE\_F3. LDH, as well as MTS assays were performed on day one, three and seven. The metabolic activity of OEC was slightly increased on day one after fucoidan treatment as shown in Figure 3.1 A). On day three and seven, however, the metabolic activity decreased to control level. The control fucoidan substances from Sigma Aldrich FV\_crude and FV\_pure were slightly more toxic to OEC on all sampled days. As visible in Figure 3.1 B), MSC reacted more sensitive to fucoidan treatment. The metabolic activity was significantly decreased on day three and seven when MSC were treated with fucoidan concentrations ranging from 10 to 200  $\mu\text{g}/\text{ml}$ . The decrease was highest when MSC were treated with the pure extract FE\_F3. Treatment with FE\_crude and FV\_pure, however, did not affect the metabolic activity. High fucoidan concentrations, especially 200  $\mu\text{g}/\text{ml}$ , affected the metabolic activity most in both, OEC and MSC.

The LDH release of OEC was equally decreased after fucoidan treatment on all sampled days. The LDH release of MSC was at control level on day one and three, but got decreased on day seven. Higher fucoidan concentrations had only a minor effect on the LDH release. These results indicate that fucoidan treatment is not toxic to OEC or MSC, even though the metabolic activity was slightly impaired by some extracts and concentrations.

To exclude that fucoidan treatment had a significant effect on MSC proliferation, the DNA amount was quantified after seven days of treatment. Figure 3.2 demonstrates that, although higher FE\_F2 and FE\_F3 concentrations slightly reduced the amount of DNA, fucoidan treatment did not have a significant impact on MSC proliferation.

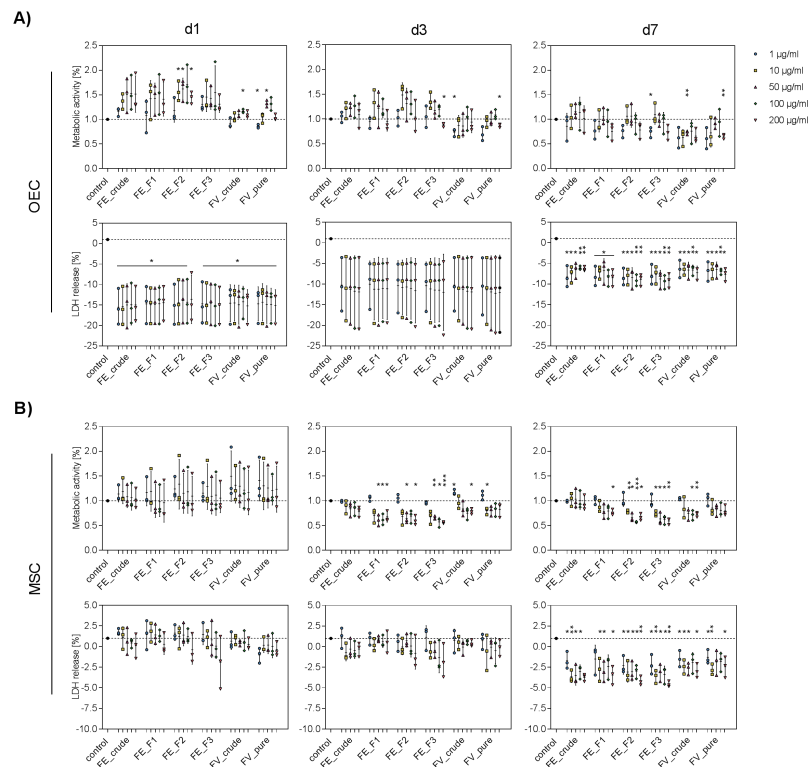


**Figure 3.1:** Membrane integrity and metabolic activity of OEC and MSC mono-cultures after treatment with enzymatically-extracted fucoidans. A) OEC and B) MSC were treated with 1, 10, 50, 100 and 200  $\mu\text{g}/\text{ml}$  fucoidan. MTS and LDH assays were performed on day one, three and seven. Significances (compared to the control) were calculated with Welch's t-test.

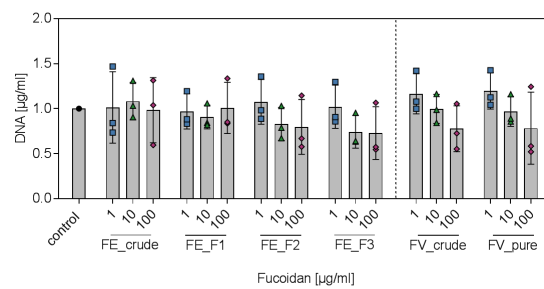


**Figure 3.2:** MSC proliferation measured by the amount of DNA after treatment with enzymatically-extracted fucoidans. MSC were treated with 1, 10 and 100  $\mu\text{g}/\text{ml}$  fucoidan. The DNA was quantified after seven days.

### 3.3 Angiogenesis, Osteogenesis and Inflammation in Mono-cultures

To reveal the effect of different enzymatically extracted fucoidan extracts on angiogenic, osteogenic and inflammatory processes in MSC and OEC mono-cultures, expression and protein production of relevant mediators were quantified. Further, ALP activity and the level of calcification were determined, as well as the interaction of fucoidan with VEGF and the effect of fucoidan on VEGF receptor 2 activation.

#### 3.3.1 Angiogenic signaling molecules VEGF, ANG-1 and SDF-1 in MSC

Figure 3.3 shows the gene expression and protein levels of VEGF, ANG-1 and SDF-1, important angiogenic signaling molecules which are mainly produced by MSC. Treatment with FE\_F1 and FE\_F2 reduced the expression of VEGF in MSC compared to the control. Even though not significant, FE\_F3 tentatively reduced VEGF gene expression as well (Figure 3.3 A)). The gene expression of ANG-1 was slightly downregulated by treatment with the control extracts FV\_crude and FV\_pure, but not affected by the extracts from *F. evanescens* (Figure 3.3 B)). Gene expression of SDF-1 was almost completely downregulated after treatment with FE\_F2 and FE\_F3 (Figure 3.3 C)). VEGF, ANG-1 and SDF-1 protein levels were similarly affected by the extracts: The higher the extract purity, the lower were the detected protein levels. FE\_F2 and FE\_F3 decreased VEGF, ANG-1 and SDF-1 to 50 % or more compared to the control cells.

#### 3.3.2 Early and late osteogenic markers in MSC

The gene expression of ALP in MSC, as well ALP activity after seven days were taken as references for early osteogenic processes. The calcification progress in MSC after 14 days was taken as a marker for late osteogenesis. How fucoidan treatment affected early and late osteogenic events is shown in Figure 3.4. Gene expression of ALP was almost completely downregulated after treatment with FE\_F1, FE\_F2 and FE\_F3, while the ALP activity was not affected by fucoidan treatment. (Figure 3.4 A)). Alizarin red staining revealed that the pure extracts FE\_F2 and FE\_F3 did not only interfere with early osteogenic processes, but also affected the calcification level, which serves as an indicator for late osteogenesis. Calcification stainings were three times lower after FE\_F2 and FE\_F3 treatment than the control stainings (Figure 3.4 B)).

#### 3.3.3 Influence of fucoidan concentration on angiogenic and osteogenic mediators

Figure 3.5 shows that the concentration of fucoidan treatment had a clear effect on VEGF, ANG-1 and SDF-1 protein levels. The higher the applied fucoidan concentration, the lower were the detected protein levels. Interestingly, low fucoidan concentrations (1 and 10  $\mu\text{g}/\text{ml}$ ) decreased the ALP activity, while treatment with 100  $\mu\text{g}/\text{ml}$  fucoidan had

no significant effect.

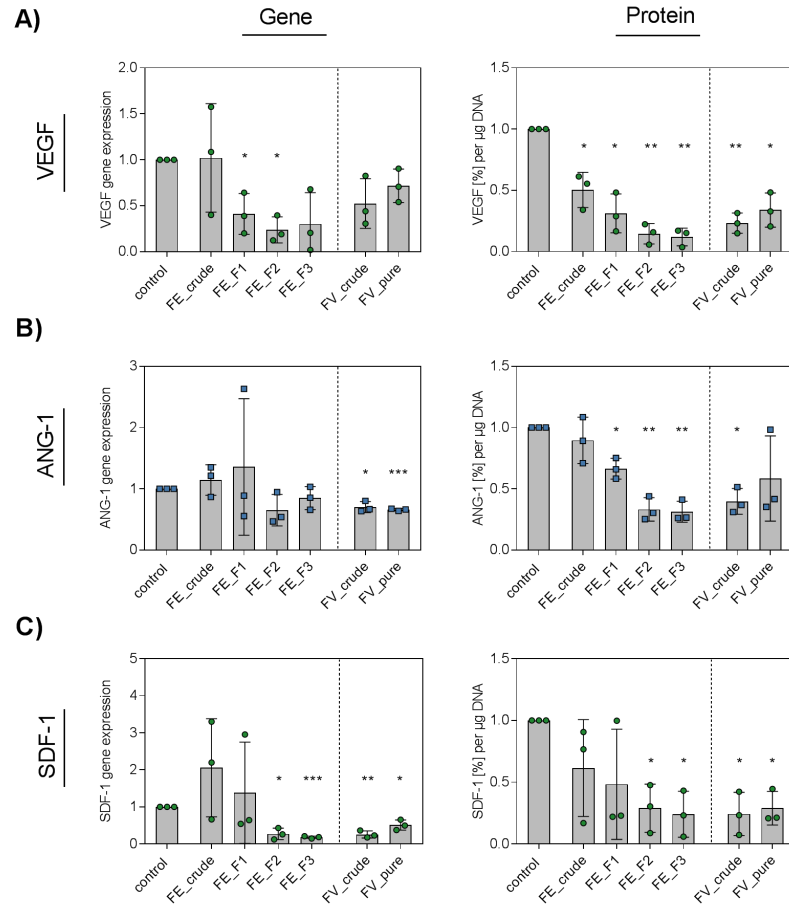


**Figure 3.3:** Expression and protein level of angiogenic mediators in MSC mono-culture after treatment with enzymatically-extracted fucoidans. MSC were treated with  $100 \mu\text{g/ml}$  fucoidan. After seven days, gene expression and protein levels in the supernatant of A) VEGF, B) ANG-1 and C) SDF-1 were quantified using qPCR and ELISA, respectively. Significances (compared to the control) were calculated with Welch's t-test.

### 3.3. Angiogenesis, Osteogenesis and Inflammation in Mono-cultures

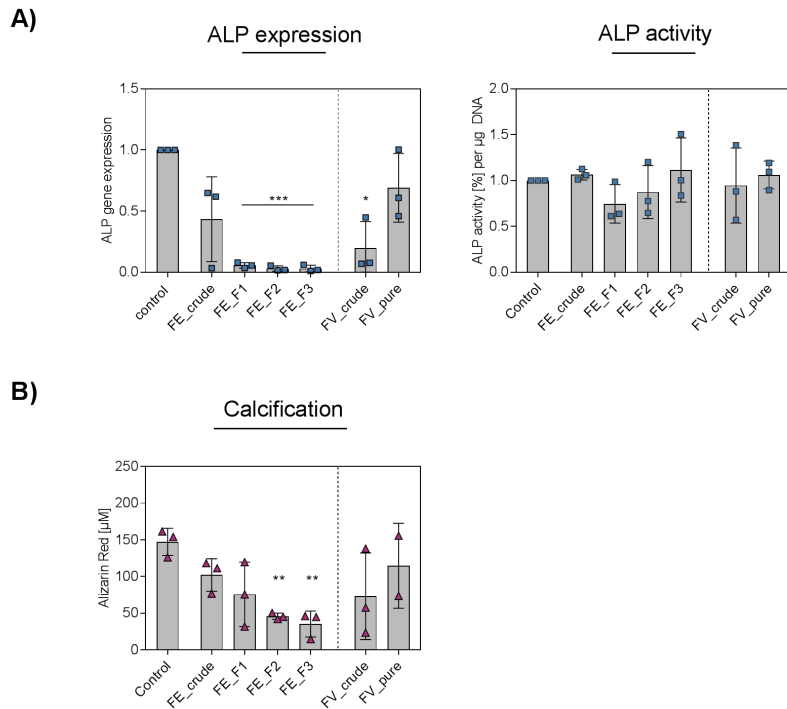


**Figure 3.4:** Early and late osteogenic markers in MSC mono-culture after treatment with enzymatically-extracted fucoidans. MSC were treated with 100  $\mu$ g/ml fucoidan. After seven days, A) ALP gene expression and activation were quantified as early osteogenic markers. C) The level of calcification using alizarin red staining was determined as a late marker for osteogenesis. Significances (compared to the control) were calculated with Welch's t-test.

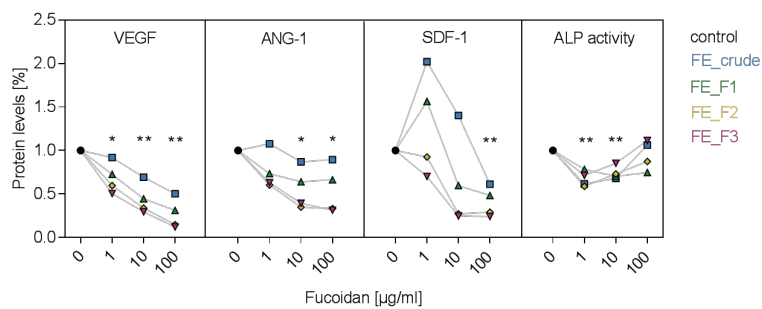


**Figure 3.5:** Effect of fucoidan concentration on angiogenic proteins and ALP activity in MSC mono-culture. MSC were treated with 1, 10 and 100  $\mu$ g/ml fucoidan. After seven days, protein levels of VEGF, ANG-1 and SDF-1 were quantified from the supernatant using ELISA. Additionally, ALP activity was determined after seven days. Significances (compared to the control) were calculated with Welch's t-test.

### 3.3.4 Affinity of fucoidan to VEGF & impact on VEGFR2 phosphorylation

The consistent results from the prior sections demonstrate that treatment with the pure extracts FE\_F2 and FE\_F3 negatively affected angiogenic and osteogenic processes in MSC mono-cultures. A simple ELISA set-up was used to address the question whether the tested fucoidan extracts were able to bind to growth factors like VEGF and therefore influence the available protein levels. Figure 3.6 shows that already small fucoidan concentrations decreased the available VEGF amount. The detected VEGF concentration was approximately three times lower after mixing with fucoidan than the control solution that did not contain fucoidan. The higher the mixed fucoidan concentration was, the lower were the detected VEGF levels.

To address whether the decreased VEGF levels due to fucoidan treatment had an effect on VEGF receptor 2 activation in OEC, the VEGFR2 phosphorylation was quantified in relation to the total amount of VEGFR2. Therefore, OEC were treated with fucoidan and stimulated with VEGF-165 simultaneously for 15 min. The results for VEGFR2 and phosphorylated VEGFR2 ELISAs are shown in Figure 3.7. The amount of total VEGFR2 was similar in all OEC and only minimally decreased in FE\_F1-treated cells (Figure 3.7 left). VEGF-165 treatment resulted in an increase of VEGFR2p by approximately 75 %, proving that VEG-165 stimulation was successful. FE\_F1- and FE\_F2-treated OEC had slightly decreased levels of VEGFR2p (Figure 3.7 middle). In relation to the total amount of VEGFR2 however, only FE\_crude treatment decreased the receptor phosphorylation significantly (Figure 3.7 right). These results indicate that fucoidan treatment had no or only minor effects on the phosphorylation of VEGFR2 in OEC.

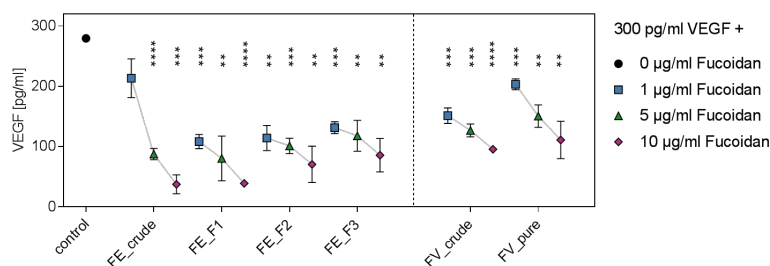


**Figure 3.6:** Interaction of enzymatically-extracted fucoidan with growth factor VEGF. 300pg/ml VEGF was mixed with 1, 5 and 10 µg/ml fucoidan. To measure the available amount of VEGF after mixture, an ELISA assay was applied. Significances (compared to the control) were calculated with Welch's t-test.

### 3.3. Angiogenesis, Osteogenesis and Inflammation in Mono-cultures

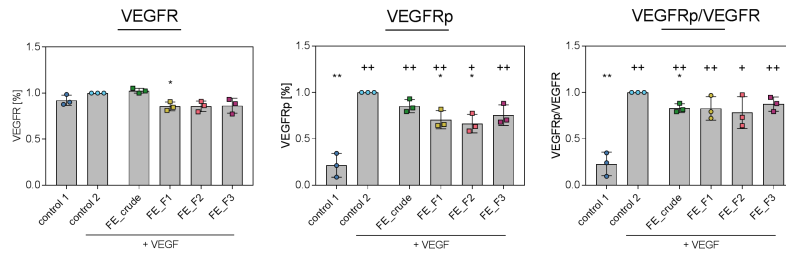


**Figure 3.7:** Phosphorylation of VEGF receptor 2 in relation to the total amount of VEGFR2 in OEC after treatment with enzymatically-extracted fucoidan. OEC were treated with 100  $\mu\text{g}/\text{ml}$  fucoidan and VEGFR2 phosphorylation was simultaneously stimulated by applying 100 ng/ml VEGF-165. Cells were harvested after 15 min and ELISAs for VEGFR2 and VEGFR2p were performed. Control cells 1 were cultured in regular medium and not treated with fucoidan, nor stimulated with VEGF-165. Control cells 2 were stimulated with VEGF-165, but not treated with fucoidan. Significances compared to control 1 (+) and to control 2 (\*) were calculated with Welch's t-test.

#### 3.3.5 Inflammatory and angiogenic signaling molecules in OEC

Endothelial cells are the main building elements of blood vessels. They migrate and reorganize during angiogenesis, but they also guide inflammatory reactions by sequestration of immune cells via cytokine release and expression of adhesion molecules. An acute inflammatory response is always one of the first steps to trigger angiogenic processes. Figure 3.8 reveals how fucoidan treatment affected the expression and extracellular levels of cytokines, adhesion molecules and angiogenic mediator ANG-2 in OEC mono-cultures. Treatment with the crude extracts FE\_crude and FE\_F1 tentatively increased gene expressions and protein levels of IL-6 and ICAM-1. However, treatment with the pure extracts FE\_F2 and FE\_F3 decreased gene expression of IL-6, ICAM-1 and VCAM-1 significantly. On protein level, this observed effect was not visible. IL-6 and ICAM-1 remained at control level after fucoidan treatment. The gene expression of ANG-2, an important angiogenic mediator, was not affected by fucoidan treatment, while protein levels were decreased after treatment with all tested fucoidan extracts, except for FE\_crude. These results indicate that the crude fucoidan extracts caused a pro-inflammatory reaction in OEC, the pure extracts, however suppressed an inflammatory response. To make a final statement about the impact of these fucoidan extract on inflammatory processes, the data shown is not sufficient. The anti-inflammatory potential of FE\_F3 was extensively investigated in a study by Kirsten et al. (manuscript in preparation).

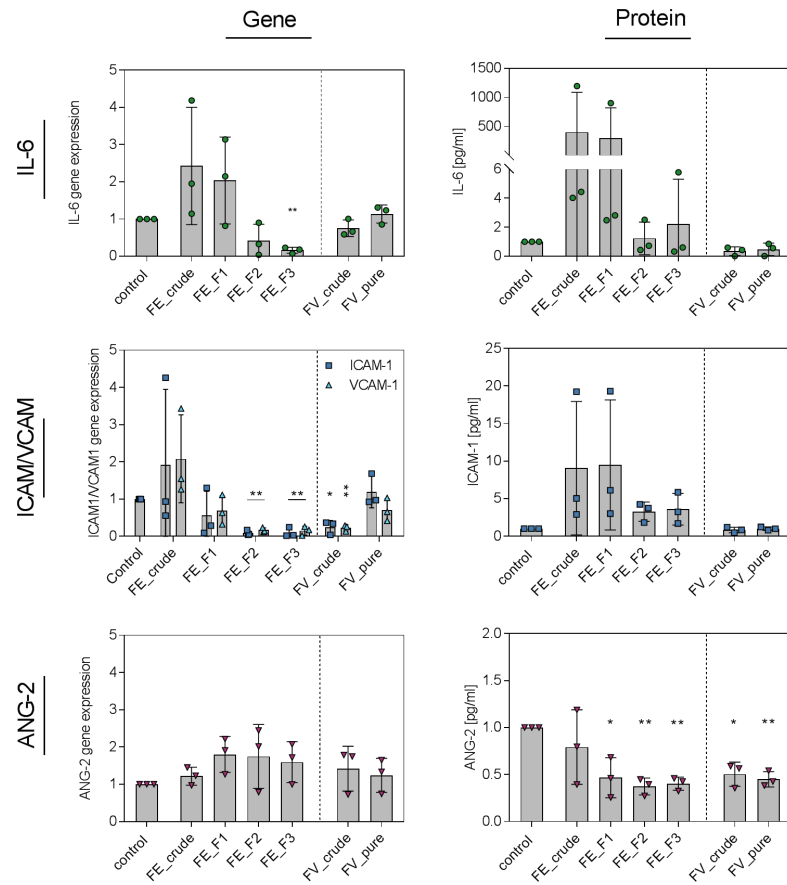


**Figure 3.8:** Expression and protein level of inflammatory and angiogenic mediators in OEC mono-culture after treatment with enzymatically-extracted fucoidans. OEC were treated with  $100\ \mu\text{g}/\text{ml}$  fucoidan. After seven days, gene expression and protein levels of IL-6, ICAM-1, VCAM-1 and ANG-2 were quantified using qPCR and ELISA, respectively. Significances (compared to the control) were calculated with Welch's t-test.

## 3.4 Angiogenesis in MSC-OEC Co-cultures

In MSC-OEC co-cultures, both cell types are able to interact. Past studies have shown that MSC-OEC co-cultures are suitable model systems to monitor the development of primitive tube-like angiogenic structures. These models offer the possibility to investigate the effect of fucoidan treatment on a functional level.

### 3.4.1 Development of angiogenic structures

To study the influence of fucoidan on the development of angiogenic structures, MSC and OEC were co-cultured, treated with fucoidan for seven days and afterwards stained for endothelial marker VE-cadherin. All co-cultures developed angiogenic tube-like structures as shown in figures 3.9 A). However, the amount of structures was highly reduced in co-cultures treated with the fucoidan fractions FE\_F1, FE\_F2 and FE\_F3. The quantification of number, length and area of the angiogenic structures revealed that treatment with 10 and 100  $\mu\text{g}/\text{ml}$  FE\_F1, FE\_F2 and FE\_F3 reduced the number of structures significantly (Figure 3.9 B)). Length and area of the angiogenic skeleton were significantly reduced after treatment with FE\_F3. These results suggest that all tested fucoidan fractions impaired the formation of angiogenic tube-like structure. Pure extracts however, suppressed the development most.

### 3.4.2 Angiogenic signaling molecules in MSC-OEC co-cultures

To reveal more details about the anti-angiogenic effect of the fucoidan fractions in MSC-OEC co-cultures, cells were treated with 10 and 100  $\mu\text{g}/\text{ml}$  fucoidan and VEGF, SDF-1, ANG-1 and ANG-2 protein levels were quantified on day four and seven in the supernatant. Additionally on day seven, the gene expressions of the mentioned signaling molecules were quantified from co-cultures which were treated with 100  $\mu\text{g}/\text{ml}$  fucoidan. Figure 3.10 shows that on day four, protein levels from fucoidan-treated co-cultures were not different to control levels, except for ANG-2. Similar to the OEC mono-cultures, ANG-2 levels were decreased with increasing purity of the extracts. On day seven, very similar to day four, ANG-2 levels were decreased most in co-cultures treated with the pure extracts. ANG-1 and SDF-1 protein levels increased from day four to day seven, but fucoidan treatment did not change the levels relatively to the control. VEGF levels were barely detectable on day four. The VEGF protein amount increased on day seven compared to day four. Different to the MSC mono-cultures, VEGF levels were higher in fucoidan-treated cells than in control cells. 100  $\mu\text{g}/\text{ml}$  fucoidan treatment had no significant impact on the gene expression of all tested signaling molecules.

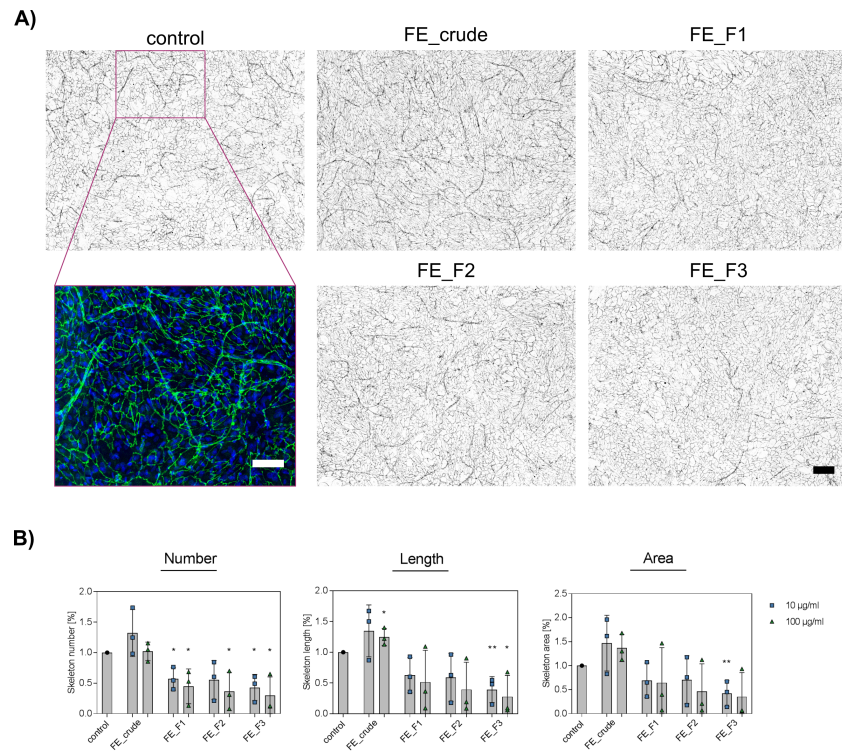


**Figure 3.9:** Development of angiogenic tube-like structures in MSC-OEC co-cultures after treatment with enzymatically-extracted fucoidans. Co-cultures were treated with 10 and 100  $\mu\text{g}/\text{ml}$  fucoidan for seven days. After seven days, cells were stained for VE-cadherin and nuclei. A) Exemplary microscopy pictures of co-cultures with angiogenic structures. Images were inverted and displayed in grey values. A close-up of developed angiogenic structures is shown in the purple frame (VE-cadherin in green, nuclei in blue, scale bars=200  $\mu\text{m}$ ). B) Quantification of angiogenic skeleton number, length and area. 27 frames in total were analyzed for each donor pair. Significances (compared to the control) were calculated with Welch's t-test.

### 3.4. Angiogenesis in MSC-OEC Co-cultures

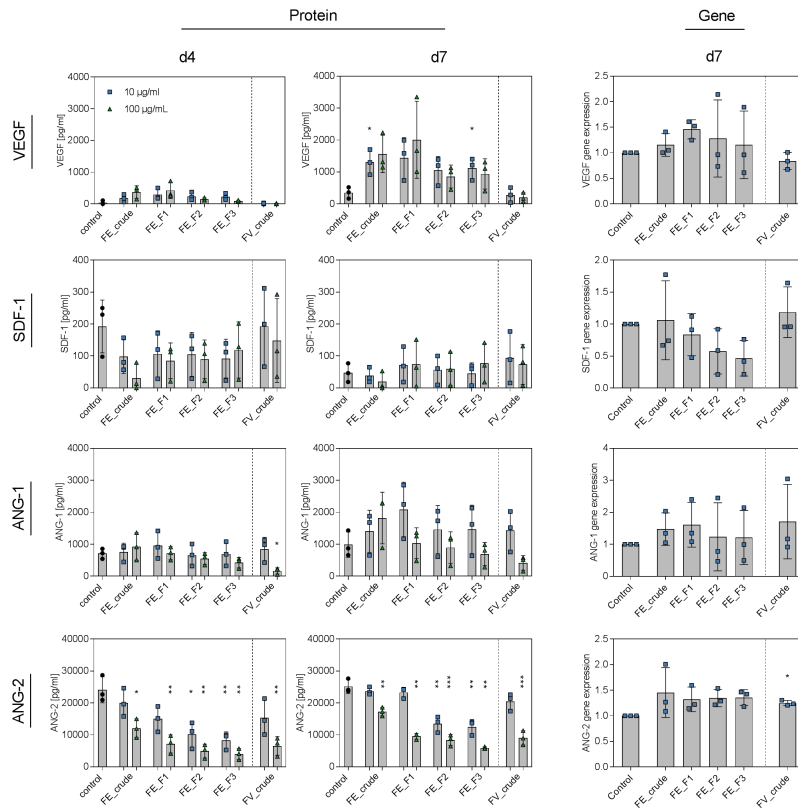


**Figure 3.10:** Expression and protein level of angiogenic mediators in MSC-OEC co-cultures after treatment with enzymatically-extracted fucoidans. For protein level quantification using ELISA, co-cultures were treated with 10 and 100  $\mu\text{g}/\text{ml}$  fucoidan for four and seven days. For gene expression analysis via qPCR, co-cultures were treated with 100  $\mu\text{g}/\text{ml}$  fucoidan for seven days. Significances (compared to the control) were calculated with Welch's t-test.

Figure 3.11 shows the expression of additional genes which play a role in angiogenic and osteogenic processes. ALP functions as a marker for early osteogenesis as explained before, MMPs degrade the ECM, so that new blood vessel can be established. While the gene expression of common mediators such as VEGF and angiopoietins was not influenced by fucoidan treatment as shown before, expressions of ALP and MMP-14 were decreased after treatment with the pure extracts FE\_F2 and FE\_F3. Similar to the mono-culture experiments, purer extracts exhibited stronger effects on the tested cell model systems.

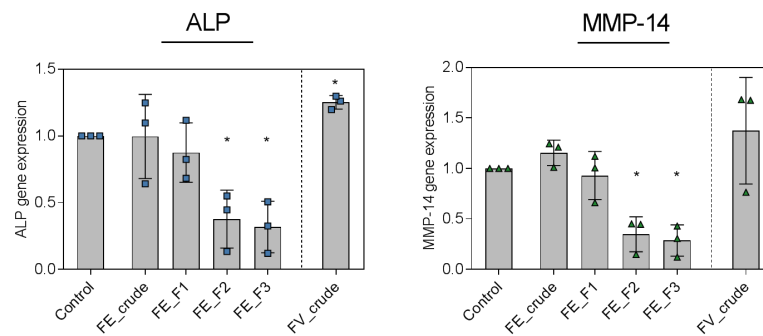


**Figure 3.11:** Gene expression of ALP and MMP-14 in MSC-OEC cocultures after treatment with enzymatically-extracted fucoidans. Cells were treated with 100  $\mu\text{g}/\text{ml}$  fucoidan and gene expression was quantified on day seven using qPCR. Significances (compared to the control) were calculated with Welch's t-test.

# 4

## Results II

---

*This chapter investigates how bioactivities of fucoidan extract FE\_F3 change after defined cleavage by fucoidanase Fhf1. The chemical properties, as well as the biological effect of medium (MMW) and low molecular weight (LMW) fucoidans obtained after enzymatic degradation were compared to high molecular weight FE\_F3 in cell culture models relevant for bone regeneration. The most important findings are summarized in the following publication:*

**Depolymerization of Fucoidan with Endo-Fucoidanase Changes Bioactivity in Processes Relevant for Bone Regeneration.** Julia Ohmes, Maria Dalgaard Mikkelsen, Thuan Thi Nguyen, Vy Ha Nguyen Tran, Sebastian Meier, Mads Suhr Nielsen, Ming Ding, Andreas Seekamp, Anne S. Meyer and Sabine Fuchs (2022) *Carbohydr. Polym.* 286

### Contents

---

4.1	Chemical Characterization of MMW and LMW . . . . .	58
4.2	Tolerance of OEC Towards MMW and LMW . . . . .	60
4.3	Angiogenesis and Inflammation in Mono-cultures . . . . .	61
4.4	Angiogenesis and Inflammation in MSC-OEC Co-cultures . .	65
4.5	Interaction of Fucoidan Extracts with MSC and OEC . . . .	68

---

## 4.1 Chemical Characterization of MMW and LMW

Fucoidan extracts were isolated from *F. evanescens* using an enzyme-assisted extraction technique. The crude (FE\_crude) extract was purified by IEX to obtain the three fucoidan fractions FE\_F1 (eluted first), FE\_F2 (eluted second) and FE\_F3 (eluted third). As shown in the prior section, FE\_F3 was the purest fraction and exhibited the strongest anti-angiogenic effect in MSC and OEC cultures. Further details on the bioactivities of the obtained fucoidan fractions can be found in [133]. HMW FE\_F3 was chosen as the substrate for hydrolysis, catalyzed by the recently discovered endo-fucoidanase Fhf1. Fhf1 cleaves  $\alpha$ -(1,4)-glycosidic bonds between non-acetylated and C2-monosulfated units in fucoidans with alternating  $\alpha$ -(1,3)-/ $\alpha$ -(1,4)-linked L-fucopyranosyls yielding LMW oligosaccharides and a MMW fraction [179]. The extraction process is schematically illustrated in Figure 2.1.

### 4.1.1 Monosaccharide composition, molecular weight, sulfate, polyphenolic and protein content

After extraction, MMW and LMW were chemically characterized. Table 4.1 lists monosaccharide composition, sulfate content, molecular weight, total phenolic and protein content of the extracts. For a better comparison, the chemical characterization of HMW FE\_F3 was added to the table as well. All extracts were mainly composed of fucose (>87 %). The compositional analysis showed that LMW was devoid of other monosaccharides. The galactose content in MMW (8 %) was comparable to the galactose content in HMW FE\_F3. Apart from galactose, MMW, as well as HMW FE\_F3 did not contain large amounts of other monosaccharides. The alginate content was negligibly low in all extracts. The overall sulfate content was lower in the LMW (~34 %) compared to the MMW fucoidan (~50 %). These results are consistent with the specificity of Fhf1 fucoidanase, which cleaves mono-sulfated fucosyl residues, leaving the disulfated residues in the MMW fraction, thus resulting in a higher sulfate content in the MMW compared to the LMW fraction. The total phenolic content and the protein content were <1.5 GAE/g and <0.6 %, respectively.

High-performance size exclusion chromatography was performed to estimate the molecular weight of the extracts. While HMW FE\_F3 had a peak at around 600 kDa, it can be categorized as a high molecular weight fucoidan. The hydrolysis product MMW is a medium molecular weight fucoidan with two peaks around 10 and 209 kDa. The LMW fraction contains oligosaccharides with a mean size of 2 kDa and therefore belongs to the group of low molecular weight fucoidans.

### 4.1.2 Chemical structures of MMW and LMW

NMR spectroscopy was applied to determine the chemical structures of MMW and LMW. The MMW fucoidan extract consisted of a repetitive and regular polysaccharide that was largely devoid of acetylation. It was disulfated in  $\rightarrow$ 3)- $\alpha$ -L-Fucp2,4-di-S-(1 $\rightarrow$  units

(Figure 4.1 A). The LMW extract was an oligosaccharide which predominantly consisted of tetrasaccharides, sulfated only at C2 of each fucose unit and C3-acetylated at the  $\rightarrow 4$ - $\alpha$ -L-Fucp2S,3OAc-(1 $\rightarrow$  residue adjacent to the reducing end (Figure 4.1 B)). In order to gain additional insights into the architecture of the fucoidan fractions, NMR spectra were further evaluated (see Supplementary Figure A.1). The evaluation showed that MMW contained signals that are consistent with the presence of  $\rightarrow 3,4$ - $\alpha$ -L-Fucp(2-SO<sub>3</sub><sup>-</sup>)-(1 $\rightarrow$ 3)- residues (Clément et al., 2010) at low density of approximately 2.4% on monomer basis (approximately one in 40 units). In contrast, branching could not be identified in the LMW fraction. The sulfate content deriving from the structures (higher sulfate content in MMW than in LMW) was consistent with the results from the titrimetric BaCl<sub>2</sub> sulfate quantification.

**Table 4.1:** Chemical characterization of fucoidanase hydrolysis products MMW and LMW including monosaccharide composition, sulfate content, molecular weight, total phenolic and total protein content. Chemical properties of HMW FE\_F3 were added for an easier comparison.

		HMW FE_F3	MMW	LMW
Neutral sugars [%mol]	Fucose	87.34±0.71	87.09±0.85	97.42±0.08
	Rhamnose	0.48±0.11	0.87±0.06	0.12±0.00
	Galactose	8.47±0.33	7.9±0.52	1.15±0.04
	Glucose	0.32±0.04	0.39±0.03	0.07±0.00
	Xylose	1.59±0.38	2.65±0.17	1.23±0.04
	Mannose	0.36±0.08	nd	nd
Uronic acid [%mol]	GluA	0.68±0.14	0.77±0.05	nd
	ManA	0.74±0.16	nd	nd
	GuluA	nd	0.32±0.02	nd
Sulfate content	SO <sub>4</sub> <sup>2-</sup> [%]	37.6±1.6	49.6±3.14	33.6±3.37
	SO <sub>4</sub> <sup>2-</sup> :Fuc <sup>1</sup>	0.9	1.1	0.9
Molecular weight [kDa]		400-500	10, 209	2
Total phenolic content [GAE/g]		0.81±0.05	1.39±0.11	0.73±0.09
Total protein content [%]		0.22±0.07	0.59±0.02	0.06±0.01

<sup>1</sup> weight ratio  
nd = not detectable

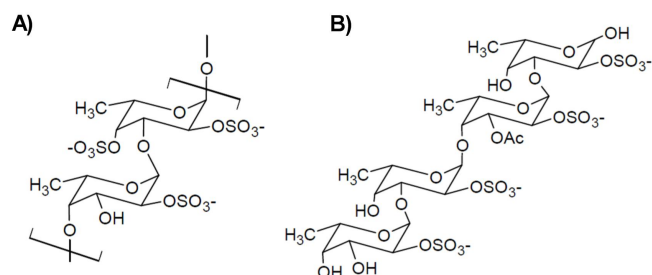


**Figure 4.1:** Chemical structures of fucoidanase Fhf1 hydrolysis products A) MMW and B) LMW. The structures were generated based on NMR analysis.

## 4.2 Tolerance of OEC Towards MMW and LMW

To study the effect of MMW and LMW on the membrane integrity in OEC, a LDH assay was performed after seven days of treatment. As shown in Figure 4.2, fucoidan treatment slightly decreased the release of LDH compared to the control cells. These results indicate that treatment with 10 and 100  $\mu\text{g}/\text{ml}$  did not impair the membrane integrity in OEC.

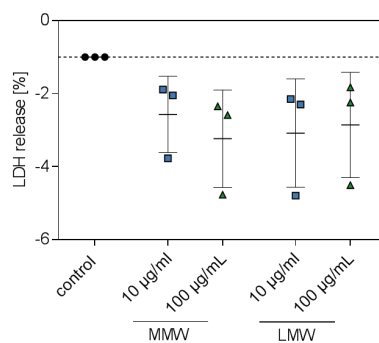


**Figure 4.2:** Membrane integrity of OEC mono-cultures after treatment with fucoidan obtained by fucoidanase hydrolysis. OEC were treated with 10 and 100  $\mu\text{g}/\text{ml}$  MMW or LMW. After seven days, a LDH assay was performed. Significances (compared to the control) were calculated with Welch's t-test

### 4.3 Angiogenesis and Inflammation in Mono-cultures

To study whether enzymatic hydrolysis changes the biological activity of fucoidan extracts in angiogenic and inflammatory processes in MSC and OEC, the expression and extracellular protein levels of relevant mediators were quantified.

#### 4.3.1 Angiogenic signaling molecules VEGF, ANG-1 and SDF-1 in MSC

VEGF, ANG-1 and SDF-1 are well known angiogenic signaling molecules which are produced by MSC. Figure 4.3 shows how VEGF, ANG-1 and SDF-1 expression and protein levels change after treating MSC with 10 and 100  $\mu\text{g}/\text{ml}$  MMW and LMW. For an easier comparison, gene expression and protein levels after 100  $\mu\text{g}/\text{ml}$  HMW FE\_F3 treatment and corresponding controls were included into the result plots. VEGF gene expression was slightly decreased after 10  $\mu\text{g}/\text{ml}$  treatment. HMW FE\_F3 treatment reduced the gene expression of VEGF and was therefore significantly lower than VEGF expression in cells that were treated with 10  $\mu\text{g}/\text{ml}$  LMW (Figure 4.3 A)). MMW and LMW treatments had no or only a very small impact on the gene expressions of ANG-1 and SDF-1. SDF-1 gene expression however, was strongly reduced by HMW FE\_F3 treatment. Therefore, gene expression in cells treated with 100  $\mu\text{g}/\text{ml}$  HMW FE\_F3 was significantly different to the expression in cells that were treated with 10  $\mu\text{g}/\text{ml}$  MMW (Figure 4.3 C)). The different effect of MMW and LMW compared to HMW FE\_F3 was more prominent for VEGF and ANG-1 protein levels. HMW FE\_F3 strongly reduced the protein amount in the supernatant. Even though, MMW and LMW also partly reduced the VEGF and ANG-1 levels, the available protein amount was much higher in these samples compared to HMW FE\_F3-treated samples. These results indicate that treatment with MMW and LMW had a weaker inhibitory effect on the mentioned angiogenic signaling molecules than HMW FE\_F3.

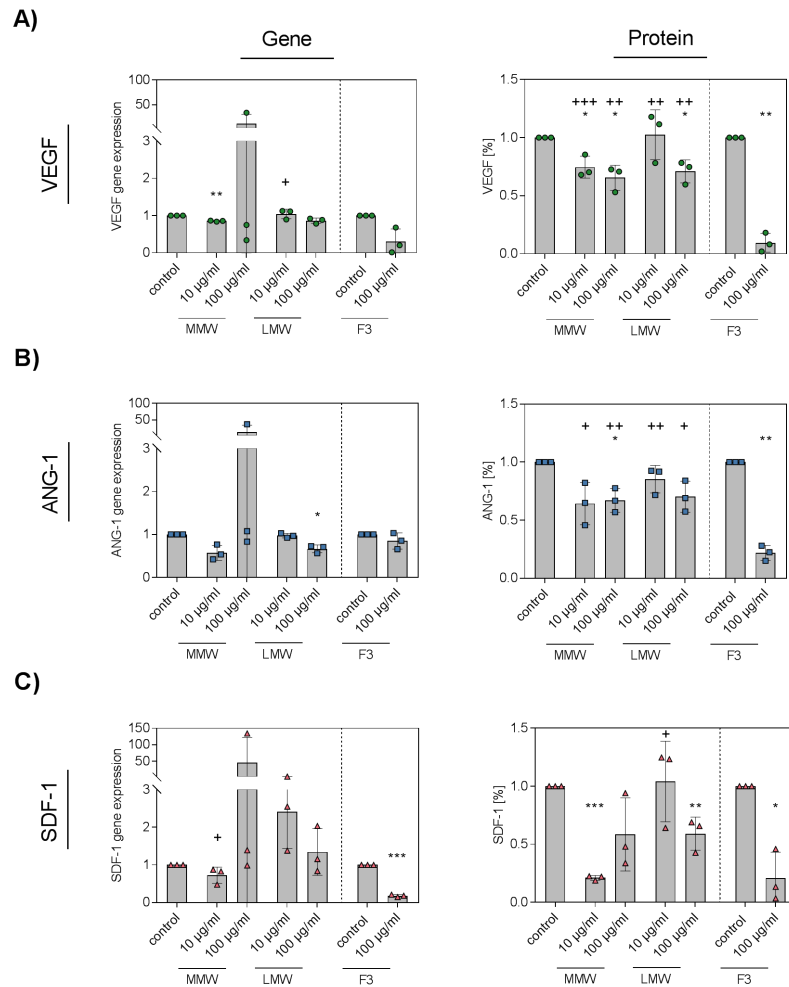


**Figure 4.3:** Expression and protein level of angiogenic mediators in MSC mono-culture after treatment with fucoidan obtained by fucoidanase hydrolysis. MSC were treated with 10 and 100 µg/ml MMW or LMW. After seven days, gene expression and protein levels in the supernatant of A) VEGF, B) ANG-1 and C) SDF-1 were quantified using qPCR and ELISA, respectively. For a better comparison, all graphs include gene expression and protein levels of MSC which were treated with 100 µg/ml HMW FE\_F3 for seven days. Significances compared to the control cells (\*) and to HMW FE\_F3-treated cells (+) were calculated with Welch's t-test.

### 4.3.2 VEGFR2 phosphorylation in OEC

In the prior section, it was shown that treatment with MMW and LMW no longer strongly reduced gene expression and protein levels of important angiogenic mediators

as it was shown for HMW FE\_F3-treated cells. It was expected that reduced VEGF protein levels caused by HMW FE\_F3 treatment would result in a weaker activation of VEGFR2 in OEC. As demonstrated in the prior chapter (see Figure 3.7), FE\_F3 treatment only tentatively decreased VEGFR2 phosphorylation. Treatment with MMW and LMW only slightly reduced VEGF protein levels. Therefore, it was not expected that MMW and LMW treatment would have an effect on the activation of VEGFR2 in OEC. Figure 4.4 demonstrates that neither MMW, nor LMW treatment reduced the amount of phosphorylated VEGFR2 in relation to the overall amount of VEGFR2. The high levels of VEGFR2p in OEC which were treated with VEGF-165 proves that VEGF-165 stimulation was successful.

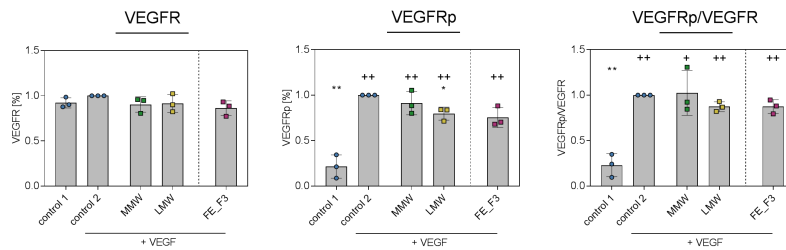


**Figure 4.4:** Phosphorylation of VEGF receptor 2 in relation to the total amount of VEGFR2 in OEC after treatment with fucoidan obtained by fucoidanase hydrolysis. OEC were treated with 100  $\mu\text{g}/\text{ml}$  MMW or LMW and VEGFR2 phosphorylation was simultaneously stimulated by applying 100 ng/ml VEGF-165. Cells were harvested after 15 min and ELISAs for VEGFR2 and VEGFR2p were performed. Control cells 1 were cultured in regular medium and not treated with fucoidan, nor stimulated with VEGF-165. Control cells 2 were stimulated with VEGF-165, but not treated with fucoidan. For a better comparison, all graphs include protein levels of VEGFR2 and VEGFR2p in OEC which were treated with 100  $\mu\text{g}/\text{ml}$  HMW FE\_F3. Significances compared to control 1 (+) and to control 2 (\*) were calculated with Welch's t-test.

### 4.3.3 Inflammatory and angiogenic signaling molecules in OEC

As mentioned before, an acute inflammatory response is one of the first steps to initiate bone repair. A lasting chronic inflammation however impairs regeneration. OEC were treated with 10 and 100  $\mu\text{g}/\text{ml}$  MMW and LMW for seven days and the effect of fucoidan treatment on inflammatory processes in OEC mono-cultures was examined. As shown in Figure 4.5 A), treatment with 10  $\mu\text{g}/\text{ml}$  MMW and 10 or 100  $\mu\text{g}/\text{ml}$  LMW had no or only a very small impact on the expression of inflammation-related mediators like IL-6, adhesion molecules ICAM-1 and VCAM-1 and  $\text{NF}\kappa\text{B}$ .

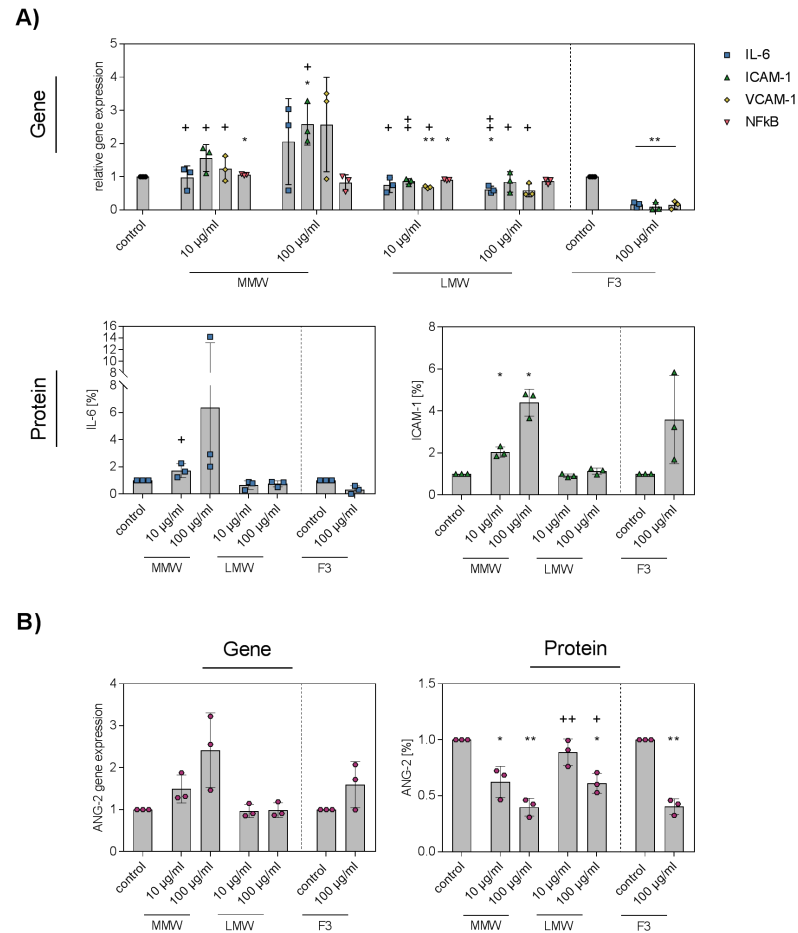


**Figure 4.5:** Expression and protein level of inflammatory and angiogenic mediators in OEC mono-culture after treatment with fucoidan obtained by fucoidanase hydrolysis. OEC were treated with 10 and 100 µg/ml MMW or LMW. After seven days, gene expression and protein levels of A) IL-6, ICAM-1, VCAM-1, NFκB and B) ANG-2 were quantified using qPCR and ELISA, respectively. For a better comparison, all graphs include gene expressions and protein levels of the mentioned mediators in OEC which were treated with 100 µg/ml HMW FE\_F3. Significances compared to the control cells (\*) and to HMW FE\_F3-treated cells (+) were calculated with Welch's t-test.

However, expression levels of IL-6, ICAM-1 and VCAM-1 were increased after treating OEC with 100  $\mu\text{g}/\text{ml}$  MMW. Contrarily, gene expressions were strongly downregulated after treatment with 100  $\mu\text{g}/\text{ml}$  HMW FE\_F3. IL-6 and ICAM-1 protein levels in the supernatant were not affected by LMW treatment in both concentrations. IL-6 and ICAM-1 protein levels however were increased after treatment with high concentrations of MMW. HMW FE\_F3 treatment had no effect on the ICAM-1 protein levels, but tentatively decreased IL-6 levels in OEC. The protein levels were mainly in accordance with the respective gene expressions. An increase of gene expression and protein levels of the mentioned inflammatory markers indicates that treatment with high concentrations of MMW caused an inflammatory response in OEC.

Figure 4.5 B) demonstrates the expression and protein levels of angiogenic signaling molecule ANG-2 in OEC. While treatment with MMW, LMW and HMW\_F3 had no effect on ANG-2 gene expression, ANG-2 protein levels were equally affected by treatment with all tested fucoidans. All fucoidans reduced ANG-2 levels by approximately 50 %. Higher fucoidan concentrations of 100  $\mu\text{g}/\text{ml}$  decreased the protein level more than lower concentrations of 10  $\mu\text{g}/\text{ml}$ .

## 4.4 Angiogenesis and Inflammation in MSC-OEC Co-cultures

To further study the impact of MMW, LMW and HMW FE\_F3 on angiogenesis and inflammation, MSC-OEC co-culture models were applied. As mentioned before, in MSC-OEC co-culture systems, both cell types are able to interact and therefore allow the conduction of functional studies. In the following, the inflammatory effect of MMW and LMW was further analyzed by studying the integrity of the endothelial cell layer after fucoidan treatment. Additionally, the angiogenic effect of MMW and LMW was further analyzed by studying the development of prevascular tube-like structures.

### 4.4.1 Integrity of the endothelial cell barrier

During an inflammatory response, endothelial cells loosen their cell contacts to enable the extravasation of immune cells from the blood stream into the affected tissue. Two well known cell junctions are adherens junctions that are associated with the transmembrane protein VE-cadherin, as well as tight junctions which need the cytoplasmic protein zona occludens-1 (ZO-1) for stabilization. Figure 4.6 A) shows how high concentrations of MMW affected the confluency of the endothelial cell layer. In contrast to the control and LMW-treated co-cultures which form a stable cell layer, MMW-treated co-cultures exhibited large areas without OEC. The analysis of the areas without OEC as presented in Figure 4.6 B), confirms that co-cultures treated with 100  $\mu\text{g}/\text{ml}$  MMW contain large areas devoid of OEC. In contrast, the area without OEC in co-cultures treated with low concentrations of MMW and treated with both concentrations of LMW was significantly smaller than in the control cells. This indicates the formation of a stable endothelial cell layer in these co-cultures. Gene expression analysis of junction proteins VE-cadherin and ZO-1 as shown in Figure 4.6 C) demonstrates that VE-cadherin expression was

downregulated in co-cultures which were treated with 100  $\mu\text{g}/\text{ml}$  MMW, while the expression of ZO-1 remained unaffected. This finding indicates that co-cultures lost their OEC integrity due to an opening of VE-cadherin-associated adherens junctions.

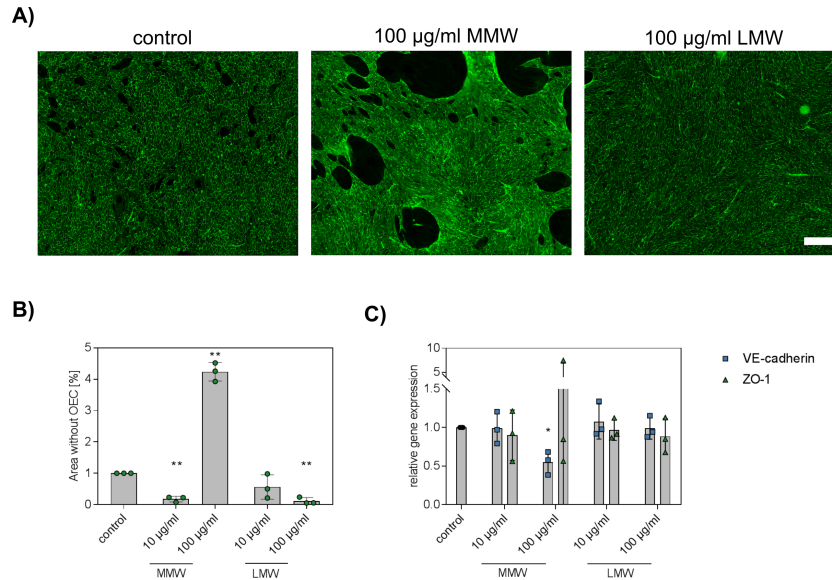


**Figure 4.6:** The integrity of the endothelial cell barrier in MSC-OEC co-cultures after treatment with fucoidan obtained by fucoidanase hydrolysis. Co-cultures were treated with 10 and 100  $\mu\text{g}/\text{ml}$  MMW and LMW for seven days. A) The co-cultures were stained for endothelial marker VE-cadherin (green). Exemplary images for control cells and co-cultures treated with 100  $\mu\text{g}/\text{ml}$  fucoidan are displayed (scale bar=300  $\mu\text{m}$ ). B) OEC-free areas were quantified for 27 frames for each donor pair. C) The gene expression of VE-cadherin and ZO-1 was determined after seven days of treatment using qPCR. Significances (compared to the control) were calculated with Welch's t-test.

#### 4.4.2 Development of angiogenic structures

To study the effect of MMW and LMW on the development of angiogenic structures, MSC-OEC co-cultures were treated with 10 and 100  $\mu\text{g}/\text{ml}$  MMW or LMW and stained on day seven for VE-cadherin. Exemplary microscopy pictures, as well as the quantification of emerged angiogenic structures are presented in Figure 4.7. As already described in the prior chapter in section 3.4.1, treatment with FE\_F3 treatment suppressed the development of angiogenic structures almost completely. In contrast, no negative impact on the development of angiogenic structures could be observed for co-cultures which were treated with MMW and LMW. The quantification of the structures revealed that length and area were even increased for some donor cells. These results are in accordance with the small impact on angiogenic signaling molecules that was observed for

#### 4.4. Angiogenesis and Inflammation in MSC-OEC Co-cultures

MSC mono-cultures after MMW or LMW treatment in section 4.3.1. This experiment shows that treatment with MMW or LMW had no inhibitory effect on the development of angiogenic structures in MSC-OEC co-cultures. It further indicates that enzymatic processing of fucoidans holds the potential to tailor the bioactivity of fucoidan extracts in regard to angiogenic processes.

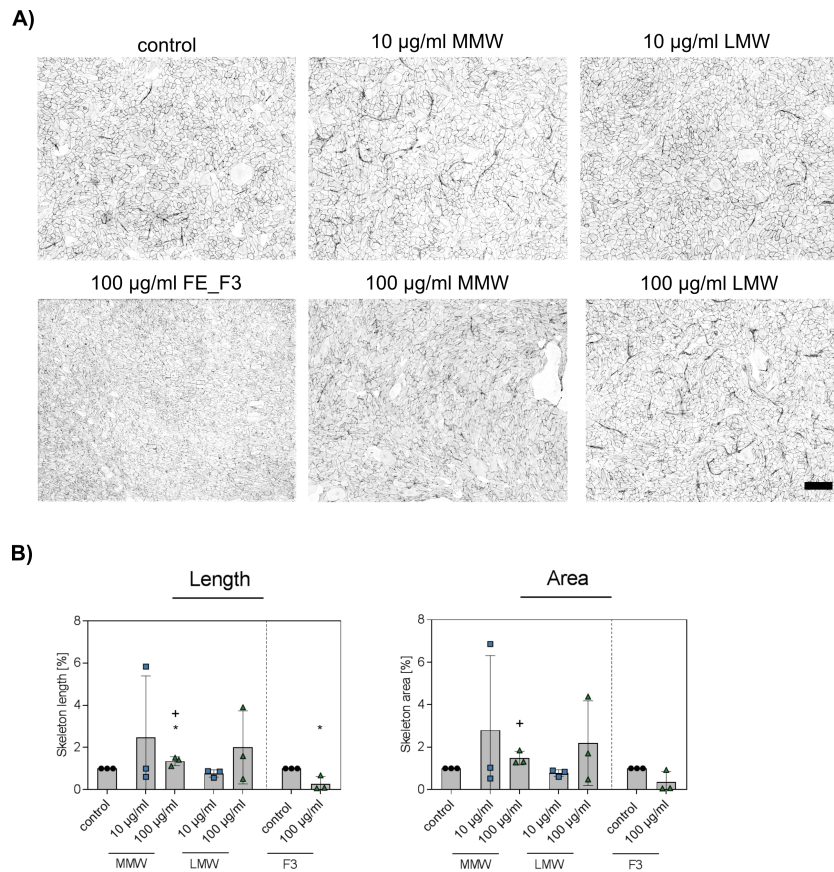


**Figure 4.7:** Development of angiogenic tube-like structures in MSC-OEC co-cultures after treatment with fucoidan obtained by fucoidanase hydrolysis. Co-cultures were treated with 10 and 100  $\mu\text{g}/\text{ml}$  MMW or LMW for seven days. After seven days, cells were stained for VE-cadherin and nuclei. A) Exemplary microscopy pictures of co-cultures with angiogenic structures. Images were inverted and displayed in grey values (scale bar = 300  $\mu\text{m}$ ). B) Quantification of angiogenic skeleton area and length. 27 frames in total were analyzed for each donor pair. For a better comparison, this figure includes the results of co-cultures treated with 100  $\mu\text{g}/\text{ml}$  HMW FE\_F3. Significances compared to the control cells (\*) and to HMW FE\_F3-treated cells (+) were calculated with Welch's t-test.

### 4.4.3 Angiogenic signaling molecules in MSC-OEC co-cultures

The prior section demonstrated that the fucoidanase hydrolysis products MMW and LMW lost their anti-angiogenic properties on a functional level which were clearly proven for HMW FE\_F3. This section investigates how angiogenic signaling molecules were affected by MMW and LMW treatment in the MSC-OEC co-culture system. Figure 4.8 shows that gene expressions of VEGF, SDF-1, ANG-1 and ANG-2 were only minimally altered by fucoidan treatment. Similar results were observed for co-cultures treated with the fractionated fucoidans FE\_F1, FE\_F2 and FE\_F3 (see section 3.4.2, Figure 3.11). Treatment with 100  $\mu\text{g}/\text{ml}$  LMW and 10  $\mu\text{g}/\text{ml}$  MMW increased the gene expression of VEGF significantly. The trend is mirrored in the VEGF protein levels which were tentatively increased after fucoidan treatment. The same effect was observed for treatment with the fractions FE\_F1, FE\_F2 and FE\_F3. Low concentrations of MMW decreased the protein level of SDF-1. Other than that, fucoidan treatment had no measurable effect on SDF-1, ANG-1 and ANG-2 protein levels. As shown in the prior section, treatment with MMW or LMW had no significant impact on the formation of angiogenic structures. Therefore, the absent effect of MMW and LMW treatment on angiogenic signaling molecules in co-cultures is in accordance with the prior results.

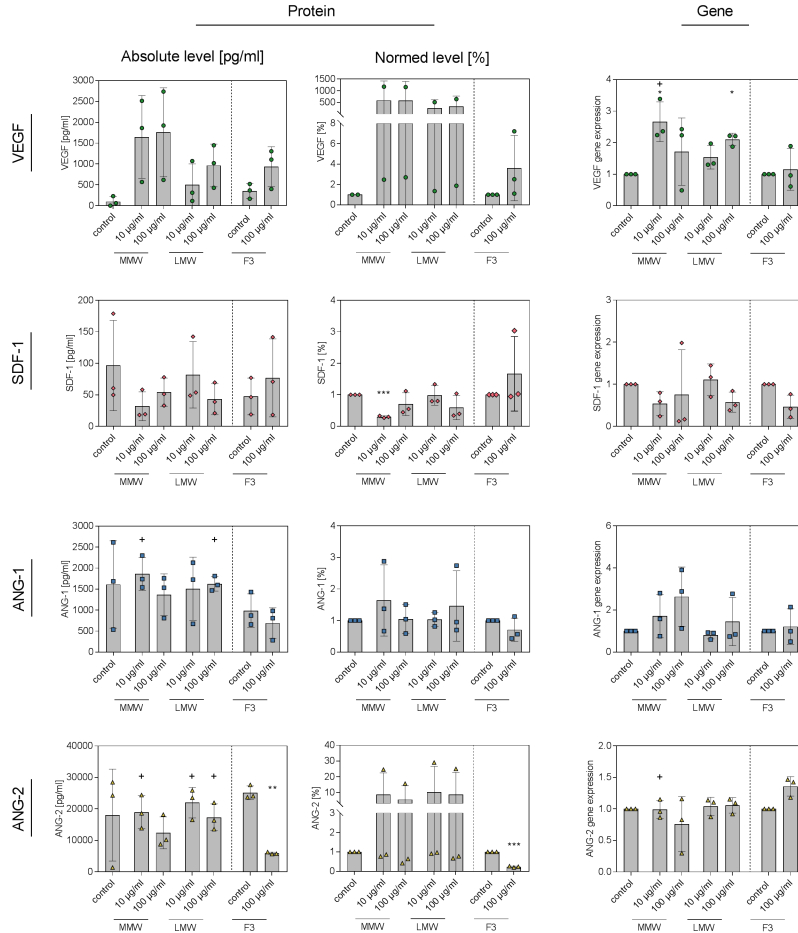
## 4.5 Interaction of Fucoidan Extracts with MSC and OEC

To assess why fucoidan hydrolysis products MMW and LMW influence angiogenic and inflammation related processes in a different way than HMW FE\_F3, the interaction of fucoidan with MSC and OEC was visualized using immunocytochemistry. Therefore, cells were incubated with 100  $\mu\text{g}/\text{ml}$  MMW, LMW and FE\_F3 for 72 h, washed repeatedly and stained for fucoidan using the BAM-4 antibody from SeaProbes. Exemplary microscopy images of stained MSC and OEC mono- and co-cultures are displayed in Figure 4.9. The light red fluorescence visible in the control cells indicates unspecific binding events of the BAM-4 antibody. The strongest fucoidan staining was observed for MSC and OEC mono-cultures which were treated with HMW FE\_F3. Almost no fucoidan staining however was observed in cultures that were treated with MMW or LMW (Figure 4.9 A) and B)). Interestingly, fucoidan staining could not be identified in any co-culture. As described in the prior sections, the co-culture environment allows OEC to develop tube-like angiogenic structures. Even though, it was shown that HMW FE\_F3 affected the development of these structures, no fucoidan staining could be detected in their vicinity (Figure 4.9 C) and D)).

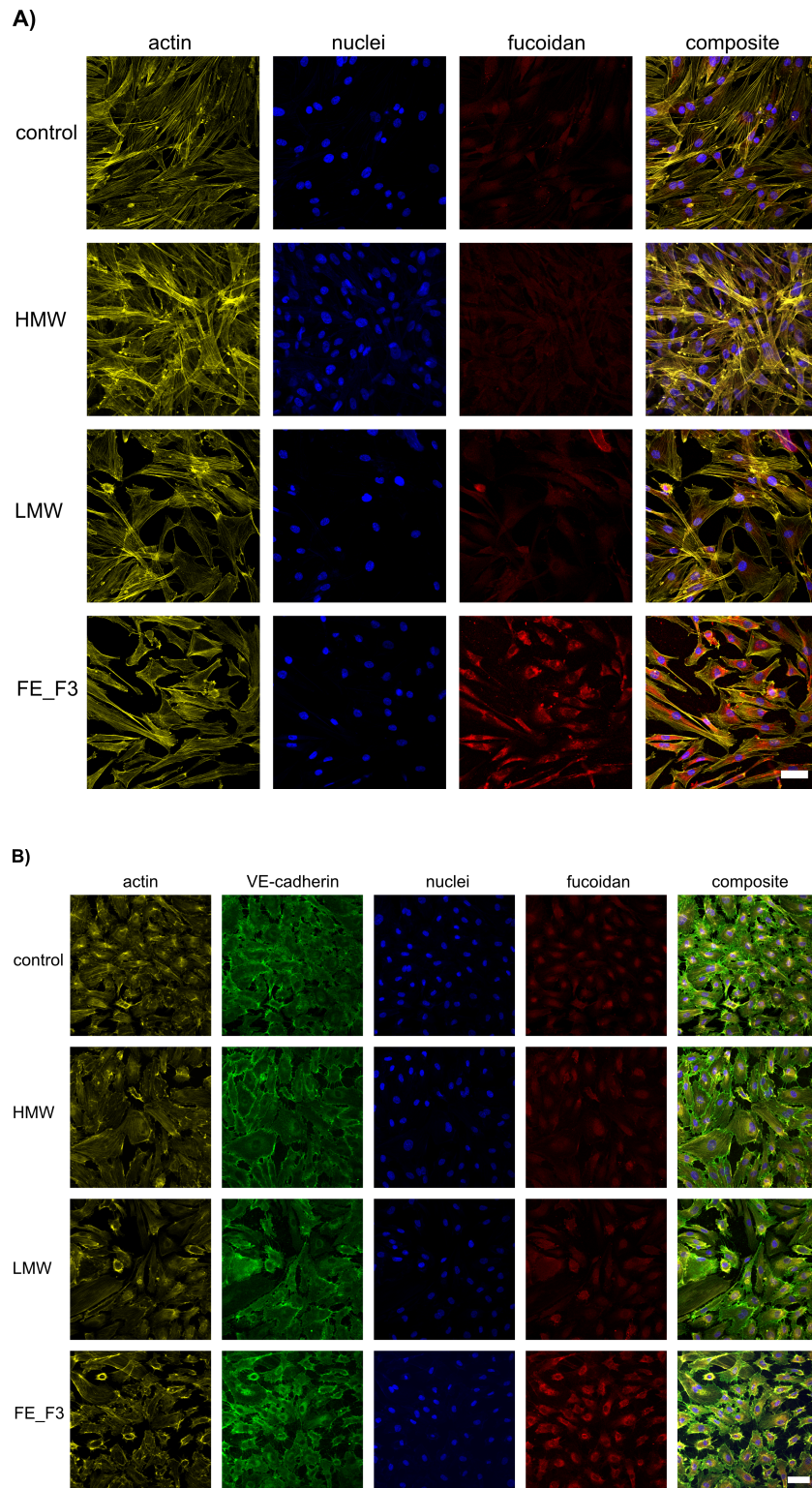
The analysis of red fluorescence intensity in relation to cell number as shown in 4.9 E) fits the observations described above. The quantification reveals that fucoidan staining on MSC cells was much stronger than on OEC. Even though, fucoidan staining was strongest for HMW FE\_F3, also MMW and LMW were detected in MSC mono-cultures. For OEC, fucoidan intensity was significantly higher after LMW and HMW FE\_F3 treatment. Supporting the observations from the microscopy pictures, no fucoidan staining could be detected in the co-culture systems. This experiment shows that

#### 4.5. Interaction of Fucoidan Extracts with MSC and OEC

FE\_F3 interacts stronger with the studied cells than hydrolysis products MMW and LMW. It also suggests that the tested fucoidans interact stronger with MSC than with OEC.



**Figure 4.8:** Expression and protein level of angiogenic mediators in MSC-OEC co-cultures after treatment with fucoidan obtained by fucoidanase hydrolysis. Co-cultures were treated with 10 or 100 µg/ml MMW or LMW. Gene expression and protein levels of VEGF, SDF-1, ANG-1 and ANG-2 were determined on day seven using qPCR and ELISA, respectively. Absolute protein levels, as well as levels normed to the control were plotted. For a better comparison, all graphs include gene expressions and protein levels of the mentioned mediators in MSC-OEC co-cultures which were treated with 100 µg/ml HMW FE\_F3. Significances compared to the control cells (\*) and to HMW FE\_F3-treated cells (+) were calculated with Welch's t-test.



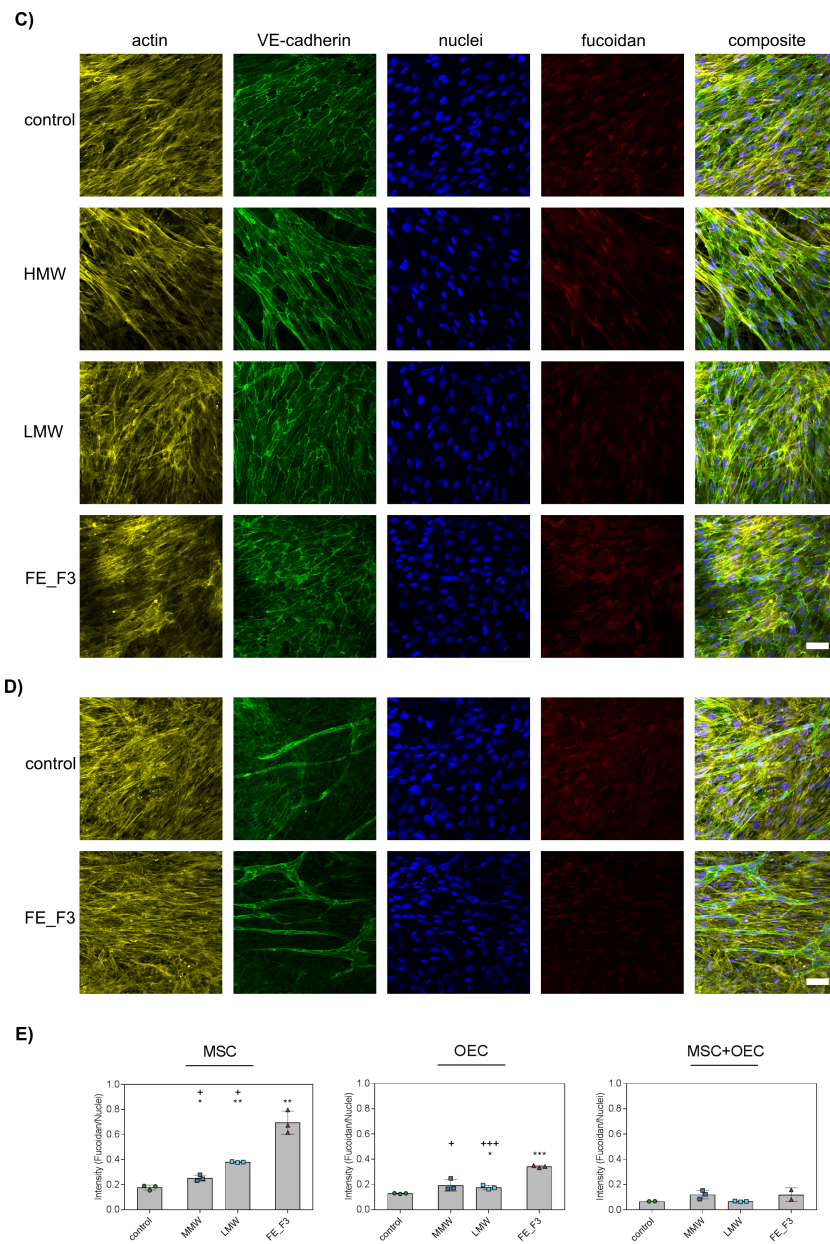


**Figure 4.9:** Interaction of enzymatically-extracted and -degraded fucoidans with MSC and OEC. Mono- and co-cultures were treated with 100  $\mu\text{g}/\text{ml}$  fucoidan for three days. Subsequently, cells were washed and stained for fucoidan (red), actin (yellow) and nuclei (blue) using BAM-4 antibody, phalloidin-TRITC and Hoechst, respectively. Cultures with OEC were also stained for VE-cadherin (green). The Figure shows exemplary microscopy pictures of A) MSC mono-cultures, B) OEC mono-cultures and C) MSC-OEC co-cultures. D) MSC-OEC co-cultures with emerged angiogenic structures. E) The fluorescence intensity of fucoidan staining was quantified in relation to the number of cells for mono- and co-cultures. Scale bars=50  $\mu$ . Significances compared to the control cells (\*) and to HMW FE\_F3-treated cells (+) were calculated with Welch's t-test.



# 5

## Results III

---

*This chapter investigates the effect of three chemically extracted and degraded fucoidan extracts (CAU1, CAU2, CAU3) on angiogenesis in co-culture models relevant for bone regeneration. Additionally, the effect of the native fucoidan (NatF) and its purified fraction (FracC) was evaluated in one experimental set.*

### Contents

---

5.1	Chemical Characterization of Chemically Extracted and Degraded Fucoidans . . . . .	74
5.2	Angiogenesis in MSC-OEC Co-cultures . . . . .	74
5.3	Interaction of Chemically Extracted Fucoidans with MSC and OEC . . . . .	79

---

## 5.1 Chemical Characterization of Chemically Extracted and Degraded Fucoidans

Native fucoidan (NatF) was isolated from *F. evanescens* applying a chemical extraction technique and subsequently purified into three fractions using IEX. The third eluted fraction FracC was tested in one experimental setup as shown in the later section 5.2.2. To obtain fragmented fucoidans, NatF was hydrolyzed by incubation with H<sub>2</sub>O<sub>2</sub> for different periods of time. Each fragmented fucoidan was further purified into three fractions using IEX. The third eluted fraction of each extract (CAU1, CAU2, CAU3) was collected for biological experiments. The procedure of chemical extraction and fragmentation is illustrated in Figure 2.1.

Results for the quantification of fucose content, degree of sulfation and molecular weight are listed in Table 5.1. The fucose content was equally high in all IEX-purified extracts. Even the native extract contained 80 % fucose. These results indicate that the co-extracted amount of alginate was low. The degree of sulfation was lowest for the native fucoidan with 0.52. It increased however to 0.61 in the purified extract FracC. The fragmented extracts contained the highest degrees of sulfation. CAU1, which was incubated for the shortest time with H<sub>2</sub>O<sub>2</sub> had the highest degree of sulfation with 0.9. The results suggest that extracts with a shorter H<sub>2</sub>O<sub>2</sub> incubation time contain a higher degree of sulfation. The native fucoidan, as well as its purified fraction FracC had a molecular weight of 400-450 kDa, belonging to the group of high molecular weight fucoidans. The decreased molecular weights of CAU1, CAU2 and CAU3 show that fragmentation with H<sub>2</sub>O<sub>2</sub> was successful. However, there was no trend visible that longer H<sub>2</sub>O<sub>2</sub> incubation times resulted in smaller fucoidan fragments. The results indicate that H<sub>2</sub>O<sub>2</sub> fragmentation occurs randomly and that incubation time has no linear effect on the molecular weight of the resulting extracts.

**Table 5.1:** Chemical characterization of chemically extracted fucoidans (NatF, FracC) and further degraded extracts (CAU1, CAU2, CAU3). Fucose content, degree of sulfation and molecular weight were determined as listed below.

	CAU1	CAU2	CAU3	NatF	FracC
Fucose [%]	93.1	93	88.4	78.6	94.5
Sulfates [%]	38.8	38.2	34	-	-
SO <sub>4</sub> <sup>2-</sup> :Fuc	0.9	0.88	0.73	0.52	0.63
Molecular weight [kDa]	26	18	155	539	371

## 5.2 Angiogenesis in MSC-OEC Co-cultures

To study the impact of chemically extracted and H<sub>2</sub>O<sub>2</sub>-fragmented fucoidan extracts on angiogenesis, MSC-OEC co-cultures were treated with CAU1, CAU2 and CAU3

and development of angiogenic structures, as well as expression and protein levels of angiogenic signaling molecules were analyzed. A co-culture with one donor pair was conducted to understand if non-fragmented extracts NatF and FracC affected angiogenic signaling molecules differently.

### 5.2.1 Development of angiogenic structures

To study the effect of CAU1, CAU2 and CAU3 on the development of angiogenic structures, MSC-OEC co-cultures were treated with 10  $\mu\text{g}/\text{ml}$  fucoidan and stained on day four and seven for VE-cadherin. Exemplary microscopy pictures for both days are shown in Figure 5.1. Almost no angiogenic structures were apparent on day four in control co-cultures, while some structures were already developed in co-cultures treated with CAU1, CAU2 and CAU3. The number of structures increased in all co-cultures from day four to day seven. The microscopy pictures from day seven show that none of the tested extracts impaired the formation of angiogenic structures in the co-culture system. Without quantification it is however difficult to judge whether fucoidan treatment increased the amount of emerged structures compared to the control.

### 5.2.2 Angiogenic signaling molecules in MSC-OEC co-cultures

To study the impact of chemically extracted fucoidans CAU1, CAU2 and CAU3 on a molecular level, MSC-OEC co-cultures were treated with 10  $\mu\text{g}/\text{ml}$  fucoidan and gene expressions, as well as protein levels of angiogenic mediators VEGF, SDF-1, ANG-1 and ANG-2 were quantified on day four and seven. Similar to the results reported before, the tested fucoidan extract had no effect on the gene expression of the mentioned signaling molecules. Only, treatment with CAU2 decreased the expression of ANG-1 slightly. While, fucoidan treatment had no impact on VEGF protein levels on both tested days, SDF-1, ANG-1 and ANG-2 level were similarly affected by treatment with CAU1, CAU2 and CAU3. Fucoidan treatment decreased the protein levels of the mentioned molecules, at which CAU3 had the strongest impact, followed by CAU2 and CAU1. A decrease of angiogenic signaling molecules in mono-cultures was reported in earlier sections for enzymatically-extracted fucoidans. However, these fucoidans also had a negative impact on the development on angiogenic structures in co-cultures which was not visible for the tested extracts CAU1, CAU2 and CAU3. In the prior section, a decrease of protein levels could be correlated with an increase in extract purity and an increase in degree of sulfation. FE\_F3 as the purest extract with the highest sulfate content impaired angiogenic processes most. Here, CAU3 (with the lowest degree of sulfation) decreased the mentioned protein levels most.

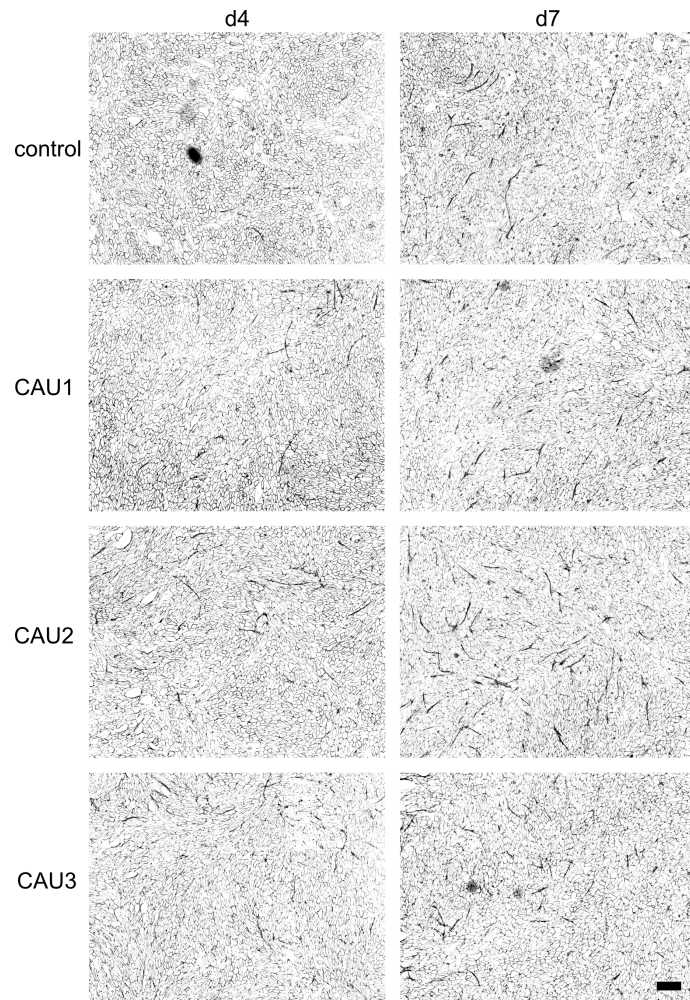


**Figure 5.1:** Development of angiogenic tube-like structures in MSC-OEC co-cultures after treatment with  $H_2O_2$ -degraded fucoidans. Co-cultures were treated with  $10 \mu g/ml$  fucoidan for four and seven days. Cells were stained for VE-cadherin and nuclei. Exemplary microscopy images were inverted and displayed in grey values (scale bar= $300 \mu m$ ).

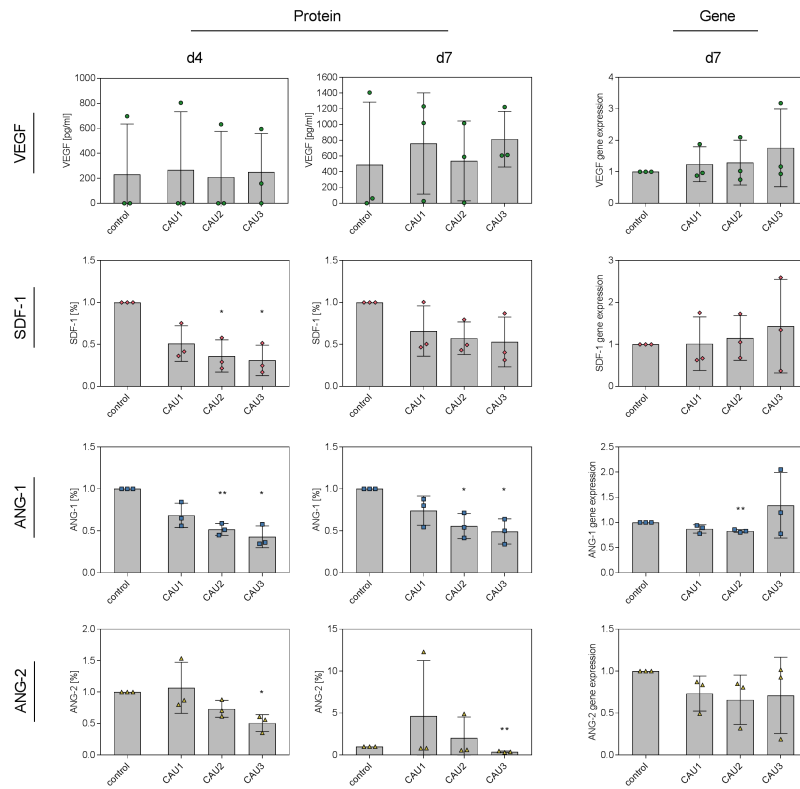


**Figure 5.2:** Expression and protein level of angiogenic mediators in MSC-OEC co-cultures after treatment with  $H_2O_2$ -degraded fucoidans. Co-cultures were treated with  $10 \mu g/ml$  fucoidan. Protein levels of VEGF, SDF-1, ANG-1 and ANG-2 were determined on day four and seven using ELISA. Gene expressions of the mentioned mediators were analyzed on day seven using qPCR. Significances (compared to the control) were calculated with Welch's t-test.

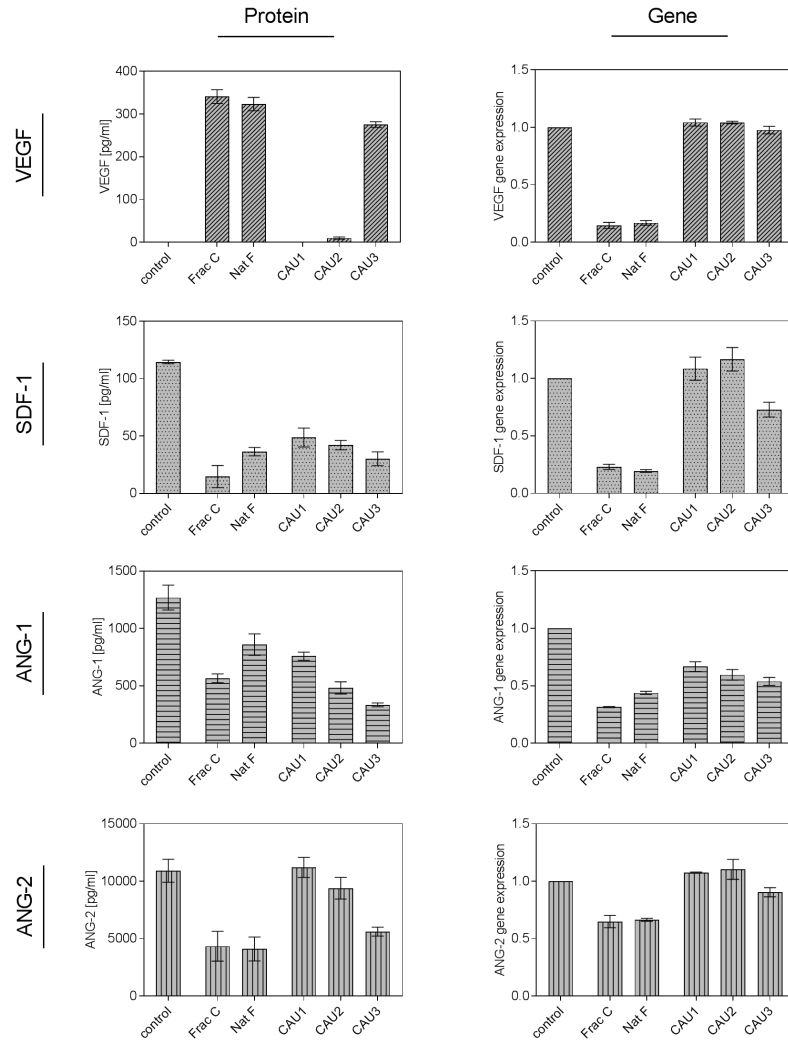
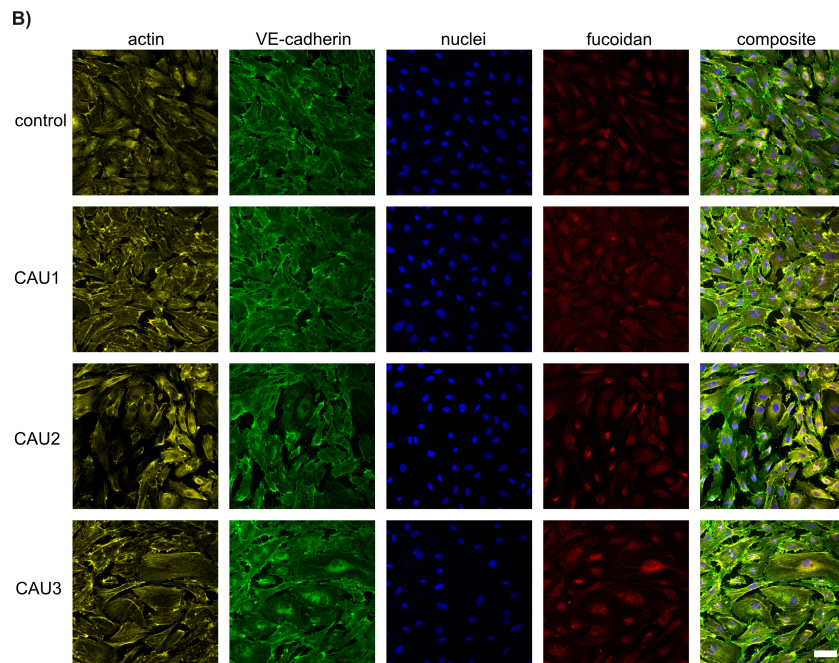
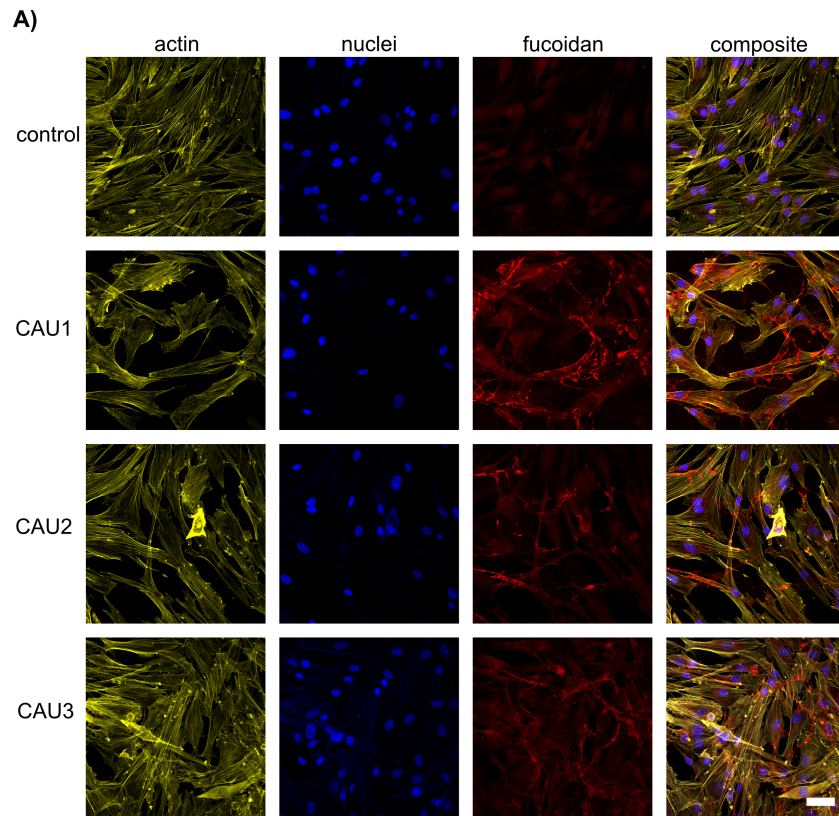


**Figure 5.3:** Expression and protein level of angiogenic mediators in MSC-OEC co-cultures after treatment with native and  $H_2O_2$ -degraded fucoidans. Co-cultures were treated with  $10 \mu g/ml$  CAU1, CAU2, CAU3 (fragmented fucoidans), NatF and FracC (native fucoidans). Gene expression and protein levels of VEGF, SDF-1, ANG-1 and ANG-2 were determined on day seven using qPCR and ELISA, respectively. Error bars indicate the technical error. Significances were not calculated, because the experiment was only performed for one donor pair.

To compare the effect of fragmented fucoidans CAU1, CAU2 and CAU3 with the intact polysaccharides, one co-culture was additionally treated with 10  $\mu\text{g}/\text{ml}$  of the native fucoidan NatF and the purified extract FracC. After seven days, gene expression and protein levels of the before mentioned mediators were quantified. The results from this experiment are displayed in Figure 5.3. Similar to the results shown in Figure 5.2, gene expression levels were mostly not affected by treatment with the fragmented extracts. Only, ANG-1 expression levels were decreased after treatment with CAU1, CAU2 and CAU3. FracC and NatF however, decreased the expressions of all tested genes to approximately 50 % or more. While, FracC and NatF strongly downregulated VEGF expression, VEGF protein levels were highly increased after treatment with the intact extracts. For the other tested signaling molecules, results from gene expression could be translated to quantified protein levels. Treatment with FracC and NatF decreased SDF-1, ANG-1 and ANG-2 protein levels by approximately 50 %. The experiment indicates that the intact fucoidan extracts NatF and FracC negatively effect the expression and protein levels of angiogenic signaling molecules. However, these results must be interpreted with caution as the experiment was only performed for one donor pair. Also, the absence of functional assays does not allow to make a final statement about the effect of the intact fucoidans NatF and FraC in the co-culture system.

### 5.3 Interaction of Chemically Extracted Fucoidans with MSC and OEC

The interaction of chemically extracted and fragmented fucoidans CAU1, CAU2 and CAU3 with MSC and OEC mono-cultures was studied using immunocytochemistry. Therefore, cells were treated with 10  $\mu\text{g}/\text{ml}$  fucoidan for three days, subsequently washed and remained fucoidan was stained using the BAM-4 antibody from SeaProbes. Exemplary microscopy pictures of the stained cells are displayed in Figure 5.4. Light red fluorescence in the control cells indicates unspecific binding events of the BAM-4 antibody. From the microscopy pictures, it can be observed that all tested fucoidans interacted with the MSC. Almost no fucoidan staining could be observed in the OEC culture. The quantification of fucoidan staining in relation to the number of cells as shown in Figure 5.4 C), confirmed the observations from the microscopy pictures. Fucoidan extracts CAU1, CAU2 and CAU3 interacted almost equally with MSC. However, only fucoidan staining after CAU3 treatment was significantly increased in OEC culture. Similar to the results for enzymatically-extracted fucoidan FE\_F3 shown in section 4.5, fucoidans interacted stronger with MSC than with OEC.



### 5.3. Interaction of Chemically Extracted Fucoidans with MSC and OEC

c)

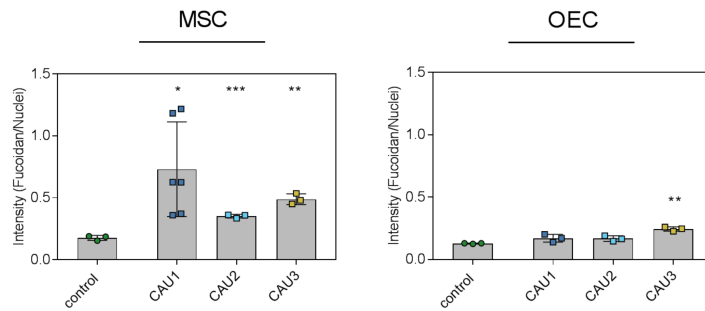


**Figure 5.4:** Interaction of  $H_2O_2$ -degraded fucoidans with MSC and OEC. Mono- and co-cultures were treated with  $10 \mu g/ml$  fucoidan for three days. Subsequently, cells were washed and stained for fucoidan (red), actin (yellow) and nuclei (blue) using BAM-4 antibody, phalloidin-TRITC and Hoechst, respectively. Cultures with OEC were also stained for VE-cadherin (green). The Figure shows exemplary microscopy pictures of A) MSC mono-cultures and B) OEC mono-cultures. C) The fluorescence intensity of fucoidan staining was quantified in relation to the number of cells for MSC and OEC. Scale bars= $50 \mu m$ . Significances (compared to the control) were calculated with Welch's t-test.



# 6

## Results IV

---

*This chapter describes the development of a thermosensitive injectable hydrogel as a delivery system for fucoidan. A protocol for fucoidan incorporation was established and physicochemical properties such as gelation time, swelling and morphology of the hydrogel were determined. 2D and 3D cell culture of human mesenchymal stem cells and endothelial cells inside and on the hydrogel were conducted to study the biocompatibility. The most important findings are summarized in the following publication.:*

**Injectable Thermosensitive Chitosan-Collagen Hydrogel as a Delivery System for Marine Polysaccharide Fucoidan.**

Julia Ohmes, Lena Marie Saure, Fabian Schütt, Marie Trenkel, Andreas Seekamp, Rengina Scherließ, Rainer Adelung and Sabine Fuchs (2022) *Mar. Drugs* 20, 402

### Contents

---

<b>6.1</b>	<b>Protocol Development for Thermosensitive Hydrogels . . . . .</b>	<b>84</b>
<b>6.2</b>	<b>Physicochemical Properties . . . . .</b>	<b>88</b>
<b>6.3</b>	<b>Biological Performance . . . . .</b>	<b>95</b>

---

## 6.1 Protocol Development for Thermosensitive Hydrogels

The following section describes the process of establishing a protocol for the production of thermosensitive hydrogels with encapsulated fucoidan. It demonstrates how to incorporate fucoidan without the formation of aggregates, presents the necessary amount of GP to achieve adequate gelation times and shows the advantages of adding collagen into the hydrogel system.

### 6.1.1 Glycerophosphate and incorporation of fucoidan

GP was added dropwise into the chitosan (95 % deacetylation, 100-250 kDa) solution to achieve a thermosensitive mixture as described first by Chenite et al. [27]. To assess whether GP isomers play a role for the development of a thermosensitive sol,  $\beta$ -GP and an isomeric GP mixture were added to the chitosan solution. As shown in Figure 6.1 A), the addition of  $\beta$ -GP results in a clear sol which gels within several minutes at 37°C. Dropwise addition of the isomeric GP however, caused the formation of a very turbid sol which gelled at 37°C into an inhomogeneous brittle hydrogel. Based on these results,  $\beta$ -GP was used for the following hydrogel preparations.

To encapsulate fucoidan into the chitosan hydrogel, different approaches were tested. The dropwise addition of fucoidan solution into chitosan- $\beta$ -GP mixture resulted in the formation of fucoidan aggregates as shown in Figure 6.1 B). Also, the dropwise addition of fucoidan solution before the addition of  $\beta$ -GP caused fucoidan aggregates as indicated by the arrows in Figure 6.1 C). The mixing of chitosan and fucoidan powder before dissolving resulted in a turbid sol (Figure 6.1 D)) with reduced ability to gelate within short time at 37°C. As demonstrated in Figure 6.1 E), premixing of  $\beta$ -GP and fucoidan solution before dropwise addition into the chitosan mixture resulted in a clear sol without fucoidan aggregates. The sol was able to gelate within short time at 37°C. For the following hydrogel preparations, fucoidan and  $\beta$ -GP solutions were always premixed before dropwise addition into the chitosan solution.

### 6.1.2 $\beta$ -GP concentration

To assess which amount of  $\beta$ -GP was necessary to achieve a sol-gel transition in adequate time, sols with 5, 6 and 7 %  $\beta$ -GP were prepared. The same sols were prepared with and without the encapsulation of 500  $\mu$ g/ml fucoidan. The gelation time at 37°C was estimated using the tube-inverting method. As shown in Figure 6.2 A), sols without fucoidan and with 5 %  $\beta$ -GP needed 20 min or more to gelate. The higher the  $\beta$ -GP content, the shorter was the measured gelation time. Hydrogels with 6 and 7 %  $\beta$ -GP needed approximately 7 and 5 min, respectively, to gelate. Addition of fucoidan into the hydrogel system had only an effect when the  $\beta$ -GP content was low. Addition of fucoidan reduced the gelation time of sols with 5 %  $\beta$ -GP to approximately 8 min.

As demonstrated in Figure 6.2 B), the pH of the formed hydrogels was slightly acidic (approximately 6.7-6.8). Neither the  $\beta$ -GP content, nor fucoidan encapsulation had a measurable effect on the pH.

## 6.1. Protocol Development for Thermosensitive Hydrogels

The turbidity of the prepared sols was dependent on the  $\beta$ -GP content. Sols with a higher  $\beta$ -content were less turbid. The encapsulation of 500  $\mu\text{g}/\text{ml}$  fucoidan into the sols increased the turbidity by around 25 % (Figure 6.2 C)).

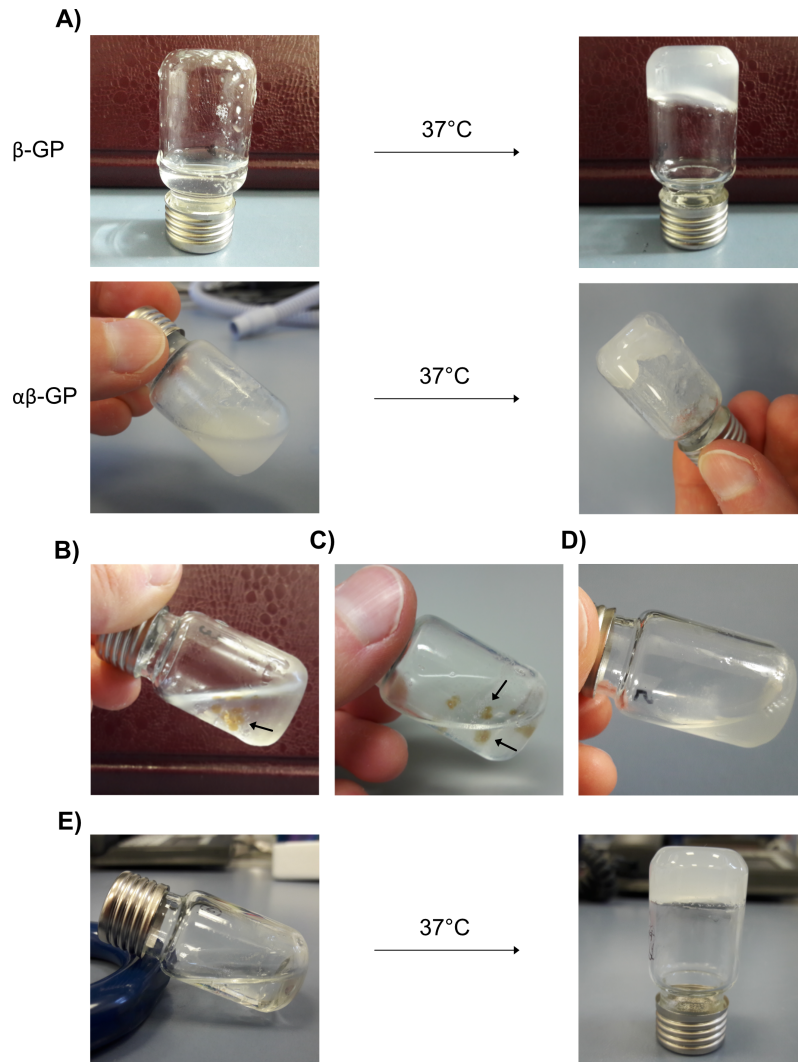


**Figure 6.1:** Development of a protocol for the preparation of injectable thermosensitive chitosan hydrogels with encapsulated fucoidan. To achieve thermosensitivity, glycerophosphate (GP) was added. A)  $\beta$ -GP addition resulted in a clear sol (top), while an isomeric GP mixture caused a very turbid sol (bottom). Addition of fucoidan in solution B) after or C) before  $\beta$ -GP addition caused fucoidan aggregates as indicated by the black arrows. D) Premixing of fucoidan and chitosan powder resulted in a turbid sol and extended the gelation time by one hour. E) Premixing of  $\beta$ -GP and fucoidan solution before addition created a clear sol which gelled within short time at 37°C.

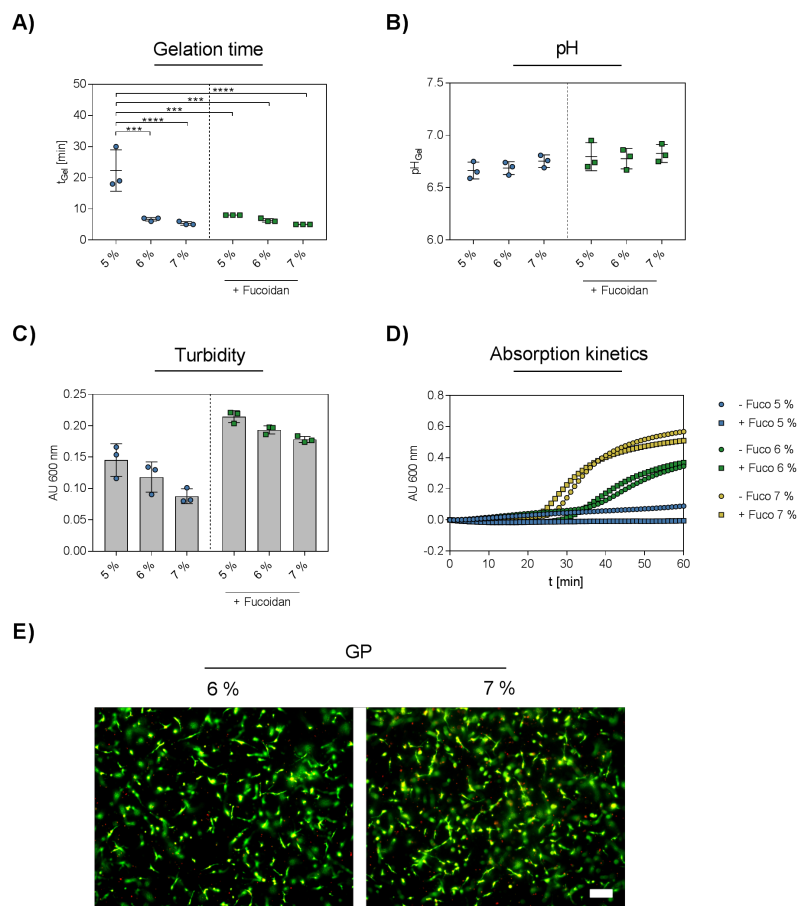


**Figure 6.2:** Chemical and physical properties of thermosensitive chitosan hydrogels with different concentrations of  $\beta$ -GP. Chitosan hydrogels were prepared using 5, 6 or 7 %  $\beta$ -GP with and without 500  $\mu$ g/ml fucoidan encapsulation. A) Gelation times at 37°C were estimated using the tube-inverting method. B) pH of the sols was measured after gelation. C) To quantify the turbidities, absorption of the sols was measured at 600 nm. D) The gelation process was monitored by measuring the absorption at 600 nm every minute for one hour. Significances were calculated using ANOVA. For C) and D), the technical replicates for one experiment were plotted (no significances were calculated). E) Life/dead staining of MSC cultured on hydrogels containing 6 and 7 %  $\beta$ -GP (scale bar = 200  $\mu$ m)

The thermosensitive sols turn opaque during gelation. To monitor the gelation process of the different sols, the absorption was measured every minute for one hour. The results are presented in Figure 6.2 D). The absorption kinetics clearly show that a higher  $\beta$ -GP content accelerates the gelation process. This trend was already indicated in A) after estimating the gelation time using the tube-inverting method. The absorption kinetics reveal that fucoidan encapsulation had no visible effect on the gelation process. The experiments demonstrate that a  $\beta$ -GP content of 7% resulted in short gelation times and in less turbid sols. Some studies reported that high amounts of  $\beta$ -GP can have a cytotoxic effects on cells [1, 191]. To rule out that an amount of 7%  $\beta$ -GP has a cytotoxic effect on MSC, cells were cultured on hydrogels containing 6 and 7%  $\beta$ -GP. On day six, life/dead staining was performed. Figure 6.2 E) shows that MSC adhered and were vital on both hydrogels. Therefore, a  $\beta$ -GP content of 7% was used for following hydrogel preparations.

### 6.1.3 Collagen type I integration

To increase the biocompatibility of the hydrogels, the integration of collagen type I into the thermosensitive chitosan system was evaluated. Therefore, collagen was added slowly into the chitosan mixture, followed by the addition of  $\beta$ -GP and fucoidan as described above. MSC were encapsulated into the hydrogels containing 1 and 1.5 mg/ml collagen and life/dead staining was performed on day six. As shown in Figure 6.3 A), cell adhesion and spreading of MSC was improved with increasing collagen content. The addition of collagen into the hydrogel system accelerated the sol-gel transition by approximately one minute (estimated by using the tube-inverting method). The gelation process was monitored by measuring the absorption of the hydrogels every minute for one hour. The absorption kinetics as presented in Figure 6.3 B) confirm that chitosan-collagen sols gelate faster than chitosan sols. The biocompatibility of the hydrogels was highly increased by integrating collagen into the system. Therefore, hydrogels were always prepared with 1.5 mg/ml collagen type I for following experiments.

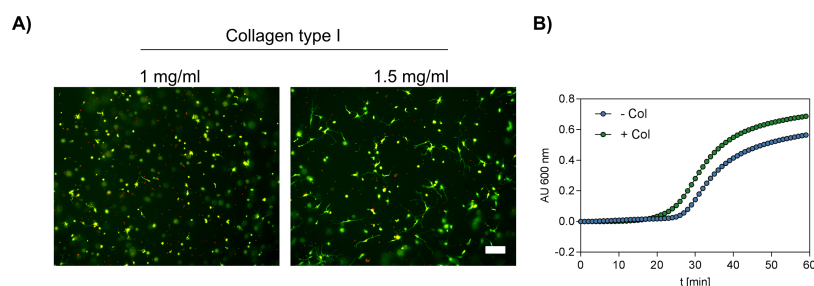


**Figure 6.3:** Integration of collagen type I into the chitosan hydrogel. Hydrogels containing 1 and 1.5 mg/ml collagen type I were prepared. A) MSC were encapsulated into the hydrogels. Vital (green) and dead (red) cells were stained on day six using calcein-AM and propidium iodide, respectively (scale bar = 200  $\mu\text{m}$ ). B) The gelation process of hydrogels with (1 mg/ml) and without collagen was monitored by measuring the absorption at 600 nm every minute for one hour.

## 6.2 Physicochemical Properties

In the following section, established chitosan-collagen hydrogels with varying encapsulated amounts of fucoidan were tested for their physicochemical properties, including gelation time, gelation temperature, pH, swelling, turbidity and microstructure. Also, a method for fucoidan detection was adapted and used to measure fucoidan release from the hydrogel over a period of time.

### 6.2.1 Gelation time, temperature, pH, swelling and turbidity

To roughly estimate the gelation time of the chitosan-collagen hydrogel with encapsulated fucoidan, the tube-inverting method was applied. Similar to the results shown before (see Figure 6.2 A)), fucoidan encapsulation had no visible effect on the gelation time. All sols stopped to flow within three to four minutes in a water bath at 37°C (see Figure 6.4 A)).

The pH of the prepared hydrogels was measured before and after gelation. The pH of the sols was approximately 6.8. After gelation, the pH turned slightly more acidic (approximately 6.6). Fucoidan encapsulation had no effect on the measured pH values. To determine the swelling capacities of the hydrogels, the ESR was calculated. Therefore, hydrogels with different fucoidan concentrations were prepared, lyophilized and subsequently rehydrated in PBS until equilibrium was reached. Figure 6.4 C) shows the ESR for the different hydrogels. Encapsulation of high fucoidan concentrations (500  $\mu\text{g}/\text{ml}$ ) decreased the ESR significantly. This result indicates that high amounts of fucoidan create a more compact gel with an impaired ability for swelling during rehydration.

The transparent sols turn into turbid gels as the gelation proceeds. Monitoring of the absorption kinetics can therefore give an impression of the gelation and whether fucoidan encapsulation has an impact on this process. As presented in Figure 6.4 D),

absorption kinetics were not significantly different for hydrogels with varying fucoidan concentrations, indicating that fucoidan encapsulation did not have an effect on the gelation process. This result is in accordance with the estimation of the gelation time using the tube-inverting method.

The encapsulation of high fucoidan amounts such as 500  $\mu\text{g}/\text{ml}$  fucoidan had a visible effect on the appearance of the sol. As illustrated in the photo in Figure 6.4 E), the sol with 500  $\mu\text{g}/\text{ml}$  fucoidan was turbid, while sols with 0-100  $\mu\text{g}/\text{ml}$  appeared transparent. This observation was confirmed by measuring the absorption at 600 nm. Hydrogels with 500  $\mu\text{g}/\text{ml}$  fucoidan were approximately four times more turbid than hydrogels with less fucoidan.

Oscillatory rheological measurements were performed to determine the viscoelastic properties of hydrogels without and with 100  $\mu\text{g}/\text{ml}$  fucoidan. The storage modulus ( $G'$ ) and the loss modulus ( $G''$ ) represent the elastic and the viscous portion of the hydrogels, respectively. These parameters allow a precise quantification of the gelation time, duration and the gelation temperature. The gel point is reached when  $G'$  becomes larger than  $G''$ . After the gelation phase where  $G'$  and  $G''$  quickly increase, a plateau is reached. Figure 6.5 A) (top) shows exemplary time sweep test for hydrogels without and with fucoidan. For the time sweep tests,  $G'$  and  $G''$  were measured at constant temperature for 16 min. The gel point and the end of the gelation process are marked with a dashed line. It was found that the sol-gel transition of hydrogels without fucoidan occurred after approximately 75 s at 37°C. The gel point of hydrogels containing 100  $\mu\text{g}/\text{ml}$  fucoidan occurred after around 59 s at 37°C. The gelation process of both hydrogels, with and without fucoidan, lasted approximately for 6 min until reaching a stable state.

Further rheological measurements were performed to determine the exact gelation temperature of hydrogels with 0 and with 100  $\mu\text{g}/\text{ml}$  fucoidan. Temperature sweep tests as shown in Figure 6.5 B) revealed that hydrogels without fucoidan started to gelate at 36.8°C. Hydrogels containing 100  $\mu\text{g}/\text{ml}$  already started to gelate at 35.3°C. These results indicate that the encapsulation of fucoidan into the hydrogel decreased the temperature at which the gel point is reached.

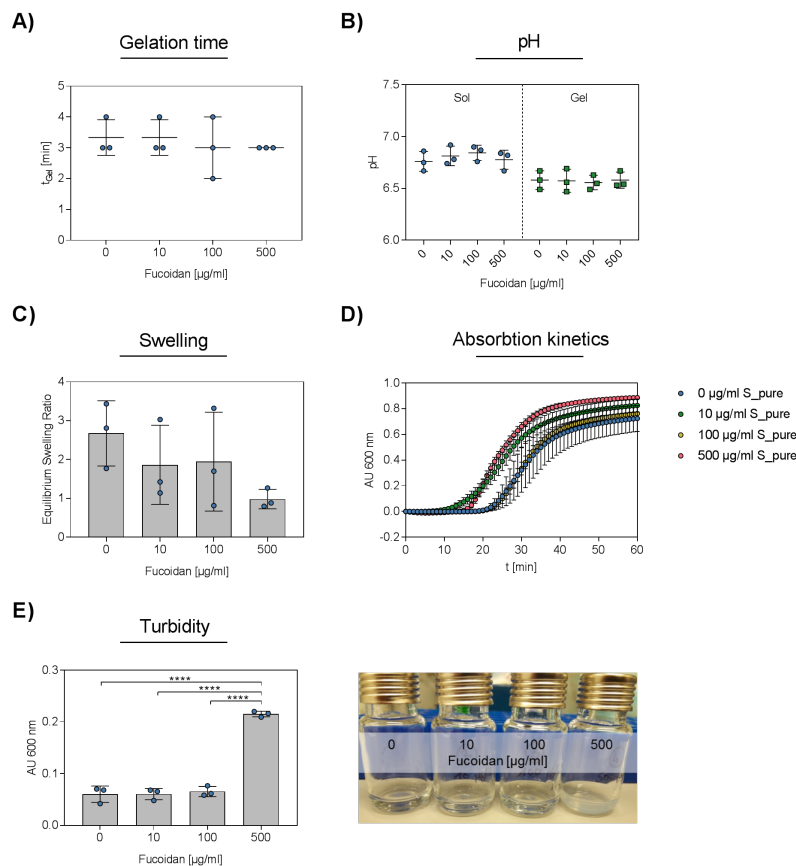


**Figure 6.4:** Physical and chemical properties of the thermosensitive chitosan-collagen hydrogel with different fucoidan concentrations. 0, 10, 100 and 500  $\mu\text{g/ml}$  fucoidan were encapsulated into the hydrogel. A) The gelation time at  $37^\circ\text{C}$  was estimated using the tube-inverting method. B) The pH of the hydrogels was measured before and after gelation. C) The swelling capacities of the hydrogels were quantified by determining the equilibrium swelling ratio. D) The gelation process was monitored by measuring the absorption at 600 nm every minute for one hour. E) The turbidity of the sols was quantified by measuring the absorption at 600 nm (left). The appearance of the hydrogels is shown on a photo (right). Results from three independent experiments were plotted. Significances were calculated using ANOVA.

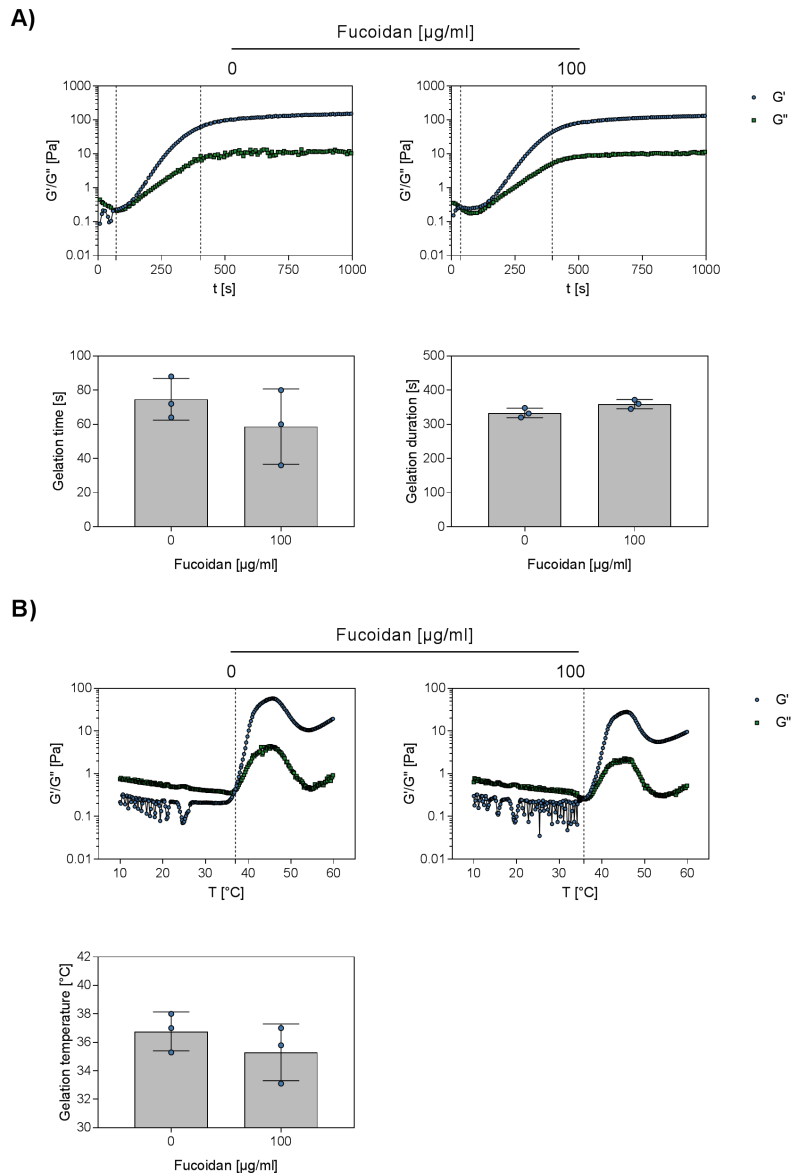


**Figure 6.5:** Rheological measurements of storage ( $G'$ ) and loss modulus ( $G''$ ) for the determination of gelation temperature, time and duration of thermosensitive chitosan-collagen hydrogels with different fucoidan concentrations. A) Time sweep tests (top) of hydrogels at  $37^\circ\text{C}$  and at a constant frequency of 1 Hz. The gel point and the end of the gelation process are marked with a dashed line. Start time of the gelation process and gelation duration were plotted (bottom). B) Temperature sweep tests (top) of hydrogels at a constant frequency of 1 Hz using a temperature gradient from 10 to  $60^\circ\text{C}$  ( $2^\circ\text{C}/\text{min}$ ). The gel point is marked with a dashed line. The gelation temperature was plotted (bottom). Experiments were repeated three times.

### 6.2.2 Internal microstructure visualized by SEM

To study the internal structure of the prepared hydrogels, SEM was applied. Therefore, samples with and without fucoidan were prepared and dried by lyophilization or critical point drying. Adequate drying of hydrogels without altering the internal structure is a well known challenge. Lyophilization of the samples resulted in visible alterations of the hydrogel shape and internal structure. The morphology and surface texture differed strongly within one hydrogel, but also differed among samples. Some similar structural elements that were observed are visualized in Figure 6.6 A). These structures consisted of larger regular pores which were partly connected by thinner filaments. Also, many samples were characterized by a sponge-like outer layer with small pores surrounding the inner of the samples which was dominated by larger pores (examples are shown in Figure 6.6 B)). Likely, these structures are formed during the dry-freezing process when outer layers of the hydrogels freeze first. The inconsistency of structural elements even within one sample suggests that lyophilization does not represent an adequate way to conserve the structural elements of a hydrogel.

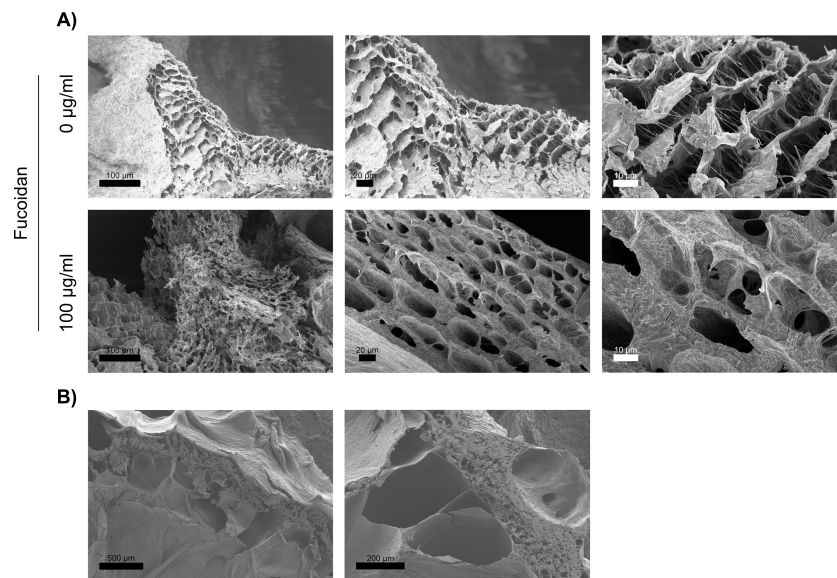


**Figure 6.6:** Internal structure of lyophilized chitosan-collagen hydrogels with and without fucoidan visualized by SEM. Samples were freeze-dried and cut in half to image the cross-sections. A) Porous structure in different magnifications of hydrogels with 0 and 100 µg/ml fucoidan. B) Exemplary visualization of sponge-like outer layer and large pores in the center of the sample.

CPD resulted in uniformly dried samples which had a very homogeneous appearance. The homogeneity was confirmed on a microscopic scale by SEM imaging. All hydrogels consisted of fluffy spheres that were entangled by long thin filaments. The distribution

of particles and filaments seemed to occur randomly. The particles tended to merge into larger aggregates causing the formation of irregular pores. The encapsulation of fucoidan caused no visible changes in the morphology of the hydrogels as shown in Figure 6.7 A). The random interaction of filaments and spheres is depicted in a high magnification in Figure 6.7 B). The filaments which most likely represent the collagen portion of the hydrogel often arranged into helix-like structures as shown in Figure 6.7 C). The fluffy nanoparticle-like spheres probably represent the chitosan portion of the hydrogel. Even though, most of the spheres had a fluffy-like appearance, some particles stood out due to their very smooth surface. An example is illustrated in Figure 6.7 D). The homogeneous samples demonstrate that the hydrogel structure is most likely better preserved and therefore more reliable after CPD than after lyophilization.

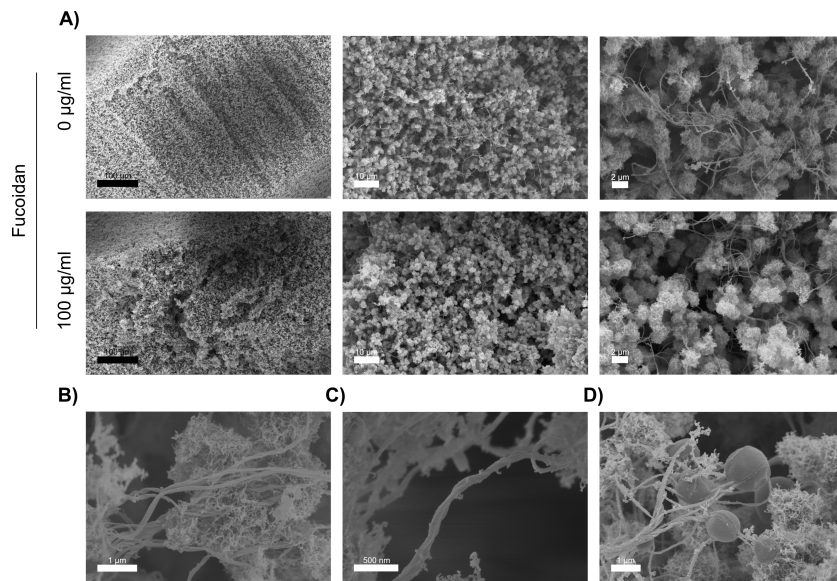


**Figure 6.7:** Internal structure of critical point dried chitosan-collagen hydrogels with and without fucoidan visualized by SEM. Before critical point drying (CPD), hydrogels were cut in half to image the cross-section. A) Homogeneous structure of hydrogels with 0 and 100  $\mu\text{g}/\text{ml}$  fucoidan characterized by spherical particles entangled by thinner filaments. B), C) and D) Exemplary visualizations of structural elements dominating the internal structure of CPD samples.

### 6.2.3 Fucoidan detection and release

To prove the encapsulation of fucoidan into the hydrogel, a protocol published by Yamazaki and colleagues [190] was adapted. Yamazaki et al. demonstrated that the nucleic acid stain SYBR Gold can be used to quantify the concentration of fucoidan solutions. Similar to DNA, the fluorescent dye binds to the fucoidan molecules and the amount of bound dye can be quantified by measuring the fluorescence. The detected fluorescence

has a linear relation to the amount of fucoidan for a specific range of concentrations (for further methodical details see section 2.7.9). To detect fucoidan inside a hydrogel, the method was adapted. Even though, the determination of absolute fucoidan concentrations inside the hydrogels using a standard curve was not possible, Figure 6.8 A) and B) show that hydrogels with more encapsulated fucoidan resulted in an increased fluorescent signal. The detection of fluorescence was carried out using two different techniques. In A), prepared hydrogels were stained using SYBR Gold and imaged with a fluorescence microscope. Exemplary pictures of the stained hydrogels with increasing amounts of fucoidan are shown. As the intensity analysis confirms, hydrogels with more encapsulated fucoidan exhibited an increased fluorescent signal. In B), the fluorescence was measured using a plate reader. Similarly, hydrogels with increased fucoidan concentrations showed a higher fluorescent signal.

The same method was applied to study the release of fucoidan from the hydrogel over a time period of six days. Figure 6.8 C) shows that approximately 60% of the detected fucoidan got released from the hydrogel within two days. After two days, the fucoidan release proceeded slower. On day six, 80% of the fucoidan was already released from the gels.

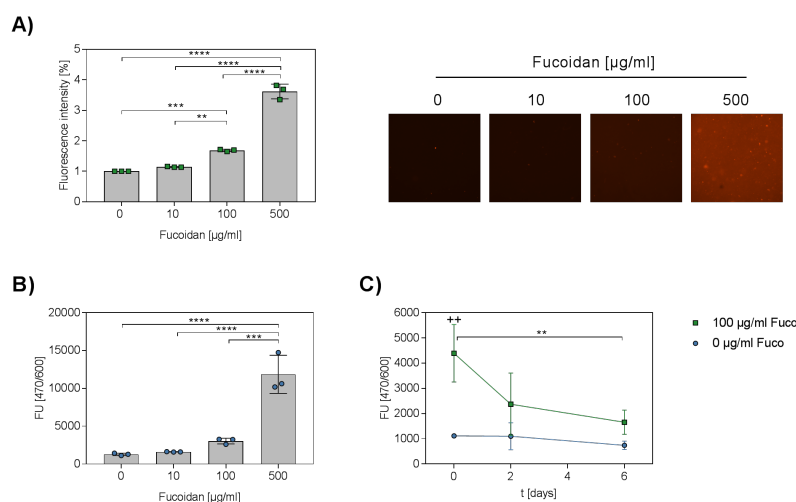


**Figure 6.8:** Detection of fucoidan inside the hydrogel and fucoidan release from the hydrogels. Hydrogels with 0, 10, 100 and 500  $\mu\text{g/ml}$  fucoidan were prepared. A) Hydrogels were prepared in Angiogenesis  $\mu$ -slides, stained with SYBR Gold and subsequently imaged using a fluorescence microscope (right). Fluorescence intensity was quantified for three frames per sample (left). B) Hydrogels were prepared in 96-well plates, stained with SYBR Gold and fluorescence was measured at 470 nm and 600 nm excitation and emission wavelength, respectively. Results from three independent experiments were plotted. Significances were calculated using ANOVA (for C): \* significances compared to different time points, + significance compared to 0  $\mu\text{g/ml}$  fucoidan.)

## 6.3 Biological Performance

The following section provides information about the biocompatibility of the thermosensitive chitosan-collagen hydrogel with integrated fucoidan. 2D and 3D cell culture of MSC and OEC was performed and the vitality of the cells was examined using fluorescence microscopy and SEM.

### 6.3.1 MSC

MSC cultured on top of the gel or encapsulated into the gel were predominantly vital as shown by the life/dead stainings in Figure 6.9. Nevertheless, differences were observed between 2D- and 3D-cultured cells. Gels with encapsulated MSC contained more dead cells compared to 2D cell cultures. For both culturing techniques, adhesion and spreading of MSC was increased on day six. MSC stained on day two were mostly characterized by a round and small phenotype, while MSC stained on day six had clearly elongated. As shown in Figure 6.9 in the bottom images, 3D-cultured MSC also appeared vital and elongated on day ten. The cell density of encapsulated MSC in one layer was understandably smaller compared to 2D-cultured MSC. Encapsulated MSC were evenly distributed throughout the different gel layers. Only, on the bottom of the wells, accumulations of MSC were observed. The encapsulation of fucoidan inside the hydrogel had no visible effect on the vitality or performance of the MSC.

To study the interaction of MSC with the biomaterial on a microscopic scale, SEM was applied. Therefore, MSC were seeded on top of the hydrogels and dried using CPD on day six. As shown by the micrographs in Figure 6.10, MSC were completely embedded into the material. They predominantly interacted with the collagen portion inside the hydrogel. As already demonstrated by the fluorescence images shown in Figure 6.9, MSC adhered and elongated inside the material. Similar to the results from life/dead staining, no differences were observed between MSC cultured on hydrogels with and without fucoidan. Life/dead staining, as well as SEM experiments indicate that MSC cultured on top of the gel or encapsulated inside the gel were vital, able to adhere and to spread. To assess whether fucoidan addition into the hydrogel had an effect on the secretion of angiogenic signaling molecule VEGF, MSC were encapsulated into the hydrogel and VEGF levels in the supernatant were quantified on day one and six. Additionally to the VEGF levels, the DNA content was quantified from the hydrogels, offering the possibility to express VEGF levels relatively to the DNA content. Figure 6.11 A) shows that the VEGF content in the supernatant increased from day one to day three by approximately 80%. However, no differences in VEGF levels could be quantified from day three to day six. The addition of fucoidan into the hydrogels had no significant effect on the secretion of VEGF into the supernatant. As indicated in Figure 6.11 B), the determined DNA from the hydrogels was the same on day one and day six. This result indicates that MSC did not significantly proliferate inside the hydrogel in the presented period of time. Similar to the VEGF secretion, fucoidan encapsulation into the hydrogels had no impact on the quantified DNA content. Even though, the VEGF secretion per  $\mu\text{g}$  DNA tentatively increased from day one to day six, the differences were

not significant (Figure 6.11 C)). This experiment suggests that fucoidan encapsulation into the hydrogel had no impact on the secretion of VEGF by MSC. It also indicates that the amount of cells inside the hydrogel was not impaired by the presence of fucoidan.

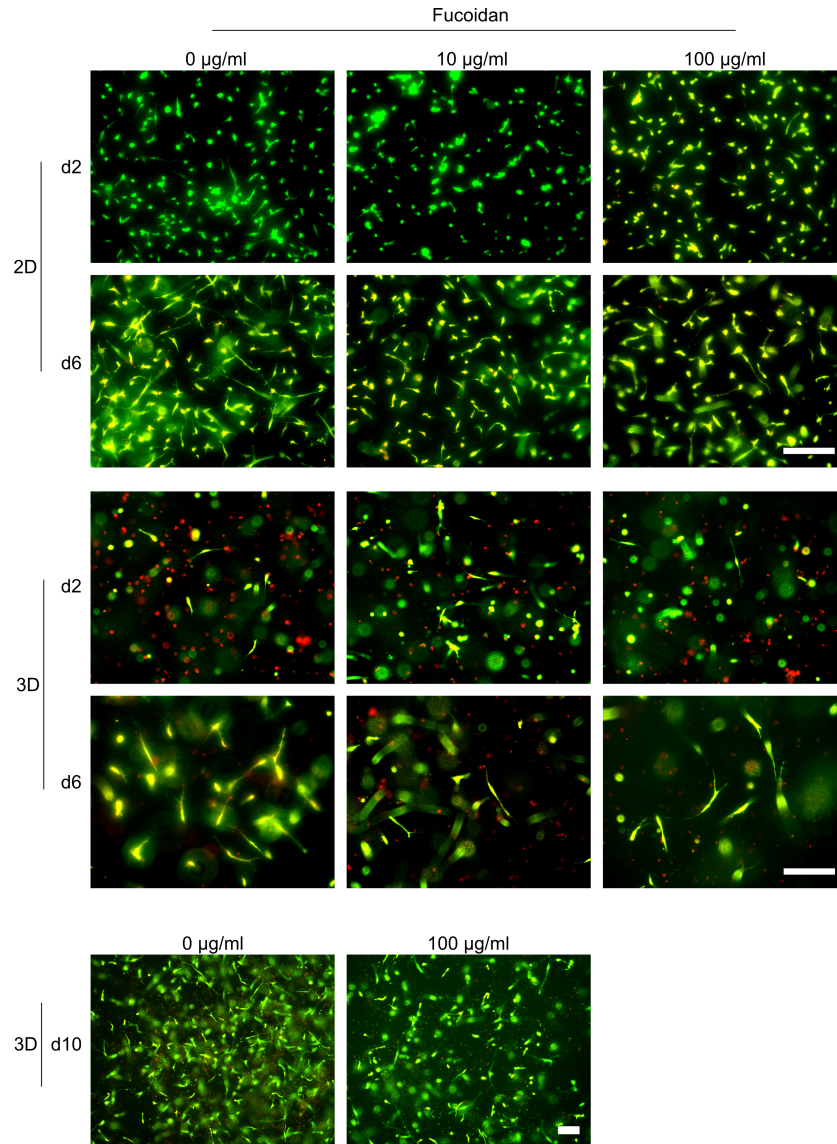


**Figure 6.9:** 2D and 3D cell culture of human MSC on and in chitosan-collagen hydrogels. Hydrogels with 0, 10 and 100 µg/ml fucoidan were prepared. For 2D culture, MSC were seeded on top of the gels; for 3D culture, MSC were encapsulated into the gel. Vital (green) and dead (red) cells were visualized on day two, six and ten using calcein-AM and propidium iodide staining, respectively. Scale bars = 200 µm.

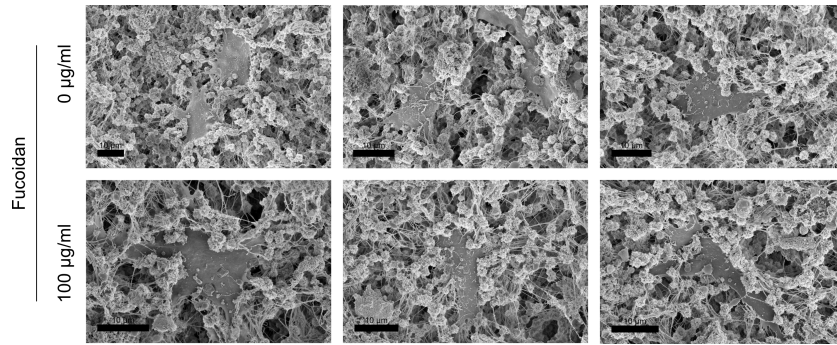


**Figure 6.10:** Interaction of MSC with the chitosan-collagen hydrogel. MSC were seeded on top of hydrogels containing 0 and 100  $\mu\text{g/ml}$  fucoidan. Hydrogels were dried using CPD on day six and subsequently imaged by SEM.

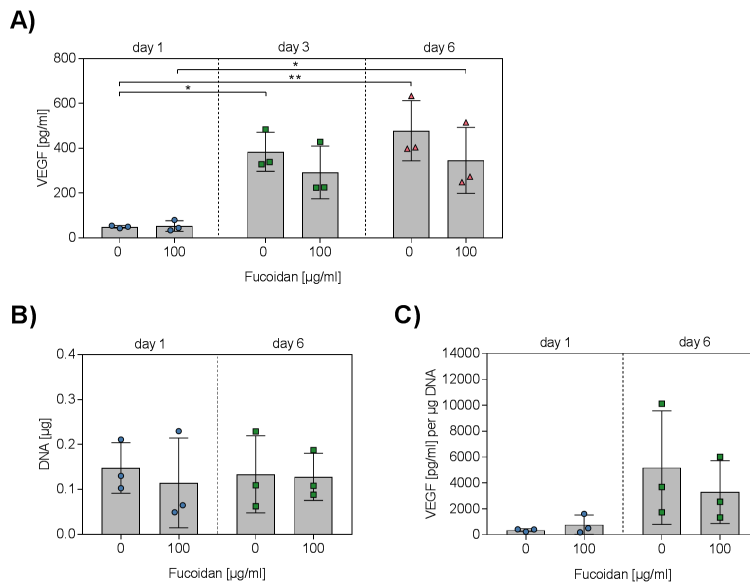


**Figure 6.11:** VEGF levels in the supernatant and DNA content from hydrogels with encapsulated MSC. MSC were encapsulated into hydrogels containing 0 and 100  $\mu\text{g/ml}$  fucoidan. A) VEGF levels were quantified using ELISA on day one, three and six. B) The DNA content of the hydrogels was quantified on day one and six. C) The VEGF levels from day one and six were expressed relatively to the DNA content of the respective hydrogels. Results from three independent experiments with three different donors were plotted. Significances compared to the control cells (\*) were calculated using ANOVA.

### 6.3.2 OEC

OEC cultured on top of the hydrogels were predominantly vital as visualized in Figure 6.12 by the life/dad staining. The amount of cells visible on the hydrogel decreased slightly from day two to day six, indicating that the cell adhesion to the hydrogel was not as strong as shown for the MSC in the latter section. Similar to the result for MSC, fucoidan encapsulation into the hydrogel had no visible impact on the vitality of the OEC. In comparison to the MSC, OEC were more sensitive in regard to encapsulation into the hydrogel. As demonstrated in Figure 6.12 in the bottom images, encapsulated OEC had a small round phenotype on day two which only slightly changed on day six. Also on day six, encapsulated OEC with a round shape dominated and were hardly able to elongate.

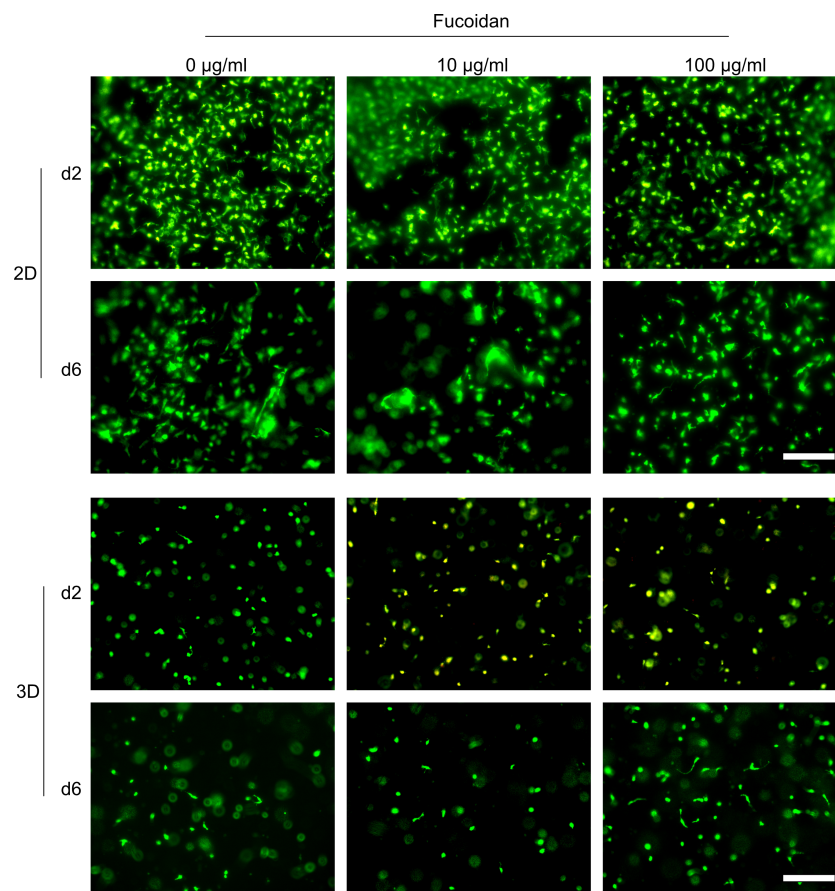


**Figure 6.12:** 2D and 3D cell culture of human OEC on and in chitosan-collagen hydrogels. Hydrogels with 0, 10 and 100  $\mu\text{g}/\text{ml}$  fucoidan were prepared. For 2D culture, OEC were seeded on top of the gels; for 3D culture, OEC were encapsulated into the gel. Vital (green) and dead (red) cells were visualized on day two and six using calcein-AM and propidium iodide staining, respectively. Scale bars = 200  $\mu\text{m}$ .

# 7

## Discussion

---

*This chapter summarizes the results and discusses them by consulting adequate examples from the literature. In the end, a conclusion and future perspectives are given.*

### Contents

---

7.1	Bioactivity of Enzymatically-Extracted Fucoidans on Angiogenesis and Osteogenesis . . . . .	100
7.2	Effect of Enzymatic Hydrolysis on the Bioactivity of the Resulting Fucoidans . . . . .	103
7.3	Preliminary Effect of Chemically Extracted and Degraded Fucoidans . . . . .	107
7.4	Injectable Chitosan-Collagen Hydrogel as a Delivery System for Fucoidan . . . . .	109
7.5	Conclusions & Future Perspectives . . . . .	112

---

## 7.1 Bioactivity of Enzymatically-Extracted Fucoidans on Angiogenesis and Osteogenesis

In the first part of the presented thesis, enzymatically-extracted fucoidans from *Fucus evanescens* were examined in regard to their bioactivities on bone regeneration processes in cell model systems mimicking bone tissue environment. To further elucidate the relationship between structure and bioactivity, chemical properties of the extracts were related to the observed bioactivities.

To isolate fucoidan from the brown algae, enzyme-assisted extraction was applied. Therefore, cell walls of the algal material were digested using alginate lyases and cellulases to release the crude fucoidan extract (FE\_crude). FE\_crude was purified with IEX resulting in three eluted fractions: FE\_F1, FE\_F2 and FE\_F3. The chemical characterization of the extracts revealed that they mainly differed in fucose and alginate, as well as sulfate content. Fucose content was the lowest in the crude extract and increased in the fucoidan fractions. FE\_F3 had the highest fucose content. Reversely, alginate content was the highest in the crude extract and decreased in the fractions. No alginate impurities were detected in the purest fraction FE\_F3. The sulfate content increased with the purity of the extracts and was highest in the FE\_F3 fraction. All extracts were HMW fucoidans with peaks ranging from 400-600 kDa. MTS and LDH assays revealed that treatment with all extracts was neither toxic, nor affected the metabolic activity of OEC and MSC. However, it was observed that MSC reacted more sensitively to higher doses of fucoidan treatment which was indicated by a reduced metabolic activity. The effect of fucoidan treatment on angiogenesis and osteogenesis was taken as a measure to evaluate fucoidan's bioactivity on bone regeneration. By quantifying the gene expression and protein levels of four prominent angiogenic regulatory molecules in MSC and OEC mono- and co-cultures and by visualizing the tube formation in the co-culture system, we found that the fucoidan extracts inhibited angiogenesis-related processes and associated key regulatory molecules.

Various studies already claimed that fucoidan acts on angiogenesis. However, as pointed out earlier in the introduction, the use of different fucoidan extracts and experimental set-ups, as well as insufficiently chemical characterization make results difficult to compare and to interpret. Similar to the presented results, Wang et al. demonstrated in two studies the anti-angiogenic effect of several fucoidan extracts. The commercially available crude extract from *Fucus vesiculosus* (by Sigma-Aldrich) was found to impair angiogenesis which was mostly related to reduced VEGF and SDF-1 protein levels [180]. The second study compared the bioactivity of fucoidans originating from three *Fucus* species, extracted by different techniques including chemical and microwave-assisted extraction. If fucoidan treatment exhibited an effect, it was consistently anti-angiogenic [181]. On the other hand, Bouvard and colleagues, Kim and colleagues, as well as Matou and colleagues observed a pro-angiogenic effect after fucoidan treatment in their model systems [18, 92, 122]. All mentioned studies used HUVECs as a cell model system. The study from Bouvard et al. examined the effect of a LMW fucoidan (4.5 kDa) from *Ascophyllum nodosum*, while Kim et al. analyzed an extract from *Laminaria japonica*

containing a broad range of molecular weights. Similar to Bouvard's study, Matou et al. analyzed an extract from *Ascophyllum nodosum*, but it contained mainly MMW polysaccharides (16-30 kDa). This variety of parameters demonstrates once again why until today the bioactivity of fucoidan cannot be ultimately defined.

In the presented thesis, the anti-angiogenic effect of the fucoidan extracts (especially the pure ones, such as FE\_F2 and FE\_F3) was related to decreased gene expressions of VEGF and SDF-1 and decreased protein levels of VEGF, ANG-1 and SDF-1 in the MSC mono-cultures. ANG-2 protein levels were decreased in OEC mono-cultures after fucoidan treatment. The VEGF-VEGFR2, as well as ANG-TIE-2 systems are crucial regulators of angiogenesis [61, 10]. Hampering of VEGF signaling due to fucoidan treatment prevents the activation of EC. Hence, tip cells are not formed and sprouting cannot proceed. VEGF also regulates the permeability of the EC layer through src [59]. Without VEGF signaling, VE-cadherin is not internalized and cell-cell contacts remain stable. The lack of a pro-angiogenic stimulus mediated through VEGF prevents the secretion of ANG-2 which functions as an antagonist for ANG-1-TIE-2 signaling [118]. EC remain in a quiescent state characterized by a high survival and low migration. Hence, the formation of prevascular structures is impaired. These conclusions are in accordance with the results from the OEC-MSC co-culture experiments. Treatment with the fucoidan fractions reduced the number of emerged tube-like angiogenic structures. The secretion of ANG-2 in the co-culture system was equally reduced after fucoidan treatment as in the OEC mono-cultures. Further, FE\_F2 and FE\_F3 treatment reduced the gene expression of MMP14 in the co-culture. The degradation of the ECM through MMPs is necessary to allow EC migrate and form new blood vessels into the tissue [148]. In contrast to the mono-culture experiments, VEGF protein levels increased in the co-cultures compared to the control. Despite fucoidan treatment, MSC kept secreting VEGF, which interestingly did not provoke the activation of OEC and subsequent formation of angiogenic structures. The assumption that fucoidan treatment impairs the phosphorylation and therefore the activation of VEGFR2 could not be confirmed. VEGF-induced phosphorylation in OEC mono-cultures was not altered by fucoidan treatment. It is worth to note that this result from OEC mono-culture does not exclude the possibility that fucoidan acts differently on VEGFR2 phosphorylation in the co-culture system.

Inflammatory processes are tightly connected to angiogenesis. Activated EC due to a pro-angiogenic or a pro-inflammatory stimulus are characterized by a similar behavior such as an increased layer permeability [141]. Results from OEC mono-cultures demonstrate that IL-6, ICAM-1 and VCAM-1 gene expression were reduced after FE\_F3 treatment. A study conducted by Kirsten et al. elaborately analyzed the effect of FE\_F3 on inflammation in LPS-stimulated OEC. According to the preliminary data shown in the presented thesis, the study demonstrated that FE\_F3 pretreatment reduced the LPS-induced inflammatory response in OEC (manuscript in preparation). These findings are in accordance with the angiogenesis-related results: A low inflammatory state in OEC favors a non-angiogenic phenotype.

To reveal whether osteogenic processes, next to angiogenesis and inflammation, were also directly influenced by treatment with the enzymatically-extracted fucoidans, ALP

expression and activity, as well as degree of calcification were quantified as early and late osteogenic differentiation markers, respectively. While, ALP activity was not altered after fucoidan treatment in MSC mono-cultures, ALP gene expression was strongly decreased in MSC mono-cultures, as well as in the co-culture system, after treatment with the fucoidan fractions. Similarly, the calcification level in MSC mono-cultures treated with FE\_F2 and FE\_F3 was decreased. Osteoblast differentiation and maturation are closely related to angiogenesis [163]. Even though, VEGF is one of the most important pro-angiogenic regulators, it also influences osteogenesis. Via paracrine signaling, VEGF triggers EC to release osteogenic factors such as BMP-2 [123]. Various studies demonstrate that VEGF is also able to directly act on osteoblasts in an autocrine way [124, 38]. Finally, Liu et al. propose an intracrine mechanism where intracellular VEGF-VEGFR2 complexes enter the nucleus and activate transcription factors which favor osteoblast differentiation [113]. Thus, a decreased VEGF level in MSC mono-cultures due to fucoidan treatment could explain the reduced osteoblast maturation indicated by decreased ALP expression and calcium deposition.

In contrast to our findings, other studies claimed the beneficial effect of fucoidan treatment on bone regeneration and osteoblast differentiation [78, 139, 91]. However most of these studies examined the effect of LMW fucoidans (< 15 kDa), while we report on the bioactivity of HMW fucoidans (> 350 kDa).

If the enzymatically-extracted fucoidans exhibited an effect on the model cells, it was consistently anti-angiogenic and anti-osteogenic. However, the intensity of the effect differed among the individual extracts. A trend was clearly visible: the higher the sulfate, respectively fucose content was, the stronger was the observed inhibiting effect on angiogenic and osteogenic processes. Pure extracts with a higher sulfate content such as FE\_F2 and FE\_F3 impaired the mentioned processes more than the crude extract with a lower fucose and sulfate content. We conclude that the purity of the extracts, as well as the sulfate content play a crucial role for defining the bioactivity of fucoidans. In accordance with our observations, Soeda and colleagues demonstrated that chemically oversulfated fucoidan from *Fucus vesiculosus*, unlike its native counterpart, reduced the formation of capillary-like structures in HUVECs [162]. Similarly to Haroun-Bouhedja and colleagues, we suggest that a higher content of sulfates increases the negative charge of the fucoidan molecules, hence facilitating the formation of fucoidan-protein complexes [70]. Indeed, it is well-known that sulfated glycosaminoglycans are able to interact with a variety of growth factors, cytokines and chemokines and that these interactions are crucial for functioning physiological processes [110]. Separate from physiological sulfated polysaccharides, the affinity of growth factors was also shown for foreign sulfated polysaccharides. Sun and colleagues demonstrated that binding of dextran sulfate and  $\gamma$ -carrageenan to fibroblast growth factor (FGF) increased the thermal stability and retained the bioactivity of the growth factor for a longer period of time [167]. Supporting the assumption that fucoidans exhibit an affinity to signaling molecules, we showed in an ELISA-based competitive binding assay that the enzymatically-extracted fucoidans suppressed the binding of VEGF to its antibody in a concentration-dependent manner. Lake and colleagues published a study which stresses the importance of sulfates

for the interaction between fucoidan and signaling molecules. They compared the effect of fucoidan on VEGF<sub>165</sub>- (contains a heparan sulfate binding site) and VEGF<sub>121</sub>-driven (does not contain a heparan sulfate binding site) chemotaxis of EC. They showed that fucoidan was only able to enhance VEGF<sub>165</sub>-driven chemotaxis of EC [103]. However, not all observed bioactivities of fucoidan can be reproduced using other sulfated polysaccharides such as heparin or chondroitin sulfate [103, 154], suggesting that apart from sulfate content, other chemical properties play a role for defining fucoidan's bioactivities. The influence of molecular weight and branching on the bioactivity of fucoidans will be discussed in more detail in the next section.

To conclude the results from the first part, we hypothesize that treatment with the enzymatically-extracted fucoidans causes OEC to remain in a quiescent state impairing the formation of angiogenic tube-like structures and hindering the maturation of osteoblast-like MSC. This status is especially favored by the purest extracts FE\_F2 and FE\_F3 (high fucose content) which also contain a higher sulfate content compared to the other extracts. Although still unclear, this effect might be caused by the binding of fucoidan to VEGF and/or the interaction with the OEC and MSC surface, thereby preventing the activation of pro-angiogenic signaling pathways.

## 7.2 Effect of Enzymatic Hydrolysis on the Bioactivity of the Resulting Fucoidans

The second part of the presented thesis investigated whether guided enzymatic hydrolysis can change the bioactivity of fucoidan in angiogenesis and inflammation, both processes relevant for successful bone regeneration and maintenance of bone health. It further investigated which chemical properties contribute to the observed effects.

Therefore, enzymatically-extracted HMW fucoidan fraction FE\_F3 was cleaved at  $\alpha$ -(1,4)-glycosidic bonds between non-acetylated and C2-monosulfated units using the newly discovered endo-fucoidanase Fhf1 from *Formosa haliotis* obtaining LMW fucoidan oligosaccharides and a MMW fucoidan fraction. FE\_F3 was chosen for enzymatic hydrolysis, because it exhibited the strongest bioactivity on OEC and MSC compared to the other fucoidan fractions (as discussed in the prior section 7.1). Further, it was the purest extract measured by its high fucose content and it had no detectable alginate, protein or polyphenol contaminations [133]. OEC and MSC mono- and co-cultures were treated with MMW and LMW fucoidan and the expression and secretion of angiogenic and inflammatory mediators were determined. The integrity of the EC layer was quantified and the formation of angiogenic structures in the co-culture system was analyzed. The observed bioactivities of MMW and LMW were directly compared to the effect of HMW FE\_F3.

As the results clearly show, MMW and LMW obtained after enzymatic hydrolysis had no longer an inhibiting effect on angiogenesis as it was proven for HMW FE\_F3. While treatment with HMW FE\_F3 decreased VEGF and ANG-1 gene expression and protein levels in MSC, treatment with MMW and LMW had only a minor effect on these mediators. Treatment with HMW FE\_F3 suppressed the formation of tube-like angiogenic

structures in the co-culture system almost completely, while MMW and LMW did not impair the formation of these structures.

The bioactivity of fucoidan is highly dependent on the chemical structure. However, the great amount of parameters taking influence on the chemical properties makes it difficult to control batch-to-batch reproducibility and to find suitable fucoidans for specific applications. A new concept to create fucoidans with defined chemical properties is the use of characterized fucoidanases which specifically cleave fucoidan into smaller fragments. Different fucoidanases have been discovered in marine organisms, but only few of them are functionally characterized. Sichert and colleagues analyzed '*Lentimonas*' sp. CC4 for fucoidanase expression and found more than 200 putative fucoidanases [158]. While the discovery and characterization of fucoidanases keep progressing, the number of studies investigating the bioactivities of the resulting fucoidan fragments is still very limited. Just recently, Nielsen et al. investigated the effect of fucoidan oligosaccharides resulting from fucoidanase cleavage together with hydroxyapatite on bone regeneration in sheep after insertion into a critical-sized defect [132]. New bone formation was analyzed by micro-CT and immunohistochemistry. Unfortunately, the native HMW fucoidan was not integrated into the study, therefore not allowing to evaluate possible bioactivity changes resulting from enzymatic cleavage. Studies by Chen et al., Kim et al. and Silchenko et al. however, compared the effect of fucoidan before and after enzymatic hydrolysis. Chen and Colleagues found that fucoidans from *Laminaria japonica* increased the tyrosinase and melanogenesis inhibition, as well as DPPH radical scavenging activities after degradation by fucoidanase from *Flavobacterium* RC2-3 [26]. Kim and colleagues observed that enzymatically degraded fucoidans from *Undaria pinnatifida* had 3-4 times reduced anticoagulating activities and did not influence the prothrombin time compared to the native fucoidan [94]. Silchenko and colleagues used fucoidanase FFA1 from *Formosa algae* to degrade fucoidan from *Sargassum horneri* and showed that oligosaccharides were not able to suppress the formation of cancer cell colonies compared to the native fucoidan which inhibited colony formation by 50 % [160]. Accordingly to our results, it becomes clear that fucoidans before and after fucoidanase hydrolysis exhibit different bioactivities. Interestingly, a number of studies found similar to our own results that fucoidans with a very small molecular weight lose or exhibit reduced effects on the studied systems: Fucoidan oligosaccharides showed reduced anticoagulating activities [94], didn't suppress cancer cell colony formation [160] or had a decreased FGF binding affinity [84].

In the recent years, it became increasingly clear that molecular weight of fucoidan plays a crucial role for defining its bioactivities [177, 66, 192]. In our own studies, we observed that fucoidans with a high molecular weight (independently from species or extraction technique) always impaired angiogenic processes. Several studies report that LMW fucoidans had a beneficial effect on angiogenesis and bone regeneration. Chabut and colleagues demonstrated that a 4 kDa fucoidan enhanced FGF-induced tube formation in EC through heparan sulfate-dependent  $\alpha 6$  integrin overexpression [24]. Bouvard and colleagues demonstrated that a 4.5 kDa fucoidan induced EC migration via PI3K/AKT signaling [18]. Hwang and colleagues found that a 1-30 kDa fucoidan fraction upregulated

the expression of osteogenic genes and increased bone density, as well as bone ash weight in vivo [78]. Authors like Matsubara and colleagues tried to categorize fucoidan's bioactivity dependent from their molecular weights. They suggest that fucoidans smaller than 20-30 kDa rather have pro-angiogenic effects than their larger counterparts [123]. However, studies reporting on the anti-angiogenic properties of LMW fucoidans [25] make clear that no universal definition exists which helps to predict the bioactivity of fucoidan dependent from their molecular weight. Nevertheless, it is undisputed that molecular weight plays a crucial role in defining fucoidan's bioactivities. Molecular weight has an impact on the total amount of sulfates displayed on the molecule and it also influences the three dimensional structure. Both parameters likely are important when it comes to the interaction of fucoidan with signaling molecules or the cellular surface. We visualized the interaction of HMW FE\_F3, MMW and LMW with OEC and MSC by immunocytochemistry and indeed found that HMW FE\_F3 interacted much stronger with the cells than MMW and LMW fucoidans. It is known that heparan sulfate, a part of heparin sulfate proteoglycans located on the cellular surface plays a crucial role during angiogenic events by modulating VEGF and FGF receptor affinity [58]. Possibly, fucoidan bound to the cellular surface alters the interaction of growth factors with its receptors by mimicking proteoglycans and therefore influencing downstream signaling pathways.

We compared the effect of MMW and LMW obtained by enzymatic hydrolysis with the effect of HMW FE\_F3 on angiogenesis and found that anti-angiogenic properties were no longer present. This finding indicates that defined enzymatic cleavage might represent a suitable technique to tailor fucoidans in regard to different applications. However, aside from the intended effects, bioactive compounds used for bone regeneration need to meet further requirements. Chronic inflammation is a major problem in bone regeneration and the maintenance of bone health which can be caused by diseases, bacterial infections or wear particles after total joint replacement [35, 81, 109]. For bone repair it is essential that applied compounds does not favor the development of a chronic inflammation. By studying the effects of MMW and LMW on inflammatory processes, we observed that higher doses of MMW triggered an inflammatory response in OEC indicated by increased expression and secretion of IL-6 and ICAM-1. Additionally, we observed the loosening of VE-cadherin-associated cell junctions, again underlining a pro-inflammatory response in OEC after treatment with 100  $\mu\text{g}/\text{ml}$  MMW. While numerous studies prove the anti-inflammatory effect of fucoidan treatment, only few studies exist indicating a pro-inflammatory effect caused by fucoidan [80, 131, 136]. Jin and colleagues studied the adjuvant function of fucoidan from *Fucus vesiculosus* and found that fucoidan induced the production of pro-inflammatory cytokines in dendritic cells. Fucoidan in combination with ovalbumin antigen enhanced the antibody production, upregulated MHC class I and II and increased T cell proliferation in vivo [83]. The same authors published in another study that fucoidan from *Undaria pinnatifida* increased the production of IL-6, IL-8 and TNF- $\alpha$  in neutrophils [82]. To exclude that a bacterial contamination in the MMW extract resulting from for example enzymatic digestion was responsible for the observed pro-inflammatory effect, the endotoxin content was quantified. The

assay resulted in very low endotoxin contents in both, MMW and LMW fucoidan. An inflammatory response triggered by bacterial impurities can therefore be excluded. By elucidating the detailed chemical structure of MMW and LMW, we tried to find chemical properties which are different in MMW and therefore might cause the inflammatory response in OEC. Next to molecular weight, the extracts differed in sulfate content and the presence of acetylation. MMW was disulfated at C2 and C4, while LMW was only sulfated at C2. The general impact of sulfates on the bioactivity of fucoidans was already discussed in the prior section in a detailed manner. While a lot of literature exists claiming the importance of sulfates in regard to bioactivity, the role of acetylation is less studied. NMR analysis revealed that LMW oligosaccharides were acetylated at C3, while the MMW fraction did not contain acetylations at any significant level. Wang and colleagues produced an acetylated fucoidan derivate and found that the antioxidant effect of the derivate was stronger compared to the native fucoidan [182]. On the other hand, Lapikova et al. observed that native fucoidan, as well as the deacetylated derivate were both able to inhibit factor Xa to the same extent, concluding that acetylation was not a determining factor for the observed bioactivity [105]. Probably acetylations do influence fucoidan's bioactivity to a certain extent. However, the lack of studies and the smaller abundance of acetylations in the chemical structure compared to sulfates indicate that acetylations likely play a minor role in determining fucoidan's bioactivities.

However, an important aspect which very likely influences fucoidan's bioactivity is its three dimensional structure. The 3D structure can be altered by charge (sulfates), molecular weight and also branching. While fucoidans from *Fucus evanescens* were originally considered as linear polymers [14], this assessment was later revised as some  $\rightarrow 3,4$ - $\alpha$ -L-Fucp-(1 $\rightarrow$ 3)-branch points were identified on desulfated and deacetylated samples [13]. NMR analysis of MMW and LMW indeed showed signals in the MMW fraction that indicate the presence of branching at low density. In contrast, the LMW oligosaccharides contained short, unbranched units with a lower charge density than the MMW fraction. Clément et al. compared the effect of branched LMW fucoidan from *Ascophyllum nodosum* with the effect of the linear polysaccharide. They found that the branched molecule exhibited a stronger anticomplementary activity. The authors explain that the presence of side chains reduced the flexibility of the fucoidan backbone. Therefore, it adopted a 3D conformation which was very similar to the target protein of C4. The interaction of branched fucoidan with C4 interrupted the complement activation [33]. As already mentioned in the prior section, it is well known that specific sulfated polysaccharides are able to interact with signaling molecules or receptors and therefore influence their bioactivity [125]. We can assume that branching altered the conformation of MMW molecules. Possibly, MMW fucoidan adopted a structure which was able to upregulate the expression of NF $\kappa$ B and secretion of IL-6 and ICAM-1 and therefore triggering a pro-inflammatory response in OEC.

Concluding the second part, enzymatic hydrolysis clearly changed the bioactivity of the obtained extracts compared to the HMW fucoidan. While HMW FE\_F3 impaired angiogenic processes in OEC and MSC, this was not observed for treatment with MMW and LMW. In contrast to high doses of MMW, LMW did not provoke an inflammatory

response in OEC. These results highlight the potential of defined enzymatic processing to select and tailor fucoidans for specific biomedical applications and also to further elucidate structure-function relationships in the context of bone regeneration.

### 7.3 Preliminary Effect of Chemically Extracted and Degraded Fucoidans

In the third part of the presented thesis, chemically extracted and H<sub>2</sub>O<sub>2</sub>-degraded fucoidan extracts varying in molecular weight were analyzed in a preliminary study in regard to their impact on angiogenic processes in MSC-OEC co-cultures.

Fucoidan from *Fucus evanescens* was chemically extracted and subsequently degraded using H<sub>2</sub>O<sub>2</sub>. The incubation time in H<sub>2</sub>O<sub>2</sub> varied, therefore resulting in three extracts with different molecular weights: CAU1 (26 kDa, MMW), CAU2 (18 kDa, MMW) and CAU3 (155 kDa, HMW). MSC-OEC co-cultures were treated with the extracts and the expression and secretion of important angiogenic mediators VEGF, SDF-1, ANG-1 and ANG-2 were quantified. Further, the impact of CAU1, CAU2 and CAU3 treatment on the formation of angiogenic tube-like structures was studied. To reveal bioactivity differences between native and degraded extracts, one co-culture was additionally treated with the native extract NatF, as well as with the purified native extract FracC. Equally, expression and secretion of the same mentioned mediators were quantified.

In contrast to the extracts MMW and LMW (see prior sections), CAU1, CAU2 and CAU3 were degraded by radical depolymerization using H<sub>2</sub>O<sub>2</sub>. The decreased molecular weight of CAU1, CAU2 and CAU3 in comparison to the native extracts NatF (539 kDa) and FracC (371 kDa) proves that radical depolymerization by H<sub>2</sub>O<sub>2</sub> is an effective way to reduce the molecular weight of fucoidans. It is noteworthy that H<sub>2</sub>O<sub>2</sub> incubation time did not correlate with the resulting molecular weights. CAU3 was incubated longest in H<sub>2</sub>O<sub>2</sub> and still had the highest molecular weight of >100 kDa. This result shows that radical depolymerization occurs randomly and that it cannot be used to intentionally produce fucoidans with specific molecular weights. This is different to enzymatic degradation which can be applied to degrade fucoidans in a defined and predictable manner [99]. Even though, enzymatic degradation is highly specific, no commercially available product exists, yet. Radical depolymerization using H<sub>2</sub>O<sub>2</sub> is simple and cheap, therefore representing a technique for fucoidan degradation which can easily be implemented in larger scale. Additionally, radical depolymerization has shown to possess anti-microbial effects on the sample [102].

Sulfate and fucose content were mostly comparable among the extracts. The consistency of these parameters makes it easier to understand the effect of molecular weight on the observed bioactivities.

To examine the effect of CAU1, CAU2 and CAU3 on angiogenic processes, MSC-OEC co-cultures were treated with the extracts and the formation of prevascular structures was observed on day four and seven using immunocytochemistry. Because angiogenic structures were not quantified, the observations and interpretations should only be taken as preliminary results. The microscopy pictures clearly showed that fucoidan treatment

did not impair the development of angiogenic structures. Possibly, treatment with CAU2 even increased the formation of angiogenic structures compared to the untreated sample. These results are similar to the ones obtained for enzymatically-degraded MMW and LMW which did not impair the formation of prevascular structures either. All mentioned extracts, except for CAU3, belong to the group of MMW or LMW fucoidans. Even though, CAU3 was categorized as a HMW, it is still much smaller than the other studied HMW fucoidans (155 kDa vs. 400 kDa) which were proven to impair the formation of prevascular structures (see chapter 3).

Fucoidan staining after treatment revealed that all H<sub>2</sub>O<sub>2</sub>-depolymerized extracts were able to interact with the cell models. The detected amount of fucoidan measured by the fluorescence intensity was highest for FE\_F3 (400-500 kDa), followed by the H<sub>2</sub>O<sub>2</sub>-depolymerized extracts (18-155 kDa), followed by the fucoidanase-degraded extracts (2-209 kDa). This result indicates that the interaction of fucoidan with the cell models might be molecular weight-dependent. The importance of molecular weight as a parameter to define fucoidan's bioactivity was already elaborately discussed in the prior section.

CAU1, CAU2 and CAU3 treatment had no effect on the gene expression of angiogenic mediators and only slightly decreased the secretion of angiopoietins in MSC-OEC co-cultures. These results are in accordance with the fact that the formation of angiogenic structures was not altered by treatment with the H<sub>2</sub>O<sub>2</sub>-depolymerized extracts.

To assess the bioactivity differences of extracts before and after radical depolymerization, one co-culture was treated with native crude and purified extracts NatF and FracC, respectively. However, these results base upon only one co-culture and should therefore be interpreted with caution. Both, NatF and FracC had a similar impact on the studied angiogenic mediators: The HMW fucoidans decreased the expression of all studied genes. This stands in contrast to the depolymerized extracts which had only an effect on the expression of ANG-1. In accordance with these results, the HMW fucoidans decreased the secretion of SDF-1, ANG-1 and ANG-2. The difference between native and depolymerized extracts on protein level was not as evident as for the gene expression. These results are similar to the ones obtained for enzymatically-extracted HMW fucoidans (especially FE\_F2 and FE\_F3) which significantly decreased the expression and secretion of the mentioned angiogenic signaling molecules.

The molecular weight of the studied enzymatically-extracted fucoidans was determined using SEC with pullulan as a calibration standard. The molecular weight of the chemically extracted fucoidans however was quantified using SEC coupled with a MALS-VIS detection system. Therefore, it was not completely accurate to compare the molecular weights of the enzymatically- and chemically extracted fucoidans before.

SEC with a calibration standard is commonly used to determine the molecular weight of fucoidans [8, 112, 130]. However, it is likely that results from this technique are not completely accurate and do not display the absolute and true molecular weight of the fucoidan sample. The determined molecular weight relies on the utilized standard which is often a narrowly distributed preparation such as pullulan or dextran. The standard used should reflect the chemical properties of fucoidan in the best way possible to deter-

mine correct molecular weights [142]. Due to fucoidan's extremely heterogeneous nature (charge, branching, 3D structure) however, no such standard exists. SEC with a MALS detection system allows to determine the accurate molecular weight of fucoidans without the need of an external calibration standard. Here, the molecular weight is directly quantified from the intensity of the scattered light [188].

To conclude, chemically extracted fucoidans exhibited a comparable bioactivity on angiogenic processes in MSC-OEC co-cultures as observed for enzymatically-extracted fucoidans with similar molecular weights. However, it is important to note that molecular weights determined by different techniques cannot be freely compared without restrictions. Even though, SEC with an external standard results in good tendencies for molecular weights of fucoidans, techniques such as SEC-MALS are necessary to determine the absolute molecular weight of fucoidans.

## 7.4 Injectable Chitosan-Collagen Hydrogel as a Delivery System for Fucoidan

In the last part of the presented thesis, a protocol for the production of an injectable hydrogel-based delivery system for fucoidan was established. By analyzing its physico-chemical properties and the biological performance, the suitability of the hydrogel for bone regeneration was evaluated.

The composite hydrogel consisted of chitosan and collagen type I.  $\beta$ -GP was included into the system to achieve thermosensitivity [27]. The addition of an isomeric  $\alpha\beta$ -GP mixture resulted in the formation of a crumbly, very heterogeneous hydrogel. The gel containing  $\beta$ -GP however was opaque and homogeneous.  $\alpha$ -GP has a linear structure and thereby causes less steric hindrance compared to  $\beta$ -GP. Wu and colleagues prepared a hydrogel composed of quaternized chitosan and  $\alpha\beta$ -GP and report that the isomeric GP mixture was suitable for the production of thermosensitive hydrogels. They assume that due to its chemical conformation, gelation with  $\alpha\beta$ -GP occurs even faster [187]. In contrast to Wu et al., we used native chitosan for the production of the hydrogel, possibly explaining the different findings. Even though, other studies exist which successfully established a thermosensitive hydrogel protocol using native chitosan and  $\alpha\beta$ -GP [194, 193], the use of  $\beta$ -GP has become general usage.

Results from our experiments show that gelation of the hydrogels occurred faster with increasing  $\beta$ -GP concentrations. Similar to our results, other studies observed as well that the gelation time decreased with increasing GP concentrations [1, 30]. In accordance with our results, Kempe and colleagues found that gelation with GP concentrations below 6% did not occur [89]. Hence, a sufficiently high concentration of  $\beta$ -GP should be chosen in order to achieve appropriate gelation times. GP addition results in the increase of pH, prevents precipitation of the hydrated gel and generates thermosensitivity at increased temperatures [151]. The molecular gelation mechanism of chitosan-GP hydrogels is explained in detail in the Introduction.

Some studies reported cytotoxic effects of high GP concentrations on several cell types [191, 93]. The cytotoxicity was related to the high osmotic pressure on cells created by

diffused GP. However, GP concentrations below 10 % in the hydrogel should not affect cell viability [1]. Life/dead stainings of MSC encapsulated in hydrogels with 6 and 7 %  $\beta$ -GP revealed that most cells remained vital. Therefore, we chose a  $\beta$ -GP content of 7 % as adequate for the hydrogel preparation.

To improve the biomimetic properties of the hydrogel, collagen type I was added into the formulation. As our experiments show, 1.5 mg/ml collagen improved the adhesion and spreading of encapsulated MSC. Additionally, collagen accelerated the gelation time by approximately one minute. Saravanan et al. explain in their review that collagen interacts with chitosan predominantly via hydrogen bonds between chitosan/collagen and GP, respectively water, via electrostatic interactions between amine groups (chitosan) and carboxyl groups (collagen), via Van der Waals and hydrophobic interactions. Collagen fibrillogenesis is triggered by the pH decrease (during gelation) and temperature increase, therefore supporting the gelation process [151]. In accordance with our results, Wang and Stegemann showed that the addition of collagen resulted in stiffer, faster gelating hydrogels [183]. Dang and colleagues report an improved pH stability and biocompatibility for L929 cells of hydrogels containing collagen compared to hydrogels with pure chitosan [37]. Further, Ding and colleagues showed that thermosensitive chitosan-collagen hydrogels exhibited good biocompatibility with MSC and supported osteoblast differentiation [41]. It becomes clear that the addition of collagen comes with a lot of advantages in regard to the chemical and physiological properties of the hydrogel.

The integration of fucoidan into the thermosensitive hydrogel system was achieved by premixing the fucoidan and  $\beta$ -GP solution before adding it into the chitosan-collagen mixture. The addition of pure fucoidan solution into the chitosan, chitosan-collagen or chitosan-collagen-GP mixture always resulted in the formation of macroscopic aggregates. Fucoidan addition did not impair the gelation process and did not alter the pH of the sol or of the hydrogel. Integration of high fucoidan amounts (500  $\mu$ /ml) increased the turbidity of the resulting sol. Also, fucoidan addition reduced the swelling capacity of the hydrogel measured by decreased ESRs.

Rheological measurements revealed that hydrogels containing 100  $\mu$ g/ml fucoidan gelled after 1 min at 37°C. This was comparable to hydrogels without fucoidan which needed around 75 s to reach the gel point. This gelation time seems appropriate for medical applications; it is long enough to allow the application via injection and to allow the gel adapting to the defect shape. On the other hand, it is short enough to prevent long waiting times and to avoid the immediate release of encapsulated fucoidan.

Temperature sweep tests demonstrated that the gelation temperature for hydrogels containing 100  $\mu$ g/ml fucoidan was 35.5°C. The gel point of hydrogels without fucoidan occurred at 36.8°C. Hence, hydrogels with fucoidan tentatively started to gelate at slightly lower temperatures than gels without fucoidan. The gelation of the hydrogels at 37°C or slightly lower temperatures is advantageous for a medical application. The cool sol can be applied at room temperature, but it will quickly start to gelate once exposed to the physiological body temperature. Several studies have been shown that the gelation temperature is determined by a combination of different parameters, such as  $\beta$ -GP content, chitosan concentration, molecular weight, as well as degree of deacetylation

[30, 36, 6]. Increased  $\beta$ -GP content and increased chitosan concentrations results in a decreased gelation temperature [30, 36]. Further, higher molecular weight and degree of deacetylation decrease the gelation temperature as well [6].

In contrast to other polysaccharides such as chitosan for example, fucoidan alone is not able to form hydrogels. Koo et al. demonstrated that aqueous fucoidan solutions exhibit low viscosity and can be characterized as pseudoplastic fluids [98]. This is in accordance with Citkowska and colleagues who showed that the viscosity of aqueous fucoidan solutions increased with increasing fucoidan concentration [31]. Due to its sulfate residues, fucoidan usually has an overall negative charge. Various studies have shown that fucoidan is able to form films or hydrogels with oppositely charged polysaccharides based on the formation of electrostatic interactions [156, 107]. The results from the rheological measurements, swelling experiments and the visual appearance (turbidity) indicate that the integration of fucoidan into the chitosan hydrogel system increased the degree of interconnectivity inside the gel. Swelling experiments revealed that hydrogels containing high amounts of fucoidan (500  $\mu$ g/ml) absorbed less water than hydrogels with no or less fucoidan. We assume that the additional molecular interactions resulted in gelation at lower temperatures and that the increased matrix interconnectivity hindered water uptake into the gel, therefore reducing the swelling capacities of hydrogels containing 500  $\mu$ g/ml fucoidan.

To our knowledge, no study exists which developed and characterized thermosensitive chitosan-collagen hydrogels with integrated fucoidan. To date, most studies investigated fucoidan as a component of nanoparticles, serving as a delivery system for drugs. The putative applications are manifold: anti-cancer, antibacterial, to treat pulmonary diseases or diabetes [116, 176, 77, 175]. The integration of fucoidan into hydrogels is less investigated in comparison to nanoparticles. However, some studies exist which developed hydrogel systems containing fucoidan. Carvalho and colleagues prepared ionically-crosslinked hydrogels with collagen, chitosan and fucoidan and found that gels containing all three polysaccharides possessed better mechanical properties than hydrogels with only two polysaccharides [22]. Sezer and colleagues prepared chitosan-fucoidan hydrogels and found in contrast to our results that hydrogels with fucoidan absorbed more water and had greater swelling capacities. The authors associate the results with the hydrophilic nature of fucoidan [156]. Murakami and colleagues found that hydrogel sheets composed of alginate, chitosan and fucoidan improved the regeneration of healing-impaired wounds in rats [126]. Karami and colleagues produced silibinin-loaded fucoidan-chitosan hydrogels and found that the formulation supported skin protection against UVB radiation [87]. Other studies describe the preparation of chitosan-fucoidan hydrogels for the encapsulation of angiogenic growth factors [128] or the development of alginate-fucoidan composite hydrogels for enhancing chondrogenesis of stem cells [88]. Additionally, some approaches are described which utilize covalent cross-linking to create hydrogel containing fucoidan. Lu and colleagues prepared genipin crosslinked hyaluronic acid-fucoidan-gelatin hydrogels for the delivery of platelet-rich plasma [115]. A study from Hsu and colleagues presents the production of methacrylated hyaluronan and fucoidan to create photo-crosslinkable hydrogels [75].

In almost all biomaterial approaches which include fucoidan, the polysaccharide rather represents a structural element with beneficial properties, such as enhancing the bioactivity of the encapsulated drug or altering mechanical properties of the hydrogel. To our knowledge, no study exists which integrates fucoidan into a hydrogel and determines its release profile comparable to a drug. Our experiments suggest that around 60 % of the encapsulated fucoidan got released from the hydrogel within two days. Only 20 % of the fucoidan remained inside the hydrogel after six days. These results indicate that fucoidan was not permanently immobilized inside the matrix. Its interactions with the other components were reversible, allowing the release of fucoidan into the supernatant over a specific period of time.

To use a biomaterial in the medical context, biocompatibility is a crucial requirement. It is defined as "the ability of a material to perform with an appropriate host response in a specific application" [186]. Interaction of human cells with the material is especially important for applications dealing with tissue regeneration. Here, the biomaterial is continuously in direct contact with the injured tissue, providing a platform for adjacent cells to migrate into the defect and initiate its regeneration [161]. To assess the biocompatibility of the thermosensitive chitosan-collagen hydrogel with integrated fucoidan, MSC and OEC were encapsulated (3D) and cultured on top (2D) of the hydrogel. Life/dead stainings revealed that 3D- and 2D-cultured MSC were elongated and adhered well to the hydrogel after six and also after ten days. SEM images demonstrate that MSC were deeply embedded into the hydrogel and interacted predominantly with the collagen portion. 2D-cultured OEC adhered and were vital after six days. However, encapsulated OEC exhibited a very small, round shape, demonstrating an impaired capability to elongate. DNA quantification for 3D-cultured MSC revealed equal DNA amounts on day one and six, indicating that MSC did not proliferate. VEGF secretion of 3D-cultured MSC was increased from day one to day six. However, no differences in VEGF secretion were detected between hydrogels with and without fucoidan. These results show that the developed hydrogel-based delivery system is biocompatible with both cell types. MSC can be encapsulated along with fucoidan into the hydrogel to support healing processes. However, to encapsulate OEC alone, structural adjustments of the hydrogel are needed. Also a co-encapsulation of OEC with another cell type such as MSC might help to improve the biocompatibility.

To conclude, thermosensitive chitosan-collagen hydrogels represent a possible delivery system for fucoidan and stem cells. The physicochemical properties of the hydrogel-based delivery system are suitable for medical applications. The biomaterial is compatible with human MSC and OEC with a limitation for OEC encapsulation.

## 7.5 Conclusions & Future Perspectives

Fucoidans are sulfated polysaccharides found in the cell wall of brown algae. Since the first discovery by Kylin in 1913, many researchers dedicate their work to this versatile sugar. Indeed, fucoidan is multifaceted in many ways. It possesses bioactivities on a wide range of physiological processes; angiogenesis, osteogenesis, inflammation, coagu-

lation and apoptosis, to name only a few. These bioactivities make fucoidan interesting as a therapeutic agent in the medical industry. However, not only its bioactivities are manifold, so is also its chemical structure and composition. Most fucoidans consist of a sulfated fucose backbone, but the amount of fucose units and sulfates, as well as their locations differ. Further, Fucoidans can variate in their monosaccharide composition, molecular weight, degree of branching, existence of acetylation and three dimensional conformation. Algae species, harvesting season, location and extraction technique are only some parameters which take influence on the chemical structure of fucoidan. Today it is clear that fucoidan's bioactivities depend on their chemical structure. The heterogeneous nature of fucoidans makes it very difficult to predict bioactivities of individual extracts. This impedes a straightforward use of the polysaccharide in the highly regulated medical industry.

This thesis aimed to elucidate the bioactivity of different fucoidans in conjunction with its chemical properties in the context of bone regeneration using human MSC and EC. The different parts of the presented thesis are schematically summarized in Figure 7.1. Part I mainly investigated the effect of enzymatically-extracted fucoidans on angiogenesis, osteogenesis and inflammation. Part II analyzed the potential of defined enzymatic hydrolysis as a tool to tailor fucoidan's bioactivities. The effect of intact and hydrolyzed fucoidans on angiogenesis and inflammation was compared. Part III studied the effect of chemically extracted and degraded fucoidans on angiogenesis. Finally, Part IV dealt with the development of an injectable thermosensitive hydrogel-based delivery system for fucoidan as a potential application in regenerative medicine.

It was found that all studied HMW fucoidans exhibited reducing effects on angiogenic mediators and the formation of angiogenic structures. Highly pure fucoidans (measured by a high fucose content and absent alginate impurities) with an increased sulfate content exhibited the strongest inhibitory effect on angiogenesis, osteogenesis and inflammation. This was related to a decreased expression and secretion of angiogenic and inflammatory mediators, to the impairing effect on the formation of angiogenic structures and to reduced osteoblast differentiation. MMW and LMW fucoidan extracts obtained from enzymatic hydrolysis lost the anti-angiogenic properties which were observed for HMW FE\_F3 fucoidan. MMW and LMW did not impair the formation of prevascular structures and had only a minor effect on the expression and secretion of angiogenic mediators. These differences were mostly attributed to the different molecular weights. In contrast to LMW, MMW caused an inflammatory response in OEC. Hence, enzymatic hydrolysis clearly changed the bioactivity of the obtained extracts. These results prove the potential of defined enzymatic processing to select and tailor fucoidans for specific biomedical applications. Chemically extracted and degraded fucoidans did not impair the formation of angiogenic structures similar to the enzymatically degraded extracts. Native chemically extracted HMW fucoidans mostly reduced expression and secretion of angiogenic mediators stronger than the degraded extracts with a lower molecular weight. A hydrogel-based delivery system for fucoidan which is injectable at lower temperatures and starts to gelate at 37°C within 1 min was established. The hydrogel was biocompatible with OEC and MSC with a limitation for OEC encapsulation.

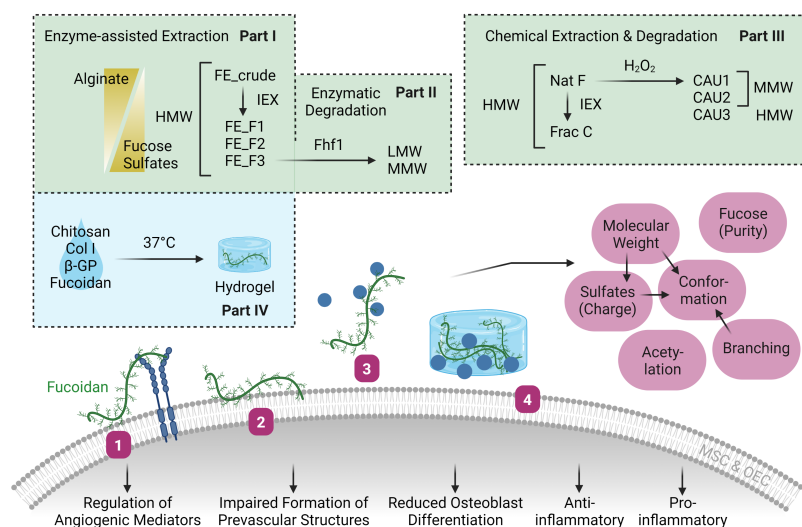


**Figure 7.1:** Summary and conclusions of the results presented in the current thesis. The thesis investigated the bioactivity of different fucoidan extracts on molecular processes relevant for bone regeneration. Bioactivities of enzymatically-extracted and -depolymerized extracts (Part I and II) were compared to chemically extracted and degraded fucoidans (Part III). A thermosensitive, injectable hydrogel as a delivery system for fucoidan was developed for the potential use in regenerative medicine (Part IV).

The results from the current thesis in conjunction with the literature suggest different possibilities how fucoidan alters signaling pathways in the studied cell models and thereby provokes the observed bioactivities. Fucoidan's negative charge probably allows it to interact with proteins. These can be surface receptors or signaling molecules. By blocking surface receptors, fucoidan prevents binding of the ligand, thereby impairing downstream signaling pathways. On the other hand, fucoidan can possess a similar conformation as the ligand, activate the receptor and enhance downstream signaling (Figure 7.1 (1)). By binding to the cell surface it might mimic sulfated glycosaminoglycans which often function as co-receptors for signaling activation (Figure 7.1 (2)). The interaction of freely diffusible fucoidan with signaling molecules might prevent their binding to the receptor (Figure 7.1 (3)). However, the integration and temporary immobilization of fucoidan inside a hydrogel might cause the reverse effect. Bound signaling molecules are temporarily immobilized and concentrated, triggering the activation of signaling pathways (Figure 7.1 (4)).

All mentioned possibilities rely on the interaction of fucoidan with different molecular structures. In turn, these interactions rely on the chemical composition of fucoidan, explaining the varying observed effects between different extracts. In the current thesis, especially the contribution of molecular weight, fucose content (purity), sulfates, acety-

lation and branching were studied and discussed. Most chemical parameters affect each other and cannot be seen in an isolated manner. In the end, almost all chemical properties determine the three dimensional conformation of the fucoidan extract.

In the future, an increased attention should be drawn to the resolution of the three dimensional structure of fucoidan molecules. It is common use to determine some basic parameters such as molecular weight and sulfate content and thereby declare the fucoidan as sufficiently chemically characterized. However, literature and results from the presented thesis clearly demonstrate that it is not as easy as that. Molecular weight, sulfates or other chemical properties never determine the bioactivity of fucoidans alone. These properties cannot be seen as isolated parameters, but must be analyzed as a unit. To further elucidate the structure-function relationship of fucoidans, an emphasis must be put on analyzing how the individual chemical properties contribute to the three dimensional structure of fucoidan. Further, it must be analyzed in detail which impact different conformations have on cellular molecular processes. To tackle this task, techniques need to be developed which allow the determination of 3D conformations in a standardized and simple way. Also methods which determine the individual chemical properties must be improved and standardized. For example, techniques omitting the use of external calibration standards need to be further established in order to determine accurate molecular weights.

Without doubt, it is always advantageous to know how a potential therapeutic agent acts on molecular processes and how observed effects can be explained. Nevertheless, if a fucoidan extract exhibits reproducibly good therapeutic effects, proven in *in vitro* and *in vivo* studies, it is not absolutely necessary to know the exact molecular mechanism. It is however extremely important for the medical use that the chemical composition of this fucoidan is stable and does not vary between batches. Therefore, extraction procedures need to be highly standardized and guarantee the continuous production of fucoidans with the same chemical structure. Results from the presented thesis have shown that defined enzymatic fucoidan processing after extraction can be a helpful tool to achieve this requirement.

Further, biological test systems need to be standardized in order to study fucoidan's bioactivity, but also to screen different extracts for a potential medical uses. These test systems should reflect human physiological processes as close as possible. Only well studied and tested fucoidans which show high medical potential *in vitro* should be tested *in vivo*. *Ex vivo* models, especially in the area of bone regeneration, could close the gap between *in vitro* and *in vivo* studies.

Finally, to apply fucoidan in the medical context, delivery systems and formulations specific to the application are needed. Even though, studies exist which describe biomaterials with integrated fucoidan, the research on this topic is still sparse. The constant demand for suitable biomaterials has fostered the research in this sector and led to the development of many promising materials, such as intelligent hydrogels, nanoparticles or bioprintable scaffolds. Already existing materials can be adapted to the integration of fucoidan to create formulations which enable the use of fucoidan as a bioactive compound for medical purposes.



# Bibliography

---

- [1] AHMADI, Raheleh ; BRUIJN, Joost D. de: Biocompatibility and gelation of chitosan–glycerol phosphate hydrogels. In: *Journal of Biomedical Materials Research Part A* 86A (2008), 9, p. 824–832. – ISSN 1549-3296
- [2] AKIYAMA, Haruhiko ; CHABOISSIER, Marie-Christine ; MARTIN, James F. ; SCHEDL, Andreas ; CROMBRUGGHE, Benoit de: The transcription factor Sox9 has essential roles in successive steps of the chondrocyte differentiation pathway and is required for expression of Sox5 and Sox6. In: *Genes & development* 16 (2002), 11, p. 2813–2828. – ISSN 0890-9369
- [3] ALBOOFETILEH, Mehdi ; REZAEI, Masoud ; TABARSA, Mehdi ; YOU, SangGuan: Bioactivities of Nizamuddiniaz zanardinii sulfated polysaccharides extracted by enzyme, ultrasound and enzyme-ultrasound methods. In: *J Food Sci Technol* 56 (2019), p. 1212–1220. – ISSN 0022-1155 (Print) 0022-1155
- [4] ALE, Marcel T. ; MEYER, Anne S.: Fucoidans from brown seaweeds: an update on structures, extraction techniques and use of enzymes as tools for structural elucidation. In: *RSC Advances* 3 (2013), p. 8131–8141
- [5] ALE, Marcel T. ; MIKKELSEN, Jørn D. ; MEYER, Anne S.: Important determinants for fucoidan bioactivity: a critical review of structure-function relations and extraction methods for fucose-containing sulfated polysaccharides from brown seaweeds. In: *Marine drugs* 9 (2011), p. 2106–2130. – ISSN 1660-3397
- [6] ALIAGHAIE, Marzieh ; MIRZADEH, Hamid ; DASHTIMOGHADAM, Erfan ; TARANEJOO, Shahrouz: Investigation of gelation mechanism of an injectable hydrogel based on chitosan by rheological measurements for a drug delivery application. In: *Soft Matter* 8 (2012), p. 7128–7137. – ISSN 1744-683X
- [7] ALVAREZ, Kelly ; NAKAJIMA, Hideo: Metallic Scaffolds for Bone Regeneration. In: *Materials* 2 (2009), 7, p. 790–832. – ISSN 1996-1944
- [8] ALWARSAMY, Madhavarani ; GOONERATNE, Ravi ; RAVICHANDRAN, Ramanibai: Effect of fucoidan from *Turbinaria conoides* on human lung adenocarcinoma epithelial (A549) cells. In: *Carbohydrate Polymers* 152 (2016), p. 207–213. – ISSN 0144-8617
- [9] AMINI, Ami R. ; LAURENCIN, Cato T. ; NUKAVARAPU, Syam P.: Bone tissue engineering: recent advances and challenges. In: *Critical reviews in biomedical engineering* 40 (2012), p. 363–408. – ISSN 0278-940X
- [10] AUGUSTIN, Hellmut G. ; KOH, Gou Y. ; THURSTON, Gavin ; ALITALO, Kari: Control of vascular morphogenesis and homeostasis through the angiopoietin–Tie system. In: *Nature Reviews Molecular Cell Biology* 10 (2009), p. 165–177. – ISSN 1471-0080

- [11] BALDWIN, Paul ; LI, Deborah J. ; AUSTON, Darryl A. ; MIR, Hassan S. ; YOON, Richard S. ; KOVAL, Kenneth J.: Autograft, Allograft, and Bone Graft Substitutes: Clinical Evidence and Indications for Use in the Setting of Orthopaedic Trauma Surgery. In: *Journal of Orthopaedic Trauma* 33 (2019). – ISSN 0890-5339
- [12] BÜHRING, Hans-Jörg ; BATTULA, Venkata L. ; TREML, Sabrina ; SCHEWE, Bernhard ; KANZ, Lothar ; VOGEL, Wichard: Novel Markers for the Prospective Isolation of Human MSC. In: *Annals of the New York Academy of Sciences* 1106 (2007), 6, p. 262–271. – ISSN 0077-8923
- [13] BILAN, Maria I. ; GRACHEV, Alexey A. ; SHASHKOV, Alexander S. ; NIFANTIEV, Nikolay E. ; USOV, Anatolii I.: Structure of a fucoidan from the brown seaweed *Fucus serratus* L. In: *Carbohydrate Research* 341 (2006), p. 238–245. – ISSN 0008-6215
- [14] BILAN, Maria I. ; GRACHEV, Alexey A. ; USTUZHANINA, Nadezhda E. ; SHASHKOV, Alexander S. ; NIFANTIEV, Nikolay E. ; USOV, Anatolii I.: Structure of a fucoidan from the brown seaweed *Fucus evanescens* C.Ag. In: *Carbohydrate Research* 337 (2002), p. 719–730. – ISSN 0008-6215
- [15] BIRCH, Kimberly A. ; EWENSTEIN, Bruce M. ; GOLAN, David E. ; POBER, Jordan S.: Prolonged peak elevations in cytoplasmic free calcium ions, derived from intracellular stores, correlate with the extent of thrombin-stimulated exocytosis in single human umbilical vein endothelial cells. In: *Journal of Cellular Physiology* 160 (1994), 9, p. 545–554. – ISSN 0021-9541
- [16] BITTKAU, Kaya S. ; NEUPANE, Sandesh ; ALBAN, Susanne: Initial evaluation of six different brown algae species as source for crude bioactive fucoidans. In: *Algal Research* 45 (2020), p. 101759. – ISSN 2211-9264
- [17] BLACK, William A. P. ; DEWAR, Eric T. ; WOODWARD, Neville: Manufacture of algal chemicals. IV—Laboratory-scale isolation of fucoidin from brown marine algae. In: *Journal of the Science of Food and Agriculture* 3 (1952), p. 122–129
- [18] BOUVARD, Claire ; GALY-FAUROUX, Isabelle ; GRELAC, Françoise ; CARPENTIER, Wassila ; LOKAJCZYK, Anna ; GANDRILLE, Sophie ; COLLIEC-JOUAULT, Sylvia ; FISCHER, Anne-Marie ; HELLEY, Dominique: Low-Molecular-Weight Fucoidan Induces Endothelial Cell Migration via the PI3K/AKT Pathway and Modulates the Transcription of Genes Involved in Angiogenesis. In: *Marine Drugs* 13 (2015), p. 7446–7462. – ISSN 1660-3397
- [19] BUCK, Donald W I I. ; DUMANIAN, Gregory A.: Bone Biology and Physiology: Part I. The Fundamentals. In: *Plastic and Reconstructive Surgery* 129 (2012). – ISSN 0032-1052
- [20] BUCKWALTER, J A. ; GLIMCHER, M J. ; COOPER, R R. ; RECKER, R: Bone Biology. In: *The Journal of Bone & Joint Surgery* 77 (1995). – ISSN 0021-9355
- [21] BUWALDA, Sytze J. ; BOERE, Kristel W. M. ; DIJKSTRA, Pieter J. ; FEIJEN, Jan ; VERMONDEN, Tina ; HENNINK, Wim E.: Hydrogels in a historical perspective: From simple networks to smart materials. In: *Journal of Controlled Release* 190 (2014), p. 254–273. – ISSN 0168-3659
- [22] CARVALHO, Duarte N. ; LÓPEZ-CEBRAL, Rita ; SOUSA, Rita O. ; ALVES, Ana L. ; REYS, Lara L. ; SILVA, Simone S. ; OLIVEIRA, J M. ; REIS, Rui L. ; SILVA, Tiago H.: Marine collagen-chitosan-fucoidan cryogels as cell-laden biocomposites envisaging tissue engineering. In: *Biomedical Materials* 15 (2020), p. 055030. – ISSN 1748-6041
- [23] CATOIRA, Marta C. ; FUSARO, Luca ; FRANCESCO, Dalila D. ; RAMELLA, Martina ; BOCCAFOSCHI, Francesca: Overview of natural hydrogels for regenerative medicine applications. In: *Journal of Materials Science: Materials in Medicine* 30 (2019), p. 115. – ISSN 1573-4838

- [24] CHABUT, Delphine ; FISCHER, Anne-Marie ; COLLIEC-JOUAULT, Sylvia ; LAURENDEAU, Ingrid ; MATOU, Sabine ; BONNIEC, Bernard L. ; HELLEY, Dominique: Low Molecular Weight Fucoidan and Heparin Enhance the Basic Fibroblast Growth Factor-Induced Tube Formation of Endothelial Cells through Heparan Sulfate-Dependent 6 Overexpression. In: *Molecular Pharmacology* 64 (2003), p. 696–702
- [25] CHEN, Meng-Chuan ; HSU, Wen-Lin ; HWANG, Pai-An ; CHOU, Tz-Chong: Low Molecular Weight Fucoidan Inhibits Tumor Angiogenesis through Downregulation of HIF-1/VEGF Signaling under Hypoxia. In: *Marine Drugs* 13 (2015). – ISSN 1660-3397
- [26] CHEN, Qianru ; KOU, Lingyun ; WANG, Fengwu ; WANG, Ying: Size-dependent whitening activity of enzyme-degraded fucoidan from *Laminaria japonica*. In: *Carbohydrate Polymers* 225 (2019), p. 115211. – ISSN 0144-8617
- [27] CHENITE, A. ; CHAPUT, C. ; WANG, D. ; COMBES, C. ; BUSCHMANN, M. D. ; HOEMANN, C. D. ; LEROUX, J. C. ; ATKINSON, B. L. ; BINETTE, F. ; SELMANI, A.: Novel injectable neutral solutions of chitosan form biodegradable gels in situ. In: *Biomaterials* 21 (2000), p. 2155–2161. – ISSN 0142-9612
- [28] CHEVOLOT, Lionel ; FOUCAULT, Alain ; CHAUBET, Frederic ; KERVAREC, Nelly ; SINQUIN, Corinne ; FISHER, Anne-Marie ; BOISSON-VIDAL, Catherine: Further data on the structure of brown seaweed fucans: relationships with anticoagulant activity. In: *Carbohydrate Research* 319 (1999), p. 154–165. – ISSN 0008-6215
- [29] CHO, Jaepyong ; HEUZEY, Marie-Claude ; BÉGIN, André ; CARREAU, Pierre J.: Physical Gelation of Chitosan in the Presence of  $\beta$ -Glycerophosphate: The Effect of Temperature. In: *Biomacromolecules* 6 (2005), 11, p. 3267–3275. – ISSN 1525-7797
- [30] CHO, Jaepyong ; HEUZEY, Marie-Claude ; BÉGIN, André ; CARREAU, Pierre J.: Chitosan and glycerophosphate concentration dependence of solution behaviour and gel point using small amplitude oscillatory rheometry. In: *Food Hydrocolloids* 20 (2006), p. 936–945. – ISSN 0268-005X
- [31] CITKOWSKA, Aleksandra ; SZEKALSKA, Marta ; WINNICKA, Katarzyna: Possibilities of Fucoidan Utilization in the Development of Pharmaceutical Dosage Forms. In: *Marine Drugs* 17 (2019), p. 458. – ISSN 1660-3397
- [32] CLARKE, Bart: Normal bone anatomy and physiology. In: *Clinical journal of the American Society of Nephrology : CJASN* 3 Suppl 3 (2008), 11, p. S131–S139. – ISSN 1555-905X
- [33] CLÉMENT, Marie J. ; TISSOT, Bérangère ; CHEVOLOT, Lionel ; ADJADJ, Elisabeth ; DU, Yuguo ; CURMI, Patrick A. ; DANIEL, Régis: NMR characterization and molecular modeling of fucoidan showing the importance of oligosaccharide branching in its anticomplementary activity. In: *Glycobiology* 20 (2010), p. 883–894. – ISSN 14602423
- [34] CONG, Qifei ; CHEN, Huanjun ; LIAO, Wenfeng ; XIAO, Fei ; WANG, Peipei ; QIN, Yi ; DONG, Qun ; DING, Kan: Structural characterization and effect on anti-angiogenic activity of a fucoidan from *Sargassum fusiforme*. In: *Carbohydrate Polymers* 136 (2016), p. 899–907. – ISSN 0144-8617
- [35] CROES, Michiel ; VAN DER WAL, Bart C. H. ; VOGELY, Charles: Impact of Bacterial Infections on Osteogenesis: Evidence From In Vivo Studies. In: *Journal of Orthopaedic Research* 37 (2019), p. 2067–2076. – ISSN 1554-527X 0736-0266
- [36] DANG, Qi F. ; YAN, Jing Q. ; LI, Jing J. ; CHENG, Xiao J. ; LIU, Cheng S. ; CHEN, Xi G.: Controlled gelation temperature, pore diameter and degradation of a highly porous chitosan-based hydrogel. In: *Carbohydrate Polymers* 83 (2011), p. 171–178. – ISSN 0144-8617

- [37] DANG, Qifeng ; LIU, Kai ; ZHANG, Zhenzhen ; LIU, Chengsheng ; LIU, Xi ; XIN, Ying ; CHENG, Xiaoyu ; XU, Tao ; CHA, Dongsu ; FAN, Bing: Fabrication and evaluation of thermosensitive chitosan/collagen/ $\alpha$ ,  $\beta$ -glycerophosphate hydrogels for tissue regeneration. In: *Carbohydrate Polymers* 167 (2017), p. 145–157. – ISSN 0144-8617
- [38] DECKERS, Martine M. ; KARPERIEN, Marcel ; VAN DER BENT, Chris ; YAMASHITA, Takeyoshi ; PAPAPOULOS, Socrates E. ; LÖWIK, Clemens W.: Expression of vascular endothelial growth factors and their receptors during osteoblast differentiation. In: *Endocrinology* 141 (2000), p. 1667–1674. – ISSN 0013-7227 (Print) 0013-7227
- [39] DELORME, Bruno ; BASIRE, Agnès ; GENTILE, Carla ; SABATIER, Florence ; MONSONIS, Frédéric ; DESOUCHES, Christophe ; BLOT-CHABAUD, Marcel ; UZAN, Georges ; SAMPOL, Joséé ; DIGNAT-GEORGE, Françoise: Presence of endothelial progenitor cells, distinct from mature endothelial cells, within human CD146+ blood cells. In: *Thrombosis and haemostasis* 94 6 (2005), p. 1270–9
- [40] DENIAUD-BOUËT, Estelle ; KERVAREC, Nelly ; MICHEL, Gurvan ; TONON, Thierry ; KLOAREG, Bernard ; HERVÉ, Cécile: Chemical and enzymatic fractionation of cell walls from Fucales: insights into the structure of the extracellular matrix of brown algae. In: *Annals of botany* 114 (2014), 10, p. 1203–1216. – ISSN 1095-8290
- [41] DING, Ke ; ZHANG, Yu L. ; YANG, Zhong ; XU, Jian Z.: A promising injectable scaffold: The biocompatibility and effect on osteogenic differentiation of mesenchymal stem cells. In: *Biotechnology and Bioprocess Engineering* 18 (2013), 2, p. 155–163. – ISSN 12268372
- [42] DOBRINČIĆ, Ana ; BALBINO, Sandra ; ZORIĆ, Zoran ; PEDISIĆ, Sandra ; KOVAČEVIĆ, Danijela B. ; GAROFULIĆ, Ivona E. ; DRAGOVIĆ-UZELAC, Verica: Advanced Technologies for the Extraction of Marine Brown Algal Polysaccharides. In: *Marine Drugs* 18 (2020). – ISSN 1660-3397
- [43] DODGSON, K. S. ; PRICE, R. G.: A note on the determination of the ester sulphate content of sulphated polysaccharides. In: *The Biochemical journal* 84 (1962), p. 106–110. – ISSN 0264-6021 1470-8728
- [44] DOMINICI, M. ; LE BLANC, K. ; MUELLER, I. ; SLAPER-CORTENBACH, I. ; MARINI, F. ; KRAUSE, D. ; DEANS, R. ; KEATING, A. ; PROCKOP, D. ; HORWITZ, E.: Minimal criteria for defining multipotent mesenchymal stromal cells. The International Society for Cellular Therapy position statement. In: *Cytotherapy* 8 (2006), Nr. 4, p. 315–7. – ISSN 1465-3249
- [45] EHRIG, Karina ; ALBAN, Susanne: Sulfated galactofucan from the brown alga *Saccharina latissima*—variability of yield, structural composition and bioactivity. In: *Marine Drugs* 13 (2014), 12, p. 76–101. – ISSN 1660-3397
- [46] EIRIN, Alfonso ; ZHU, Xiang-Yang ; KRIER, James D. ; TANG, Hui ; JORDAN, Kyra L. ; GRANDE, Joseph P. ; LERMAN, Amir ; TEXTOR, Stephen C. ; LERMAN, Lilach O.: Adipose tissue-derived mesenchymal stem cells improve revascularization outcomes to restore renal function in swine atherosclerotic renal artery stenosis. In: *Stem cells (Dayton, Ohio)* 30 (2012), 5, p. 1030–1041. – ISSN 1549-4918
- [47] ERIKSEN, Erik F. ; AXELROD, Douglas W. ; MELSEN, Flemming: *Bone histomorphometry*. New York (N.Y.) : Raven, 1994. – ISBN 0781701228
- [48] FATHERAZI, S. ; MATSA-DUNN, D. ; FOSTER, B. L. ; RUTHERFORD, R. B. ; SOMERMAN, M. J. ; PRESLAND, R. B.: Phosphate regulates osteopontin gene transcription. In: *Journal of dental research* 88 (2009), 1, p. 39–44. – ISSN 1544-0591
- [49] FERRARA, Napoleone ; GERBER, Hans-Peter ; LECOUTER, Jennifer: The biology of VEGF and its receptors. In: *Nature Medicine* 9 (2003), p. 669–676. – ISSN 1546-170X

- 
- [50] FIEDLER, Ulrike ; SCHARPFENECKER, Marion ; KOIDL, Stefanie ; HEGEN, Anja ; GRUNOW, Verena ; SCHMIDT, Jarno M. ; KRIZ, Wilhelm ; THURSTON, Gavin ; AUGUSTIN, Hellmut G.: The Tie-2 ligand Angiopoietin-2 is stored in and rapidly released upon stimulation from endothelial cell Weibel-Palade bodies. In: *Blood* 103 (2004), p. 4150–4156. – ISSN 0006-4971
- [51] FUCHS, Sabine ; DOHLE, Eva ; KOLBE, Marlen ; KIRKPATRICK, Charles J.: Outgrowth Endothelial Cells: Sources, Characteristics and Potential Applications in Tissue Engineering and Regenerative Medicine. In: *Bioreactor Systems for Tissue Engineering II: Strategies for the Expansion and Directed Differentiation of Stem Cells* (2010), p. 201–217. ISBN 978-3-642-16051-6
- [52] FUCHS, Sabine ; HERMANN, Maria I. ; KIRKPATRICK, Charles J.: Retention of a differentiated endothelial phenotype by outgrowth endothelial cells isolated from human peripheral blood and expanded in long-term cultures. In: *Cell and Tissue Research* 326 (2006), p. 79–92. – ISSN 1432-0878
- [53] FUCHS, Sabine ; JIANG, Xin ; SCHMIDT, Harald ; DOHLE, Eva ; GHANAATI, Shahram ; ORTH, Carina ; HOFMANN, Alexander ; MOTTA, Antonella ; MIGLIARESI, Claudio ; KIRKPATRICK, Charles J.: Dynamic processes involved in the pre-vascularization of silk fibroin constructs for bone regeneration using outgrowth endothelial cells. In: *Biomaterials* 30 (2009), p. 1329–1338. – ISSN 0142-9612
- [54] FUKUCHI, Yumi ; NAKAJIMA, Hideaki ; SUGIYAMA, Daisuke ; HIROSE, Imiko ; KITAMURA, Toshio ; TSUJI, Kohichiro: Human Placenta-Derived Cells Have Mesenchymal Stem/Progenitor Cell Potential. In: *Stem Cells* 22 (2004), 9, p. 649–658. – ISSN 1066-5099
- [55] FUKUHARA, Shigetomo ; SAKO, Keisuke ; MINAMI, Takashi ; NODA, Kazuomi ; KIM, Hak Z. ; KODAMA, Tatsuhiko ; SHIBUYA, Masabumi ; TAKAKURA, Nobuyuki ; KOH, Gou Y. ; MOCHIZUKI, Naoki: Differential function of Tie2 at cell–cell contacts and cell–substratum contacts regulated by angiopoietin-1. In: *Nature Cell Biology* 10 (2008), p. 513–526. – ISSN 1476-4679
- [56] GAINETDINOV, Raul R. ; PREMONT, Richard T. ; BOHN, Laura M. ; LEFKOWITZ, Robert J. ; CARON, Marc G.: Desensitization of G Protein-Coupled Receptors and Neuronal Functions. In: *Annual Review of Neuroscience* 27 (2004), 6, p. 107–144. – ISSN 0147-006X
- [57] GALEA, Gabriel L. ; ZEIN, Mohamed R. ; ALLEN, Steven ; FRANCIS-WEST, Philippa: Making and shaping endochondral and intramembranous bones. In: *Developmental Dynamics* 250 (2021), 3, p. 414–449. – ISSN 1058-8388
- [58] GALLAGHER, John: Fell-Muir Lecture: Heparan sulphate and the art of cell regulation: a polymer chain conducts the protein orchestra. In: *International Journal of Experimental Pathology* 96 (2015), p. 203–231. – ISSN 0959-9673 (Print) 0959-9673
- [59] GAVARD, Julie ; PATEL, Vyomesh ; GUTKIND, Silvio: Angiopoietin-1 Prevents VEGF-Induced Endothelial Permeability by Sequestering Src through mDia. In: *Developmental Cell* 14 (2008), 1, p. 25–36. – ISSN 15345807
- [60] GEHLING, Ursula M. ; ERGUÜN, Süüleyman ; SCHUMACHER, Udo ; WAGENER, Christoph ; PANTEL, Klaus ; OTTE, Marcus ; SCHUCH, Gunter ; SCHAFHAUSEN, Philippe ; MENDE, Thorsten ; KILIC, Nerbil ; KLUGE, Katrin ; SCHAÜFER, Birgit ; HOSSFELD, Dieter K. ; FIEDLER, Walter: In vitro differentiation of endothelial cells from AC133-positive progenitor cells. In: *Blood* 95 (2000), p. 3106–3112. – ISSN 0006-4971
- [61] GERHARDT, Holger: VEGF and endothelial guidance in angiogenic sprouting. In: *Organogenesis* 4 (2008), 10, p. 241–246. – ISSN 1547-6278

- [62] GERHARDT, Holger ; GOLDING, Matthew ; FRUTTIGER, Marcus ; RUHRBERG, Christiana ; LUNDKVIST, Andrea ; ABRAMSSON, Alexandra ; JELTSCH, Michael ; MITCHELL, Christopher ; ALITALO, Kari ; SHIMA, David ; BETSHOLTZ, Christer: VEGF guides angiogenic sprouting utilizing endothelial tip cell filopodia. In: *The Journal of cell biology* 161 (2003), 6, p. 1163–1177. – ISSN 0021-9525
- [63] GINEBRA, Maria-Pau ; ESPANOL, Montserrat ; MAAZOUZ, Yassine ; BERGEZ, Victor ; PASTORINO, David: Bioceramics and bone healing. In: *EFORT open reviews* 3 (2018), 5, p. 173–183. – ISSN 2058-5241
- [64] GÓMEZ-GAVIRO, Maria V. ; LOVELL-BADGE, Robin ; FERNÁNDEZ-AVILÉS, Francisco ; LARA-PEZZI, Enrique: The Vascular Stem Cell Niche. In: *Journal of Cardiovascular Translational Research* 5 (2012), p. 618–630. – ISSN 1937-5395
- [65] GROSSO, Andrea ; BURGER, Maximilian G. ; LUNGER, Alexander ; SCHAEFER, Dirk J. ; BANFI, Andrea ; MAGGIO, Nunzia D.: It Takes Two to Tango: Coupling of Angiogenesis and Osteogenesis for Bone Regeneration. In: *Frontiers in bioengineering and biotechnology* 5 (2017), 11, p. 68. – ISSN 2296-4185
- [66] GUPTA, Dhanak ; SILVA, Melissa ; RADZIUN, Karolina ; MARTINEZ, Diana C. ; HILL, Christopher J. ; MARSHALL, Julie ; HEARNDEN, Vanessa ; PUERTAS-MEJIA, Miguel A. ; REILLY, Gwendolen C.: Fucoidan Inhibition of Osteosarcoma Cells is Species and Molecular Weight Dependent. In: *Marine Drugs* 18 (2020), p. 104. – ISSN 1660-3397
- [67] HADJIDAKIS, DIMITRIOS J. ; ANDROULAKIS, Ioannis I.: Bone Remodeling. In: *Annals of the New York Academy of Sciences* 1092 (2006), 12, p. 385–396. – ISSN 0077-8923
- [68] HAHN, Thomas ; LANG, Siegmund ; ULBER, Roland ; MUFFLER, Kai: Novel procedures for the extraction of fucoidan from brown algae. In: *Process Biochemistry* 47 (2012), p. 1691–1698. – ISSN 1359-5113
- [69] HAMIDOUCHE, Zahia ; HAÏ, Eric ; VAUDIN, Pascal ; CHARBORD, Pierre ; SCHÜLE, Roland ; MARIE, Pierre J. ; FROMIGUÉ, Olivia: FHL2 mediates dexamethasone-induced mesenchymal cell differentiation into osteoblasts by activating Wnt/ $\beta$ -catenin signaling-dependent Runx2 expression. In: *The FASEB Journal* 22 (2008), 11, p. 3813–3822. – ISSN 0892-6638
- [70] HAROUN-BOUHEDJA, Ferial ; ELLOUALI, Mostafa ; SINQUIN, Corinne ; BOISSON-VIDAL, Catherine: Relationship between Sulfate Groups and Biological Activities of Fucans. In: *Thrombosis Research* 100 (2000), p. 453–459. – ISSN 0049-3848
- [71] HOLMES, David: Closing the gap. In: *Nature* 550 (2017), p. S194–S195. – ISSN 1476-4687
- [72] HOLMES, David I R. ; ZACHARY, Ian: The vascular endothelial growth factor (VEGF) family: angiogenic factors in health and disease. In: *Genome Biology* 6 (2005), p. 209. – ISSN 1474-760X
- [73] HONG, Dun ; CHEN, Hai-Xiao ; XUE, Yun ; LI, Dong-Mei ; WAN, Xiao-Chen ; GE, Renshan ; LI, Ji-Cheng: Osteoblastogenic effects of dexamethasone through upregulation of TAZ expression in rat mesenchymal stem cells. In: *The Journal of Steroid Biochemistry and Molecular Biology* 116 (2009), p. 86–92. – ISSN 0960-0760
- [74] HSIAO, Hui-Hua ; WU, Tien-Chiu ; TSAI, Yung-Hsiang ; KUO, Chia-Hung ; HUANG, Ren-Han ; HONG, Yong-Han ; HUANG, Chun-Yung: Effect of Oversulfation on the Composition, Structure, and In Vitro Anti-Lung Cancer Activity of Fucoidans Extracted from *Sargassum aquifolium*. In: *Marine Drugs* 19 (2021). – ISSN 1660-3397

- [75] HSU, Fu-Yin ; CHEN, Jheng-Jie ; SUNG, Wen-Chieh ; HWANG, Pai-An: Preparation of a Fucoidan-Grafted Hyaluronan Composite Hydrogel for the Induction of Osteoblast Differentiation in Osteoblast-Like Cells. In: *Materials (Basel, Switzerland)* 14 (2021), 3, p. 1168. – ISSN 1996-1944
- [76] HUANG, Haiqin ; QI, Xiaole ; CHEN, Yanhua ; WU, Zhenghong: Thermo-sensitive hydrogels for delivering biotherapeutic molecules: A review. In: *Saudi pharmaceutical journal : SPJ : the official publication of the Saudi Pharmaceutical Society* 27 (2019), 11, p. 990–999. – ISSN 1319-0164
- [77] HUANG, Yi-Cheng ; LI, Rou-Ying: Preparation and characterization of antioxidant nanoparticles composed of chitosan and fucoidan for antibiotics delivery. In: *Marine Drugs* 12 (2014), 7, p. 4379–4398. – ISSN 1660-3397
- [78] HWANG, Pai-An ; HUNG, Yu-Lan ; PHAN, Nam N. ; HIEU, Bui-Thi-Ngoc ; CHANG, Po-Ming ; LI, Kuan-Lun ; LIN, Yen-Chang: The in vitro and in vivo effects of the low molecular weight fucoidan on the bone osteogenic differentiation properties. In: *Cytotechnology* 68 (2016), p. 1349–1359. – ISSN 0920-9069 1573-0778
- [79] JAIN, Rakesh K.: Molecular regulation of vessel maturation. In: *Nature Medicine* 9 (2003), p. 685–693. – ISSN 1546-170X
- [80] JAYAWARDENA, Thilina U. ; SANJEEWA, Asanka ; NAGAHAWATTA, D. P. ; LEE, Hyo-Geun ; LU, Yu-An ; VAAS, A. P. J. P. ; ABEYTUNGA, D. T. U. ; NANAYAKKARA, C. M. ; LEE, Dae-Sung ; JEON, You-Jin: Anti-Inflammatory Effects of Sulfated Polysaccharide from *Sargassum Swartzii* in Macrophages via Blocking TLR/NF- $\kappa$ b Signal Transduction. In: *Marine Drugs* 18 (2020). – ISSN 1660-3397
- [81] JIAO, Hongli ; XIAO, E. ; GRAVES, Dana T.: Diabetes and Its Effect on Bone and Fracture Healing. In: *Current Osteoporosis Reports* 13 (2015), p. 327–335. – ISSN 1544-1873 (Print) 1544-1873
- [82] JIN, Jun-O ; YU, Qing: Fucoidan delays apoptosis and induces pro-inflammatory cytokine production in human neutrophils. In: *International Journal of Biological Macromolecules* 73 (2015), p. 65–71. – ISSN 0141-8130
- [83] JIN, Jun-O ; ZHANG, Wei ; DU, Jiang-Yuan ; WONG, Ka-Wing ; ODA, Tatsuya ; YU, Qing: Fucoidan can function as an adjuvant in vivo to enhance dendritic cell maturation and function and promote antigen-specific T cell immune responses. In: *PLoS One* 9 (2014), p. e99396. – ISSN 1932-6203
- [84] JIN, Weihua ; JIANG, Di ; ZHANG, Wenjing ; WANG, Chunyu ; XIA, Ke ; ZHANG, Fuming ; LINHARDT, Robert J.: Interactions of fibroblast growth factors with sulfated galactofucan from *Saccharina japonica*. In: *International Journal of Biological Macromolecules* 160 (2020), p. 26–34. – ISSN 0141-8130
- [85] JONES, Elena A. ; KINSEY, Sally E. ; ENGLISH, Anne ; JONES, Richard A. ; STRASZYNSKI, Liz ; MEREDITH, David M. ; MARKHAM, Alex F. ; JACK, Andrew ; EMERY, Paul ; MCGONAGLE, Dennis: Isolation and characterization of bone marrow multipotential mesenchymal progenitor cells. In: *Arthritis & Rheumatism* 46 (2002), 12, p. 3349–3360. – ISSN 0004-3591
- [86] KADOYA, Y. ; REVELL, P. A. ; AL-SAFFAR, N. ; KOBAYASHI, A. ; SCOTT, G. ; FREEMAN, M. A. R.: Bone formation and bone resorption in failed total joint arthroplasties: Histomorphometric analysis with histochemical and immunohistochemical technique. In: *Journal of Orthopaedic Research* 14 (1996), 5, p. 473–482. – ISSN 0736-0266

- [87] KARAMI, Masood A. ; MAKHMALZADEH, Behzad S. ; POORANIAN, Mahsa ; REZAI, Anahita: Preparation and optimization of silibinin-loaded chitosan–fucoidan hydrogel: an in vivo evaluation of skin protection against UVB. In: *Pharmaceutical Development and Technology* 26 (2021), 2, p. 209–219. – ISSN 1083-7450
- [88] KARUNANITHI, Puvanan ; MURALI, Malliga R. ; SAMUEL, Shani ; RAGHAVENDRAN, Hanumanantha Rao B. ; ABBAS, Azlina A. ; KAMARUL, Tunku: Three dimensional alginate-fucoidan composite hydrogel augments the chondrogenic differentiation of mesenchymal stromal cells. In: *Carbohydrate Polymers* 147 (2016), p. 294–303. – ISSN 0144-8617
- [89] KEMPE, Sabine ; METZ, Hendrik ; BASTROP, Martin ; HVILSOM, Annette ; CONTRI, Renata V. ; MÄDER, Karsten: Characterization of thermosensitive chitosan-based hydrogels by rheology and electron paramagnetic resonance spectroscopy. In: *European Journal of Pharmaceutics and Biopharmaceutics* 68 (2008), 1, p. 26–33. – ISSN 09396411
- [90] KENKRE, Julia S. ; BASSETT, John H.: The bone remodelling cycle. In: *Annals of Clinical Biochemistry* 55 (2018), 5, p. 308–327. – ISSN 17581001
- [91] KIM, Beom S. ; KANG, Hyo-Jin ; PARK, Ji-Yun ; LEE, Jun: Fucoidan promotes osteoblast differentiation via JNK- and ERK-dependent BMP2–Smad 1/5/8 signaling in human mesenchymal stem cells. In: *Experimental & Molecular Medicine* 47 (2015), p. e128–e128. – ISSN 2092-6413
- [92] KIM, Beom S. ; PARK, Ji-Yun ; KANG, Hyo-Jin ; KIM, Hyung-Jin ; LEE, Jun: Fucoidan/FGF-2 induces angiogenesis through JNK- and p38-mediated activation of AKT/MMP-2 signalling. In: *Biochemical and Biophysical Research Communications* 450 (2014), p. 1333–1338. – ISSN 0006-291X
- [93] KIM, Sungwoo ; NISHIMOTO, Satoru K. ; BUMGARDNER, Joel D. ; HAGGARD, Warren O. ; GABER, M W. ; YANG, Yunzhi: A chitosan/ $\beta$ -glycerophosphate thermo-sensitive gel for the delivery of ellagic acid for the treatment of brain cancer. In: *Biomaterials* 31 (2010), p. 4157–4166. – ISSN 0142-9612
- [94] KIM, Woo J. ; KOO, Yean-Kyoung ; JUNG, Mi-Kyung ; MOON, Hye R. ; KIM, Sung M. ; SYNYTSYA, Andry ; YUN-CHOI, Hye S. ; KIM, Yeong S. ; PARK, Jae K. ; PARK, Yong I.: Anticoagulating activities of low-molecular weight fuco-oligosaccharides prepared by enzymatic digestion of fucoidan from the sporophyll of Korean *Undaria pinnatifida*. In: *Archives of Pharmacal Research* 33 (2010), p. 125–131. – ISSN 0253-6269 (Print) 0253-6269
- [95] KO, Frank C. ; SUMNER, D R.: How faithfully does intramembranous bone regeneration recapitulate embryonic skeletal development? In: *Developmental Dynamics* 250 (2021), 3, p. 377–392. – ISSN 1058-8388
- [96] KOLBE, Marlen ; DOHLE, Eva ; KATERLA, Denise ; KIRKPATRICK, Charles J. ; FUCHS, Sabine: Enrichment of outgrowth endothelial cells in high and low colony-forming cultures from peripheral blood progenitors. In: *Tissue engineering. Part C, Methods* 16 (2010), 10, p. 877–886. – ISSN 1937-3392
- [97] KOLBE, Marlen ; XIANG, Zhou ; DOHLE, Eva ; TONAK, Marcus ; KIRKPATRICK, Charles J. ; FUCHS, Sabine: Paracrine Effects Influenced by Cell Culture Medium and Consequences on Microvessel-Like Structures in Cocultures of Mesenchymal Stem Cells and Outgrowth Endothelial Cells. In: *Tissue Engineering Part A* 17 (2011), p. 2199–2212
- [98] KOO, Jae-Geun ; JO, Kil-Suk ; PARK, Jin-Hee: Rheological properties of fucoidans from *Laminaria religiosa*, sporophylls of *Undaria pinnatifida*, *Hizikia fusiforme* and *Sagassum fulvellum* in Korea. In: *Korean Journal of Fisheries and Aquatic Sciences* 30 (1997), Nr. 3, p. 329–333

- [99] KUSAYKIN, Mikhail I. ; SILCHENKO, Artem S. ; ZAKHARENKO, Alexander M. ; ZVYAGINTSEVA, Tatyana N.: Fucoidanases. In: *Glycobiology* 26 (2016), p. 3–12. – ISSN 0959-6658
- [100] KYLIN, Harald: Zur Biochemie der Meeresalgen. 83 (1913), p. 171–197
- [101] LAHRSEN, Eric ; SCHOENFELD, Ann-Kathrin ; ALBAN, Susanne: Size-dependent pharmacological activities of differently degraded fucoidan fractions from *Fucus vesiculosus*. In: *Carbohydrate Polymers* 189 (2018), p. 162–168. – ISSN 0144-8617
- [102] LAHRSEN, Eric ; SCHOENFELD, Ann-Kathrin ; ALBAN, Susanne: Degradation of Eight Sulfated Polysaccharides Extracted from Red and Brown Algae and Its Impact on Structure and Pharmacological Activities. In: *ACS Biomaterials Science & Engineering* 5 (2019), 3, p. 1200–1214
- [103] LAKE, Andrew C. ; VASSY, Roger ; BENEDETTO, Mélanie D. ; LAVIGNE, Damien ; VISAGE, Catherine L. ; PERRET, Gérard Y. ; LETOURNEUR, Didier: Low Molecular Weight Fucoidan Increases VEGF165-induced Endothelial Cell Migration by Enhancing VEGF165 Binding to VEGFR-2 and NRP1. In: *The Journal of Biological Chemistry* 281 (2006), p. 37844–37852
- [104] LANGENBACH, Fabian ; HANDSCHEL, Jörg: Effects of dexamethasone, ascorbic acid and  $\beta$ -glycerophosphate on the osteogenic differentiation of stem cells in vitro. In: *Stem Cell Research & Therapy* 4 (2013), p. 117. – ISSN 1757-6512
- [105] LAPIKOVA, E. S. ; DROZD, N. N. ; TOLSTENKOV, A. S. ; MAKAROV, V. A. ; ZVYAGINTSEVA, T. N. ; SHEVCHENKO, N. M. ; BAKUNINA, I. U. ; BESEDNOVA, N. N. ; KUZNETSOVA, T. A.: Inhibition of thrombin and factor Xa by *Fucus evanescens* fucoidan and its modified analogs. In: *Bulletin of Experimental Biology and Medicine* 146 (2008), p. 328–333. – ISSN 0007-4888 (Print) 0007-4888
- [106] LAVERTU, Marc ; FILION, Dominic ; BUSCHMANN, Michael D.: Heat-Induced Transfer of Protons from Chitosan to Glycerol Phosphate Produces Chitosan Precipitation and Gelation. In: *Biomacromolecules* 9 (2008), 2, p. 640–650. – ISSN 1525-7797
- [107] LEE, Hyun M. ; KIM, Jong-Ki ; CHO, Tae-Sub: Applications of ophthalmic biomaterials embedded with fucoidan. In: *Journal of Industrial and Engineering Chemistry* 18 (2012), p. 1197–1201. – ISSN 1226-086X
- [108] LI, Lei ; SCHEIGER, Johannes M. ; LEVKIN, Pavel A.: Design and Applications of Photoresponsive Hydrogels. In: *Advanced Materials* 31 (2019), 6, p. 1807333. – ISSN 0935-9648
- [109] LIN, Tzu hua ; TAMAKI, Yasunobu ; PAJARINEN, Jukka ; WATERS, Heather A. ; WOO, Deanna K. ; YAO, Zhenyu ; GOODMAN, Stuart B.: Chronic inflammation in biomaterial-induced periprosthetic osteolysis: NF- $\kappa$ B as a therapeutic target. In: *Acta biomaterialia* 10 (2014), p. 1–10. – ISSN 1878-7568 1742-7061
- [110] LINDAHL, Ulf ; COUCHMAN, John ; KIMATA, Koji ; ESKO, Jeffrey D.: Proteoglycans and Sulfated Glycosaminoglycans. In: *Essentials of Glycobiology* (2015), p. 207–221
- [111] LIU, Mei ; ZENG, Xin ; MA, Chao ; YI, Huan ; ALI, Zeeshan ; MOU, Xianbo ; LI, Song ; DENG, Yan ; HE, Nongyue: Injectable hydrogels for cartilage and bone tissue engineering. In: *Bone Research* 5 (2017), p. 17014. – ISSN 2095-6231
- [112] LIU, Xin ; LIU, Bin ; WEI, Xiaolei ; SHI, Yaping ; JIA, Airong ; WANG, Changyun: Structural elucidation of fucoidans from *Sargassum pallidum*. In: *Journal of Applied Phycology* 33 (2021), p. 523–531. – ISSN 1573-5176
- [113] LIU, Yanqiu ; BERENDSEN, Agnes D. ; JIA, Shidong ; LOTINUN, Sutada ; BARON, Roland ; FERRARA, Napoleone ; OLSEN, Bjorn R.: Intracellular VEGF regulates the balance between osteoblast and adipocyte differentiation. In: *Journal of Clinical Investigation* 122 (2012), p. 3101–3113. – ISSN 0021-9738 (Print) 0021-9738

- [114] LOI, Florence ; CÓRDOVA, Luis A. ; PAJARINEN, Jukka ; LIN, Tzu hua ; YAO, Zhenyu ; GOODMAN, Stuart B.: Inflammation, fracture and bone repair. In: *Bone* 86 (2016), 5, p. 119–130. – ISSN 1873-2763
- [115] LU, Hsien-Tsung ; CHANG, Wan-Ting ; TSAI, Min-Lang ; CHEN, Chien-Ho ; CHEN, Wei-Yu ; MI, Fwu-Long: Development of Injectable Fucoidan and Biological Macromolecules Hybrid Hydrogels for Intra-Articular Delivery of Platelet-Rich Plasma. In: *Marine Drugs* 17 (2019), 4, p. 236. – ISSN 1660-3397
- [116] LU, Kun-Ying ; LI, Rou ; HSU, Chun-Hua ; LIN, Cheng-Wei ; CHOU, Shen-Chieh ; TSAI, Min-Lang ; MI, Fwu-Long: Development of a new type of multifunctional fucoidan-based nanoparticles for anticancer drug delivery. In: *Carbohydrate Polymers* 165 (2017), p. 410–420. – ISSN 0144-8617
- [117] LV, Feng-Juan ; TUAN, Rocky S. ; CHEUNG, Kenneth M C. ; LEUNG, Victor Y L.: Concise Review: The Surface Markers and Identity of Human Mesenchymal Stem Cells. In: *Stem Cells* 32 (2014), 6, p. 1408–1419. – ISSN 1066-5099
- [118] MAISONPIERRE, Peter C. ; SURI, Chitra ; JONES, Pamela F. ; BARTUNKOVA, Sona ; WIEGAND, Stanley J. ; RADZIEJEWSKI, Czeslaw ; COMPTON, Debra ; MCCLAIN, Joyce ; ALDRICH, Thomas H. ; PAPADOPOULOS, Nick ; DALY, Thomas J. ; DAVIS, Samuel ; SATO, Thomas N. ; YANCOPOULOS, George D.: Angiopoietin-2, a Natural Antagonist for Tie2 That Disrupts in vivo Angiogenesis. In: *Science* 277 (1997), p. 55–60
- [119] MARUYAMA, Masahiro ; RHEE, Claire ; UTSUNOMIYA, Takeshi ; ZHANG, Ning ; UENO, Masaya ; YAO, Zhenyu ; GOODMAN, Stuart B.: Modulation of the Inflammatory Response and Bone Healing. In: *Frontiers in Endocrinology* 11 (2020). – ISSN 1664-2392
- [120] MASTER, Zubin ; JONES, Nina ; TRAN, Jennifer ; JONES, Jamie ; KERBEL, Robert S. ; DUMONT, Daniel J.: Dok-R plays a pivotal role in angiopoietin-1-dependent cell migration through recruitment and activation of Pak. In: *The EMBO journal* 20 (2001), 11, p. 5919–5928. – ISSN 0261-4189
- [121] MATICA, Mariana A. ; AACHMANN, Finn L. ; TØNDERVIK, Anne ; SLETTA, Håvard ; OSTAFE, Vasile: Chitosan as a Wound Dressing Starting Material: Antimicrobial Properties and Mode of Action. In: *International journal of molecular sciences* 20 (2019), 11, p. 5889. – ISSN 1422-0067
- [122] MATOU, Sabine ; HELLEY, Dominique ; CHABUT, Delphine ; BROS, Andrée ; FISCHER, Anne-Marie: Effect of fucoidan on fibroblast growth factor-2-induced angiogenesis in vitro. In: *Thrombosis Research* 106 (2002), p. 213–221. – ISSN 0049-3848
- [123] MATSUBARA, Kiminori ; XUE, Changhu ; ZHAO, Xue ; MORI, Masaharu ; SUGAWARA, Tatsuya ; HIRATA, Takashi: Effects of middle molecular weight fucoidans on in vitro and ex vivo angiogenesis of endothelial cells. In: *International Journal of Molecular Medicine* 15 (2005), Nr. 4, p. 695–699. – ISSN 1107-3756
- [124] MIDY, V. ; PLOUET, J.: Vasculotropin/Vascular Endothelial Growth Factor Induces Differentiation in Cultured Osteoblasts. In: *Biochemical and Biophysical Research Communications* 199 (1994), p. 380–386. – ISSN 0006-291X
- [125] MULLOY, Barbara: The specificity of interactions between proteins and sulfated polysaccharides. In: *Anais da Academia Brasileira de Ciencias* 77 (2005), p. 651–664. – ISSN 0001-3765
- [126] MURAKAMI, Kaoru ; AOKI, Hiroshi ; NAKAMURA, Shingo ; NAKAMURA, Shin ichiro ; TAKIKAWA, Megumi ; HANZAWA, Motoaki ; KISHIMOTO, Satoko ; HATTORI, Hidemi ; TANAKA, Yoshihiro ; KIYOSAWA, Tomoharu ; SATO, Yasunori ; ISHIHARA, Masayuki: Hydrogel blends of chitin/chitosan, fucoidan and alginate as healing-impaired wound dressings. In: *Biomaterials* 31 (2010), p. 83–90. – ISSN 0142-9612

- [127] NADAR, Shamraja S. ; RAO, Priyanka ; RATHOD, Virendra K.: Enzyme assisted extraction of biomolecules as an approach to novel extraction technology: A review. In: *Food Research International* 108 (2018), p. 309–330. – ISSN 0963-9969
- [128] NAKAMURA, Shingo ; NAMBU, Masaki ; ISHIZUKA, Takamitsu ; HATTORI, Hidemi ; KANATANI, Yasuhiro ; TAKASE, Bonpei ; KISHIMOTO, Satoko ; AMANO, Yoshiko ; AOKI, Hiroshi ; KIYOSAWA, Tomoharu ; ISHIHARA, Masayuki ; MAEHARA, Tadaaki: Effect of controlled release of fibroblast growth factor-2 from chitosan/fucoidan micro complex-hydrogel on in vitro and in vivo vascularization. In: *Journal of Biomedical Materials Research Part A* 85A (2008), 6, p. 619–627. – ISSN 1549-3296
- [129] NEUPANE, Sandesh ; BITTKAU, Kaya S. ; ALBAN, Susanne: Size distribution and chain conformation of six different fucoidans using size-exclusion chromatography with multiple detection. In: *Journal of Chromatography A* 1612 (2020), p. 460658. – ISSN 0021-9673
- [130] NGUYEN, Thuan T. ; DALGAARD MIKKELSEN, Maria ; NGUYEN TRAN, Vy H. ; TRANG, VO Thi D. ; RHEIN-KNUDSEN, Nanna ; HOLCK, Jesper ; RASIN, Anton B. ; CAO, Hang Thi T. ; VAN, Tran Ti T. ; MEYER, Anne S.: Enzyme-Assisted Fucoidan Extraction from Brown Macroalgae *Fucus distichus* subsp. *evanescens* and *Saccharina latissima*. In: *Marine Drugs* 18 (2020). – ISSN 1660-3397
- [131] NI, Liying ; WANG, Lei ; FU, Xiaoting ; DUAN, Delin ; JEON, You-Jin ; XU, Jiachao ; GAO, Xin: In vitro and in vivo anti-inflammatory activities of a fucose-rich fucoidan isolated from *Saccharina japonica*. In: *International Journal of Biological Macromolecules* 156 (2020), p. 717–729. – ISSN 0141-8130
- [132] NIELSEN, Mads S. ; DALGAARD MIKKELSEN, Maria ; PTAK, Signe H. ; HEJBØL, Eva K. ; OHMES, Julia ; NGUYEN THI, Thuan ; NGUYEN HA, Vy T. ; FRETTE, Xavier ; FUCHS, Sabine ; MEYER, Anne ; SCHRØDER, Henrik D. ; DING, Ming: Efficacy of marine bioactive compound fucoidan for bone regeneration and implant fixation in sheep. In: *Journal of Biomedical Materials Research Part A* 110 (2022), 4, p. 861–872. – ISSN 1549-3296
- [133] OHMES, Julia ; XIAO, Yuejun ; WANG, Fanlu ; DALGAARD MIKKELSEN, Maria ; NGUYEN, Thuan T. ; SCHMIDT, Harald ; SEEKAMP, Andreas ; MEYER, Anne S. ; FUCHS, Sabine: Effect of Enzymatically Extracted Fucoidans on Angiogenesis and Osteogenesis in Primary Cell Culture Systems Mimicking Bone Tissue Environment. In: *Marine Drugs* 18 (2020). – ISSN 1660-3397
- [134] OLIVEIRA, Catarina ; GRANJA, Sara ; NEVES, Nuno M. ; REIS, Rui L. ; BALTAZAR, Fátima ; SILVA, Tiago H. ; MARTINS, Albino: Fucoidan from *Fucus vesiculosus* inhibits new blood vessel formation and breast tumor growth in vivo. In: *Carbohydrate Polymers* 223 (2019), p. 115034. – ISSN 0144-8617
- [135] PAPAPETROPOULOS, Andreas ; FULTON, David ; MAHBOUBI, Keyvan ; KALB, Robert G. ; O'CONNOR, Daniel S. ; LI, Fengzhi ; ALTHIERI, Dario C. ; SESSA, William C.: Angiopoietin-1 inhibits endothelial cell apoptosis via the Akt/survivin pathway. In: *Journal of Biological Chemistry* 275 (2000), 3, p. 9102–9105. – ISSN 00219258
- [136] PARK, Hye Y. ; HAN, Min H. ; PARK, Cheol ; JIN, Cheng-Yun ; KIM, Gi-Young ; CHOI, Il-Whan ; KIM, Nam D. ; NAM, Taek-Jeong ; KWON, Taeg K. ; CHOI, Yung H.: Anti-inflammatory effects of fucoidan through inhibition of NF- $\kappa$ B, MAPK and Akt activation in lipopolysaccharide-induced BV2 microglia cells. In: *Food and Chemical Toxicology* 49 (2011), p. 1745–1752. – ISSN 0278-6915
- [137] PARK, Soo-Jeong ; LEE, Kyo W. ; LIM, Dae-Seog ; LEE, Suman: The Sulfated Polysaccharide Fucoidan Stimulates Osteogenic Differentiation of Human Adipose-Derived Stem Cells. In: *Stem Cells and Development* 21 (2011), 11, p. 2204–2211. – ISSN 1547-3287

- [138] PENG, Tingying ; THORN, Kurt ; SCHROEDER, Timm ; WANG, Lichao ; THEIS, Fabian J. ; MARR, Carsten ; NAVAB, Nassir: A BaSiC tool for background and shading correction of optical microscopy images. In: *Nature Communications* 8 (2017), p. 14836. – ISSN 2041-1723
- [139] PEREIRA, Jessica ; PORTRON, Sophie ; DIZIER, Blandine ; VINATIER, Claire ; MASSON, Martial ; SOURICE, Sophie ; GALY-FAUROUX, Isabelle ; CORRE, Pierre ; WEISS, Pierre ; FISCHER, Anne-Marie ; GUICHEUX, Jerome ; HELLEY, Dominique: The in vitro and in vivo effects of a low-molecular-weight fucoidan on the osteogenic capacity of human adipose-derived stromal cells. In: *Tissue Engineering Part A* 20 (2014), p. 275–284. – ISSN 1937-335X (Electronic) 1937-3341 (Linking)
- [140] PHILLIPS, Jennifer E. ; GERSBACH, Charles A. ; WOJTOWICZ, Abigail M. ; GARCIA, Andrés J: Glucocorticoid-induced osteogenesis is negatively regulated by Runx2/Cbfa1 serine phosphorylation. In: *Journal of Cell Science* 119 (2006), 2, p. 581–591. – ISSN 0021-9533
- [141] POBER, Jordan S. ; SESSA, William C.: Evolving functions of endothelial cells in inflammation. In: *Nature Reviews Immunology* 7 (2007), p. 803–815. – ISSN 1474-1733
- [142] PODZIMEK, Stepan: Truths and myths about the determination of molar mass distribution of synthetic and natural polymers by size exclusion chromatography. In: *Journal of Applied Polymer Science* 131 (2014), 4. – ISSN 0021-8995
- [143] REDDI, Hari: Role of morphogenetic proteins in skeletal tissue engineering and regeneration. In: *Nature Biotechnology* 16 (1998), p. 247–252. – ISSN 1546-1696
- [144] REHMAN, Jalees ; LI, Jingling ; ORSCHELL, Christie M. ; MARCH, Keith L.: Peripheral Blood “Endothelial Progenitor Cells” Are Derived From Monocyte/Macrophages and Secrete Angiogenic Growth Factors. In: *Circulation* 107 (2003), 3, p. 1164–1169
- [145] RINAUDO, Marguerite: Chitin and chitosan: Properties and applications. In: *Progress in Polymer Science* 31 (2006), p. 603–632. – ISSN 0079-6700
- [146] RIZWAN, Muhammad ; YAHYA, Rosiyah ; HASSAN, Aziz ; YAR, Muhammad ; AZZAHARI, Ahmad D. ; SELVANATHAN, Vidhya ; SONSUDIN, Faridah ; ABOULOULA, Cheyma N.: pH Sensitive Hydrogels in Drug Delivery: Brief History, Properties, Swelling, and Release Mechanism, Material Selection and Applications. In: *Polymers* 9 (2017), 4, p. 137. – ISSN 2073-4360
- [147] ROHWER, Kevin ; NEUPANE, Sandesh ; BITTKAU, Kaya S. ; PÉREZ, Mayra G. ; DÖRSCHMANN, Philipp ; ROIDER, Johann ; ALBAN, Susanne ; KLETTNER, Alexa: Effects of Crude *Fucus distichus* Subspecies *evanescens* Fucoidan Extract on Retinal Pigment Epithelium Cells-Implications for Use in Age-Related Macular Degeneration. In: *Marine Drugs* 17 (2019), 9, p. 538. – ISSN 1660-3397
- [148] RUNDHAUG, Joyce E.: Matrix metalloproteinases and angiogenesis. In: *Journal of cellular and molecular medicine* 9 (2005), p. 267–285. – ISSN 1582-1838
- [149] RUTKOVSKIY, Arkady ; STENSLØKKEN, Kåre-Olav ; VAAGE, Ingvar J.: Osteoblast Differentiation at a Glance. In: *Medical science monitor basic research* 22 (2016), 9, p. 95–106. – ISSN 2325-4416
- [150] SAHARINEN, Pipsa ; EKLUND, Lauri ; MIETTINEN, Juho ; WIRKKALA, Riikka ; ANISIMOV, Andrey ; WINDERLICH, Mark ; NOTTEBAUM, Astrid ; VESTWEBER, Dietmar ; DEUTSCH, Urban ; KOH, Gou Y. ; OLSEN, Bjorn R. ; ALITALO, Kari: Angiopoietins assemble distinct Tie2 signalling complexes in endothelial cell-cell and cell-matrix contacts. In: *Nature Cell Biology* 10 (2008), p. 527–537. – ISSN 1476-4679

- [151] SARAVANAN, Sekaran ; VIMALRAJ, Selvaraj ; THANIKAIVELAN, Palanisamy ; BANUDEVI, Sivanantham ; MANIVASAGAM, Geetha: A review on injectable chitosan/beta glycerophosphate hydrogels for bone tissue regeneration. In: *International Journal of Biological Macromolecules* 121 (2019), p. 38–54. – ISSN 0141-8130
- [152] SCHINDELIN, Johannes ; ARGANDA-CARRERAS, Ignacio ; FRISE, Erwin ; KAYNIG, Verena ; LONGAIR, Mark ; PIETZSCH, Tobias ; PREIBISCH, Stephan ; RUEDEN, Curtis ; SAALFELD, Stephan ; SCHMID, Benjamin ; TINEVEZ, Jean-Yves ; WHITE, Daniel J. ; HARTENSTEIN, Volker ; ELICEIRI, Kevin ; TOMANCAK, Pavel ; CARDONA, Albert: Fiji: an open-source platform for biological-image analysis. In: *Nature Methods* 9 (2012), p. 676–682. – ISSN 1548-7105
- [153] SCHNEIDER, Caroline A. ; RASBAND, Wayne S. ; ELICEIRI, Kevin W.: NIH Image to ImageJ: 25 years of image analysis. In: *Nature Methods* 9 (2012), p. 671–675. – ISSN 1548-7105
- [154] SCHNEIDER, Tino ; EHRIG, Karina ; LIEWERT, Inga ; ALBAN, Susanne: Interference with the CXCL12/CXCR4 axis as potential antitumor strategy: superiority of a sulfated galactofucan from the brown alga *Saccharina latissima* and Fucooidan over heparins. In: *Glycobiology* 25 (2015), p. 812–824. – ISSN 0959-6658
- [155] SEMENZA, Gregg L.: Hypoxia-inducible factors in physiology and medicine. In: *Cell* 148 (2012), 2, p. 399–408. – ISSN 1097-4172
- [156] SEZER, Ali D. ; CEVHER, Erdal ; HATIPOGLU, Fatih ; OGURTAN, Zeki ; BAS, Ahmet L. ; AKBUGA, Jülide: Preparation of Fucooidan-Chitosan Hydrogel and Its Application as Burn Healing Accelerator on Rabbits. In: *Biological and Pharmaceutical Bulletin* 31 (2008), p. 2326–2333
- [157] SHARIATINIA, Zahra: Pharmaceutical applications of chitosan. In: *Advances in Colloid and Interface Science* 263 (2019), p. 131–194. – ISSN 0001-8686
- [158] SICHERT, Andreas ; CORZETT, Christopher H. ; SCHECHTER, Matthew S. ; UNFRIED, Frank ; MARKERT, Stephanie ; BECHER, Dörte ; FERNANDEZ-GUERRA, Antonio ; LIEBEKE, Manuel ; SCHWEDER, Thomas ; POLZ, Martin F. ; HEHEMANN, Jan-Hendrik: Verrucomicrobia use hundreds of enzymes to digest the algal polysaccharide fucooidan. In: *Nature Microbiology* 5 (2020), p. 1026–1039. – ISSN 2058-5276
- [159] SILBERFELD, Thomas ; LEIGH, Jessica W. ; VERBRUGGEN, Heroen ; CRUAUD, Corinne ; DE REVIERS, Bruno ; ROUSSEAU, Florence: A multi-locus time-calibrated phylogeny of the brown algae (Heterokonta, Ochrophyta, Phaeophyceae): Investigating the evolutionary nature of the “brown algal crown radiation”. In: *Molecular Phylogenetics and Evolution* 56 (2010), p. 659–674. – ISSN 1055-7903
- [160] SILCHENKO, Artem S. ; RASIN, Anton B. ; KUSAYKIN, Mikhail I. ; KALINOVSKY, Anatoly I. ; MIANSONG, Zhang ; CHANGHENG, Liu ; MALYARENKO, Olesya ; ZUEVA, Anastasiya O. ; ZVYAGINTSEVA, Tatyana N. ; ERMAKOVA, Svetlana P.: Structure, enzymatic transformation, anticancer activity of fucooidan and sulphated fucooligosaccharides from *Sargassum horneri*. In: *Carbohydrate Polymers* 175 (2017), p. 654–660. – ISSN 0144-8617
- [161] SLAUGHTER, Brandon V. ; KHURSHID, Shahana S. ; FISHER, Omar Z. ; KHADEMOSSEINI, Ali ; PEPPAS, Nicholas A.: Hydrogels in regenerative medicine. In: *Advanced materials (Deerfield Beach, Fla.)* 21 (2009), 9, p. 3307–3329. – ISSN 1521-4095
- [162] SOEDA, Shinji ; SHIBATA, Yoshiaki ; SHIMENO, Hiroshi: Inhibitory Effect of Oversulfated Fucooidan on Tube Formation by Human Vascular Endothelial Cells. In: *Biological and Pharmaceutical Bulletin* 20 (1997), p. 1131–1135

- [163] STEGEN, Steve ; VAN GASTEL, Nick ; CARMELIET, Geert: Bringing new life to damaged bone: The importance of angiogenesis in bone repair and regeneration. In: *Bone* 70 (2015), p. 19–27. – ISSN 8756-3282
- [164] STEIN, Gary S. ; LIAN, Jane B. ; WIJNEN, Andre J. van ; STEIN, Janet L. ; MONTECINO, Martin ; JAVED, Amjad ; ZAIDI, Sayyed K. ; YOUNG, Daniel W. ; CHOI, Je-Yong ; POCKWINSE, Shirwin M.: Runx2 control of organization, assembly and activity of the regulatory machinery for skeletal gene expression. In: *Oncogene* 23 (2004), p. 4315–4329. – ISSN 1476-5594
- [165] STEVENS, Troy ; GARCIA, Joe G N. ; SHASBY, Michael ; BHATTACHARYA, Jahar ; MALIK, Asrar B.: Mechanisms regulating endothelial cell barrier function. In: *American Journal of Physiology-Lung Cellular and Molecular Physiology* 279 (2000), 9, p. L419–L422. – ISSN 1040-0605
- [166] STREET, John ; BAO, Min ; DEGUZMAN, Leo ; BUNTING, Stuart ; PEALE JR, Franklin V. ; FERRARA, Napoleone ; STEINMETZ, Hope ; HOEFFEL, John ; CLELAND, Jeffrey L. ; DAUGHERTY, Ann ; VAN BRUGGEN, Nicholas ; REDMOND, Paul ; CARANO, Richard A D. ; FILVAROFF, Ellen H.: Vascular endothelial growth factor stimulates bone repair by promoting angiogenesis and bone turnover. In: *Proceedings of the National Academy of Sciences of the United States of America* 99 (2002), 7, p. 9656–9661. – ISSN 0027-8424
- [167] SUN, Changye ; LIU, Mengxin ; SUN, Panwen ; YANG, Mingming ; YATES, Edwin A. ; GUO, Zhikun ; FERNIG, David G.: Sulfated polysaccharides interact with fibroblast growth factors and protect from denaturation. In: *FEBS open bio* 9 (2019), p. 1477–1487. – ISSN 2211-5463
- [168] TADA, Hiroyuki ; NEMOTO, Eiji ; FOSTER, Brian L. ; SOMERMAN, Martha J. ; SHIMAUCHI, Hidetoshi: Phosphate increases bone morphogenetic protein-2 expression through cAMP-dependent protein kinase and ERK1/2 pathways in human dental pulp cells. In: *Bone* 48 (2011), p. 1409–1416. – ISSN 8756-3282
- [169] TAKAYUKI, Asahara ; TOYOAKI, Murohara ; SULLIVAN, Alison ; SILVER, Marcy ; VAN DER RIEN, Zee ; TONG, Li ; WITZENBICHLER, Bernhard ; SCHATTEMAN, Gina ; ISNER, Jeffrey M.: Isolation of Putative Progenitor Endothelial Cells for Angiogenesis. In: *Science* 275 (1997), 2, p. 964–966
- [170] TANG, Guoke ; LIU, Zhiqin ; LIU, Yi ; YU, Jiangming ; WANG, Xing ; TAN, Zhihong ; YE, Xiaojian: Recent Trends in the Development of Bone Regenerative Biomaterials. In: *Frontiers in cell and developmental biology* 9 (2021), 5, p. 665813. – ISSN 2296-634X
- [171] TEIXEIRA, M. M. ; WILLIAMS, T. J. ; HELLEWELL, P. G.: Role of prostaglandins and nitric oxide in acute inflammatory reactions in guinea-pig skin. In: *British journal of pharmacology* 110 (1993), 12, p. 1515–1521. – ISSN 0007-1188
- [172] TIMMERMANS, Frank ; HAUWERMEIREN, Filip V. ; SMEDT, Magda D. ; RAEDT, Robrecht ; PLASSCHAERT, Frank ; BUYZERE, Marc L D. ; GILLEBERT, Thierry C. ; PLUM, Jean ; VANDEKERCKHOVE, Bart: Endothelial Outgrowth Cells Are Not Derived From CD133+ Cells or CD45+ Hematopoietic Precursors. In: *Arteriosclerosis, Thrombosis, and Vascular Biology* 27 (2007), 7, p. 1572–1579
- [173] TONDREAU, Tatiana ; MEULEMAN, Nathalie ; DELFORGE, Alain ; DEJENEFTE, Marielle ; LEROY, Rita ; MASSY, Martine ; MORTIER, Christine ; BRON, Dominique ; LAGNEAUX, Laurence: Mesenchymal Stem Cells Derived from CD133-Positive Cells in Mobilized Peripheral Blood and Cord Blood: Proliferation, Oct4 Expression, and Plasticity. In: *Stem Cells* 23 (2005), 9, p. 1105–1112. – ISSN 1066-5099
- [174] TORODE, Thomas A. ; MARCUS, Susan E. ; JAM, Murielle ; TONON, Thierry ; BLACKBURN, Richard S. ; HERVÉ, Cécile ; KNOX, Paul: Monoclonal antibodies directed to fucoidan preparations from brown algae. In: *PLoS ONE* 10 (2015), 2. – ISSN 19326203

- [175] TSAI, Li-Chu ; CHEN, Chien-Ho ; LIN, Cheng-Wei ; HO, Yi-Cheng ; MI, Fwu-Long: Development of multifunctional nanoparticles self-assembled from trimethyl chitosan and fucoidan for enhanced oral delivery of insulin. In: *International Journal of Biological Macromolecules* 126 (2019), p. 141–150. – ISSN 0141-8130
- [176] VENKATESAN, Jayachandran ; SINGH, Sandeep K. ; ANIL, Sukumaran ; KIM, Se-Kwon ; SHIM, Min S.: Preparation, Characterization and Biological Applications of Biosynthesized Silver Nanoparticles with Chitosan-Fucoidan Coating. In: *Molecules (Basel, Switzerland)* 23 (2018), 6, p. 1429. – ISSN 1420-3049
- [177] VIÑAS, Milena Álvarez ; FLÓREZ-FERNÁNDEZ, Noelia ; GONZÁLEZ-MUÑOZ, María J. ; DOMÍNGUEZ, Herminia: Influence of molecular weight on the properties of Sargassum muticum fucoidan. In: *Algal Research* 38 (2019), p. 101393. – ISSN 2211-9264
- [178] VIGUET-CARRIN, S. ; GARNERO, P. ; DELMAS, P. D.: The role of collagen in bone strength. In: *Osteoporosis International* 17 (2006), p. 319–336. – ISSN 1433-2965
- [179] VUILLEMIN, Marlene ; SILCHENKO, Artem S. ; CAO, Hang Thi T. ; KOKOULIN, Maxim S. ; TRANG, Vo Ti D. ; HOLCK, Jesper ; ERMAKOVA, Svetlana P. ; MEYER, Anne S. ; DALGAARD MIKKELSEN, Maria: Functional Characterization of a New GH107 Endo- $\alpha$ -(1,4)-Fucoidanase from the Marine Bacterium *Formosa haliotis*. In: *Marine Drugs* 18 (2020). – ISSN 1660-3397
- [180] WANG, Fanlu ; SCHMIDT, Harald ; PAVLESKA, Dijana ; WERMANN, Thees ; SEEKAMP, Andreas ; FUCHS, Sabine: Crude Fucoidan Extracts Impair Angiogenesis in Models Relevant for Bone Regeneration and Osteosarcoma via Reduction of VEGF and SDF-1. In: *Marine Drugs* 15 (2017). – ISSN 1660-3397 (Electronic) 1660-3397 (Linking)
- [181] WANG, Fanlu ; XIAO, Yuejun ; NEUPANE, Sandesh ; PTAK, Signe H. ; RÖMER, Ramona ; XIONG, Junyu ; OHMES, Julia ; SEEKAMP, Andreas ; FRETTE, Xavier ; ALBAN, Susanne ; FUCHS, Sabine: Influence of Fucoidan Extracts from Different Fucus Species on Adult Stem Cells and Molecular Mediators in In Vitro Models for Bone Formation and Vascularization. In: *Marine Drugs* 19 (2021), 3, p. 194. – ISSN 1660-3397
- [182] WANG, Jing ; LIU, Li ; ZHANG, Quanbin ; ZHANG, Zhongshan ; QI, Huimin ; LI, Pengcheng: Synthesized oversulphated, acetylated and benzoylated derivatives of fucoidan extracted from *Laminaria japonica* and their potential antioxidant activity in vitro. In: *Food Chemistry* 114 (2009), p. 1285–1290. – ISSN 0308-8146
- [183] WANG, Limin ; STEGEMANN, Jan P.: Thermogelling chitosan and collagen composite hydrogels initiated with beta-glycerophosphate for bone tissue engineering. In: *Biomaterials* 31 (2010), 5, p. 3976–3985. – ISSN 1878-5905
- [184] WANG, Xiaoyi ; JIANG, Huijiao ; GUO, Lijiao ; WANG, Sibao ; CHENG, Wenzhe ; WAN, Longfei ; ZHANG, Zhongzhou ; XING, Lihang ; ZHOU, Qing ; YANG, Xiongfeng ; HAN, Huanhuan ; CHEN, Xueling ; WU, Xiangwei: SDF-1 secreted by mesenchymal stem cells promotes the migration of endothelial progenitor cells via CXCR4/PI3K/AKT pathway. In: *Journal of Molecular Histology* 52 (2021), p. 1155–1164. – ISSN 1567-2387
- [185] WHYTE, J. N. C. ; SOUTHCOTT, B. A.: An extraction procedure for plants: extracts from the red alga *Rhodomela larix*. In: *Phytochemistry* 9 (1970), p. 1159–1161. – ISSN 0031-9422
- [186] WILLIAMS, D. F.: *The Williams Dictionary of Biomaterials*. Liverpool University Press, 1999. – ISBN 9780853237341
- [187] WU, Jie ; SU, Zhi-Guo ; MA, Guang-Hui: A thermo- and pH-sensitive hydrogel composed of quaternized chitosan/glycerophosphate. In: *International Journal of Pharmaceutics* 315 (2006), p. 1–11. – ISSN 0378-5173

- [188] WYATT, Philip J.: Light scattering and the absolute characterization of macromolecules. In: *Analytica Chimica Acta* 272 (1993), p. 1–40. – ISSN 0003-2670
- [189] XIAO, Guozhi ; GOPALAKRISHNAN, Rajaram ; JIANG, Di ; REITH, Elizabeth ; BENSON, Douglas ; FRANCESCHI, Renny T.: Bone Morphogenetic Proteins, Extracellular Matrix, and Mitogen-Activated Protein Kinase Signaling Pathways Are Required for Osteoblast-Specific Gene Expression and Differentiation in MC3T3-E1 Cells. In: *Journal of Bone and Mineral Research* 17 (2002), 1, p. 101–110. – ISSN 0884-0431
- [190] YAMAZAKI, Yoshie ; NAKAMURA, Yuko ; NAKAMURA, Tatsuo: A fluorometric assay for quantification of fucoidan, a sulfated polysaccharide from brown algae. In: *Plant Biotechnology* 33 (2016), p. 117–121
- [191] YAN, Jihong ; YANG, Liu ; WANG, Guirong ; XIAO, Yang ; ZHANG, Baohong ; QI, Nianmin: Biocompatibility Evaluation of Chitosan-based Injectable Hydrogels for the Culturing Mice Mesenchymal Stem Cells In Vitro. In: *Journal of Biomaterials Applications* 24 (2009), 5, p. 625–637. – ISSN 0885-3282
- [192] YANG, Chen ; CHUNG, Donghwa ; SHIN, Il-Shik ; LEE, HyeonYong ; KIM, JinChul ; LEE, YongJin ; YOU, SangGuan: Effects of molecular weight and hydrolysis conditions on anticancer activity of fucoidans from sporophyll of *Undaria pinnatifida*. In: *International Journal of Biological Macromolecules* 43 (2008), p. 433–437. – ISSN 0141-8130
- [193] ZHAO, Qing S. ; JI, Qiu X. ; XING, Ke ; LI, Xiao Y. ; LIU, Cheng S. ; CHEN, Xi G.: Preparation and characteristics of novel porous hydrogel films based on chitosan and glycerophosphate. In: *Carbohydrate Polymers* 76 (2009), p. 410–416. – ISSN 0144-8617
- [194] ZHOU, Hui Y. ; CHEN, Xi G. ; KONG, Ming ; LIU, Cheng S.: Preparation of chitosan-based thermosensitive hydrogels for drug delivery. In: *Journal of Applied Polymer Science* 112 (2009), 5, p. 1509–1515. – ISSN 0021-8995
- [195] ZINDEL, Joel ; KUBES, Paul: DAMPs, PAMPs, and LAMPs in Immunity and Sterile Inflammation. In: *Annual Review of Pathology: Mechanisms of Disease* 15 (2020), 1, p. 493–518. – ISSN 1553-4006

# Acronyms

---

<b>ALP</b>	Alkaline phosphatase	<b>FGF</b>	Fibroblast growth factor
<b>ANG</b>	Angiopoietin	<b>FHL</b>	Four and a half LIM domains protein
<b>BMP</b>	Bone morphogenic protein	<b>FV</b>	Fucus vesiculosus
<b>BSA</b>	Bovine serum albumin	<b>GAE</b>	Gallic acid equivalents
<b>Col I</b>	Collagen type I	<b>GP</b>	Glycerophosphate
<b>COX</b>	Cyclooxygenase	<b>GPCR</b>	G-protein coupled receptor
<b>CPC</b>	Cetylpyridinium chloride	<b>HIF</b>	Hypoxia inducible factor
<b>CPD</b>	Critical point drying	<b>HLA-DR</b>	Human leukocyte antigen DR isotype
<b>CXCR</b>	C-X-C motif chemokine receptor	<b>HMW</b>	High molecular weight
<b>DAMP</b>	Damage-associated molecular pattern	<b>HUVEC</b>	Human umbilical vein endothelial cells
<b>DMEM</b>	Dulbecco's Modified Eagle's Medium	<b>ICAM</b>	Intercellular adhesion molecule
<b>Dok-R</b>	Downstream of kinase-related protein	<b>IEX</b>	Ion-exchange chromatography
<b>DPPH</b>	2,2-diphenyl-1-picrylhydrazyl	<b>IL</b>	Interleukin
<b>EBM</b>	Endothelial basal medium	<b>LDH</b>	Lactate dehydrogenase
<b>EC</b>	Endothelial cells	<b>LFMP</b>	Low fat milk powder
<b>ECM</b>	Extracellular matrix	<b>LPS</b>	Lipopolysaccharide
<b>EGM</b>	Endothelial growth medium	<b>LMW</b>	Low molecular weight
<b>ELISA</b>	Enzyme-linked immunosorbent assay	<b>MALS-VIS</b>	Multi-angle light scattering-viscosity
<b>EPC</b>	Endothelial progenitor cells	<b>MAPK</b>	Mitogen-activated protein kinase
<b>ESR</b>	Equilibrium swelling ratio	<b>MHC</b>	major histocompatibility complex
<b>FAK</b>	Focal adhesion kinase	<b>MKP</b>	Mitogen-activated protein kinase phosphatase
<b>FBS</b>	Fetal bovine serum	<b>MLC</b>	Myosin light chain
<b>FE</b>	Fucus evanescens	<b>MMP</b>	Matrix metalloproteinase
		<b>MMW</b>	Medium molecular weight

## Bibliography

---

<b>MSC</b>	Mesenchymal stem cells	<b>RPL13A</b>	Ribosomal protein L13a
<b>NF<math>\kappa</math>B</b>	nuclear factor kappa-light-chain-enhancer of activated B cells	<b>Runx</b>	Runt-related trascription factor
<b>NMR</b>	Nuclear magnetic resonance	<b>SDF</b>	Stromal-derived factor
<b>NO</b>	Nitric oxide	<b>SEC</b>	Size exclusion chromatography
<b>ODM</b>	Osteogenic differentiation medium	<b>SEM</b>	Scanning electrone microscopy
<b>OEC</b>	Outgrowth endothelial cells	<b>Sox</b>	SRY-box transcription factor
<b>PAMP</b>	Pathogen-associated molecular pattern	<b>TLR</b>	Toll-like receptor
<b>PBS</b>	Phosphate-buffered saline	<b>TNF</b>	Tumor necrosis factor
<b>PFA</b>	Paraformaldehyde	<b>TNFR</b>	Tumor necrosis factor receptor
<b>PGI<sub>2</sub></b>	Prostaglandin I <sub>2</sub>	<b>VCAM</b>	Vascular cell adhesion molecule
<b>PI3K</b>	Phosphoinositide 3-kinase	<b>VEGF</b>	Vascular endothelial growth factor
<b>PLC</b>	Phospholipase C	<b>VEGFR</b>	Vascular endothelial growth factor receptor
<b>PS</b>	Penicillin/Streptomycin	<b>VEGFR<sub>p</sub></b>	Phosphorylated vascular endothelial growth factor receptor
<b>ROI</b>	Region of interest	<b>ZO</b>	Zona occludens

# List of Figures

---

1.1	Long bone anatomy and regeneration. . . . .	3
1.2	Phase I and phase II inflammation in endothelial cells. . . . .	4
1.3	Molecular processes during angiogenesis. . . . .	6
1.4	Bone regeneration via intramembranous and endochondral ossification. . .	8
1.5	Photos and backbone structures of brown algae <i>Fucus evanescens</i> and <i>Fucus vesiculosus</i> . . . . .	12
2.1	Extraction and processing of fucoidan extracts. . . . .	21
2.2	Human outgrowth endothelial cells (OEC) isolated from peripheral blood.	24
2.3	Human osteoblast-like mesenchymal stem cells (MSC) isolated from can- cellous bone. . . . .	25
2.4	Workflow for biological experiments using MSC and OEC mono- and co- cultures as model systems. . . . .	26
2.5	Fucoidan staining with primary antibodies BAM-1 and BAM-4. . . . .	31
2.6	Dot blot for proving the affinity of primary antibody BAM-4 to the studied fucoidan extracts. . . . .	32
2.7	Amplitude sweep test to determine the linear viscoelastic region of the hydrogels without and with 100 $\mu\text{g}/\text{ml}$ fucoidan. . . . .	35
2.8	Preparations for critical point drying. . . . .	36
2.9	SYBR Gold nucleic acid gel stain for quantifying fucoidan in solution according to the protocol of Yamazaki et al. . . . .	37
3.1	Membrane integrity and metabolic activity of OEC and MSC mono- cultures after treatment with enzymatically-extracted fucoidans. . . . .	46
3.2	MSC proliferation measured by the amount of DNA after treatment with enzymatically-extracted fucoidans. . . . .	46
3.3	Gene expression and protein level of angiogenic mediators in MSC mono- culture after treatment with enzymatically-extracted fucoidans. . . . .	48
3.4	Early and late osteogenic markers in MSC mono-culture after treatment with enzymatically-extracted fucoidans. . . . .	49
3.5	Effect of fucoidan concentration on angiogenic proteins and ALP activity in MSC mono-culture. . . . .	49
3.6	Interaction of enzymatically-extracted fucoidan with growth factor VEGF.	50

---

3.7	Phosphorylation of VEGF receptor 2 in relation to the total amount of VEGFR2 in OEC after treatment with enzymatically-extracted fucoidan.	51
3.8	Expression and protein level of inflammatory and angiogenic mediators in OEC mono-culture after treatment with enzymatically-extracted fucoidans.	52
3.9	Development of angiogenic tube-like structures in MSC-OEC co-cultures after treatment with enzymatically-extracted fucoidans.	54
3.10	Expression and protein level of angiogenic mediators in MSC-OEC co-cultures after treatment with enzymatically-extracted fucoidans.	55
3.11	Gene expression of ALP and MMP-14 in MSC-OEC co-cultures after treatment with enzymatically-extracted fucoidans.	56
4.1	Chemical structures of fucoidanase Fhfl hydrolysis products.	60
4.2	Membrane integrity of OEC mono-cultures after treatment with fucoidan obtained by fucoidanase hydrolysis.	60
4.3	Gene expression and protein level of angiogenic mediators in MSC mono-culture after treatment with fucoidan obtained by fucoidanase hydrolysis.	62
4.4	Phosphorylation of VEGF receptor 2 in relation to the total amount of VEGFR2 in OEC after treatment with fucoidans obtained by fucoidanase hydrolysis.	63
4.5	Expression and protein level of inflammatory and angiogenic mediators in OEC mono-culture after treatment with fucoidan obtained by fucoidanase hydrolysis.	64
4.6	The integrity of the endothelial cell barrier in MSC-OEC co-cultures after treatment with fucoidans obtained by fucoidanase hydrolysis.	66
4.7	Development of angiogenic tube-like structures in MSC-OEC co-cultures after treatment with fucoidans obtained by fucoidanase hydrolysis.	67
4.8	Expression and protein level of angiogenic mediators in MSC-OEC co-cultures after treatment with fucoidan obtained by fucoidanase hydrolysis.	69
4.9	Interaction of enzymatically-extracted and -degraded fucoidans with MSC and OEC.	71
5.1	Development of angiogenic tube-like structures in MSC-OEC co-cultures after treatment with H <sub>2</sub> O <sub>2</sub> -degraded fucoidans.	76
5.2	Expression and protein level of angiogenic mediators in MSC-OEC co-cultures after treatment with H <sub>2</sub> O <sub>2</sub> -degraded fucoidans.	77
5.3	Expression and protein level of angiogenic mediators in MSC-OEC co-cultures after treatment with native and H <sub>2</sub> O <sub>2</sub> -degraded fucoidans.	78
5.4	Interaction of H <sub>2</sub> O <sub>2</sub> -degraded fucoidans with MSC and OEC.	81
6.1	Development of a protocol for the preparation of injectable thermosensitive chitosan hydrogels with encapsulated fucoidan.	85
6.2	Chemical and physical properties of thermosensitive chitosan hydrogels with different concentrations of $\beta$ -GP.	86
6.3	Integration of collagen type I into the chitosan hydrogel.	88

---

6.4	Physical and chemical properties of the thermosensitive chitosan-collagen hydrogel with different fucoidan concentrations. . . . .	90
6.5	Rheological measurements of storage ( $G'$ ) and loss modulus ( $G''$ ) for the determination of gelation temperature, time and duration of thermosensitive chitosan-collagen hydrogels with different fucoidan concentrations. . . . .	91
6.6	Internal structure of lyophilized chitosan-collagen hydrogels with and without fucoidan visualized by SEM. . . . .	92
6.7	Internal structure of critical point dried chitosan-collagen hydrogels with and without fucoidan visualized by SEM. . . . .	93
6.8	Detection of fucoidan inside the hydrogel and fucoidan release from the hydrogels. . . . .	94
6.9	2D and 3D cell culture of human MSC on and in chitosan-collagen hydrogels. . . . .	96
6.10	Interaction of MSC with the chitosan-collagen hydrogel. . . . .	97
6.11	VEGF levels in the supernatant and DNA content from hydrogels with encapsulated MSC. . . . .	97
6.12	2D and 3D cell culture of human OEC on and in chitosan-collagen hydrogels. . . . .	98
7.1	Summary and conclusions of the results presented in the current thesis. . . . .	114
A.1	$^1\text{H}$ - $^{13}\text{C}$ HSQC spectra of the fucoidanase hydrolysis products MMW and LMW. . . . .	143

(Figures 1.2, 1.3, 1.4, 2.1, 2.4, 2.8 and 7.1 were created with BioRender.com. Figure 1.1 was adapted from "Bone with Callout (Layout)" by BioRender.com (2022). Retrieved from <https://app.biorender.com/biorender-templates>)



# List of Tables

---

2.1	Endotoxin levels of fucoidan extracts used in the current thesis. . . . .	22
2.2	Fucoidan extracts from <i>Fucus evanescens</i> (FE) and <i>Fucus vesiculosus</i> (FV) used in the presented thesis. . . . .	26
2.3	QuantiTect Primer Assays (Qiagen) for qPCR used in the current thesis. .	28
2.4	DuoSet <sup>®</sup> ELISA Development Systems (R&D) used in the current thesis.	29
2.5	List of materials used for the presented thesis. . . . .	40
2.5	List of all materials used for the presented thesis (continued). . . . .	41
2.5	List of all materials used for the presented thesis (continued). . . . .	42
3.1	Chemical characterization of enzymatically-extracted fucoidans FE_crude, FE_F1, FE_F2 and FE_F3. . . . .	44
4.1	Chemical characterization of fucoidanase hydrolysis products MMW and LMW. . . . .	59
5.1	Chemical characterization of chemically extracted fucoidans (NatF, FracC) and further degraded extracts (CAU1, CAU2, CAU3). . . . .	74
A.1	Donor information and passage numbers for OEC and MSC used in the presented thesis. . . . .	142



A

**Appendix**

---

## A.1 OEC and MSC Donor Information

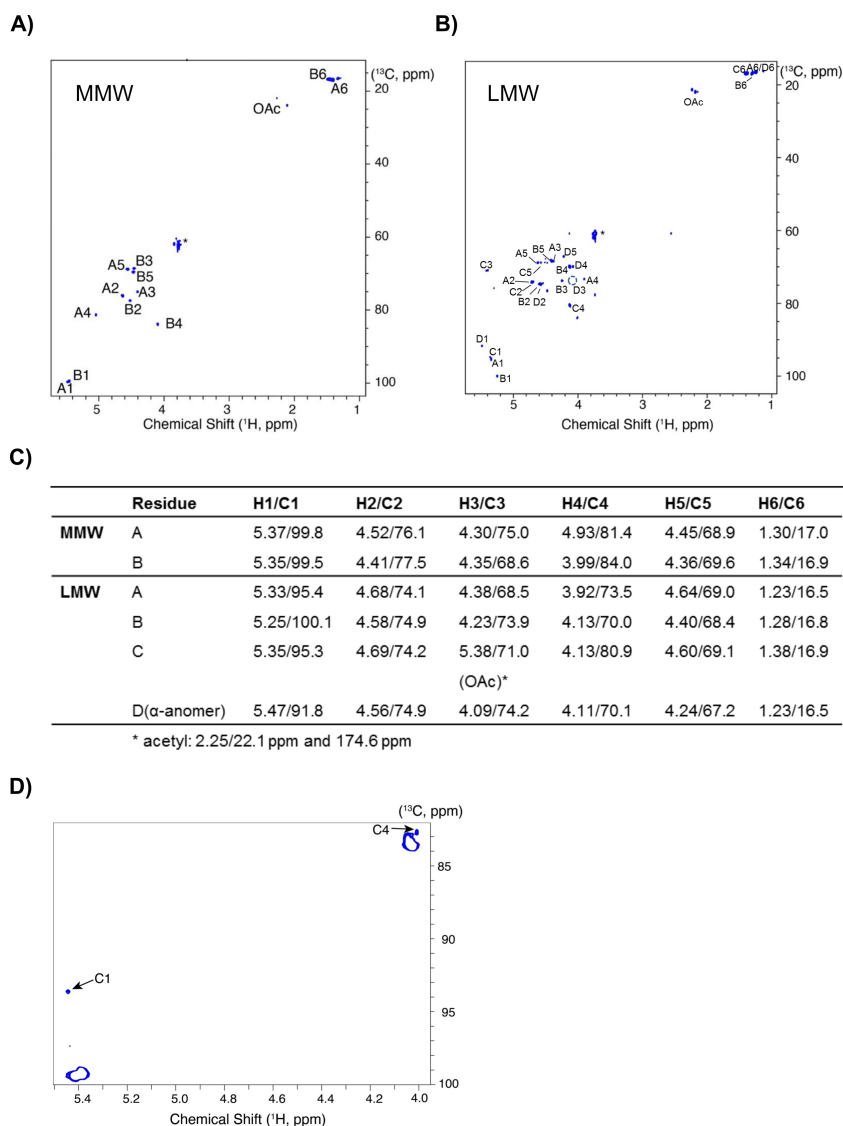
**Table A.1:** Donor information and passage numbers for OEC and MSC used in the presented thesis.

OEC				
No.	Passage No.	Sex	Age	Blood type
74	9	m	37	AB+
147	5, 8, 10	f	25	A+
152	7, 9	-	-	-
252	4, 5, 6, 11	w	20	A+
264	5, 6	m	66	0
274	4, 7	m	62	A+

MSC				
No.	Passage No.	Sex	Age	Blood type
15-1	4	f	50	-
16-2	4, 5	f	57	-
17-4	5	-	-	-
18-1	5	m	48	-
18-4	4, 5	m	78	-
18-7	5	f	69	-
18-8	4, 5	m	-	-
19-2	4, 5	f	76	-

## A.2 NMR Spectroscopy



**Figure A.1:**  $^1\text{H}$ - $^{13}\text{C}$  HSQC spectra (800 MHz instrument, 323 K) of the fucoidanase hydrolysis products A) MMW and B) LMW. The corresponding table is shown in C). Residual Tris buffer signal is indicated by an asterisk. For the MMW spectrum, acetyl group signals are largely absent, while di-sulfation is observed in this fraction. For the LMW spectrum acetyl group signals are evident near 2.25 (1H)/22.1 (13C) ppm. Di-sulfation is not observed in this fraction. The position of the broadened D3 signal is indicated by a dashed circle. D) Spectral region of the  $^1\text{H}$ - $^{13}\text{C}$  HSQC recorded on MMW. Arrows indicate the CH groups at C1 and C4 for a minor (2.4 %) unit, whose chemical shifts are consistent with a  $\rightarrow 3,4$ - $\alpha$ -L-Fucp(2-SO<sub>3</sub><sup>-</sup>)-(1 $\rightarrow$ 3)- branch point [33]. The presence of 3,4-branch points in the *F. evanescens* fucoidan was previously postulated by [13].

### A.3 Certificate of Analysis Chitosan 95/100

HMC+

**HEPPE MEDICAL CHITOSAN GmbH**  
 CEO: Dipl. Biotechnol. Katja Richter

Heinrich-Damerow-Straße 1  
 D-06120 Halle (Saale)  
 Tel: +49 (0) 345 27 896 300  
 Fax: +49 (0) 345 27 896 378  
 info@medical-chitosan.com  
 www.medical-chitosan.com

HypoVereinsbank Halle (Saale)  
 Account: 356 864 832 BLZ: 800 200 86  
 SWIFT: HYVE DE MM 440  
 IBAN: DE33 8002 0086 0356 8648 32

Volksbank Halle (Saale) eG  
 Account: 0001 160 966 BLZ: 800 937 84  
 SWIFT: GENO DE F1 HAL  
 IBAN: DE83 8009 3784 0001 1609 66

VAT.ID: DE 249 728 508  
 Amtsgericht Stendal HRB 5561

## Certificate of Analysis

**Product line:** *Chitoceuticals*

Product: Chitosan 95/100  
 CAS: 9012-76-4  
 Product No.: 24704  
 Batch No.: 212-021118-01  
 Storage conditions: < 25 °C, dry and well closed  
 Production date: 02.11.2018  
 Expiry date: 02.11.2021

Parameter	Method	Limit	Result
Appearance of solid product	HMC QK-PA-0001	white to light yellow	complies
Appearance of solution	HMC QK-PA-0002	clear, colorless to slightly yellowish	complies
Degree of deacetylation	HMC QK-PA-00 03	≥ 92.6%	94.6 %
Viscosity (1 % in 1 % acetic acid, 20 °C)	HMC QK-PA-0004	71 - 150 mPas	116 mPas
Ashes (sulphated)	HMC QK-PA-0005	≤ 1 %	0.2 %
Dry matter content	HMC QK-PA-0006	≥ 90 %	95.6 %
Insolubles	HMC QK-PA-0010	≤ 2 %	complies
Heavy metals			
Pb	HMC QK-PA-0019	≤ 40 ppm	complies
Hg	HMC QK-PA-0020	≤ 0.2 ppm	complies
Cd	HMC QK-PA-0020	≤ 0.5 ppm	complies
As	HMC QK-PA-0020	≤ 0.5 ppm	complies
Protein content	HMC QK-PA-0008	≤ 0.5 %	complies
Microbiological tests			
Total bacterial count	HMC QK-PA-0022	≤ 1000 CFU/g substance	complies
Yeast & mould	HMC QK-PA-0022	≤ 100 CFU/g substance	complies
For reference			
Molecular weight (by GPC): 100 - 250 kDa			

Halle (Saale), 25.02.2019

Katja Richter  
Head of QA/QC

Page: 1/1  
Rev: 02